ZEOLITE ENCAPSULATED COMPLEXES OF RUTHENIUM: SYNTHESIS, CHARACTERISATION AND CATALYTIC ACTIVITY STUDIES

Thesis submitted to the
Cochin University of Science and Technology
In partial fulfilment of the requirements for the degree of

Doctor of philosophy
In
Chemistry
Under the faculty of science

By

ANNU ANNA VARGHESE

DEPARTMENT OF APPLIED CHEMISTRY
COCHIN UNIVERSITY OF SCIENCE AND TECHNOLOGY
Kochi-22, India

DECEMBER 2008

******Dedicated to my loving parents,
my dear husband
and my beloved sons
****

Certificate

*This is to certify that the thesis entitled "**Zeolite encapsulated complexes of ruthenium: synthesis, characterisation and catalytic activity studies**" submitted by **Ms. Annu Anna Varghese** is an authentic and bonafide record of the original research work carried out by the author under my supervision, in partial fulfilment of the requirements for the degree of Doctor of Philosophy of Cochin University of Science and Technology and further, the results embodied in this thesis, in full or in part have not been presented before for the award of any other degree.*

Kochi-22

06-12-2008

Prof. K.K. Mohammed Yusuff

Department of Applied Chemistry
Cochin University of Science and Technology,
Kochi-22

Declaration

I hereby declare that the work presented in this thesis entitled **"Zeolite encapsulated complexes of ruthenium: synthesis, characterisation and catalytic activity studies"** submitted for the award of Ph.D Degree is based on the original work done by me under the guidance of Dr.K.K.Mohammed Yusuff , Professor of Catalysis, Department of Applied Chemistry, Cochin University of Science and Technology, and that it has not formed part of any thesis submitted previously for the award of any other degree.

Kochi-22
06-12-2008

Annu Anna Varghese

Acknowledgement

I gratefully acknowledge my deep sense of gratitude to all who provided help and support to me during the course of my research work. I invariably feel short of words to express my heartfelt gratitude and deep indebtedness to Dr.K.K.Mohammed Yusuff, my supervising guide for his efficient guidance through the awesome path of research with great patience. His constant encouragement, fruitful discussions and valuable suggestions at different stages were really a great inspiration.

I express my sincere thanks to Dr.K.Girish Kumar, Head, Department of Applied Chemistry, CUSAT for providing the necessary facilities for my work. I extend my gratefulness to Dr.S.Sugunan, Dr.M.R.Prathapachandra Kurup, Dr.S.Prathapan and the other faculty members of the department for their source of inspiration for my research work.

I take this opportunity to express my heartfelt thanks to Dr.Jyothy Mariam John for her timely guidance, brilliant suggestions and help right from the initial stages of my work. I sincerely appreciate the help rendered by Dr.Rani Abraham during the preparation of my thesis.

I recall with gratitude the selfless help and involvement of my friends Ms.Manju Sebastian and Mr.Arun.V at different stages of this work. I am also thankful to Dr.N.Sridevi, Dr.Preetha.G.Prasad, Dr.Pearly Sebastian, Dr.S.Mayadevi, Dr.Anas.K and my labmates Robinson, Leeju, Varsha and Digna who gave me support and reassurance in different ways. I am so grateful to acknowledge the constant support and encouragement of Dr. Winnie Varghese, Principal and other members of the faculty, Department of Chemistry, M.A.College, Kothamangalam.

I also thank CUSAT and CSIR, New Delhi for providing financial assistance in the form of research fellowship. I also acknowledge the services provided by the authorities of SAIF, Sophisticated Tests and Instrumentation Centre, Kochi; SAIF, IIT, Bombay and IISc, Bangalore. I also remain thankful to the Office Staff, Department of Applied Chemistry.

I would like to record my deep love for my beloved parents and all other family members and my entire circle of friends and relatives for imparting affectionate encouragement and

confidence with their earnest prayers and sustained support in fulfilling this dream. I am very much indebted to my husband Dr.George Abraham for his unfailing support and endearing source of encouragement. I express my deep sense of affection and love to my little angels Abel and Joel for inspiring me with their beautiful smiles.

Above all, I submit my heartfelt gratefulness before the supreme power of God Almighty for guiding me through the critical stages in my life.

Annu AnnaVarghese

Preface

Catalysis form the backbone of modern chemical industry and scientists all over the world are in search of highly efficient catalysts with high activity and good selectivity. Moreover with vast advances in science and technology during the recent decades, catalysts are expected to become more effective and environment friendly. The most impressive examples of catalyst designs are found in the field of homogeneous catalysis by transition metal complexes. But neat complexes of transition metals are associated with major drawbacks like loss of activity and difficulty of separation. Most of the problems encountered by homogeneous catalysts can be overcome by immobilizing them on a suitable matrix. Immobilized catalysts couple the high activity of a homogeneous system and good workability of a heterogeneous system.

Among the different supports used for anchoring of metal complexes, zeolites are the most effective as they can tune the coordination environment around the metal by modifying the electrostatic properties of the ligand. The process of encapsulation provides a simple way of coupling the reactivity of transition metal complexes with the robustness and stereochemistry of a zeolite. The metal encapsulated complexes of Schiff bases, especially those of ruthenium, can mimic biomolecules and act as structural and functional mode of many metalloenzymes. The coordination chemistry of ruthenium complexes have been an area of particular interest because of their ability to act as efficient catalysts in oxidation and hydrogenation processes. All these developments in the field of coordination chemistry have prompted us to direct our research work in the synthesis of zeolite encapsulated complexes of ruthenium and investigate their catalytic activity in certain reactions of industrial significance.

The thesis is divided into eight chapters. Chapter I is a general introduction on the relevance of zeolite encapsulated transition metal complexes as versatile catalysts in organic synthesis and polymer chemistry. The materials and methods employed for the present study are given in chapter II. Chapter III deals with the synthesis and

characterization of ruthenium complexes of Schiff bases derived from salicylaldehyde within the supercages of the zeolite. Chapter IV is divided into two sections. Section A consists of the zeolite encapsulated complexes of aminobenzoic acids whereas the section B gives an account of the dimethylglyoxime complex. Chapter V presents our studies on the encapsulated complexes of ruthenium with the Schiff bases derived from pyridine carboxaldehydes. Chapter VI of the thesis focuses on the catalytic activity of the synthesized complexes in the decomposition of hydrogen peroxide and studies on the action of the encapsulated complexes on the oxidation of cyclohexanol are presented in Chapter VII. Chapter VIII deals with our detailed investigation on phenol hydroxylation in presence of the encapsulated complexes. The general conclusions derived from the study are summarized at the end of the thesis.

Contents

Chapter IV

Section A

Section B

****

Chapter I

INTRODUCTION

Chapter I

INTRODUCTION

Catalysis is an area of prime importance in the frontier area of chemistry. The term 'catalysis' refers to the enhancement of a particular chemical reaction by the appropriate use of a suitable material. The basic characteristics essential for a catalyst are high activity, good selectivity and regenerability. Nowadays, all the products manufactured utilize the rate enhancement and energy saving property of catalysts in the various steps of their industrial production. The industrial reactions accelerated by the presence of a catalyst are associated with the production of a large quantity of inorganic effluents, which are difficult to dispose off. One of the major concerns in the field of catalysis is the minimization of waste production in various chemical processes.

The growing demands for the design of environment friendly products and processes have led to the development of green chemistry. In view of the growing concern over environmental pollution and with further advance of catalytic sciences, chemical industries are forced to adopt new safe and eco-friendly technologies with less consumption of energy and raw materials. Chemical reactions involving catalysis are more preferred as they are highly effective under milder conditions and generate minimum wastes. Thus there is a constant urge for the need to develop regenerable and effective solid catalysts.

Basically there are three different fields of catalysis: homogeneous, heterogeneous and biological (enzymatic) catalysis. Homogeneous catalysts include transition metal complexes existing in a series of oxidation states and acting as good catalysts for many chemical reactions. The disadvantages associated with them have put greater emphasis on the development of new and improved heterogeneous catalytic systems. The most widely used technique to heterogenize complexes is to encapsulate them in zeolite pores. The supported complexes possess several advantages when compared to their homogeneous counterparts. Keeping in mind the different commercial

benefits associated with the heterogenization of complexes, efforts are being made to develop relatively new zeolite catalysts for providing a break through in the industrial field of active and selective organic transformations. With this view, a large number of Schiff base complexes have been synthesized inside zeolite cages and studied.

1.1. SCHIFF BASE COMPLEXES

Recent years have witnessed a great deal of interest in the research of different types of Schiff base complexes of transition elements[1-4]. The interest in the design and synthesis of novel transition metal complexes containing Schiff bases lies in their biological and catalytic activity in many reactions[5,6]. Many Schiff base complexes possess interesting biological properties such as antibacterial and antitumour activities[7-9]

Depending on the nature of the Schiff base ligands, there are immense applications of their complexes in the chemical field. Schiff bases with variable donation sites could be monodentate, bidentate, tridentate or tetradentate forming mono or polynuclear complexes[10]. The tetradentate Schiff base complexes are employed to design metal complexes related to synthetic and natural oxygen carriers.

In many studies, Schiff bases deserve a relevant role for several reasons like:

(a) The major advantage of Schiff bases is that they can be obtained by simple self-condensation of various aldehydes with suitable amines.

(b) They can have additional donor groups like oxygen, sulphur, phosphorus etc. which makes them good candidates for metal ion complexation and for mimicking biological systems.

(c) Schiff bases can be functionalized by the insertion of appropriate groups in the aliphatic or aromatic chains of the precursors used.

(d) Another advantage is the ease of preparation of Schiff base complexes by template effect and the designed complexes can be directly obtained by this procedure.

Complexes of Schiff bases with oxygen and nitrogen as donor atoms were found to be very effective reagents aiding the oxidation of alcohols and alkenes[11]. The coordination chemistry of Schiff base complexes are widely investigated since they

provide ample opportunities for inducing substrate chirality, tuning metal centered electronic factor and enhancing solubility and stability of both homogeneous and heterogeneous catalysts[12-17].

Schiff bases act as the most attractive and convenient ligands for ruthenium complexes. This can be attributed to several reasons:

(a) The use of appropriate Schiff bases with suitable electron withdrawing or electron donating groups can tune the steric and electronic effects around the ruthenium core.
(b) The donor atoms nitrogen and oxygen on the Schiff bases are capable of exerting two opposite electronic effects. The phenolic oxygen acting as a hard donor can stabilize the higher oxidation state of ruthenium and the soft donor, imine nitrogen stabilizes the lower oxidation state of ruthenium.
(c) The preparation of Schiff bases is very simple and they can be obtained in high yield by condensation of aldehydes with different amines[18, 19].

All these desirable properties of Schiff bases have made it relevant to synthesize a large number of bidentate, tridentate and tetradentate transition metal complexes of Schiff bases. There are instances of tetradentate Ru-salen[20-27] class of compounds acting as quite stable catalysts even at room temperatures. They show remarkably high dia- and enantioselectivity in catalysing a large number of organic reactions. The versatile application of salen complexes in organic synthesis and polymer chemistry include the promotion of several organic transformations like olefin metathesis reactions, cross metathesis, enzyme metathesis, alkyne dimerization and enol-ester syntheses. Schiff bases contribute largely towards the progress of coordination chemistry of transition metals by providing a foundation for the development of contemporary macrocyclic chemistry[28]. The rising interest in the study of unsymmetrical Schiff base complexes with transition metal cations is due to the action of such complexes as relevant models to bio-inorganic molecules such as metalloproteins and metalloenzymes[29-33]. Asymmetric Schiff base complexes are used as redox catalysts[34] in many organic reactions and as models for irregular metal ion binding to peptides[35, 36]. Various hydrogenation and oxidation reactions including

selective oxidation of styrene in presence of zeolite encapsulated salen complexes are reported[37-39].

1.2. HOMOGENEOUS CATALYSIS BY TRANSITION METAL COMPLEXES

The study of transition metal complexes has witnessed a spectacular development during the recent few decades due to their increasing potential as versatile catalysts in organic synthesis and polymer chemistry. In accordance with growing environmental concerns and the demand for more efficient and cheaper processes, the use of homogeneous transition metal complexes to catalyse organic reactions have received widespread attention in recent years[40-42]. Thus there is a continuing interest for the design and synthesis of new compounds that can function as catalysts in reactions of industrial significance and modification of the properties of already synthesized molecules. All chemical reactions involving catalysis are associated with changes in the oxidation state and coordination environment of the central metal ion and ligand field environment.

The coordination environment around the central metal ion directs the properties of the complexes, hence complexation of transition metal atoms by ligands of different types have been of great significance. Transition metal atoms possess nine orbitals in total that include one s, three p and five d orbitals and there are cases where all the nine orbitals participate in bond formation with ligands. The existence of central transition metal atom in different oxidation states were found to be most promising in catalytic studies and the transition metal compounds, by virtue of their readily available multioxidation states, occupy a key position in the development of coordination chemistry[43]. If all the nine orbitals of the metal atom are filled completely, then addition of a ligand involve substitution reactions of S_N1 type. The reaction proceeds by dissociation of one ligand from the complex forming a coordinatively unsaturated species with only sixteen electrons in the valence shell. This unsaturated species show high tendency to bind with incoming ligands so as to increase the electron count to eighteen. The catalytic mechanism is driven by the jumping of transition metal ion between these two states[44].

Many positive aspects are associated with homogeneous catalysts. They can operate at low temperatures and pressures and yield products with higher selectivity and purity. Moreover, reaction mechanisms of homogeneous catalysis are better understood than the surface reactions of heterogeneous systems. The reversible binding of molecular oxygen to transition metal complexes can modify their properties to a great extent[45]. The mixed ligand complexes of transition metals containing ligands with N, S and N, S, O donors show interesting stereochemical, electrochemical and electronic properties[46].

There are numerous examples of a wide variety of reactions catalysed by homogeneous transition metal complexes. The pioneering work by Ziegler and coworkers paved the foundation for the development of homogeneous catalysis. The first effective homogeneous catalyst designed for hydrogenation is the square planar rhodium complex, chlorotris(triphenyl phosphine)rhodium(I), which is well known as Wilkinson's catalyst. The water-gas shift reaction involving the conversion of CO to CO_2 is catalyzed by a variety of homogeneous metal carbonyl complexes like $[HFe(CO)_4]^-$, $[Rh(CO)_2I_2]^-$ and $[Ru(bpy)_2(CO)C]^+$. The hydroformylation[47] reaction producing about 5 million tons of aldehydes and aldehyde derivatives annually makes use of cobalt or rhodium complexes to accelerate the reaction. One of the great successes of homogeneous catalysis is in the conversion of methanol to acetic acid. The Monsanto acetic acid process can be initiated using the rhodium complex, $[Rh(CO)I_2]^-$. Another notable development in this field is the successful use of palladium catalysts in the Wacker process for the production of acetaldehyde from ethylene[48]. The one reaction that requires special mention is the enantioselective electrocatalytic epoxidation of olefins in the presence of chiral Schiff base complexes of manganese[49].

Homogeneous catalysts have limited applications due to their high susceptibility to reaction conditions and the difficulty of their separation from the product mixture. The low thermal and chemical stabilities of such systems result in their slow decomposition. All the problems encountered by homogeneous catalysts can be overcome by immobilizing them on a suitable matrix. The immobilization of homogeneous catalysts leads to higher thermal and chemical stabilities[50-60]. The product selectivity and substrate specificity is increased to a greater extent by sterric crowding

around the metal atom. In addition to all these qualities, the ease of separation of the supported catalysts makes them more beneficial when compared to their homogeneous counterparts.

1.3. HETEROGENISATION OF HOMOGENEOUS SYSTEMS

Recent years have witnessed a great deal of interest in the study of heterogeneous catalytic systems due to their importance as catalysts for many reactions. Heterogenised homogeneous catalysts possess the advantages of both homogeneous and heterogeneous systems. They offer several advantages such as the simplification of the reaction procedures, easy separation of products, recyclability of expensive catalysts, possibility to design continuous flow processes, good control of morphology of polymers and high polymer bulk density[61-65].

The term heterogenisation refers to the process of immobilization of homogeneous transition metal complexes by anchoring them to an inert polymer or inorganic support. This type of bonding to a solid surface stabilizes the complex and generates catalytically active centers[66]. The supported complexes possess higher selectivity and greater catalytic activity than their homogeneous analogues. Infact, the greatest challenge in catalysis is the development of systems with good selectivity and in this context, there is an urgent need to develop highly efficient ecofriendly heterogeneous catalytic systems.

Several methods can be employed for supporting homogeneous catalysts that can be broadly classified into two categories. The organic supports widely used are polymers like polystyrene; poly(4-vinyl pyridine) etc. and the inorganic supports include silica, alumina, zeolites, clay etc. Interest in inorganic supports has arisen because of their unique characteristics of flexibility and stability. Inorganic supported catalysts by means of their rigid structure can act as bio-functional catalysts[67]. Of all the supports used, the use of zeolite molecular sieves has gained considerable importance due to their ability to tailor the structure of the catalyst to maximize their activity[68, 69]. The process of encapsulation provides a simple way of coupling the reactivity of transition metal complexes with the robustness and stereochemistry of a zeolite.

1.3.1. Zeolites

Zeolites are porous metal oxides, typically aluminosilicates, which contain extensive cavities and well-defined channel structures with, pore diameters in the 3-12Å range[70-72]. Zeolite was discovered by the Swedish scientist Axel Frederick Cronstedt[73]. He found that heating of zeolite crystals release the water contained in them as gas bubbles and this prompted him to name the mineral as 'zeolite', which means 'boiling stone' in Greek. The channels and cages of the zeolite structure are only accessible to those molecules with the correct shape and dimensions. The incorporation of catalytic sites within such a structure provides the basis of molecular shape-selective catalysis. The parallels between zeolite chemistry and biological oxidation systems have been highlighted by the research work of Herron *et al.*[74, 75].

1.3.1.1. Structural aspects of zeolites

Zeolites are crystalline aluminosilicates with an open lattice framework and contain silica and alumina tetrahedra joined through oxygen bridges to form a three-dimensional structure. They belong to the tectosilicate family of minerals[76-79]. The interconnection of Si and Al tetrahedra through oxygen bridges play a major role in enhancing the thermal stability of the molecule. The zeolite structure is found to be stable even at higher temperatures of about 700°C[80]. The primary building units of tetrahedra can arrange themselves in different ways to form different rings of various dimensions. These rings are joined together to form complex secondary building units[81].

The general formula of the zeolite structure is $M_{x/n}(AlO_2)_x(SiO_2)_y.nH_2O$. The charge carried by the tetrahedral Al framework is found to be neutralized by the M^{n+}cation[82].

The chemistry of zeolites has been an area of particular interest because of their high activity and unique size and shape-selective catalytic properties. The zeolite pores act as reaction centers for binding and catalysis of molecules[83]. The development of zeolites as potential catalysts in various organic reactions started after the inspiring work by Barrer in the early 1940's. The microporous highly crystalline structure of

zeolites has provided them the ability to act as 'molecular sieves'. The windows and cavities within the zeolites are large enough to allow the entry of molecules upto 9Å in diameter into the crystalline structure.

1.3.1.2. Classification of Zeolites

Zeolites can be classified in different ways[84, 85].

(i) Classification based on Si/Al ratio

(a) Zeolites with low Si/Al ratio between 1and1.5.

eg:- Zeolite A, Zeolite X etc.

(b) Zeolites with intermediate Si/Al ratio between 2 and 5.

eg:- Zeolite L, Zeolite Y, erionite etc.

(c) Zeolites with high Si/Al ratio.

eg:- ZSM-5, ZSM-11, mordenite, ferrierite.

(ii) Classification based on pore diameter

(a) Small pore zeolites

eg:- Linde A, chabazite.

(b) Intermediate pore zeolites

eg:- ZSM-5, ZSM-11, ferrierite.

(c) Large pore zeolites

eg:- Linde L, ZeoliteX , ZeoliteY etc.

1.3.1.3. Structure of Zeolite A, X and Y

In these zeolites twenty four tetrahedra constitute a sodalite unit which is a three dimensional array of SiO_4 and AlO_4 tetrahedra in the form of a truncated octahedron with 24 vertices and six four- membered rings and eight six-membered rings. The basic building units of sodalite have an internal diameter of 6.6Å and the enclosed void space is called the sodalite cage. These units that are connected by hexagonal prisms constitute a larger void space called the supercage. The cavity of the sodalite unit is known as the βcage while the cavity of the supercage is the α-cage.

Zeolites A, X and Y belong to the faujasite type of zeolites. Zeolite A is formed when the sodalite units are joined through the four-membered ring faces (D4R) whereas zeolites X and Y are formed by the joining of the hexagonal six-membered faces of the sodalite units (D6R). The Si/Al ratio of zeolite X is about 1.25 and that of zeolite Y is about 2.5. The diameters of α-cage and βcage are approximately 13Å and 6.6Å respectively. The unit cell formula and mole ratio of SiO_2/Al_2O_3 of zeolites X and Y are represented in the table 1.1.

Table 1.1.

Type of Zeolite	Unit cell formula	SiO_2/Al_2O_3 Mole ratio
Zeolite X	$Na_{86}(AlO_2)_{86}(SiO_2)_{106}.nH_2O$	25:1
Zeolite Y	$Na_{56}(AlO_2)_{56}(SiO_2)_{136}.nH_2O$	5:1

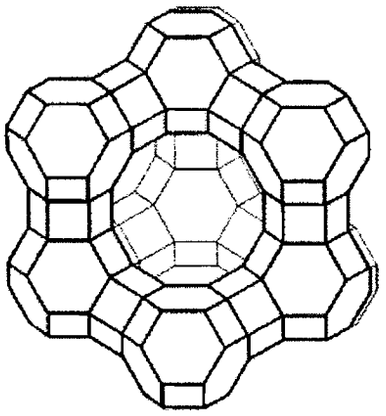

Fig. 1.1 The cavity and channel structure of zeolite-Y

All these structural aspects of zeolites have resulted in an interesting behaviour of zeolites, which include high catalytic activlty, ion exchange capacity, shape selectivity, specific adsorption behaviour and good flexibility for adjustment by isomorphous substitution of the constituents in the framework. The large internal surface area and the uniform dimensions of the windows present have made them attractive supports for many guests. The most commonly used aluminosilicates is zeolite-Y with regular surfaces and well-defined coordination sites. The incorporation of various materials into the internal voids of the zeolite lattice modifies the adsorption

and catalytic properties of the host and guest species to a greater extent. The catalytic properties of zeolites depend on several factors such as the degree of dehydration and the type of cation, which has been exchanged into the zeolite. The exchanged cations serve to balance the negative charges created by the tetrahedral units in the lattice framework.

1.3.2. Catalytic activity of zeolites

The well-defined cages and channels of the zeolite serve as a sort of reaction flask with suitable molecular dimension for the enapsulation of metal complexes. There are two distinct kinds of catalytic activity for zeolites.

(a) Based on their Bronsted acidity[86-89].

(b) Based on the presence of transition metal cations[90-93]

The reason for the Bronsted acidity is the presence of a heteroatom like aluminium in a silica framework[94]. The hydrogen atom bonded to the oxygen adjacent to the tetrahedrally incorporated heteroatom has a tendency to free itself as a proton thereby leaving a macroanionic framework. The evidence for the existence of this proton is given by probes like IR spectroscopy, high resolution NMR spectroscopy etc. The introduction of a strongly polarizing cation into the cavities of the zeolite by means of ion exchange will facilitate the formation of free protons and make them good Bronsted acid catalysts. The above-mentioned process of acid catalysis of zeolites serves as the basis for several useful syntheses like the industrial production of ethyl benzene. The presence of cations of different transition metals in the microenvironment of the interior of the zeolites enhances the action of various redox reactions.

The recognition of the significance of shape-selectivity in the study of zeolites brings into attention the kinship between zeolitic and enzymatic catalysts. Similar to enzymatic action, only the reactants possessing the requisite dimensions to gain entry into the interior of the zeolite are favoured and certain products according to their ability to diffuse out are preferentially released from within the internal area of the zeolite. The active sites constituting the detachable protons are expected to be distributed uniformly throughout the bulk of the zeolite.

1.3.2.1. Zeolite-encapsulated transition metal complexes

The zeolite encapsulation has both advantages and disadvantages. The major advantages can be listed as follows.

(1) The metal ions are uniformly dipersed throughout the zeolite support that prevents polynuclear cluster formation of metal ions.
(2) The process of encapsulation enables a metal complex to be physically trapped in the pores and not necessarily bound to the oxide surface.
(3) The framework structure of many zeolites including the dimensions and arrangements of the cages are roughly equivalent to those that are encountered in enzyme catalysis, thus allowing comparative studies between them.
(4) The high thermal stability of the zeolites combined with the large internal surface area and their size and shape selectivity enable them to act as attractive solid supports.
(5) Zeolites can effectively function as both the solvent and the counter ion in the formation of metal complexes.

In addition to the above-cited benefits, there are some disadvantages associated with the use of zeolite supports.

(1) The window size in a zeolite restricts the size of the ligand that can be used in the preparation of the complex.
(2) Due to the anionic nature of the zeolite lattice, encapsulation is usually restricted to cationic complexes.
(3) The problem of diffusion arises during catalysis as many of the cavities are already filled with large complexes.

1.3.2.2. Synthesis of zeolite- encapsulated complexes

Several methods have been developed for encapsulation of transition metal complexes inside the three-dimensional pore structure of zeolite. The most widely used methods are

(a) Flexible ligand method

In this method of complexation the flexible nature of the ligand is taken into consideration. The ligand molecules are small enough to diffuse through the zeolite pores and form complexes with the metal ions in the cavities of the zeolite host material. The metal complexes thus formed are too large to escape from the zeolite void. This idea was first introduced by Herron in the synthesis of encapsulated complexes of bis(salicylaldehyde)ethylenediamine (salen) in the cavities of faujasite[95]. The initial step, in this process is the preparation of transition metal ion exchanged zeolite by the method of ion exchange. In the metal exchanged zeolite, the metal ion is surrounded by water molecules; hydroxide or oxide ions of the zeolite structure and these weak ligands can readily be replaced by other coordinating ligands. The salen can enter the cavities of the zeolite through the restricting windows and react with the transition metal ions already present within the supercages of the zeolite. The complex thus formed adopts a suitable geometry and cannot diffuse out of the zeolite pores. The salen complexes of Fe(III)[96], Co(II), Mn(II)[97], Rh(II)[98] and Pd(II)[99] are already synthesized by this method. A similar method was adopted for the synthesis of bipyridyl complexes of iron, manganese, copper and ruthenium[100, 101]. The encapsulated complexes prepared by this technique exhibit good catalytic activity[102] and the catalysis have been reported to depend upon the transition metal ion and the nature of the Schiff base ligands[103]. The flexible ligand method was also adopted for the synthesis of highly selective bis - and tris-coordination complexes.

(b) Ship-in-a-bottle synthesis

This method of encapsulation involves the synthesis of the metal complex from smaller components of the ligand within the zeolite voids or assembling it from smaller species around the transition metal ions. The ship-in-a-bottle synthesis was first used by Romanovsky and co-workers to prepare zeolite-encapsulated transition metal complexes of phthalocyanines[104-106]. The phthalocyanine complexes of iron, cobalt, nickel, copper and manganese were prepared by this method[107-110]. The first stage of preparation involves the introduction of metal ion into the zeolite structure by means of ion exchange in the form of carbonyl complex or metallocenes. This is followed by

addition of 1, 2-dicyanobenzene (DCB) and the reaction occurs at high temperature to form metal phthalocyanine complexes inside the cage structure.

Another method of preparation involves treating the ion exchanged zeolite with 1, 2-dicyanobenzene under vacuum in the temperature range of 250-350°C. The formation of the complex proceeds according to the equation as

$$M^{2+}Y + 4DCB + H_2O \rightarrow MPcY + \tfrac{1}{2} O_2 + 2H^+$$

The optimum temperature required for the formation of a particular complex depends on the structure of the zeolite and nature of the transition metal ion. Yet another way of intrazeolite ligand synthesis and complexation occurs by the adsorption of the transition metal carbonyl complex within the zeolite followed by the synthesis of the phthalocyanine ligand around the transition metal introduced into the cavities. It can occur either by decomposition of carbonyl to form small metal clusters or by a direct ligand exchange of carbonyl by 1, 2-dicyanobenzene. The presence of uncomplexed transition metal ions can be greatly reduced by using metallocenes as suppliers of transition metal ions instead of carbonyl complexes. Tetra-t-butyl substituted phthalocyanine complexes of iron and perfluorophthalocyanines of iron, cobalt, copper and manganese are incorporated in zeolites by adopting this technique[111, 112]. There are similar reports of encapsulation of tetramethylporphyrins in zeolite Y.

(c) Template synthesis

During the method of synthesis by template method, a pre-formed metal complex acting as a template is added to the synthesis gel. The metal complex acting as the templating agent must be stable during all stages of the synthesis. The above condition restricts the formation of a large number of complexes by this method. But there are various advantages associated with this method of synthesis. The important one is that well-defined encapsulated metal complexes with a pre-determined coordination can be obtained. Template method has been used in the synthesis of zeolite encapsulated phthalocyanine complexes of iron, cobalt, nickel, copper and manganese.

1.3.3. Catalysis by zeolite-encapsulated transition metal complexes

The use of zeolite-encapsulated transition metal complexes to catalyse organic reactions has gained considerable attention in recent years on account of their fascinating properties. Homogeneous catalysts immobilized in the cage system of zeoliteY are expected to be stabilized against aggregation or bimolecular deactivation. Furthermore, the zeolite cage system may favour unique selectivity of a catalytic reaction due to changed complex geometries, transition-state modifications and diffusional selectivity for the substrate molecules. The evidence for the location of metal complexes inside the zeolite cages are obtained from a large number of data like the changes in spectra with respect to solution analogues, scanning electron microscopy before and after soxhlet extractions, failure to extract the complexes with strong donor solvents and recovery of the complexes after dissolution of the zeolite with acid. The combined effects of the shape selectivity of zeolites and high dispersive power of metal ions of transition metal exchanged zeolites are of great interest in catalytic studies. But it is crucial to understand the distribution of metal ions in such systems and to find out if large complex molecules formed inside the intracrystalline spaces are under distortion or affected in any way by the zeolite lattice leading to unusual physical and chemical behaviour[113].

Reports about metal phthalocyanine complexes trapped within the zeolite cages are already available[114]. These large macrocyclic metal complexes have a tendency to aggregate or dimerize in solution and act as inhibitors to certain redox processes[115]. The zeolite encapsulated iron-phthalocyanine complexes are found to act as effective catalysts in the selective oxidation of cyclohexane to cyclohexanone in the presence of tert-butyl peroxide[116]. The corresponding simple phthalocyanine complexes of iron were found to undergo oxidative destruction under the same reaction conditions[117]which brings into focus the unique catalytic properties of zeolite. The synthesis and structural properties of zeolite encapsulated phthalocyanine complexes of cobalt, copper, nickel, manganese, ruthenium are already reported[118-122]. All these encapsulated complexes enhance the rate of hydroxylation of phenol in the presence of hydrogen peroxide, which is an industrially important reaction[123]. The cobalt analogue is an active catalyst

in the oxidation of ethylbenzene with molecular oxygen and the copper complexes catalyse the epoxidation reaction of styrene[124].

Zeolites X and Y can be used for the synthesis of several organic compounds[125-127]. Various reactions like hydration of olefins, dehydration of alcohols, ester formation, transesterification etc. are catalysed by zeolite systems[128, 129]. The emergence of supported salen complex of manganese as an important catalyst for the oxidation of olefins has find major applications in pharmaceutical industry[130, 131]. Zeolite entrapped carbonyl clusters of osmium act as selective stable catalysts for CO hydrogenation[132]. The experiments conducted on tris(2,2'-bipyridine)iron(II) complexes of zeoliteY provides evidence for the dynamic feature of complex equilibrium in presence of a ligand-eliminating process with the cage openings acting as sinks for such a draining system. Detailed studies are conducted on the formation of paramagnetic oxygen adducts in cobalt exchanged-Y type zeolites containing adsorbed ethylenediamine[133]. An anionic Co(II) cyanide complex which reversibly binds oxygen inside zeoliteY has been prepared[134].

Zeolite encapsulated complexes exhibit some fine properties of the enzymes and so they are called 'zeoenzymes'[135]. The entrapped complexes exhibit the high specificity and activity of the enzymes since the channels and cages within the three-dimensional pore structure of zeolites are similar to those present in natural enzymes[136-138]. A number of such complexes are reported to mimic certain enzymes[139-144]. Zeolite encapsulated porphyrin type complexes mimicking the enzyme cytochrome P-450 is a topic of intense research in recent years[145-148]. An efficient mimic of cytochrome P-450 was developed by Jacobs *et al.* by the encapsulation of iron pthalocyanine complex within zeoliteY and then embedding it in polydimethylsiloxane membrane[149]. This environment friendly system behaves in a similar manner as true enzymes in the oxidation of alkanes at room temperature[150-152]. The embedded form shows a six-fold increase in activity when compared to the nonembedded form.

Reports of zinc and iron porphyrin complexes incorporated in the cages of zeolite have attracted wide attention due to their high activity in photosensitizesd oxidation reactions[153--155]. The encapsulation of copper acetate dimers in zeoliteY find application as catalysts in the hydroxylation of phenol[156].

The zeolite supported Schiff base complexes display an enhanced activity and selectivity in a multitude of organic reactions. In view of the highly desirable attributes of such complexes, a vast number of supported Schiff base complexes have been designed and synthesized. The entrapment of a chiral salen complex of manganese aids the asymmetric epoxidation of alkenes. Zeolite Y encapsulated Cu(salen) complex prepared by Ratnasamy *et al.*[157] are efficient catalysts in the selective oxidation of cyclohexanol to cyclohexanone in the presence of hydrogen peroxide[158]. A similar analogue of Co(salen) complex and V(salen) complex with tetragonal distortion show catalytic activity towards phenol hydroxylation[159]. These distortions in molecular geometries as a result of encapsulation lead to depletion of electron density at the metal sites and subsequent increase in catalytic activity. The entrapped Co(salen) complex has been reported to act as a zeoenzme to study the oxygen binding properties of haemoglobin[160].

Much attention has recently been given to bipyridyl complexes trapped in zeolite cages due to their specific properties. The epoxidation of alkenes is hindered by several complications arising from the competing process of their auto-oxidation. The epoidation can be realized in practice by engaging zeolite supported Mn(II) bipyridine complexes[161]. The photocatalytic activity exhibited by encapsulated bipyridine complexes of ruthenium is of considerable significance[162, 163]. They act as an efficient oxygen sensor material and can efficiently oxidize intrazeolite water to dioxygen[164, 165].

Several metal carbonyl clusters grafted on zeolite supports are studied in detail to understand their action as catalysts. There are reports of zeolite-encapsulated clusters of iron, rhodium, iridium, palladium, osmium and molybdenum[166-170]. They can be prepared by the usual procedure of ion exchange followed by carbonylation[171]. Clusters of osmium carbonyl supported on zeolite[172] can catalyze the hydrogenation of carbon monoxide to form hydrocarbons. Another interesting class of carbonyl clusters is the intrazeolite half-sandwich compounds of rhodium and iridium[173].

A lot of work has been done to explain the reason behind the enhanced catalytic activity of encapsulated metal complexes of salen in the selective oxidation of methane using tert-butyl hydroperoxide under mild conditions. It is very interesting to note that simple complexes show only mild activity in comparison with the supported analogues.

The oxidative coupling of 2, 6-dimethyl phenol was catalyzed by engaging zeolite supported pyridine derivative complexes of Cu(II), $[Cu(2\text{-ethylpyridine})_n]^{n+}$ which was first synthesized by Kazusaka *et al*[174]. Zeolite-Y encapsulated copper complexes of Schiff bases derived from salicylaldehyde and 2-aminomethylbenzimidazole are effective catalysts for the oxidation of phenol and styrene in the presence of hydrogen peroxide[175].

Efficient catalysts for the oxidation of α-pinene under commercially viable and environmentally acceptable reaction conditions have been developed with encapsulation of [Co(II)Saloph] and [Ru(III)saloph] complexes in zeolite[176]. The thermal stability of carbonyl complexes of nickel supported inside zeolites has become a subject of wide investigation.[177]. The application of intrazeolite compounds in the separation and purification of gases can be achieved on knowing the sterric distortion of materials in zeolites. The first experimental evidence for the distortion of intrazeolite compounds is obtained from the studies of $[FeL_3]^{2+}$ ions (where L = ethylenediamine, bipyridine and phenanthrene) in zeolite supercages[178]. The mononuclear dioxygen complexes of cobalt act as model compounds for oxygen carriers and they have been stabilized by immobilization of the complexes inside zeolite[179, 180]. Zeolite encapsulated picolinate complexes of vanadium when compared to their homogeneous forms show high oxidative power and increased selectivity. The higher reactivity can be explained on the basis of the intermediate peroxo vanadium species formed during the oxidative process. The formation of encapsulated six coordinate cobalt(II) methyl isocyanide complexes with D_{4h} symmetry illustrates the formation of fully coordinated complexes in the supercages of zeolite. The hydroxylation of phenol can be accelerated by engaging various supported complexes like Cu(II) thiazoylhydrazone, Co(II) phenanthroline and VO(Salen) in zeolite Y. Bis(dimethylglyoxime) complexes of different transition metals entrapped in zeolite lattice find immense applications as catalysts in a large number of synthetic reactions. Notable among them is the selective oxidation of propene[181].

The excellent catalytic activities of the encapsulated complexes of different transition metals have prompted us to synthesize a family of ruthenium complexes

within the zeolite supercages and to investigate their action in a series of organic reactions of industrial significance.

1.4. CATALYTIC ACTIVITY OF RUTHENIUM COMPLEXES

The coordination chemistry of ruthenium complexes is of special significance in view of their application in biological processes and as catalysts in chemical and photochemical industry[182-185]. In spite of the fast trend in the research on different transition metal complexes, very little importance has been given to their ruthenium analogues[186-189]. The recent years have witnessed a great deal of interest in the synthesis of complexes of ruthenium using ligands of various classes, particularly of Schiff bases. Studies on the chemistry of such complexes have brought into attention their importance in oxidation processes[190, 191]. The coordination chemistry of Ru(II) and Ru(III) complexes has been widely investigated because of their use in catalytic oxidation and hydrogenation processes[192-194]. A distinctive feature of ruthenium complexes is that they are found to be very stable, exhibit a good tolerance towards organic functionalities, air and moisture and display high activity and chemoselectivity in chemical transformations.

The Schiff base complexes of ruthenium containing oxygen and nitrogen as donor atoms act as efficient catalysts in the oxidation of alkenes and alcohols[195-197]. Reports about the Schiff base complexes of Ru(II) with appended CO and triphenyl phosphine groups prepared by Wilkinson *et al.* are available[198]. The catalytic effect of ruthenium complexes in the homogeneous catalysis of carbonyl complexes and oxo reactions are well established[199-203]. Moreover they act as excellent catalysts in different organic transformation reactions including reduction and oxidation reactions, hydrolysis etc.

There are reports about the catalytic activity of ruthenium complexes containing tertiary phosphine and tertiary arsine ligands[204, 205]. Studies are conducted on the oxidation of alcohols by some supported Schiff base complexes of ruthenium[206-209]. The reactions studied involve the oxidation of cholesterol, geraniol etc. effected by ruthenium complexes in the presence of N-methylmorpholine-N-oxide and N,N-dimethylaniline-N-oxide[210]. The interesting properties of ruthenium complexes

containing nitrogen and oxygen donors such as their redox stability, excited-state reactivities and excited-state lifetimes have rekindled the growing interest in the investigation of such complexes.

The coordination environment around ruthenium plays the key role in their part as catalysts towards the reduction of unsaturated organic compounds in mild coordinating media[211, 212]. Ruthenium exhibits a wide range of oxidation states, which is responsible for their versatile electron-transfer properties [213-217]. The action of ruthenium complexes depend on the stability and interconvertibility of the various oxidation states characteristic of the metal and are influenced to a great extent by the binding of the ligands to the metal. Hence the synthesis of ruthenium complexes by employing different ligands is receiving widespread attention nowadays. The electron-transfer, photochemical and catalytic properties shown by ruthenium metal is the reason behind the considerable interest in the coordination chemistry of the metal[218]. The real impetus towards this fast growing interest is the successful use of some tridentate Schiff base complexes of ruthenium in several catalytic asymmetric reactions[219, 220].

Complexes of ruthenium show promising applications as homogeneous catalysts in carbonylation, hydroformylation and oxo reactions[221-224]. Some Ru(III) Schiff base complexes derived from aldehydes like salicylaldehyde, picolinaldehyde and several amines have been investigated to study the nature of binding and catalytic activity in high valent stable ruthenium complexes[225]. There are several instances of these complexes behaving as catalysts in the reductive carbonylation of nitrobenzene to phenylurethane by a phosgene-free route and in the oxidation reaction of cyclohexene to its epoxide[226].

The chemistry of bipyridine complexes of ruthenium deserves special mention as a result of their photocatalytic activity. The numerous experiments conducted by researchers with the bipyridine complexes have proved that their zeolite encapsulated complexes are easily susceptible to coordination of another molecule of Ru(II) complex which make them highly selective photocatalysts. Another interesting feature is the imparting of luminescent properties to intrazeolite bis-terpyridine complexes of the type $[Ru(tpy)_2]^{2+}$ existing as non-luminescent in free solution[227]. Mixed ligand ruthenium complexes have been found to catalyze many reactions such as hydrogenation,

oxidation, carbonylation, hydroformylation etc. due to their wide range of reversible and accessible oxidation states[228, 229]. The tetradentate salen and porphyrin complexes of ruthenium are highly enantioselective in their potential use as catalysts in various reactions of great industrial importance.

Binuclear ruthenium (III) complexes of the type $[RuX_2(EPh_3)_2]L$ (where X= Cl, Br; E = P or As; L = schiff base anion) are prepared by the reaction of the appropriate diamines with salicylaldehyde or benzoylacetone in a 2:1 molar ratio. The prepared complexes with octahedral geometry have been used as catalysts in aryl-aryl couplings. Tris(2,2'-bipyridine) ruthenium(II) complex $[Ru^{II}(bpy)_3]^{2+}$ can be synthesized within the large cavities of zeoliteY by heating a mixture of bipyridine and $Ru^{III}Y$ zeolites. The spectroscopic properties of the complexes were found to be similar to $[Ru^{II}(bpy)_3]^{2+}$complexes in aqueous solution. But a distinctive feature of the zeolite complexes is their anomalous variability in photophysical behaviour, which depends on the degree of complex loading within the zeolite and the extent of hydration. All these studies showed the importance of zeolites as attractive supports for ruthenium complexes and the possibility of alteration of coordination environments to enhance desired photoreactions and photocatalytic processes[230]. The experiments conducted by Dwyer and Gyarfas showed the formation of ozone and hydrogen peroxide on dissolution of tris(bipyridine) salts of Ru(III) in water[231].

Extensive studies have been conducted on octahedral hexacoordinated ruthenium(II) complexes[232] containing 2,2'-bipyridine ligands (bpy) due to their vast applications as chiral building blocks for supramolecular assemblies[233, 234] and as chiral probes for biological molecules[235, 236]. The photoluminescent and electroluminescent properties of the bipyridine complexes make them good light-emitting devices[237-239]. ZeoliteY encapsulated $Ru(bpy)_3^{2+}$acts as an highly efficient photocatalyst. The entrapmemt of the bipyridine complex in zeolite supercages results in dramatic increase in emission intensity and lifetime providing access to practically important potential photochemical reactivity of the complex. The desirable properties of Ru-phosphane complexes like their excellent enantioselectivities; broad substrate scope; fast reactions; high substrate to catalyst ratios etc. have made them key intermediates of antibiotic carbapenems[240] and antibacterial levofloxacin[241]. Dinitrogen complexes of ruthenium

have been investigated to provide a model emulating the low temperature fixation of nitrogen. The synthesis of dinitrogen complexes of the type $[Ru(NH_3)N_2]^{2+}$ involve the exchange reaction of $[Ru(NH_3)NO]^{3+}$ and then action with hydrazine.

The heterogeneous Schiff base carbene complexes of ruthenium provide recyclable and efficient solid catalysts with significant activity than their homogeneous counterparts. High product yield was obtained with these immobilized ruthenium complexes for enol-ester synthesis, Kharasch addition, ring-closing metathesis (RCM) and ring-opening metathesis polymerization (ROMP) reactions. Ruthenium(III) complexes have been widely applied as efficient catalysts in hydrogen transfer reactions between alcohols and ketones. The arene ruthenium(II) and ruthenium(0) complexes act as good catalysts for many important reactions of alkenes which even include enantioselective hydrogen transfer to ketones and imines in the presence of enantiometrically pure chiral amino alcohols or diamines producing higher yields[242-244]. The contribution of catalytic enantioselective hydrogenation is very important as syntheses of complex molecules and production of chemicals and pharmaceuticals are based on this reaction. The assessment of,γ,δ- unsaturated aldehydes using [3,3]-sigmatropic rearrangement of allyl vinyl ethers face many limitations in the introduction of vinyl ether group. But an alternative method have been developed for selective alkene isomerisation by the incorporation of ruthenium hydride or ruthenium carbonyl derivatives[245-250].

There are various reports about the use of ruthenium(III) complexes as non-toxic and homogeneous catalysts[251-254]. The kinetics and mechanism of Ru(III) catalyzed oxidation of asparagine and aspartic acid by N-bromosuccimide[255] were investigated and similar studies were made regarding the mechanism of Ru(III) catalyzed oxidative reactions of lactose and maltose by potassium bromate in alkaline medium[256].

The condensation of 2-aminobenzoic acid with alehydes like salicylaldehyde and pyridine-2-carboxaldehyde yield a series of tridentate Schiff base ligands which are used in the synthesis of mixed chelate complexes of ruthenium. These complexes characterized by analytical and spectral studies were used to study catalysis of hydrocarbon oxidations for cyclohexene, cyclohexane, cyclohexanol, toluene, benzyl

alcohol, tetrahydrofuran etc using oxygen atom transfer agents like H_2O_2, t-BuOOH, NaOCl, $KHSO_5$ and pyridinium-N-oxide[257]. The ruthenium complexes of the type $[Ru(CO)(PPh_3)_2Z(L)]$ where Z = PPh_3, pyridine or piperidine ; L = anion of the Schiff base were synthesized by condensing anthranilic acid with salicylaldehyde, acetyl acetone etc. The catalytic studies of those complexes proved them to be very effective for oxidation of primary alcohols in the presence of N-methylmorpholine-N-oxide as co-oxidant[258]. Ruthenium complexes possessing an octahedral geometry have been prepared and characterized with ligands derived by reaction of 4-aminobenzoic acid with anisaldehyde, 2-nitrobenzene and 4-chlorobenzene[259]. An octahedral structure has been tentatively assigned to hexa-coordinated Ru(III) complexes with anthranilic acid cinnamaldehyde, anthranilic acid p-tolualdehyde and anthranilic acid p-anisaldehyde[260].

1.5. SCOPE OF THE PRESENT INVESTIGATION

Catalysis is a key technology that helps to solve the various challenges faced by the growing population regarding limited resources and environmental problems. Scientists all over the world are in search of highly efficient catalysts with good selectivity and high activity. Catalysis forms the backbone of modern chemical industry and there is an urgent need to develop catalysts that are easily separable from the reaction mixture and highly recyclable. Moreover with vast advances in science and technology, catalysts are expected to become more safe and eco-friendly.

The most impressive examples of catalyst designs are found in the field of homogeneous catalysis by transition metal complexes. But neat complexes of transition metals are associated with major drawbacks like loss of activity and difficulty of separation thereby making the process more expensive. It is possible to improve the properties of complexes such as selectivity, thermal stability, recyclability and ease of catalyst separation. by immobilizing them on various supports. Immobilized catalysts couple the high activity of a homogeneous system and good workability of a heterogeneous system.

Among the different supports used for anchoring of metal complexes, zeolite Y is the most effective as it can impart size and shape selectivity. Zeolite Y with cavities and channels of molecular dimensions of different sizes and shapes can fine tune the

coordination environment around the metal by modifying the electrostatic properties of the ligand. The encapsulation of complexes increase the life span of the catalyst by providing stability to the material thereby preventing the dimerisation of metal complexes already present. The metal encapsulated complexes of Schiff bases can mimic biomolecules and act as structural and functional mode of many metalloenzymes. Hence they have gained the attention of researchers in the field of active heterogeneous catalysis. All these developments in the field of coordination chemistry have prompted us to direct our research work in the design and synthesis of zeolite encapsulated transition metal complexes. The present study was undertaken with the following objectives.

1) Synthesis and characterization of zeolite encapsulated ruthenium complexes of some simple ligands, which might function as good bio-friendly catalysts.
2) Synthesis and characterization of zeolite supported ruthenium complexes of some Schiff bases derived from salicylaldehyde or pyridine carboxaldehydes.
3) To study the effect of the zeolite matrix on the structure and geometry of the synthesized complex.
4) To determine the catalytic activity of the synthesized complexes in various reactions of industrial significance like
   (i) Decomposition of hydrogen peroxide.
   (ii) Selective hydroxylation of phenol to hydroquinone.
   (iii) Oxidation of cyclohexanol.
5). To make a comparative study of the catalytic activity of neat complexes and analogous encapsulated complexes.

Keeping all the above mentioned objectives in mind, the zeolite encapsulated metal complexes of the following ligands were prepared and characterized.

1. Salicylaldehyde semicarbazone (SSC)
2. N,N'-bis(salicylaldimine)-*o*-phenylenediamine (SOD)
3. N,N'-bis(salicylaldimine)-*p*-phenylenediamine (SPD)
4. Anthranilic acid (AA)
5. 4-Aminobenzoic acid (ABA)
6. Dimethylglyoxime (DMG)

7. N,N'-bis(3-pyridylidene)-1,2-phenylenediamine (PCO)
8. N,N'-bis(3-pyridylidene)-1,4-phenylenediamine (PCP)
9. N,N'-bis(2-pyridylidene)-1,2-phenylenediamine (CPO)
10. N,N'-bis(2-pyridylidene)-1,4-phenylenediamine (CPP)

The present study dealing with the design and synthesis of new encapsulated complexes and their applications as catalysts are incorporated in detail in this thesis.

References

1. Mc Carthy, P. J.; Hovey, R. J.; Ueno, K.; Martell, A. E. J.Am.Chem.Soc. **1955,** 77, 5820

2. Ali, M. A.; Livingstone, S. E. Coord.Chem. Rev, **1974,** 13, 126.

3. Srinivasan, K.; Michand, P.; Kochi, J. K. J.Am.Chem.Soc. **1986,** 108, 2309.

4. Bhattacharya, P. K. Proc.Indian Acad.Sci.(Chem.Sci.). **1990,** 102, 247.

5. Serron, S.A.; Haar, C.M.; Nolan, S. P.; Brammer, L. Organometallics. **1997,** 16, 5120.

6. Bindu, P.; Kurup, M. R. P.; Satyakeerty, T.R. Polyhedron. **1998,** 18, 321.

7. Chattopadhyay, S.K.; Ghosh, S. Inorg.Chim.Acta. **1987,** 131, 15.

8. Chattopadhyay, S.K.; Ghosh, S. Inorg.Chim.Acta. **1989,** 163, 245.

9. Bregant, F.; Pacor, S.; Ghosh, S.; Chattopadhyay, S.K.; Sava, G. Anti Cancer Res. **1993**, 13, 1007.

10. Enikolopyan, N.S.; Bogdanova, K.A.; Askarov, K.A.; Russ.Chem. Rev, **1983,** 52, 13

11. Kureshy, R. I.; Khan, N. H.; Abdi SHR. J.Mol.Cat. **1995,** 96, 117.

12. De Clercq, B.; Verpoort. F. Macromolecules. **2002,** 35, 8943.

13. Opstal, T.; Verpoort. F. Synlett. **2002,** 6, 935.

14. Opstal, T.; Verpoort. F. Angew.Chem.Int.Edit. **2003,** 42, 2876.

15. Pal, S. N.; Pal, S. Inorg.Chem. **2001**, 40, 4807.

16. De Clercq, B.; Verpoort. F. Adv.Synth.Catal. **2002**, 34 ,639.

17. De Clercq, B.; Lefebvre, F.; Verpoort. F. Appl.Catal.A **2003**, 247, 345.

18. Guerriero, P.; Tamburini, S.; Vigato, P.A. Coord.Chem. Rev. **1995,** 139,17.

19. Vigato, P.A.; Tamburini, S.Chem.Rev, **2004**, 248, 1717.

20. Miller, J.A.; Jin, W.; Nguyen, S.B. Angew.Chem. Int.Ed. **2002,** 41,2953

21. Miyata, A.; Furakawa, M.; Irie, R.; Katsuki, T. Tetrahedron Lett. **2002**,43,3481.

22. Miyata, A.; Murakami, M.; Irie, R.; Katsuki, T. Tetrahedron Lett. **2001**,42,7067.

23. Murakami, M.; Uchida, T.; Katsuki, T. Tetrahedron Lett. **2001**,42,7071

24. Murakami, M.; Uchida, T.; Irie, R.; Katsuki, T. Tetrahedron Lett. **2000,** 41, 5119.

25. Irie, R.; Masutani, K.; Katsuki, T. Synlett .**2000,** 1433.

26. Takeda, T.; Irie, R.; Shinoda, Y.; Katsuki, T. Synlett. **1999**,1157.

27. Uchida, T.; Irie, R.; Katsuki, T. Synlett. **1999**,1163.

28. Fenton, D.E.; Vigato, P.A. Chem.Soc. Rev, **1988**, 17, 69.

29. Williams, R.J.P. Biochem.Soc.Trans. **1990**, 18, 689.

30. Wilkinson, G. Comprehensive Coordination Chemistry, Pergamon, Oxford. **1987**, 5, 494 & 726.

31. Cotamagana, J.; Vargas, J.; Latorre, R.; Alvarado, A.; Mena, G. Coord.Chem. Rev, **1992**,119, 67.

32. Pandey, Y.S.; Pandey, H.N.; Mathur, P. Polyhedron. **1994**, 13, 3111

33. Siecker, R.E.; Jensen, L.C.; Saunders-Lochr, J. Nature (London). **1981**,291, 263

34. Boghaei, D.M.; Sabounchei, S.J.S.; Rayati, S. Synth. React.Inorg.Met-Org.Chem. **2000**, 30,1535.

35. Hill, H. A. O. Inorg. Biochem, **1979**, I, 199.

36. Hodgson, M.S.; Eccles, K.O.; Lontie, T.K. J.Am.Chem.Soc. **1981**,103,984.

37. Kowalak, S.; Weiss, R.C.; Balkus, K.J. J.Chem.Soc.Chem.Commun. **1991**, 57.

38. Kimura, T.; Fukuoka, A.; Ichikawa, M. Catal.Lett. **1990**, 4, 279.

39. Varkey, S.P.; Jacob, C.R. Ind. J.Chem. **1998**, 37A , 407.

40. Nakamura, A.; Tsulsui, M. Principles and applications of Homogeneous catalysis, Wiley, New York .**1980**.

41. Masters, C. Homogeneous transition metal catalysis, Chapman & Hall-London, New York .**1981**.

42. Olive, G.H.; Olive, S. Coordination and catalysis, Verlag Chemie, New York. **1977**.

43. Krimura, E.; Sakonaka, A.; Machida, R. J.Am.Chem. Soc. **1984**, 104.

44. Parshall.G.W.; Ittel.S.D. Homogeneous catalysis 2nd edition, Wiley, New York. **1996**.

45. Niederhoffer, E.C.; Timmons, J.H.; Martell, A. E. Chem.Rev. **1984,** 84, 137.

46. Greaney.M.A.; Coyle.C.L.; Harma.M.A.; Jordan.A.; Stiefel.E.I. Inorg.Chem. **1989**, 28, 912-920.

47. Antolovic, D.; Davidson, E. R. Am.Chem.Soc. **1987,** 109, 5828.

48. Smidt, J.; Hafner, W.; Jira, R.; Sedlneier, J.; Sieber, R.; Rulttinger, R.; Kojer. Angew. Chem. **1959,** 71 , 176.

49. Jacobsen, E.N.; Schaus, S.E.; Dossetter, A.G.; Jamison, T.F. US Patent-**1999**-255480.

50. Krause, J.O.; Nuyken, O.; Wurst, K.; Buchmeiser, M.R.; Chemistry **2004**, 10, 777.

51. Yang, L.; Mayr, M.; Wurst, K.; Buchmeiser, M.R. Chemistry **2004**, 10, 5761.

52. Cannon, S.J.; Dunne, A.M.; Blechert, S. Angew. Chem. **2002**,41,3989.

53. Cannon, S.J.; Dunne, A.M.; Blechert, S. Angew. Chem. Int.Ed. **2002**, 41, 3835.

54. Cannon, S.J.; Blechert, S. Bioorg.Med.Chem. Lett. **2002**, 12 1873.

55. Jafarpour,L.; Heck,M.P.; Baylon,C.; Lee,H.L.; Mioskowski, C.; Nolan, S.P. Organometaalics. **2002**, 21, 671.

56. Yao, Q.W. Angew.Chem. Int.Ed. **2000**, 39, 3896.

57. Ahmed, M.; Arnauld, T.; Barrrett, A.G.M.; Braddock, D.C.; Procopiou, A. Synlett. **2000**, 9, 1007.

58. Heckel, A.; Seebach, D. Angew.Chem. Int.Ed. **2000**, 39, 1.

59. Gibson, S.E.; Swamy, V.M. Adv.Synth.Catal. **2002**, 344, 619.

60. Dowden, J.; Savovic, J. Chem. Commun. **2001,** 37.

61. Garber, S.B.; Kingsbury, J.S.; Gray, B.L.; Hovedya, A.H. J.Am.Chem. Soc. **2000**, 122, 8168.

62. Kingsbury, J.S.; Garber, S.B.; Giftos, J.M.; Gray, B.L.; Okamoto, M.M.; Farrer, R.A.; Fourkas, J.T.; Hovedya, A.M. Angew.Chem. Int.Ed. **2001**, 40, 4251.

63. Hultzisch, K.C.; Hovedya, A.H.; Jernelius, J.A.; Schrock, R.R. Angew.Chem. Int.Ed. **2002**, 41, 589.

64. Clark, J.H.; Macquarrie, D.J. Chem. Soc.Rev, **1996**, 25, 303.

65. Clark, J.H.; Macquarrie, D.J. Org.Process. Res.Dev. **1997**, 1, 149.

66. Corma, A.; Garcia, H. Chem. Rev, **2000**, 102 ,3837.

67. Murrell, L.L. Advanced materials in catalysis, Academic Press, New York **1977**.

68. Romanovsky, B.V.; Zakharov, V.Yu.; Borisova, T.G. Modern Problems of Physical Chemistry (Ed.K.V.Topchieva), Moscow.Univ.Publ.**1982**, P170,

69. Lunsford, J.H. Catal.Rev.Sci. Eng. **1975**, 12, 137.

70. Jacobs. P.A.; Mortier. W.J.; Uytterhoeven. J.B. J.Inorg.Nucl. Chem. **1978**, 40,1919

71. Bein.T.; Jacobs.P.A. J. Chem. Soc. Faraday Trans. I **1983**, 79, 1819; **1984**, 80, 1391.

72. Breck,D.W.Z. Molecular Sieves, Krieger, Malabar FL, **1984**.

73. Cronstedt, A.F. Akad.Handl. **1756** ,17, 120.

74. Herron, N.; Tolman, C.A. J. Am.Chem. Soc.**1987,** 109, 2837.

75. Herron,N.; Stucky, G.D.; Tolman, C.A. J. Am. Chem. Soc. **1986**, 1521.

76. Dwyer, J.; Karim, K. J. Chem.Soc. Chem.Commun.**1991**, 905.

77. Barrer, R.M. Zeolites and Clay Minerals as Sorbents and Molecular sieves, Academic Press, London.**1978**.

78. Smith, J.V. Adv.Chem.Ser. **1971**, 101,171.

79. Smith, J.V. Chem.Rev. **1988**, 88,149.

80. Corma, A.; Augustin Martinez. Adv.Mater. 7. **1995**, 2, 137.

81. Rabo, J.A. Zeolite Chemistry and Catalysis, ACS Monograph 171, American Chemical Society, Wasington DC. **1976**.

82. Meir, W.M.; Olson, D.H. Atlas of Zeolite Structure Types, 2nd edition, Butterwork, London. **1987**.

83. Lungford, J.H. Catal. Rev. Sci.Eng.; **1975**, 12, 137.

84. Barrer, R.M. Hydrothermal Chemistry of Zeolites, Academic Press, NewYork. **1982**.

85. Barrer, R.M. Hydrothermal Chemistry of Zeolites, Academic Press, London. **1983**.

86. Rabo, J.A. Catal.Rev.Sci.Eng. **1982**, 24, 202.

87. Derouane, E.G.; Whittingham. M.S.; Jacobson, A.J. (Eds). Intercalation Chemistry, Academic Press, New York. **1982**, 101.

88. Thomas, J.M. Proc.Int.Congr.Catal.8th I , **1984**, 31.

89. Ramdas, S.; Thomas, J.M.; Cheetham, A.K.; Betteridge, P.W.; Davies, E.K. Angew.Chem. **1984**, 96, 629.

90. Maxwell, I.E. Adv.Catal.**1982**, 31, I.

91. Boreskov, G.K.; Minachev, K.M. (Ed.). Applications of Zeolites in Catalysis, Akademiai Kiado, Budapest.**1979**.

92. Heinemann, H. Catal.Sci.Technol.I ,**1981**.

93. Hedden, K.; Weitkamp, J. Chem. Ing.Tech.**1983**, 55, 907.

94. Haag, W.O.; Lago, R.M.; Weisz, P.B. Nature (London).**1984**, 309, 589.

95. Herron, N. Inorg.Chem. **1986**, 25, 4714.

96. Gaillion, L.; Sajot, N.; Bedioui, F.; Devynck, J.; Balkus Jr, K.J. J. Electroanal. Chem. **1993**, 345, 157.

97. Bowers, C.; Dutta, P.K. J.Catal.**1990**, 112, 271.

98. Balkus Jr, K.J.; Welch, A.A.; Gnade, B.E. Zeolites.**1990**, 19,722.

99. Kowalak, S.; Weiss R.C.; Balkus Jr, K.J. J. Chem.Soc.Chem.Commun.**1991**, 57.

100. Wilde, W.de.; Lunsford, J.H. Inorg.Chim.Acta.**1979**, 34, L229.

101. Wilde, W.de.; Peeters, G.; Lunsford, J.H. J. Phys. Chem. **1980**, 84, 2306.

102. Knops-Gerrits, P.P.; De Vos, D.E.; Thibault- Starzyk, F.; Jacobs, P.A. Nature **1994**, 369, 543.

103. Bedioui, F.; Roue, L.; Devynck, J.; Balkus Jr, K.J Stud.Surf.Sci.Catal.**1994**, 84, 917.

104. Romanovsky, B.V. in Proc.8th Int.Congr.Catal., Vol.4, Verlag Chemie, Weinheim .**1984,** 657.

105. Zakharov, V.Y.;Romanovsky, B.V. Vest.Mosk.Univ., Ser.2 Khim. **1977,** 18, 142.

106. Romanovsky, B.V.; Gabrielov, A.G. J.Mol.Catal.**1992,** 74, 293.

107. Balkus Jr, K.J.; Ferraris, J.P. J.Phys.Chem. **1990**, 94, 8019.

108. Meyer, G.; Wohrle, D.; Mohl, M.; G.Schulz-Ekloff, Zeolites .**1984,** 4, 30.

109. Ferraris, J.P.; Balkus Jr, K.J.; Schade, A. J.Incl.Phenom.**1992**, 14, 163.

110. Ziqi Jiang.; Zuwei Xi. Fenzi Cuihua 6.**1992,** 6, 467.

111. Bedioui, F.; Roue, L.; Gaillion, L.; Devynck, J.; Bell, S.L.; Balkus Jr, K.J. Preprints Div. Of Petroleum Chemistry, ACS 38. **1993**, 3, 529.

112. Balkus Jr, K.J.; Gabrielov, A.G.; Bell, S.L.; Bedioui, F.; Roue, L.; Devynck, J. Inorg. Chem. **1994,** 33, 67.

113. Vanko, G.; Homonnay, Z.; Nagy, S.; Attila Vertes.; Gabriella Pal-Borbely.; Hermann, K. Beyer. J. Chem.Soc.Chem.Commun.**1998**, 785-786.

114. Algaura, F.; Estever, M.A.; Fornes, V.; Garcia, H.; Primo, J. New. J. Chem. **1998**, 333.

115. Balkus Jr, K.J.; Felipe Diaz, J. New Journal of Chemistry, **1996,** 20, 12.

116. Parton, R.F.; Pere, G.J.; Neys, P.E.; Jacobs, P.A. Stud. Surf. Sci.Catal. **1991,** 59, 395.

117. Mansuy, D. Coord. Chem. Rev, **1993**, 125, 129.

118. Mozo, E.P.; Gabriunas, N.; Lucacioni, F.; Acosta, D.; Patrono, P.; Ginestra, A.L.; Reiz, P.; Delmon, B. J. Phys. Chem. **1993,** 97,12819.

119. Mozo, E.P.; Gabriunas, N.; Maggi, R.; Acosta, D. Reiz, P.; Delmon, B. J. Mol. Catal.**1994,** 91,251.

120. Raja, R.; Ratnaswamy, P. J. Catal. **1997,** 170, 244.

121. Seelan, S.; Sinha, A.K.; Sreenivas, D.; Sivasankar, S. J. Mol.Catal.A: Chem. **2000**, 157,103.

122. Romanovsky, B.V.; Gabrielov, A.G. J.Mol.Catal.**1992,** 74, 293.

123. Seelan, S.; Sinha, A.K. Appl.Catal.A: General. **2003,**238,201.

124. Van Der Voort, P.; Babitch, I.B.; Grobet, P.J.; Verberckmoes, A.A.; Vansant, E.F. J.Chem. Soc; Faraday.Trans; **1996**,92, 3635.

125. Landis, P.S.; Venuto, P.B. J. Catal.**1966,** 6,245.

126. Venuto P.B.; Landis, P.S. Adv.Catal **1968**, 18, 259.

127. Venuto P.B. Chem.Tech.**1971**, 215.

128. Hoelderich,W.F.; Hesse, M.; Naeumann, F. Angew. Chem. Int. Edit. Engl. **1988**, 27, 226.

129. Iwamoto, M.; Tajima, M.; Kagawa, S. J. Catal.**1986**,101, 195.

130. Katasuki, T. Coord. Chem. Rev, **1995**, 140.

131. Zhang,W.; Loebach, J.L.; Wilson, S.R.; Jacobson, E.N. J. Am. Chem. Soc. **1990**, 112,2801.

132. Zhou, P.L; Gates, B.C. J. Chem.Soc., Chem.Commun, **1989**.

133. Howe, R.F.; Lunsford, J.H. The Journal of Phys.Chem. **1975**, 79, 17.

134. Taylor, R.J.; Drago, R.S.; Hage, J.P. Inorg. Chem. **1992**,31, 253-258.

135. Parton, R.F.; Vankelecom, Ivo F.J.; Casselman, M.J.A.; Bezoukhanova, C.P.; Uytterhoeven, J.B.; Jacobs, P.A. Nature. **1994,** 370,541.

136. Herron, N. New J. Chem. **1989**, 13, 761.

137. Herron, N. Chem.Tech.Sept. **1995**, 542.

138. De Vos, D.E.; Thibault-Starzyk, F.; Knops-Gerrits, P.P.; Parton, R.F.; Jacobs, P.A. Macromol. Symp.**1994,** 80,157.

139. Gallion, L.; Sajot, N.; Bedioui, F.; Devynck, J.; Balkus Jr, K.J. J.Electroanal. Chem.**1993,** 345,157.

140. Bedioui, F.; De Boysson, E.; Devynck, J.; Balkus Jr, K.J. J. Chem.Soc., Faraday Trans.**1991,** 87,3831.

141. Herron, N. J.Coord.Chem.**1986,** 19, 25.

142. Herron, N. Inorg.Chem.**1988**, 25, 4714.

143. De Vos, D.E.; Starzyk, F.T.; Jacob, P.A. Angew Chem. Int.Engl. **1994**,33, 431.

144. Herron, N. Chem.Technol.**1989,** 9, 542.

145. Nakamura, M.; Tatsumi, T.; Tominaga, H. Bull. Chem.Soc.Jpn. **1990**,63, 3334.

146. Can, Y.W.; Wilson, R.B. Preprints Div. Of Petroleum Chemistry, ACS 33.**1988**,3,453.

147. Groves, J.T.; Nemo, T.E. J.Am.Chem.Soc.**1983,** 105,5786.

148. Herron, N.; Tolman, C.A. J.Am.Chem.Soc.**1987,** 109, 2837.

149. Vankelecom, I.F.J.; Parton, R.F.; Casselman, M.J.A.; Uytterhoeven, J.B.; Jacobs, P.A. J. Catal. **1996,** 163, 457.

150. Vankelecom, Ivo F.J. Chem.Rev, **2002,** 102, 3779.

151. Bowers, C.; Dutta, P.K. J.Catal.**1990**, 122, 271.

152. Xavier, K.O.; Chacko, J.; Mohammed Yusuff, K.K. J.Mol.Catal.**2002**, 178, 275.

153. Nakamura, M.; Tatsumi, T.; Tominaga, H. Bull.Chem.Soc.Japan; **1990**, 63, 3334.

154. Swzulbinski, W.S.; Kincaid, J.R. Inorg.Chem. **1998**,37, 5614.

155. Deshpande, S.; Srinivas, D.; Ratnasamy, P. J.Catal. **2000** 188, 261.

156. Ozin, G.A.; Caroline Gil. Chem.Rev, **1989**, 89,1749.

157. Anderson, J.R.; Boudart, M. Catalysis- Science and Technology, Springer. **1996**, 11.

158. Ratnasamy, C.; Murugkar, A.; Padhye, S. Ind. J.Chem.**1996**, 36A, I.

159. Ulagappan, N.; Krishnasamy, V. Ind. J.Chem;**1996**, 35A, 787.

160. Herron, N. Chem.Tech.Sept.**1995**, 542.

161. Knops-Gerrits, P.P.; Vos,D.de.; Thibault-Starzyk, F. Jacobs, P.A. Nature **1994**,369, 543.

162. Sykora, M.; Maruszewski, K.; Treffert-Ziemelis, S.M.; Kincaid, J.R. J. Am.Chem.Soc;**1998**, 120, 3490.

163. Sykora, M.; Kincaid, J.R. Nature.**1997**, 387, 162.

164. Meier, B.; Werner, T.; Klimat, I.; Wolfbin, O.S. Sensors and Actuators B.**1995**, 29,240.

165. Ledney, M.; Dutta, P.K. J.Am.Chem. Soc.**1995**, 117, 7687.

166. Rao, L.F.; Fukuoka, A.; Kosugi, N.; Kuroda, H.; Ichikawa, M.; Rode, B.J.; Davis, M.E.; Hanson, B.E. J.Catal.**1985**, 96, 574.

167. Iwamaoto, M.; Kagawa, S. J. Phys.Chem.**1986**, 90, 5244.

168. Bergeret, G.; Gallezot, P.; Lefebore, F. Stud.Surf.Sci.Catal.**1986**, 28, 401.

169. Sheu, L.; Knozinger, H.; Sachtler, W.H.M. Catal.Lett. **1989**, 2, 129.

170. Y-Sing, Y.; Howe, R.F. J. Chem.Soc. Faraday Trans.**1986**, 82, 2887.

171. Jacobs, P.; Gates, B.C.; Guezi, L.; Knozinger, H. Metal Clusters in Catalysis, Eds. Elsevier, Amsterdam.**1986.**

172. Zhou, P.L.; Gates, B.C. J.Chem.Soc. Chem. Commun. **1989,** 347.

173. Ozin, G.A.; Haddleton, D.M.; Gil, C.J. J.Phys. Chem. **1989,** 347.

174. Ukisu, Y.; Kazusaka, A.; Nomura, M. J.Mol.Catal.**1991**, 70, 165.

175. Maurya, M.R.; Anil, K.C.; Shri Chand. J. Mol. Catal. A. Chem. **2006,** 263, 227.

176. Joseph, T.; Sawant, D.P; Gopinath, C.S.; Halligudi, S.B.; Journal of Molecular Catalysis A: Chemical **2002,** 184, 289-299.

177. Michali, J.K.; Narayana, M.; Kevan, L. The Journal of Phys.Chem. **1984,** Vol 88, No:22.

178. Umemura, Y; Minai, Y; Tominaga. T. J.Chem.Soc, Chem. Commun, **1993.**

179. Mizuno, K.; Imamura, S.; Lunsford, J.H. Inorg.Chem.**1984,** 23,3510-3514.

180. Martell.A.E, Acc.Chem. Res.**1982,** 15,155.

181. David, L.; Cozar, O.; Sumalan, L.; Tetean, R.; Cracium, C.; Prop, N. Stud.Univ. Babes-Bolyai, Phys. **1996,** 41(1), 43.

182. Murry, K.S.; Van den Bergen, A.M.; West, B.O. Aust. J.Chem.Soc. **1978,** 31, 203.

183. Calendrazzo, F.; Floriani, C.; Henzi, R.; Epllattenier, F.L. J.Chem.Soc (A), **1969,** 1378.

184. Khan, M.M.T.; Shaikh, Z.A. Ind. J.Chem, **1992,** 31A,191.

185. Ramesh, R.; Natarajan, K. Synth. React. Inorg. Met-Org. Chem. **1996**,26, 47.

186. Khan, M.M.T.; Misra, A.S.; Rao, P.; Sreelatha, Ch. J. Mol.Catal., **1988,** 44, 107.

187. Khan, M.M.T.; Khan, N.H.; Kureshy, R.I.; Boricha, A.B.; Shaikh, A.Z. Inorg.Chim.Acta, **1990,**170, 213.

188. Ramesh, R.; Suganthy, P.K.; Natarajan, K. Synth. React. Inorg.Met-Org.Chem. **1996**,26,47.

189. Khan, M.M.T.; Srinivas, D.; Kureshy, R.I.; Khan, N.H. Inorg. Chem. **1990,** 29, 2320.

190. El-Hendawy, A.M.; El-Shahawi, M.S. Polyhedron. **1989,**8, 2813.

191. Che, C.M.; Ho, C.; Lan, T.C. J. Chem. Soc., Dalton Trans. **1991,**129.

192. Karvembu, R.; Natarajan, K. Polyhedron. **2002,** 21, 219-223.

193. Chatterjee, D.; Mitra. A.; Roy. B.C. J. Mol. Catal. **2000**, 161, 17-21.

194. Yang, H.; Alvarez, M.; Lugan, N.; Mathieu, R. J.Chem. Soc., Chem. Commun. **1995,** 1721-1722.

195. Kureshy.R.I.; Khan.N.H.; Abdi SHR. J.Mol.Cat.**1995**, 96 ,117.

196. El-Hendawy, A.M.; Alkubaisi, A.H.; El-Ghany El-Kourashy A.; Shanab M.M. Polyhedron. **1993,** 12, 2343.

197. El-Hendawy, A.M.; El-Ghany El-Kourashy, A.; Shanab, M.M. Polyhedron. **1992,** 11, 523.

198. Thornback, J.R.; Wilkinson, G. J.Chem. Soc. Dalton Trans, **1978**, 110.

199. Suss-Fink, G. Schimdt, G.F. J.Mol.Catal. **1987,**42, 361.

200. Squarez, T.; Fontal, B. ibid, **1985,** 32, 191.

201. Jenner, G.; Bitsi, G.; Schleiffer, E. ibid, **1987,**39, 233.

202. Taqui Khan, M.M.; Halligudi, S.B.; Abdi, S.H.R. J.Mol.Catal. **1988,** 44, 179, **1988,** 45, 215.

203. Taqui Khan, M.M.; Halligudi, S.B.; Shukla, S. Angew. Chem. Int.Ed.Engl. **1988,** 27,1735.

204. Leung, W.H.; Che, C.M. Inorg. Chem. **1989,** 28 ,4619.

205. Wong, W.K.; Chen, X.P.; Gao, J.P.; Chi, Y.G.; Pan, W.X.; Wang, W.Y. J.Chem.Soc.Dalton Trans. **2002,** 113.

206. Saridha, K.; Karvembu, R.; Viswanathamurthi, P.; Yasodhai, S. Synthesis and Reactivity in Inorganic, Metal- Organic and Nano- Metal Chemistry, **2005**, 35, 707.

207. Jeewoth, T.; Li Kam Wah, H.; Bhowon, M.G.; Ghoorohoo, D.; Babooram, K. Synth. React. Inorg. Met-Org. Chem. **2000,** 30, 1023.

208. Bhowon, M.G. Indian J.Chem. **2000**, 39A, 1207.

209. Chatterjeea, D.; Mitra, A.; Roy, B.C. J. Mol.Cat. **2000,** 161, 17.

210. Sharpless, K.B.; Akashi, K.; Oshima, K. Tetrahedron Lett. **1976,** 29, 2503.

211. Mukherjee, D.K.; Palit, B.K.; Saha, C.R. J. Mol.Catal. **1994,**88, 57.

212. Islam, S.M.; Bose, A.; Palit, B.K.; Saha, C.R. J.Catal. **1998**,173, 268.

213. Seddon, K.R. Coord.Chem.Rev, **1981,** 35, 41.

214. Kalyansundaram, K. Coord.Chem.Rev, **1982,** 46, 159.

215. Seddon, E.A.; Seddon, K.R. The Chemistry of Ruthenium. Elsevier, Amsterdam. **1984**.

216. Ghosh, B.K.; Chakravorthy, A. Coord. Chem. Rev, **1989**,25, 239.

217. Wong, W.T. Coord. Chem. Rev, **1994,** 131, 45.

218. Reimers, J.R.; Hush, N.S. Inorg.Chem. **1990,** 29, 3686.

219. Cogan, D.A.; Liu, G.C.; Kim, K.J.; Backes, B.J.; Ellman, J.A. J.Am. Chem. Soc. **1998,** 120, 8011-8019.

220. Liu, G.C.; Cogan, D.A.; Ellman, J.A. J. Am. Chem. Soc. **1997,** 119, 9913-9914.

221. Schrauzer, G.N. Transition Metals in Homogeneous Catalysis. Marcel Dekker Inc., New York. **1971.**

222. Suss-Fink, G.; Schimdt, G.F. J. Mol. Catal.**1987,** 42, 361.

223. Taqui Khan, M.M.; Martell, A.E. Homogeneois Catalysis by Metal Complexes, vol.I and II, Academic Press, New York.**1974**.

224. Shilov, A.E. Fundamental Research In Homogeneous Catalysis, vol.I, Gordon & Breach, New York.**1986**.

225. Taqui Khan, M.M.; Sreelatha, Ch.; Mirza, S.A.; Ramachandraiah, G.; Abdi, S.H.R. Inorg. Chim. Acta. **1988,** 154, 103.

226. Taqui Khan, M.M.; Mirza, S.A.; Prakash Rao, A.; Sreelatha, Ch. J.Mol. Catal.**1988**,44, 107.

227. Bhuiyan, A.A.; Kincaid, J.R. Inorg. Chem.**1998,** 37, 2525.

228. Sung, K.M.; Huh, S.; Jun, M.J. Polyhedron, **1999,** 18, 469.

229. Goldstein, A.S.; Beer, R.H.; Drago, R.S. J.Am. Chem. Soc. **1994**,116, 2424.

230. Quayle, W.H; Lunsford, J.H. Inorganic Chemistry. **1982,** Vol.21, No.1.

231. Dwyer, F.P.; Gyarfas, E.C. J.Am.Chem. Soc. **195,** 74, 4669.

232. Caspar, R.; Amouri, H.; Gruselle, M.; Cordier, C.; Malezieux, B.; Duval, R.; Leveque, H. Eur. J.Inorg. Chem.**2003,** 499-505.

233. Ali, Md.M.; Mac-Donnell, F.M. J.Am.Chem.Soc.**2000,** 122, 11527-11528.

234. Okamoto, K.; Matsuoka, Y.; Wakabayashi, N.; Yamagishi, A.; Hoshino, N. Chem.Commun .**2002.** 282-283.

235. Hartshorn, R.; Barton, J.K. J.Am.Chem.Soc.**1992**, 114, 5919-5925.

236. Shimidzu, T.; Iyoda, T.; Izaki, K. J.Phys.Chem.**1985,** 89, 642-645.

237. Durr, H.; Bossman, S. Acc.Chem.Res.**2001,** 34, 905-917.

238. Rudmann, H.; Shimada, S.; Rubner, M.F. J.Am.Chem.Soc.**2002**, 124, 4918-4921.

239. Buda, M.; Kalyuzhny, G.; Bard, A.J. J.Am.Chem.Soc.**2002,** 124, 6090-6098.

240. Noyori, R. J.Am.Chem.Soc.**1988,** 110, 629.

241. Kitamura, M.; Okhuma, T.; Inoue, S.; Sayo, N.; Kumobayashi, H.; Akutagawa, S.; Ohta, T.; Takaya, H.; Noyori, R. J.Am.Chem.Soc. **1988,** 110, 629.

242. Takehara, J.; Hashiguchi, S.; Fujii, A.; Inoue, S.; Ikariya, T.; Noyori, R. Chem.Commun.**1996,** 233.

243. Fujii, A.; Hashiguchi, S.; Uematsu, N.; Ikariya, T.; Noyori, R. J.Am. Chem. Soc. **1996**, 118, 2521.

244. Uematsu, N.; Fujii, A.; Hashiguchi, S.; Ikariya, T.; Noyori, R. J.Am. Chem. Soc. **1996,**118, 4916.

245. Wakamatsu, H.; Nishida, M.; Adachi, N.; Mori, M. J.Org.Chem.**2000,** 65, 3966.

246. Krompiec, S.; Pigulla, M.; Szczepankiewicz, W.; Bieg, T.; Kuznik, N.; Leszczynska- Sedja, K.; Kubichi, M.; Borowiak, T. Tetrahedron Lett. **2001,** 42, 7095.

247. Salvini, A.; Frediani, P.; Piacenti, F. J.Mol.Catal.A: Chemical **2000,**159, 185.

248. Salvini, A.; Piacenti, F.; Frediani, P.; Devescovi, A.; Caporali, M. J.Organomet. Chem. **2001**, 625, 255.

249. Dallmann, K.; Buffon, R. J.Mol.Catal.A: Chemical.**2002,** 185, 187.

250. Dallmann, K.; Buffon, R. J.Mol.Catal.A: Chemical. **2001,** 172, 81.

251. Srivastava,S. Oxid. Comm. **1992,**15 (1), 34- 42.

252. Srivastava, S.; Singh,S. J.Saudi Chem.Soc. **2003,** 415- 422.

253. Srivastava, S; Tripathi, H.; Singh, K.; Trans.Metal Chem. **2001,**26,727-729.

254. Singh, K.; Tripathi, H.; Awasthi, A.; Srivastava, S. Oxid. Comm. **2001,** 24(3), 388-392.

255. Srivastava, S; Khare, P; Singh, S; Srivastava, P. Bulletin of the Catalysis Society of India, **2008,**7, 1-11.

256. Srivastava, S; Chaudhary, L. Bulletin of the Catalysis Society of India, **2008,** 7, 20-27.

257. Chatterjee, D.; Mitra, A.; Shepherd, R.E. Inorganica Chimica Acta. **2004,** 357, 980- 990.

258. Jayabalakrishnan, C.; Karvembu, R.; Natarajan, K. Transition Metal Chemistry. **2002**, 27, 790-794.

259. Bhowon, M.G.; Nedhool, D. Synth. React. Inorg. Met. Org. Chem. **1999,** 29, 607-620.

260. Thangadurai, T.D.; Gowri, M.; Natarajan, N. Synth. React. Inorg. Met. Org. Chem. **2002**, 32 (2), 329-343.

Chapter II

MATERIALS AND METHODS

Chapter II

MATERIALS AND METHODS

2.1. INTRODUCTION

This chapter deals with the details regarding the reagents used for synthesis. It also describes the methods employed for the synthesis of ligands, metal exchanged zeolite and zeolite-encapsulated complexes. The details of the various analytical and physico-chemical methods used for the characterization of the synthesized complexes and the methods used to study the catalytic activities of the different complexes under study are also presented in this chapter.

2.2. REAGENTS

O-phenylenediamine (Loba Chemie), *p*-phenylenediamine (Loba Chemie), dimethylglyoxime (E.Merck), salicylaldehyde (E.Merck), ethylene glycol (Aldrich), semicarbazide hydrochloride(Loba Chemie), anthranilic acid (E.Merck), 4-amino-benzoic acid (E.Merck), methanol, pyridine-3-carboxaldehyde (E.Merck) and pyridine-2-carboxaldehyde (E.Merck) were used as starting materials for the preparation of ligands. The metal salt used is $RuCl_3.3H_2O$ (Loba Chemie).

All reagents used were of analytical grade unless otherwise specified. *o*-phenylenediamine and *p*-phenylenediamine were purified by the following method[1]. The diamine was dissolved in water to which activated charcoal was added. The resultant solution was boiled, filtered and allowed to cool. The crystallised diamine was dried and kept in a desiccator. The solvents used were either 99% pure or purified by standard procedures[2].

The support used is zeolite Y with a Si/Al ratio of 2.6 and surface area of 650 m^2/g obtained from Zeolyst International, Netherlands.

2.3. SYNTHESIS OF LIGANDS

2.3.1. Synthesis of salicylaldehyde semicarbazone (SSC)

To an aqueous solution of semicarbazide hydrochloride (1 g, 0.008 mole), sodium acetate (1.5 g, 0.01 mole) and salicylaldehyde (0.5 g, 0.004 mole) were added slowly with constant stirring. Then the mixture was refluxed for about two hours on a water bath. The product obtained was filtered, washed with ethanol and recrystallised from 1-propanol[3].

2.3.2. Synthesis of N,N'-bis(salicylaldimine)-*o*-phenylenediamine (SOD)

The *o*-phenylenediamine (1.08 g, 0.01 mole) dissolved in very little amount of benzene was added dropwise to the salicylaldehyde solution (2.91 cm^3, 0.02 mole) in benzene using a dropping funnel with constant stirring. The yellow solid obtained was separated by filtration and washed using ether. The ligand thus obtained was recrystallised twice from methanol and stored in vacuum in a desiccator.

2.3.3. Synthesis of N,N'-bis(salicylaldimine)- *p*-phenylenediamine (SPD)

The *p*-phenylenediamine was recrystallised twice from hot water. To an ethanolic solution of *p*-phenylenediamine (1.08 g, 0.01 mole), salicyladehyde (2.91 cm^3, 0.02 mole) was added and the resultant solution was refluxed on a water bath for about 3 hours. The bright orange solid obtained by this technique was recrystallised twice from methanol and kept dry over anhydrous calcium chloride in a desiccator.

2.3.4. Purification of anthranilic acid (AA)

Anthranilic acid was purified by dissolving very small portions in methanol and allowing them to form crystals. The crystals thus obtained were again recrystallised using the same solvent and stored over anhydrous calcium chloride.

2.3.5. Purification of 4 –aminobenzoic acid (ABA)

Similar procedure was employed for obtaining pure 4–aminobenzoic acid crystals. The solid crystals obtained after recrystallization from methanol were placed in a desiccator over anhydrous calcium chloride.

2.3.6. Purification of dimethylglyoxime (DMG)

The purification of dimethylglyoxime was done by recrystallising them from methanol. The pure crystals of DMG obtained were dried over anhydrous calcium chloride.

2.3.7. Synthesis of N,N'–bis(3-pyridylidene)–1,2–phenylenediamine (PCO)

The starting materials required for the synthesis of this ligand are pyridine – 3 – carboxaldehyde and *o*-phenylenediamine. The diamine purchased as such cannot be used for this preparation. It can be used only after recrystallisation as described earlier. Recrystallised *o*-phenylenediamine (1.08 g, 0.01 mole) was refluxed with ethanolic solution of pyridine–3-carboxaldehyde (2.14 g, 0.02 mole) for about five hours. The reaction mixture was then filtered to get yellow crystals of the ligand. It was washed several times with benzene, recrystallised from ethanol and dried in vacuum over anhydrous calcium chloride in a desiccator.

2.3.8. Synthesis of N,N'–bis(3–pyridylidene)–1,4–phenylenediamine (PCP)

An ethanolic solution of pyridine-3-carboxaldehyde (2.14 g, 0.02 mole) and *p*-phenylenediamine (1.08 g, 0.01 mole) were allowed to reflux on a water bath for five hours to get the product. The yellow solid formed was filtered, washed several times with benzene and recrystallised from ethanol. Then it was dried in vacuum over anhydrous calcium chloride.

2.3.9. Synthesis of N,N'–bis(2–pyridylidene)– 1,2–phenylenediamine (CPO)

Pyridine-2-carboxaldehyde (2.14 g, 0.02 mole) in ethanol was taken in a roundbottom flask. Recrystallised *o*-phenylenediamine (1.08 g, 0.01 mole) was added to this with stirring. The reaction mixture was boiled under reflux on a water bath for five hours. The product formed was obtained by filtration. Yellow crystals of CPO were washed with benzene, recrystallised twice from ethanol and dried in vacuum over anhydrous calcium chloride.

2.3.10. Synthesis of N,N'–bis(2–pyridylidene)–1,4–phenylenediamine (CPP)

The ligand N,N'–bis(2–pyridylidene)–1,4–phenelenediamine (CPP) was synthesized by a procedure similar to that of CPO. The mixture of recrystallized *p*-phenylenediamine (1.08 g, 0.01 mole) and pyridine-2-carboxaldehyde (2.14 g, 0.02 mole) in ethanol was refluxed on a water bath for five hours. The crystals separated were collected, washed with benzene and recrystallised from ethanol to get the pure ligand.

2.4. SUPPORTS USED

The zeolite- Y used for encapsulation was modified by the following techniques.

2.4.1. Preparation of sodium exchanged zeolite (NaY)

The zeolite-Y obtained was modified using the standard ion exchange procedure which is based on the method suggested by Edward *et al.*[4]. Zeolite-Y (5 g) was mixed with a solution of NaCl (0.1 M, 500 ml) and stirred for 24 hours at room temperature to remove any extra ions present by converting them into Na^+ ions. The solution was then filtered to get sodium-exchanged form of the zeolite, which was made chloride free by washing with distilled water till the filtrate becomes free of chloride ions. The NaY thus formed was dried at 100°C for two hours.

2.4.2. Preparation of metal exchanged zeolite (RuY)

The sodium ions in NaY were replaced by transition metal ions by stirring sodium-exchanged zeolite (5 g) with metal chloride solution (0.001 M) at 90°C for 24 hours. It should be noted that low concentration of metal salt solution was used since there are chances for dealumination at higher concentrations[5]. The slurry obtained after the stipulated time was filtered and washed with distilled water several times to make it free from anions. It was then dried in a Muffle furnace at 450°C for four hours[6].

2.4.3. Preparation of zeolite encapsulated metal complexes

Transition metal cations exchanged into zeolite-Y are capable of forming well-defined complexes with certain ligands within the large cavities of the zeolite

framework[7]. The three-dimensional pore structure of zeolites offer the possibility for the preparation of complexes inside the zeolite which are otherwise unstable in solution. This trapping is usually described as making a 'ship-in-a-bottle' complex. The zeolites with the aid of their unique ligating and solvating properties stabilize the transition metal complexes. The stabilization can be achieved by anchoring of the complexes to the zeolite lattice by coordination to framework oxygens[8]. The encapsulated metal complexes were prepared using the flexible ligand method where flexible ligand molecules enter the supercages of the zeolite and react with the metal ions already present in the cage. This method generally involves two kinds of encapsulation.

2.4.3.1. Encapsulation by heating in a sealed ampule

This method involves the mixing of the metal exchanged zeolite (2 g) with excess of the ligand and heating the mixture in a closed glass ampule at an optimum temperature in a Muffle furnace for a definite period of time. During this process, the ligand molecules diffuse into the metal exchanged zeolite uniformly and hence complex formation occurs. The advantage is that the large size of the complex prevents its diffusion out of the zeolite structure. The complex formed was soxhlet extracted with suitable solvents to remove unreacted ligands and surface species. The process of soxhlet extraction was continued till the extracting solvent became colourless. The uncomplexed metal ions in the zeolite were removed by back exchange with NaCl solution (0.01 M, 250 ml) for 24 hours. It was then filtered, washed with distilled water to make it free of chloride ions and finally dried at 100°C for two hours[9]. The prepared complex was stored in vacuum over anhydrous calcium chloride.

2.4.3.2. Encapsulation by refluxing the metal exchanged zeolite with the ligand

The metal exchanged zeolite MY (5 g) was added to a solution of the ligand in a suitable solvent and this mixture was refluxed for 24 hours on a water bath. As heating progresses, the ligand molecules enter the zeolite pores and undergo complexation with the metal ions already present there.

The encapsulated complex was purified by soxhlet extraction with suitable solvents for the removal of the surface species. It was then stirred with sodium chloride

solution (0.01 M, 250 ml) to remove any uncomplexed metal ions present in the zeolite. Then it was filtered, made free of chloride ions by washing with distilled water. The zeolite-encapsulated complex thus obtained was stored in vacuum over anhydrous calcium chloride after drying at 100°C for two hours. Further details with regard to the synthesis of encapsulated complexes are given in the respective chapters.

2.5. REAGENTS FOR CATALYTIC ACTIVITY STUDIES

Phenol (Merck), cyclohexanol (Merck), hydrogen peroxide (30% aqueous solution, E.Merck) and tert-butyl hydroperoxide (Merck, 70%) were used for catalytic studies. The solvents used for these studies were either of 99% purity or purified by known laboratory procedures. The experimental setup and the results of these catalytic studies are presented in the relevant chapters.

2.6. CHARACTERIZATION METHODS

The synthesis of the transition metal complexes inside the zeolite pores pose many important questions regarding their stability, retention of the zeolite framework, extent of encapsulation etc. In order to get a correct picture of the distribution of the metal complex within the zeolite framework and a clear understanding of the extent to which encapsulation has taken place, various analytical and physico-chemical techniques have been employed. The details of these techniques are presented in this chapter.

2.6.1. Elemental analysis

2.6.1.1. CHN analysis

Microanalysis for carbon, hydrogen and nitrogen in the synthesized ligands, neat complexes and encapsulated complexes were done on an Elementar model Vario EL III at SAIF, Sophisticated Test and Instrumentation Centre, Kochi. These results give an idea about the composition of the ligands and complexes and provide a method to determine the presence of uncomplexed metal ions in the lattice structure.

2.6.1.2. Analysis of Si, Al, Na and transition metal ion in the zeolite sample

A small amount of the zeolite sample was accurately weighed (w) and taken in a beaker. About 40ml of conc.H_2SO_4 was added and heated strongly. It was then cooled, diluted with water (200 ml) and filtered using an ashless filter paper. The filtrate was collected in a standard flask. The residue was heated in a platinum crucible, cooled and weighed (w_1). Hydrofluoric acid was then added in drops and heated strongly to dryness to remove silica as H_2SiF_6. This process was repeated three to four times. The remaining solid was then ignited to 800°C for about 1 hour, cooled and weighed (w_2). The amount of silica present in the sample can be calculated using the equation:

$$\% SiO_2 = (w_1 - w_2) \times 100 / w$$

The residue in the crucible was treated with potassium persulphate and fused till a clear melt was obtained. It was dissolved in water and combined with the earlier filtrate collected in the standard flask. The metals present in this solution were determined by ICP- AES method. The Si to Al ratio provides the unit cell formula and the ion exchange capacity of the zeolite. The comparison of the ratio of the encapsulated complexes with that of the pure zeolite shows the retention of the zeolite framework after encapsulation.

2.6.2. Surface area and pore volume analysis

The surface areas of the synthesized complexes were measured to ensure whether encapsulation of metal complexes had occurred and the knowledge of surface area values provide important applications in catalytic studies. The surface areas of the samples were determined by the multipoint BET method[10] of nitrogen adsorption at liquid nitrogen temperature using 'Micromeritics Gemini 2360 surface area analyzer'. This method involves the measurement of the amount of gas adsorbed by the respective samples. Initially a very small amount of the sample is accurately weighed and taken in a clean dry sample tube. This was heated to about 473 K and kept at this temperature for about 3 hours in an atmosphere of nitrogen gas. The volatile impurities on the surface of the catalyst were completely removed by the heat treatment. Then the sample was allowed to cool to room temperature and again the sample tube containing the

complex was weighed. The sample was kept fixed in the instrument and cooled to very low temperature of about 77 K using liquid nitrogen. The adsorption of nitrogen on the surface of the sample lowers the pressure inside the chamber and equilibrium is established between the adsorbed gas and the free gas phase. The BET equation used for calculating the surface area is

$P / V (P_0 - P) = 1 / V_m C + (C-1) P / V_m C P_0$ where

V = volume of the gas adsorbed at relative pressure P/P_0

V_m = volume of the gas in the monolayer

P_0 = saturation vapour pressure of the adsorbate

C = BET constant which is related to the heat of adsorption

The plot of the left side of the BET equation against P/ P_0 gives a straight line with slope $(C-1) / V_m C$ and intercept $1 / V_m C$. The volume of gas in the monolayer, V_m can be obtained from these values and hence the number of moles of nitrogen adsorbed (X_m) can be calculated. BET surface area is calculated using the equation, $S_{BET} = X_m N A_m 10^{-20}$ where N = Avogadro number and A_m = cross sectional area of the adsorbate molecule. The equation used for calculating the total pore volume of the sample is $V_{tot} = V.D$ where D = density conversion factor.

2.6.3. X-ray diffraction analysis

The X-ray diffraction patterns of the parent zeolite, ion exchanged zeolite and encapsulated complexes were recorded to know their crystalline nature. The comparisons of these diffraction patterns enable us to tell whether any changes occur in the internal crystalline structure of the zeolite upon encapsulation[11]. The X-ray diffractometer used to study the sample is Bruker AXSD8 advance diffractometer. The apparatus consists of a stationary X-ray source, Ni filtered radiation with wavelength 1.5404 Å and a movable detector to scan the intensity of the diffracted radiation as a function of the angle 2θ between the incident and the diffracted beam.

2.6.4. Thermogravimetric analysis

Thermogravimetric analysis is an effective tool to study the nature of decomposition of the metal complexes. In this technique, the sample under consideration is heated at a controlled rate in an atmosphere of nitrogen and the weight loss of the substance is recorded as a function of temperature. The major advantage of this method is that it can directly give an idea about the thermal stability of a material. The thermograms obtained are characteristic for a given sample due to the unique sequence of physico-chemical reactions occurring over definite temperature ranges, which in turn depends upon the structure of the molecule[12]. The changes in weight occur as a result of the rupture or formation of various physical and chemical bonds at elevated temperatures. This may lead to the evolution of volatile products or the formation of heavier reaction products. TG analyses were carried out on a Perkin Elmer, Diamond TG/DSC at a heating rate of 10°C per minute in an atmosphere of nitrogen.

2.6.5. SEM analysis

Scanning electron microscopy analysis of the zeolite encapsulated complexes before and after soxhlet extraction was done using JEOL-JSM-840A SEM. It reveals the presence of materials adsorbed on the surface of the support and the morphological changes associated with encapsulation. A narrow beam of electrons from a tungsten filament is passed through the sample. In order to protect the zeolite sample from surface charging and thermal damage due to collision with electron beam, a thin film of gold is coated over them. The amount of back-scattered or secondary radiation is noted as a function of the primary beam. The major advantage of this method is its ability to give a picture of the effectiveness of soxhlet extraction in removing the substances adsorbed on the surface.

2.6.6 Infrared spectra

The IR spectra provide valuable information regarding the structure of the complex and the nature of the functional groups present. Hence it can be used as an effective tool to confirm the formation of the complexes within the zeolite pores and to

detect the coordination of ligands to the transition metals. Infrared spectra of the ligands, simple complexes and the metal encapsulated complexes in the region 4000-400 cm^{-1} were recorded using Shimadzu 8000 Fourier Transform Infrared Spectrophotometer. Each zeolite encapsulated complex exhibits a characteristic IR pattern[13] and these vibrations are observed in the region 1250-400 cm^{-1}. The shift of characteristic bands on chelation is sometimes masked by the well-defined strong bands of zeolite.

2.6.7. Electronic spectra

The diffuse reflectance spectra were recorded at room temperature in the range 250-850 nm using Ocean Optics, Inc.SD 2000, Fiber Optic Spectrometer with a charged coupled device (CCD) detector. Sodium exchanged zeolite, NaY is used as the blank for zeolite samples. The spectra were computer processed and plotted as percentage reflectance versus wavelength. To get the spectra in the absorbance mode, one has to apply Kubelka- Munk equation, which is as follows.

$$\log \left((1 - r_\alpha)^2 / 2r_\alpha \right) = \log k - \log S$$

Here $r_\alpha = R_\alpha$ (sample) / R_α(standard)

R_α (sample) is the diffuse reflectance of the sample and R_α (standard) is taken as 1. K is the absorption coefficient and S is the scattering coefficient. The Kubelka-Munk factor, $F(R) = (1- r_\alpha)^2/2r_\alpha = K/S$. The plot of $(1-r_\alpha)^2/2r_\alpha$ as a function of wavelength gives the absorption curve.

2.6.8. EPR spectra

The EPR spectra of the powdered zeolite encapsulated complexes in DMF were recorded at liquid nitrogen temperature and the standard used was tetracyanoethylene (TCNE) with g value of free electron = 2.0027. The EPR spectra of transition metal complexes contain a wealth of information about their electronic structures. The degeneracy of the d orbitals and the presence of the unpaired electrons give rise to orbital contributions as a result of which anisotropic g values are obtained.

2.7. CATALYTIC STUDIES

2.7.1. Gas Chromatography

The analysis of the reactants and products of the different catalytic reactions was conducted using a Chemito 8510 Gas Chromatograph. The various components in the reaction mixture were separated using an SE-30 column. The peaks appearing on the recorder are characteristic of the different components and the peak area is found to be proportional to the amount of the component present in the mixture.

References

1. Perrin, D.D.; Armarego, W.L.F.; Perrin, D.R. Purification of Laboratory Chemicals, 2nd Edn. Pergamon Press, New York, **1980**.
2. Furniss, B.S.; Hannaford, A.J.; Smith, P.W.G.; Tatchell, A.R. Vogels' Text Book of Practical Organic Chemistry- 5th edition –ELBS- Longman Singapore Publishers, **1996**.
3. Patole, J.; Dutta, S.; Padhye, S.; Sinn, E. Inorganic Chimica Acta, **2001**, 318, 207.
4. Yonemoto, E.H.; Kim, Y.II.; Schmehl, R.H.; Wallin, J.O.; Shoulders, B.A; Richardson, B.R.; Haw, J.F.; Mallouk, T.E. J.Am. Chem. Soc. **1994**, 116, 10537.
5. Menon,P.G. Lectures on Catalysis, 41st Ann. Meeting, Ind. Acad. Sci., Ramasheshan S. (Ed.), **1975**.
6. Taylor, R.J.; Drago, R.S., George, J.E. J.Am. Chem. Soc.**1989**, 111, 6610.
7. Howe, R.F.; Lunsford, J.H. The Journal of Physical Chemistry, **1975**, 79, 17.
8. Vansant, E.F.; Lunsford, J.H. J. Chem. Soc. Faraday Trans. **1973**, 19, 1028.
9. Ulagappan, N.; Krishnasamy, V. Ind. J. Chem. **1996**, 35 A 787.
10. Brunauer, S.; Emmett, P.H.; Teller, E. J. Am. Chem. Soc. **1938**, 60, 309.
11. Paez-Mozo E; Gabriunas, N.; Lucaccioni, F.; Acosta, D.D.; Patrono, P; Loginestra, A.; Ruiz, P.; Delmon, B. J. Phys. Chem. **1993**, 97,12819.
12. Textbook of Quantitative Analysis- Jeffery et al.
13. Breck, D.W. Zeolite Molecular Sieves Structure Chemistry and Use, Wiley Interscience Publications, **1973**, Vol.1.

Chapter III

ZEOLITE ENCAPSULATED RUTHENIUM COMPLEXES OF THE SCHIFF BASES DERIVED FROM SALICYLALDEHYDE

Chapter **III**

ZEOLITE-Y ENCAPSULATED RUTHENIUM COMPLEXES OF THE SCHIFF BASES DERIVED FROM SALICYLALDEHYDE

3.1. INTRODUCTION

Transition metal complexes of Schiff bases derived from salicylaldehyde act as biomimetic catalysts for oxygen atom transfer[1], as catalysts for enantioselective epoxidations[2] and aziridinations[3], as catalysts for mediating organic redox reactions[4] and as mediators for other oxidative processes[5]. The Schiff bases have interesting structural properties[6]. Salen ligands are capable of supporting metals in a variety of oxidation states and there are large possibilities for the oxidation of the metal or the ligand. It is therefore important to understand the fundamental oxidation chemistry of salen metal complexes.

The heterogenisation of Schiff base complexes derived from salicylaldehyde find wide applications for various reactions like selective oxidation[7], carboxylation, decarboxylation[8], cyclisation, amination, isomerisation and rearrangement[9, 10] of different compounds. The complexes of salicylaldehyde semicarbazone with copper are found to show superoxide activity. They are also found to possess antifungal, antibacterial[11,12], anti-inflammatory, antitumour, antileukaemic and other such related properties[13].

Co(salen) complexes encapsulated in zeolite-Y form stable dioxygen adducts thereby mimicking haemoglobin. The Schiff base complexes of N,N'-ethylenebis (salicylidenaminate) and N,N'-o-phenylenebis(salicylidenaminate) have been extensively used as functional mimics of metalloproteins in dioxygen binding and oxidation of olefins and aromatic compounds using H_2O_2, iodosyl benzene and NaOCl. The key factor for the biomimetic activity is their flexible nature and ability to adopt a variety of geometries to generate active sites for the various oxidation reactions[14, 15]. It have been reported that encapsulated Co(salophen) complexes act as efficient oxygen activators in the Pd-catalysed aerobic oxidation of 1,3-cyclohexadiene to 1,4- diacetoxy-

2-cyclohexene[16-18]. VO(saloph) complexes (where saloph = bis(salicylaldehyde) -*o*-phenylenediimine) encapsulated in zeolite-Y by flexible ligand synthesis exhibited high catalytic activity and selectivity in the epoxidation of trans-stilbene and styrene[19]. The higher activity may be due to the relaxed geometry of VO(saloph) and the easy access of the active site to the substrate molecules.

The kinetics of the reductive carbonylation of nitrobenzene in ethanol yielding phenylurethane as the single product was investigated in the presence of the catalyst [Ru(saloph)Cl_2][20]. The same complex was used to perform the kinetic study of hydroformylation of 1-hexene, cyclohexene and cyclooctene in ethanolic medium[21]. Ru(III)Saloph-Y and Co(II)Saloph-Y were tested in the allylic oxidation of α-pinene to its oxygenated products and the ruthenium complex was found to be more active than the cobalt analogue[22]. The catalytic studies conducted by Halligudi *et al.* have found that [Ru(saloph)Cl_2] showed good activity in oxidative carbonylation of cyclohexylamine to give cyclohexylurethane with a turnover rate of 30 mol product per mol catalyst per hour[23].

The Schiff base in the equatorial position of the octahedral complex [Ru(SOD)Cl_2] (where SOD=N,N'-bis(salicylaldimine)-*o*-phenylenediamine) contain two nitrogen and two oxygen atoms. The presence of labile trans chlorides in the coordination sphere of the metal ion is indicated by its higher catalytic activity involving replacement of chloride ions, which provide vacant coordination sites for coordination to the metal ion[24].

The semicarbazones act as a bidentate or tridentate ligand depending on the aldehyde residue attached to the semicarbazide moiety. The stability of such type of complexes is greatly enhanced by the coordination of oxygen atom to the transition metal ion. The metal complexes derived from semicarbazones are widely studied due to their activity against influenza[25], protozoa[26], small pox[27], viral diseases and certain kinds of tumours[28] and due to their wide use as pesticides[29] and fungicides[30]. Semicarbazones constitute a special class of azomethines that act as ionic or neutral moieties[31]. The chemistry of semicarbazone complexes is very interesting as the α-N atom of the Schiff base remains uncoordinated and only the β-N coordinates to the

metal complexes. All these distinctive features of semicarbazone complexes have made it worthwhile to encapsulate the metal complexes of semicarbazones inside the zeolite framework and to study their structural and catalytic properties. The encapsulated complexes derived from the Schiff base salicylaldehyde semicarbazone, have got wide applications and many simple complexes of SSC are already reported[32].

The structure and biocidal activity of various semicarbazone complexes of transition metals have been widely studied; but very few reports are available on ruthenium complexes[3-37]. Ruthenium carbonyl complexes with salicylaldehyde semicarbazone and thiosemicarbazone have been prepared and characterised[38]. The IR spectral data of these complexes suggest that the ligand SSC is binegative and tridentate and that the coordination sites are β-nitrogen, carbonyl oxygen and O of phenolic OH after deprotonation. There are no chances of coordination through α-nitrogen due to considerable strain[39]. The absorptions attributed to ν_{sym} and ν_{asy} of the NH_2 group in the spectrum of the free ligand remain unaltered in the metal complexes confirming the noninvolvement of the terminal NH_2 group in coordination. The prominent band due to secondary ν_{NH} in the ligand disappeared in the spectrum of the complex, which indicates the deprotonation of the ligand prior to coordination through the secondary –NH group. A strong band assigned to phenolic ν_{C-O} stretching in the free Schiff base undergoes shift to higher frequency on complexation indicating that additional coordination is through phenolic oxygen. The analytical and spectral data have proposed an octahedral structure for the ruthenium complex of SSC.

A search through the literature reveals that zeolite-Y encapsulated ruthenium complexes of SSC, SOD and SPD have not yet been studied. In view of these aspects, zeolite encapsulated ruthenium complexes of the Schiff bases SSC, SOD and SPD have been synthesized and characterized. The results of these studies are presented in this chapter. The structures of the ligands SSC, SOD and SPD are given in figures 3.1, 3.2 and 3.3. respectively.

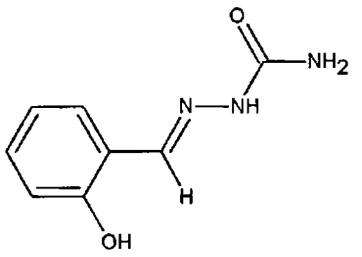

Figure 3.1. Structure of salicylaldehyde semicarbazone (SSC)

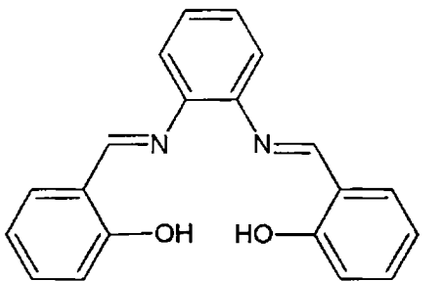

Figure 3.2. Structure of N,N'-bis(salicylaldimine)-*o*-phenylenediamine (SOD)

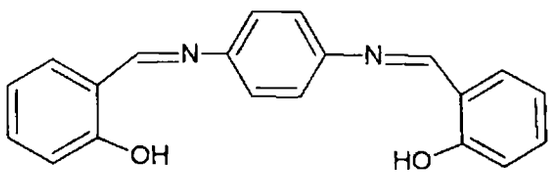

Figure 3.3. Structure of N,N'-bis(salicylaldimine)-*p*-phenylenediamine (SPD)

3.2. EXPERIMENTAL

The details concerned with the synthesis of the ligands SSC, SOD, SPD and the metal exchanged zeolite are presented in chapter II.

3.2.1. Synthesis of zeolite encapsulated ruthenium complexes of salicylaldehyde semicarbazone (RuYSSC)

The zeolite encapsulated ruthenium complex of the Schiff base SSC was prepared from the ruthenium-exchanged zeolite using the flexible ligand method. The ligand salicylaldehyde semicarbazone was mixed thoroughly with the ruthenium-exchanged zeolite RuY (5 g) in the ligand to metal ratio 1:1. It is desirable to use a slight excess of the ligand to ensure maximum complexation. Then the above mixture

is heated at 200°C for 6 hours in a sealed glass ampule. This enables the diffusion of the ligand into the supercages of the zeolite to form the encapsulated complex. The unreacted ligand and surface species present are removed by soxhlet extraction of the material first with methanol and then with chloroform. The uncomplexed metal ions in the zeolite and ionisable portions of the ligand were removed by ion exchange with NaCl solution (0.01 M, 500 ml) for 24 hours. It was filtered, washed free of chloride ions and finally dried at 100°C for two hours and the RuYSSC thus obtained was stored in vacuum over anhydrous calcium chloride.

3.2.2. Synthesis of zeolite encapsulated ruthenium complexes of N,N'-bis(salicylaldimine)-*o*-phenylenediamine(RuYSOD) and N,N'-bis(salicylaldimine)-*p*-phenylenediamine (RuYSPD)

The encapsulation of ruthenium complexes of N,N'-bis(salicylaldimine)-*o*-phenylenediamine and N,N'-bis(salicylaldimine)-*p*-phenylenediamine were also achieved by flexible ligand method[40-44]. The metal exchanged zeolite RuY (5 g) was added to the ligand SOD dissolved in methanol (50 ml). The concentration of the ligand was adjusted in such a way to obtain 1:1 ligand to metal ratio. The mixture was refluxed on a water bath for about 12 hours. The penetration of the ligand molecules through the zeolite pores result in the formation of large metal complexes inside the framework. The product formed was then filtered and soxhlet extracted with methanol and dichloromethane for several days till the extract became colorless. This ensures the complete removal of the surface species. The complex was then back exchanged with NaCl solution (0.01 M, 250 ml) for 24 hours to replace all uncomplexed metal ions with sodium ions, then repeatedly washed with distilled water to make the complex chloride free and dried in vacuum. The resulting encapsulated complex denoted by RuYSOD was stored in vacuum over anhydrous calcium chloride. The complex RuYSPD was also prepared according to the similar procedure.

3.3. CHARACTERIZATION

The details regarding the techniques used for characterization are presented in chapter II.

3.4. RESULTS AND DISCUSSION

3.4.1. Chemical analysis

The analytical data of the sodium exchanged zeolite-Y and ruthenium exchanged zeolite-Y are given below in table 3.1. The amount of silica, alumina and Si/Al ratio are very decisive in determining the stability and crystallinity of the resulting complexes.

Table 3.1. Analytical data of metal exchanged zeolites

Zeolite Sample	% Si	% Al	% Na	% Metal
NaY	20.84	8.02	9.32	
RuY	20.72	7.85	7.20	1.98

The Si to Al ratio of NaY is found to be 2.6 which corresponds to a unit cell formula $Na_{54}(AlO_2)_{54}(SiO_2)_{138}.nH_2O$[45]. This ratio is retained even after the metal exchange, which confirms that dealumination has not occurred during the exchange reaction. This proves beyond doubt that the zeolite framework is unaltered by encapsulation. The retention of Si to Al ratio was observed in earlier studies also[46, 47].

In the preparation of metal exchanged zeolite, very dilute solutions of metal ions are used, as high concentration of metal chloride may result in dealumination and destruction of the framework[48]. If x represent the fraction of Ru^{3+} ions exchanged with Na^+ ions in the zeolite, then the equation representing the ion exchange is

$$Na_{54}Y + x\,M^{3+} \rightarrow M_xNa_{54-3x}Y + 3x\,Na^+$$

The degree of ion exchange and the unit cell formula of the metal exchanged zeolite can be calculated from the obtained data. The percentage of metal in RuY gives the unit cell formula of ruthenium-exchanged zeolite as $Na_{43.14}\,Ru_{3.62}\,(SiO_2)_{138}(AlO_2)_{54}.\,nH_2O$.

The unit cell formula is a representation of the composition of a unit cell in the metal exchanged zeolites. The degree of ion exchange for RuY is 20.11%.

3.4.2. Elemental analysis

The analytical data of the encapsulated complexes are given in table 3.2.

Table 3.2. Analytical data of the encapsulated complexes RuYSSC, RuYSOD and RuYSPD

Compound	Colour	Elements % found (% calculated)						
		% Si	% Al	%Na	%M	% C	% H	% N
SSC	Greenish Yellow					53.18 (53.63)	4.98 (5.06)	23.16 (23.45)
RuYSSC	Bright Green	20.36	7.83	6.32	0.6	1.26	2.99	0.097
SOD	Yellow					75.63 (75.93)	4.83 (5.10)	8.83 (8.86)
RuySOD	Grey	20.66	7.93	6.99	0.82	1.47	2.96	0.17
SPD	Bright Orange					75.52 (75.93)	5.16 (5.10)	8.65 (8.86)
RuYSPD	Dark Grey	20.62	7.88	6.56	0.78	1.43	2.76	0.16

In all the complexes, the Si/Al ratio is found to be 2.6, which is an indication of the retention of the zeolite framework without any damage after complex formation. The analytical data of the encapsulated complexes shows that the percentage of metal is slightly in excess of what is required for the formation of 1: 2 complexes. This may be due to the presence of uncomplexed metal ions in the zeolite cages even after back exchange. The uncomplexed metal ions present are usually removed during back exchange with NaCl solution. But in some cases excess concentration of metal ions may result due to the occupation of more than one metal ion in the same cage of the zeolite. There are chances for the complex formed or trapped ions to hinder the

approach of further ligands and prevent further complex formation with other metal ions.

The percentages of carbon, hydrogen and nitrogen indicate the encapsulation of complexes in the zeolite cages. The amount of carbon present gives only a qualitative idea about the entrapment of the complexes. The entrapment of complexes within the zeolite pores can be clearly understood on knowing the position of metal ions in the zeolite Y. The different metal ions have preference for specific sites in the structure. The dehydration of MY results in the removal of water molecules coordinated to it and there are chances for the lattice oxygen to occupy the vacant coordination sites. The rehydration of the modified zeoliteY is followed by a back migration of the cation towards the zeolite framework. Thus the metal ions in a zeolite are in a dynamic system that involves the migration of metal for coordination. The presence of large ligands makes it difficult for them to enter the small cages and then the most probable site for complex formation is the supercage. Hence there is the migration of metal ions to the supercages for complexation. The metal- oxygen bonds in the lattice are broken during this process in which the complexes are formed and there are chances for the formation of new bonds with the ligands[49-53].

3.4.3. Surface area and pore volume

The surface area and pore volume of zeolite-Y, sodium exchanged zeolite (NaY), ruthenium exchanged zeolite (RuY) and the encapsulated complexes RuYSSC, RuYSOD and RuYSPD are determined by BET method and the results are presented in table 3.3.

Table 3.3. Surface area and Pore volume values

Sample	Surface area (m^2/g)	Pore volume (cc/g)
Zeolite Y	799	0.40
NaY	692	0.34
RuY	682	0.35
RuySSC	435	0.22
RuYSOD	380	0.21
RuYSPD	365	0.20

There is not much difference in the surface area of NaY and RuY whereas there is a significant decrease in surface area upon encapsulation of complexes[54]. There is a decrease of 36.22% for RuYSSC and decrease of 44.28% and 46.48% for the SOD and SPD complexes respectively. The surface area of zeolite is mainly internal surface area and the blocking of pores due to complex formation results in a decrease in surface area[55]. The decrease in surface area is a clear indication of the formation of complexes within the zeolite cages[56]. The lowering of surface area and pore volume with encapsulation has been reported earlier[57].

3.4.4. X-ray diffraction patterns

XRD patterns obtained for NaY, RuY and the encapsulated complexes RuYSSC, RuYSOD and RuYSPD are given in the figure 3.4. The comparison of these patterns show that the XRD patterns of the encapsulated complexes exactly match with that of the metal exchanged zeolite and NaY. This is a strong evidence for the fact that the zeolite framework remains intact on encapsulation[58].

The characterization by diffraction technique is very important as it provides valuable information on crystallinity and changes in unit cell parameters occurring during encapsulation[59-61]. Similarity in diffraction patterns of RuY and encapsulated complexes suggests that the reduction in surface area is not due to the breakage of crystalline structure of the zeolite but due to encapsulation of complexes within the super cages of the zeolite.

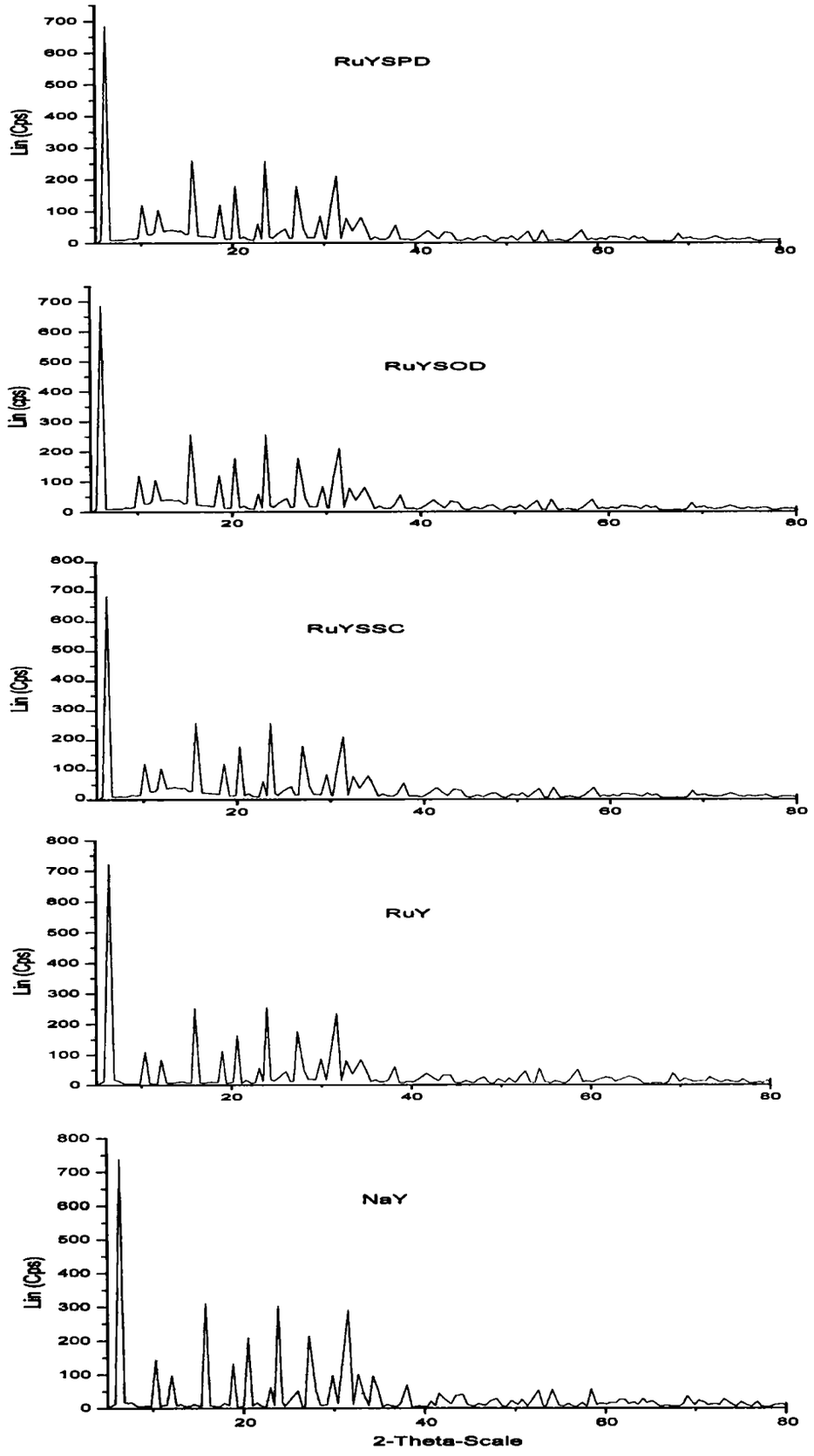

Figure 3.4. XRD spectra of (i) NaY (ii) RuY (iii) RuYSSC (iv) RuYSOD (v) RuYSPD

3.4.5. SEM analysis

Scanning electron micrographs of the zeolite encapsulated complexes before and after soxhlet extraction are depicted in figures 3.5 and 3.6. In the micrographs taken before soxhlet extraction aggregates of species are visible on the surface but in the micrographs taken after soxhlet extraction the surface appears to be clean. This shows that soxhlet extraction with a suitable solvent can be successfully employed for removing the surface species present. During the soxhlet extraction procedures, the extraction is done for a longer period of time so that well-defined crystals of complexes formed should be free from any tint of ions present on the external surface. Clear zeolite surfaces are reported in the case of phthalocyanine and salen complexes[62, 63].

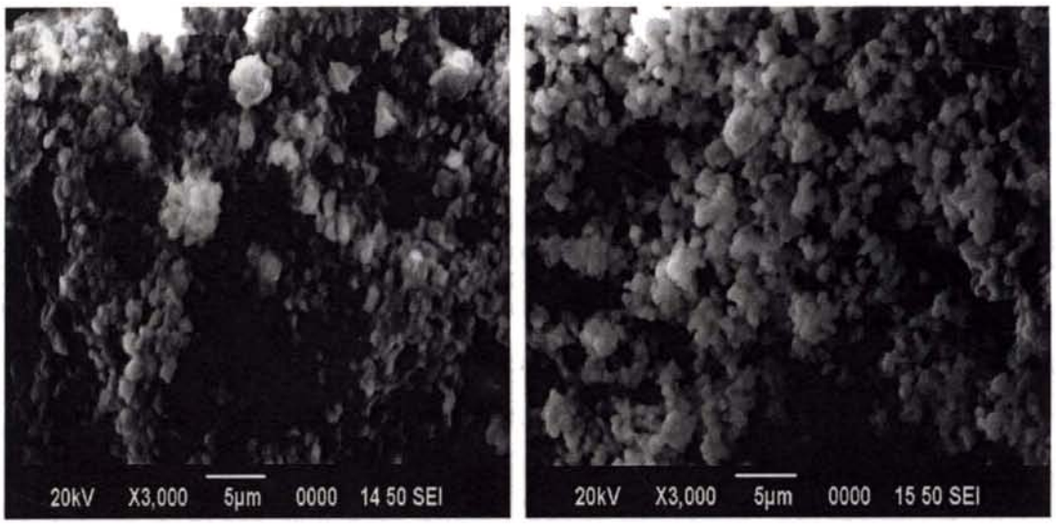

(i) (ii)

Figure 3.5. Scanning electron micrographs of RuYSSC (i) before and (ii) after soxhlet extraction

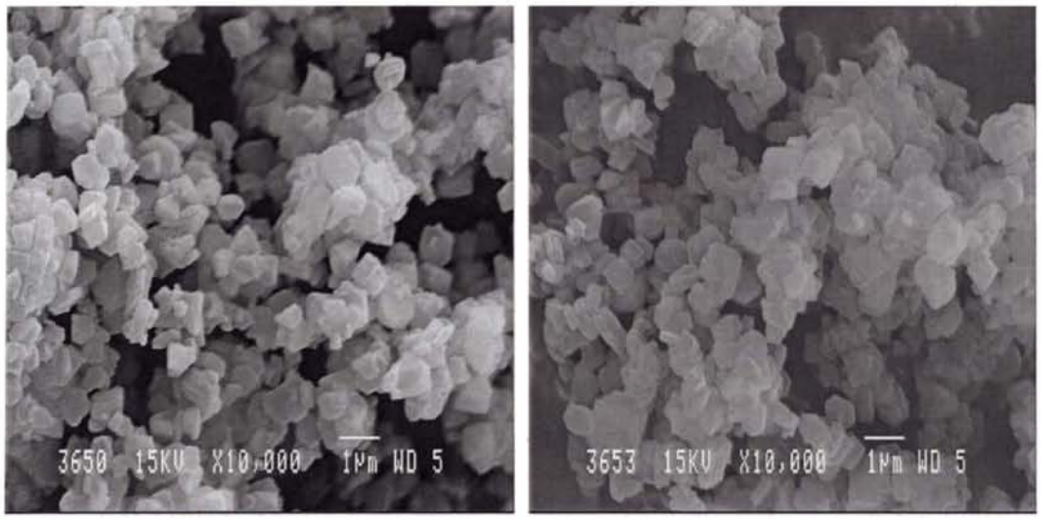

(i) (ii)

Figure 3.6. Scanning electron micrographs of RuYSOD (i) before and (ii) after soxhlet extraction

3.4.6. TG analysis

The thermal behaviour of the zeolite samples were studied and their TG/DTG and TG/DSC curves were recorded at a heating rate of 10°C per minute up to 1100°C in an atmosphere of nitrogen. The corresponding changes in weight occur due to the rupture or formation of chemical bonds on raising the temperature or due to the removal of volatile products[64]. There are many reports about the thermal behavior of simple complexes of RuYSSC studied by Petrovic and co-workers[65]. The thermal stability of heterogeneous complexes is found to be greater than the analogous homogeneous ones[66]. The TG/DTG patterns of RuYSSC, RuYSOD and RuYSPD are given in figures 3.7, 3.8 and 3.9 respectively. The TG data for the samples are presented in table 3.4. The well-defined TG patterns obtained in the case of simple complexes may not be obtained for the zeolite samples. One reason for this discrepancy might be the low concentration of metal complexes within the supercages of the zeolite. However, TG data provide clear information about decomposition temperature of the complexes under study.

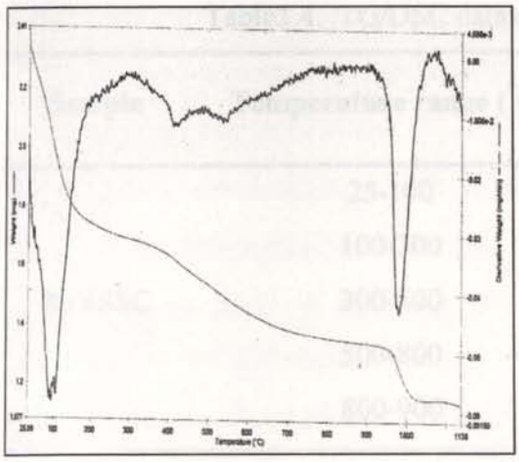

Figure 3.7(a) TG/DTG curve of RuYSSC

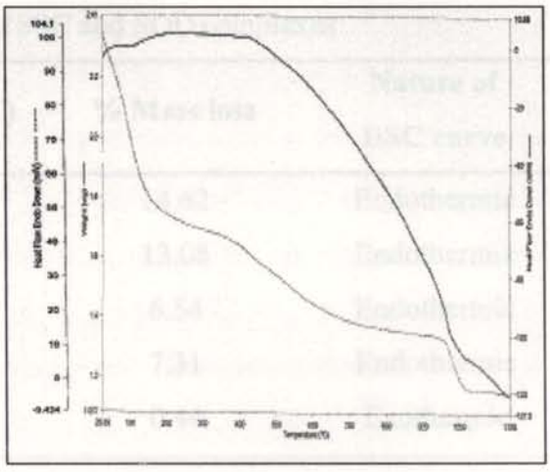

Figure 3.7(b) TG/DSC curve of RuYSSC

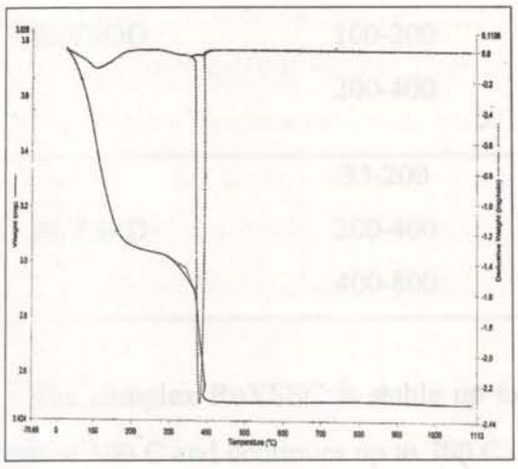

Figure 3.8(a) TG/DTG curve of RuYSOD

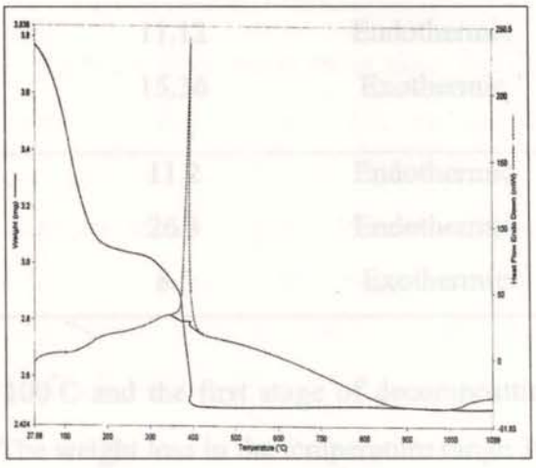

Figure 3.8(b) TG/DSC curve of RuYSOD

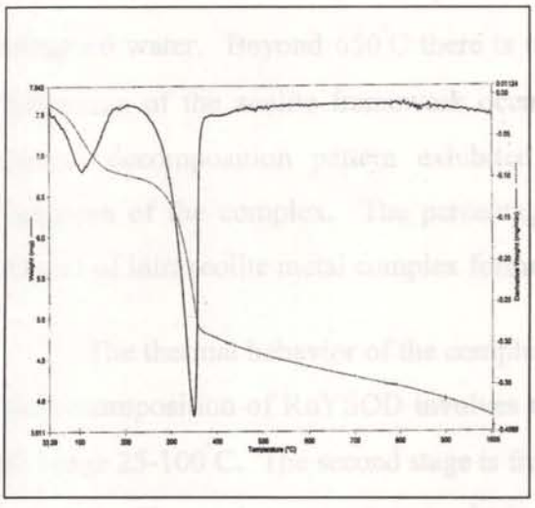

Figure 3.9(a) TG/DTG curve of RuYSPD

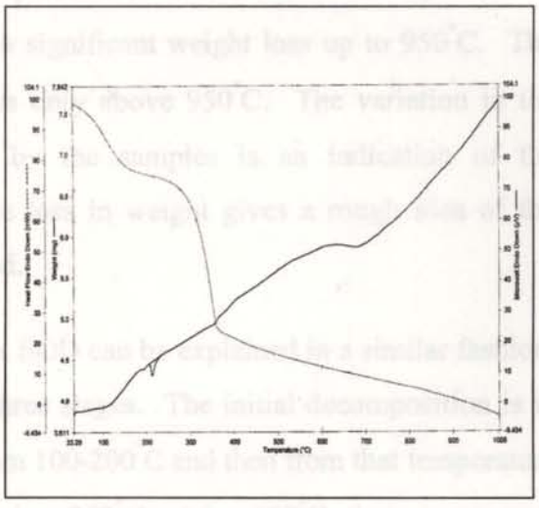

Figure 3.9(b) TG/DSC curve of RuYSPD

Table3.4. TG/DSC data of SSC and SOD complexes

Sample	Temperature range (°C)	% Mass loss	Nature of DSC curve
RuYSSC	25-100	14.62	Endothermic
	100-300	13.08	Endothermic
	300-500	6.54	Endothermic
	500-800	7.31	Endothermic
	800-900	0.44	Exothermic
RuYSOD	25-100	7.4	Endothermic
	100-200	11.12	Endothermic
	200-400	15.36	Exothermic
RuYSPD	33-200	11.2	Endothermic
	200-400	26.3	Endothermic
	400-800	8.5	Exothermic

The complex RuYSSC is stable up to 100°C and the first stage of decomposition starts at 100°C and continues up to 300°C. The weight loss in the temperature range 30-100°C could be due to the loss of free water molecules. The mass loss occurring between 100°C and 300°C with peak temperature at 106°C indicates expulsion of entrapped water. Beyond 650°C there is no significant weight loss up to 950°C. The destruction of the zeolite framework occurs only above 950°C. The variation in the thermal decomposition pattern exhibited by the samples is an indication of the formation of the complex. The percentage loss in weight gives a rough idea of the amount of intrazeolite metal complex formed.

The thermal behavior of the complex SOD can be explained in a similar fashion. The decomposition of RuYSOD involves three stages. The initial decomposition is in the range 25-100°C. The second stage is from 100-200°C and then from that temperature to 395°C. The peak temperature is obtained as 383°C. After 400°C, there is no mass loss up to 1000°C, which implies that the decomposition is almost complete at 400°C. The mass loss during the initial stages of decomposition can be attributed to the loss of

water molecules that may also include coordinated water. The partial decomposition of the zeolite sample occurs in the range 200-400°C. The decomposition of RuYSPD is seen to take place in three stages. The weight loss is found to be 11.2% till 200°C. The next stage of decomposition starts from 200°C and the loss of 26.3% in the range 200-400°C indicate deaquation of the sample. The peak temperature is observed at 349°C. The change in mass of 8.5% in 400-500°C range may be on account of the decomposition of the organic part of the molecule. The destruction of the zeolite framework occurs above 800°C.

3.4.7. FTIR spectra

There are detailed reports available on the framework structure of many zeolites carried out by Flasigen *et al.* in the mid IR region of 200-1300 cm^{-1}. The fundamental vibrations of the zeolite framework are contained in this region, which makes it essential to have a detailed study of the vibrations in that region. The characteristic spectral bands of the zeolite can be classified into two groups. The first group consists of the internal vibrations of the primary units of the structure and the other group comprises of the bands arising due to the linkage between the primary units. The second set of bands depends mainly on the structure of the zeolite samples. The IR spectrum of RuY is almost the same as that of zeolite Y which shows that the basic zeolite structure remains intact on metal exchange[67-69]. The IR spectrum of RuY is given in figure 3.10.

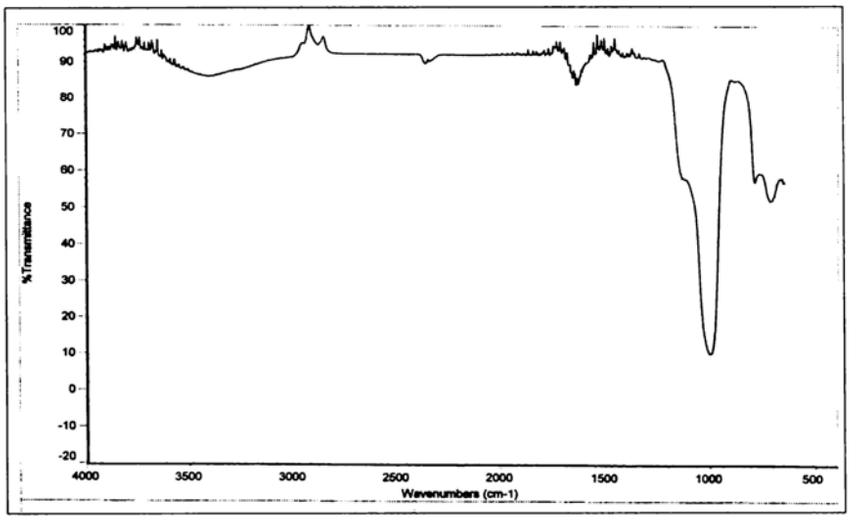

Figure 3.10. Infrared spectrum of RuY

The bands in the region 700-900 cm^{-1} may be due to symmetric stretching and that around 900-1250 cm^{-1} is due to asymmetric stretching. The IR spectral data of the ligands and the encapsulated complexes are given in figures 3.11- 3.13. The IR spectra of the ligands and the supported complexes recorded using KBr pellet in the region 400-4000 cm^{-1} are given in tables 3.5 and 3.6 respectively.

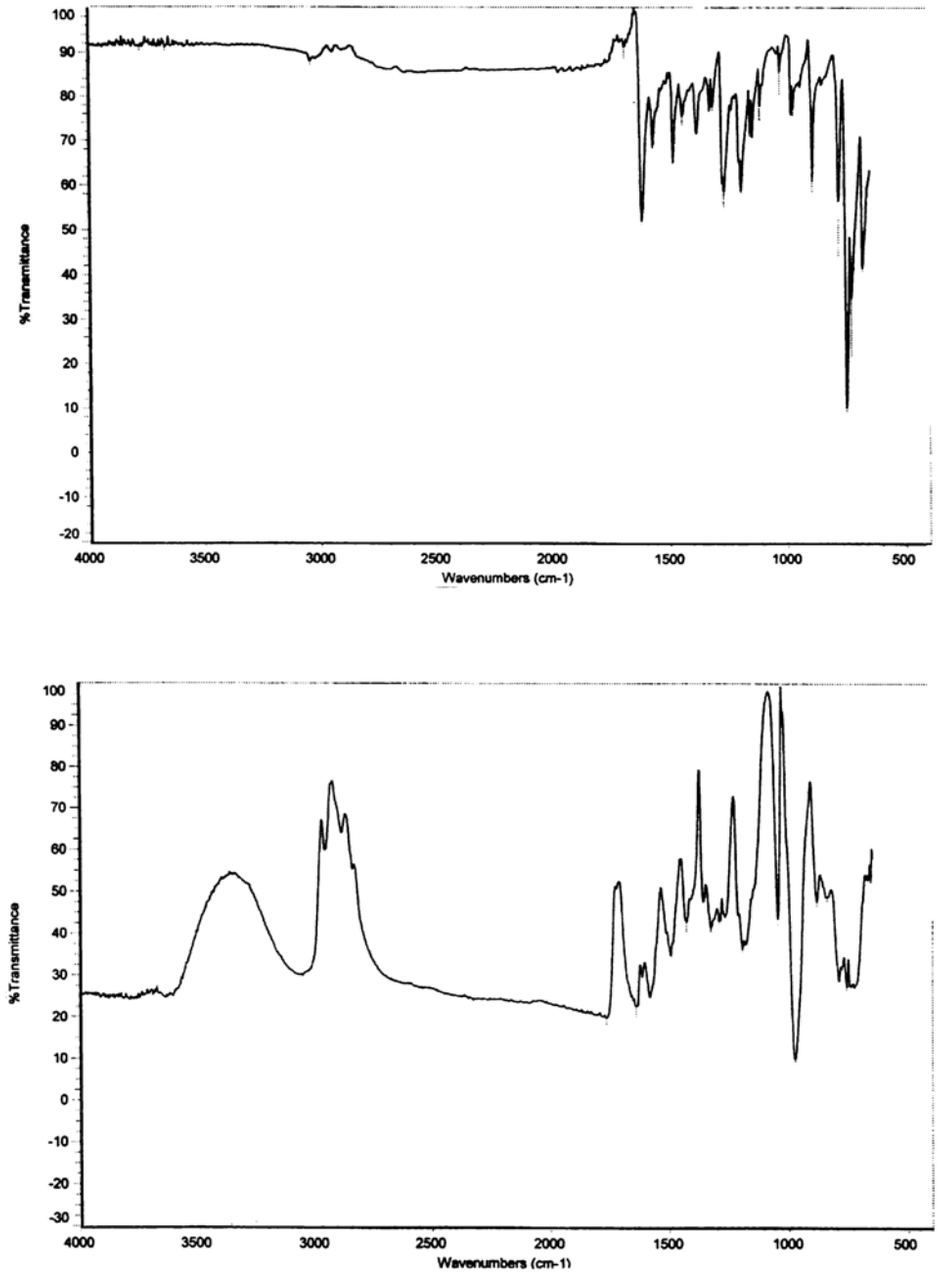

Figure 3.11. Infrared spectra of SSC and RuYSSC

Table 3.5. IR bands of SSC and RuYSSC

SSC (cm^{-1})	RuYSSC (cm^{-1})	Assignments
	569	$\nu_{zeolite}$
682	658	
728	725	
749	759	
783	791	
852	838	
893	883	
974	974	
983		
1030	1046	ν_{N-N}
1114		
1147		ν_{symC-C}
1157		
1195	1193	
1268	1265	$\nu_{C=O(phenolic)}$
1315	1288	
1330	1324	δ_{NH}
1384	1356	
1445	1447	ν_{C-C}
1485	1427	$\nu_{C=N}$
1571	1580	
1618	1613	$\nu_{C=O(carbonyl)}$
1691	1639	
1945	1718	
	2885	
3042	3054	
3663	3633	$\nu_{freeO-H}$
3775		

The spectral data of the encapsulated complexes confirms the formation of complexes inside the zeolite cages[70]. The ligand SSC could coordinate through the nitrogen atom of the azomethine group, the oxygen of the phenolic hydroxyl group and oxygen of the carbonyl group. The band occurring at 1485 cm^{-1} in the spectrum of the pure SSC ligand due to C=N stretching vibration of the azomethine group gets shifted to a lower frequency of 1427 cm^{-1} in the zeolite encapsulated semicarbazone indicating the involvement of azomethine nitrogen in coordination. The band seen at 1268 cm^{-1} due to phenolic C=O group shifts to a lower frequency of 1265 cm^{-1} in the complex which suggests the coordination through C-O of the phenolic group. The absorption band at 1618 cm^{-1} could be assigned to the vibration of the carbonyl group. The shifting of this band to 1613 cm^{-1} is indicative of the complexation involving the participation of the carbonyl group.

The bands around 1046 $cm^{-1}$and 729 cm^{-1} may be due to the rocking and wagging modes of water. The bands seen around 3040-3660 cm^{-1} is due to the merging of ν_{O-H} and ν_{N-H} frequencies. The ν_{O-H} stretching vibration of water is seen as a broad band around 3250-3650 cm^{-1} in the spectrum of the supported complex. This is a clear indication of the presence of water molecules of the zeolite in the complex.

Some bands observed in the spectrum of the ligand are not seen in the spectrum of the encapsulated complex as they are masked by the strong absorption bands of the zeolite. Certain new bands seen in the spectrum of the complex are those of the zeolite support.

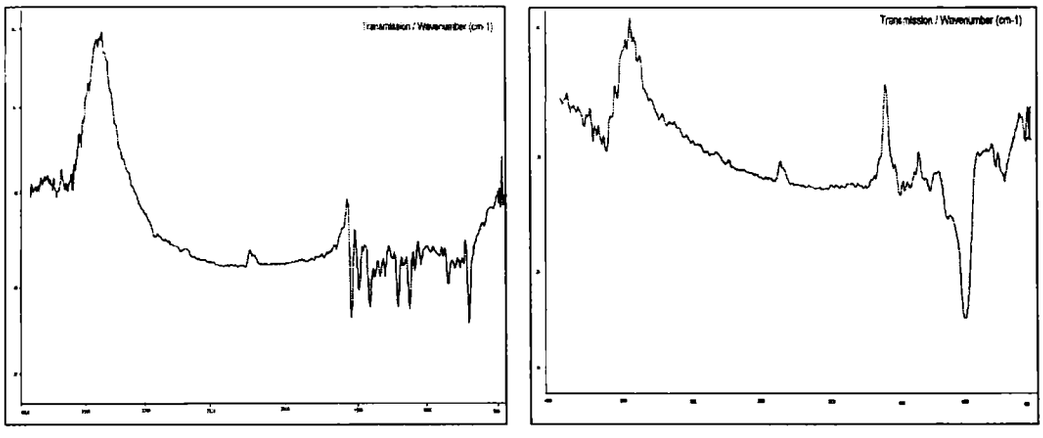

Figure 3.12. Infrared spectra of SOD and RuYSOD

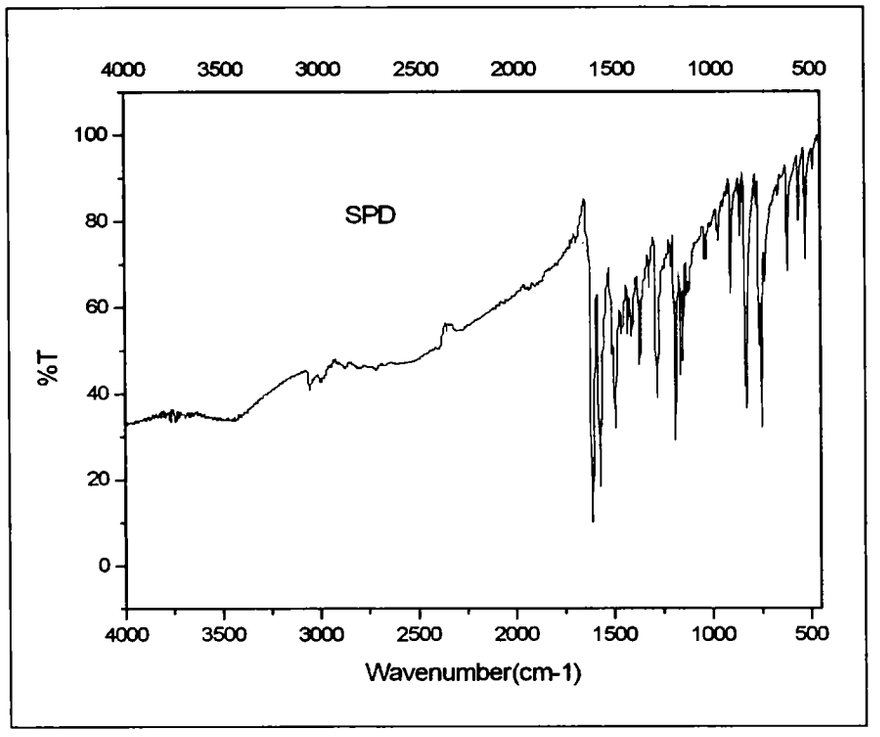

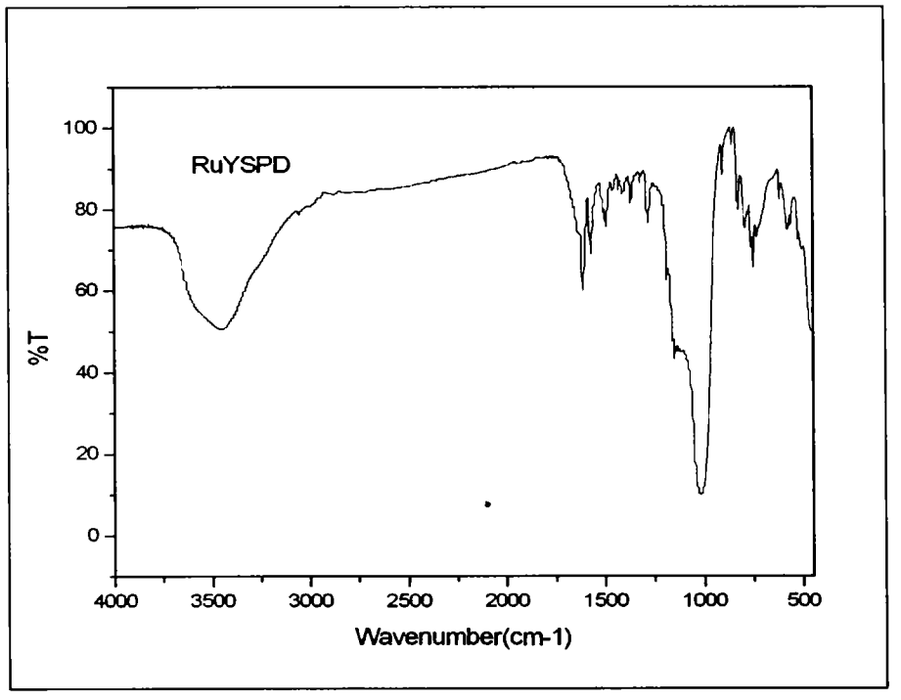

Figure 3.13. Infrared spectra of SPD and RuYSPD

assignments are given in table 3.7. These bands agree well with that for a Ru(III) complex having an octahedral structure[74, 75]. The electronic spectrum of the complex RuYSSC is given in figure 3.14.

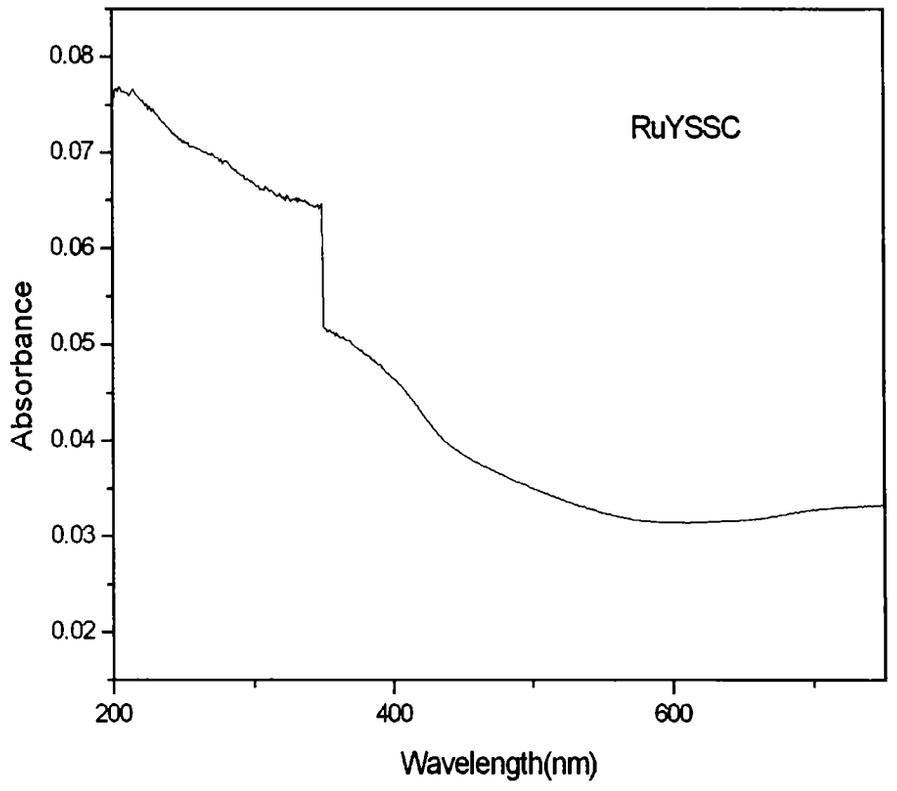

Figure 3.14. Electronic spectrum of RuYSSC

Table 3.7. Electronic spectral data

Sample	Absorbance Max.		Tentative Assignments
	nm	cm^{-1}	
RuYSSC	247	40490	Charge transfer
	313 (sh)	31950	$A_{2g}, {}^2T_{1g} \leftarrow {}^2T_{2g}$
	440	22730	${}^2E_g \leftarrow {}^2T_{2g}$
	606 (sh)	16580	${}^4T_{1g} \leftarrow {}^2T_{2g}$
	881 (sh)	11350	${}^4T_{2g} \leftarrow {}^2T_{2g}$
	951 (sh)	10520	${}^4T_{1g} \leftarrow {}^2T_{2g}$
RuYSOD	242	41320	Charge transfer
	308 (sh)	32470	$A_{2g}, {}^2T_{1g} \leftarrow {}^2T_{2g}$
	446	22420	${}^2E_g \leftarrow {}^2T_{2g}$
	600 (sh)	16660	${}^4T_{1g} \leftarrow {}^2T_{2g}$
	876 (sh)	11420	${}^4T_{2g} \leftarrow {}^2T_{2g}$
	945	10580	${}^4T_{1g} \leftarrow {}^2T_{2g}$
RuYSPD	244	40980	Charge transfer
	310 (sh)	32260	$A_{2g}, {}^2T_{1g} \leftarrow {}^2T_{2g}$
	445	22470	${}^2E_g \leftarrow {}^2T_{2g}$
	602 (sh)	16610	${}^4T_{1g} \leftarrow {}^2T_{2g}$
	875 (sh)	11430	${}^4T_{2g} \leftarrow {}^2T_{2g}$
	942	10620	${}^4T_{1g} \leftarrow {}^2T_{2g}$

3.4.9. EPR spectra

The electron paramagnetic resonance spectra of the complexes help us to determine the electronic state and geometry of the encapsulated complexes[75]. The EPR spectra of the complexes were recorded at liquid nitrogen temperature to gather information regarding the symmetry of the ligand field. The spectra are represented in figures 3.15 – 3.17. and the EPR parameters are tabulated in table 3.8.

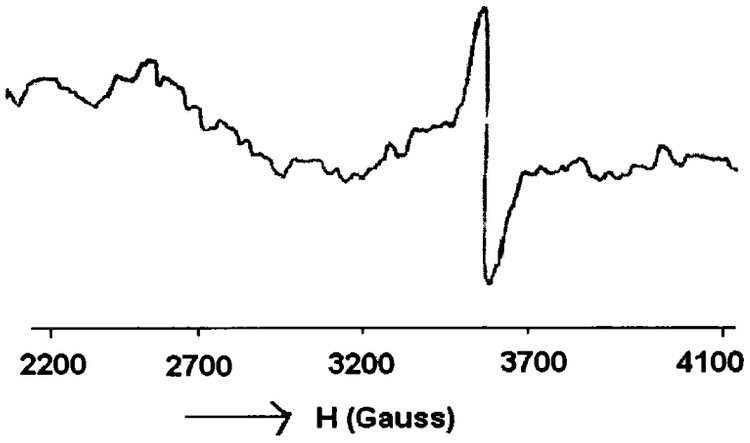

Figure 3.15. EPR spectrum of RuYSSC

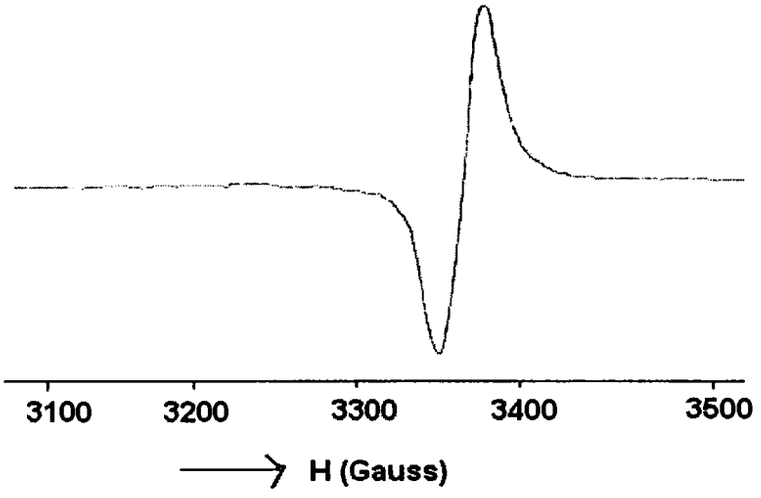

Figure 3.16. EPR spectrum of RuYSOD

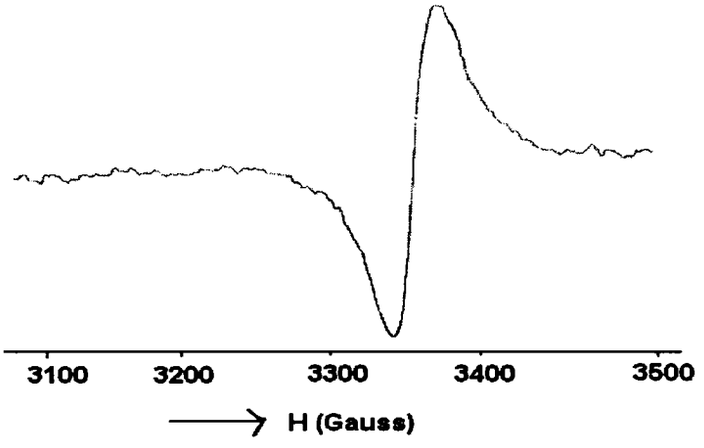

Figure 3.17. EPR spectrum of RuYSPD

Table 3.8. EPR spectral parameters

Complex	EPR parameters
RuYSSC	$g_1 = 2.11$; $g_2 = 2.14$; $g_3 = 2.01$
RuYSOD	$g_{\parallel} = 1.99$; $g_{\perp} = 2.06$
RuYSPD	$g_{\parallel} = 2.01$; $g_{\perp} = 2.12$

A well resolved hyperfine splitting pattern is obtained for encapsulated complexes that are similar to that in dilute solutions indicating the formation of the monomeric complexes within the zeolite supercages. The spectrum of RuYSSC gives three g values indicating rhombohedral distortion of octahedral geometry. The presence of two g values for RuYSOD and RuYSPD is indicative of the six coordinate environments around the ruthenium atom in the complexes and present an axial symmetry. The interactions of the zeolite framework with the encapsulated complex could induce some distortions in the expected structure.

17. Zsigmond, A.; Notheisz, F.; Frater, Z.; Backvall, J.E. Stud. Surf. Sci. Catal. **1997**, 108, 453.

18. Zsigmond, A.; Notheisz, F.; Szegletes, S.; Backvall, J.E. Stud. Surf. Sci. Catal. **1995**, 94, 728.

19. Joseph,T.; Srinivas, D.; Gopinath, C.S.; Halligudi, S.B. Catalysis Letters, **2002**, 83, 3-4.

20. Taqui Khan, M.M.; Halligudi, S.B.; Shukla, S.; Shaikh, Z.A. Journal of Molecular Catalysis, **1990**, 57, 307- 312.

21. Taqui Khan, M.M.; Sumita Rao, N.; Halligudi, S.B. Journal of Molecular Catalysis, **1990**, 63, 137- 146.

22. Joseph, T.; Sawant, D.P.; Gopinath, C.S.; Halligudi, S.B. Journal of Molecular Catalysis A : Chemical **2002**, 184 , 289- 299.

23. Halligudi, S.B.; Bhatt, K.N.; Taqui Khan, M.M. Journal of Molecular Catalysis, **1991**, 68.

24. Taqui Khan, M.M..; Halligudi, S.B.; Shukla, S.; Shaikh, Z.A. Journal of Molecular Catalysis, **1990**, 57, 301- 305.

25. Orlova, N.N.; Aksenova, V.A.; Selidovkin, D.A.; Bagdanova, N.S.; Pershin, G.N. Russ. Pharm. Toxico, **1968**, 348 .

26. Butler, K. U.S. patent No: 3, **1968**, 382, 266.

27. Bauer, D.J.; St.Vincent, L.; Kempe, C.H.; Downe, A.W. Lancet, **1963**, 20, 494 .

28. Petering, A.W.; H.H.Buskik, H.H.; Underwood, G.E.; Cancer Res., **1964**, 64, 367.

29. Johnson, C.W.; Jolyner, J.W.; Perry, R.P. Antibiot. Chemother, **1952**, 2, 636.

30. Benns, B.G.; Gingers, B.A.; Bayley, C.H. Appl. Microbiol., **1961**, 8, 353.

31. Raizada, M.S.; Srinivastava, M.N. Syn. React. Inorg.Met.Org.Chem.**1993**, 22, 393.

32. Patole, J.; Dutta, S.; Padhye, S.; Sinn, E. Inorg. Chim. Acta, **2001**, 318, 207

33. Singh, K.; Singh, R.V.; Tandon, J.P. Syn. React. Inorg. Met. Org.Chem. **1987**, 17, 385.

34. Basuli, F.; Peng, S.M.; Bhattacharya, S. Inorg. Chem, **1997**, 36, 5645.

35. Chinnusamy, V.; Natarajan, K. Syn.React.Inorg.Met. Org.Chem. **1993**, 23, 889.

36. Basuli, F.; Ruf, M.; Pipernot, C.G.; Bhattacharya, S. Inorg. Chem,**1998**, 37, 6113 .

37. Dharmaraj, N.; Natarajan, K. Syn. React. Inorg. Met. Org.Chem. **1997**, 27, 601.

38. Thangadurai, T.D., Natarajan, K. Transition Metal Chemistry, **2002**, 27, 840-843.

39. Das, M.; Livingstone, S.E. Coodin. Chem. Rev, **1974**, 13, 101.

40. Jacob, C.R.; Varkey, S.P.; Ratnasamy, P. Appl. Catal. A. Gen **1988**, 1568, 3453.

41. Schulz- Ekloof, S.; Ernst, S.; 'Handbook of Heterogeneous Catalysis', Ertil, G.; Knozinger, J.; Weitramp, J.; (Eds), Wiley-VCH, **1997**, 734.

42. Bowers, C.; Dutta, P.K. J.Catal. **1990**, 122 , 271.

43. Kowalak, S.; Weisis, R.C.; Balkur Jr, K.J. J. Chem. Soc. Chem. Commun. **1991**, 57.

44. Devos, D.E.; Feijen, E.J.P.; Schoonheydt, R.A.; Jacobs, P.A. J. Am. Chem. Soc. **1994**, 116, 4746.

45. Tollman, C.; Herron, N. Symposium on Hydrroc.Oxidation, 194th National Meeting of the American Chemical Society, New Orleans, L.A, **1987**, Aug 30-Sept.4.

46. Strutz, J.; Diegruber, H.; Jaeger, N.I.; Mosler, R. Zeolites. **1983**, 3, 102.

47. Mizuno, K.; Luunsford, J.H. Inorg. Chem. **1983**, 22, 3483.

48. Menon, P.G.; Ramasheshan, S. (Ed.) Lectures on Cat. 41stAnn. Meet. Ind. Acad. Sci.**1975**.

49. Egerton, T.A.; Hagan, A.; Stone, F.S.; Vickerman, J.C. J. Chem. Soc.Faraday Trans. **1972**, 168, 723.

50. Vansant, E.F.; Lunsford, J.H. J. Phys. Chem. **1972**, 76, 2860.

51. Lunsford, J.H.; Vansant, E.F. J. Phys. Soc; Faraday Trans II, **1973**, 69, 1028.

52. Dutta, P.K.; Lunsford, J.H. J. Chem. Phys. **1977**, 6 (10) 4716.

53. Jermijn, J.W.; Johnson, T.J.; Vansant, E.F.; Lunsford, J.H. J. Phys. Chem **1973**, 77, 2964.

54. Balkus K.J.Jr.; Gabrielov, A.G. J. Inclusion Phenom. Mol. Recogn. Chem, **1995**, 21, 159.

55. Mozo, E.P.; Gabriunas, N.; Lucaccioni, F.; Acosta, D.D.; Patrono, P.; Givestra, A.L.; Reiz, P; Delmon, B. J. Phys. Chem. **1993**, 97, 12819.

56. Balkus, K.J.; Gabrielov, Jr.A.G. J. Incl. Phenom. Mol. Rec. Chem. **1995**, 21, 159

57. Varkey, S.P.; Jacob, C.R. Ind. J. Chem. **1998**, 37A , 407.

58. Herron, N.; Stucky, G.D.; Tolman, C.A. J. Chem. Commun, **1986**, 1521.

59. Simpson, H.D.; Steinfink, H. J. Am. Chem. Soc. **1969**, 91, 6225.

60. Simpson, H.D.; Steinfink, H. J. Am. Chem. Soc. **1969**, 91, 6229.

61. Gallezot, P.; Taarit, Y.B.; Imelik, B. J. Catal. **1972**, 26, 205.

62. Thomas, J.M.; Catlow, C.R.A. Progr. Inorg. Chem. **1988**, 35, 1.

63. Raja, R.; Ratnasam, P. J. Catal, **1997**, 170, 244.

64. Diegruber, H.; Plath, P.J.; Schulz-Ekloff, G.; Mohal, M. J. Mol. Catal. **1984**, 24, 115.

65. Petrovic, A.F.; Petrovic, D.M.; Leovac, V.M.; Budimi, M. J. Thermal studies and Calorimetry, **1999**, 58, 589.

66. Flasigen, E.M.; Khatami, H.; Szymanski, H.A. 'Molecular Seive Zeolites', Adv. Chem. Ser., 101, American Chemical Society, Washington.D.C, **1971**, 201.

67. Flanigen, E.M. in Zeolite Chemistry and Catalysis, Rabo,J.A (Ed).; ACS Monograph, American Chemical Society, Washington D C, **1976**.

68. Jacobs, P.A.; Beyer, H.K.; Valyon, J. Zeolites 1, **1981**, 161.

69. Bindu Jacob, Ph.D Thesis, CUSAT, **1998**.

70. Edgardo, P,M.; Nyole, G.; Fabio,L.; Acosya, D.D.; Pasquale, P.; Aldo, L.G.; Patricio, R.; Bernard, D. J. Phy. Chem. **1993**, 97,12819.

71. Chandra, S.; Singh, R. Indian J. Chem. **1988**, 27 A, 417.

72. Patel, I.A.; Thaker, B.T. Indian. J. Chem. **1999**, 38 A, 427.

73. Yusuff, K.K.M.; Sreekala, R. J. Polym. Sci: Part A, Polym. Chem. **1992**, 30, 2595

74. Kortum, G. Reflectance Spectroscopy Principles, Methods, Applications, Springer-Verlag- Berlin, **1969**.

75. Lever, A.B.P. Inorganic Spectroscopy, Second Edition, Elsevier, NewYork, **1984**.

76. Wertz, J.E.; Borton, J.R. Electron Spin Resonance: Elementary theory & Practical Applications, Mc Graw-Hill, **1972**.

Chapter IV

Section A

ZEOLITE -Y ENCAPSULATED RUTHENIUM COMPLEXES OF ANTHRANILIC ACID AND 4-AMINOBENZOIC ACID

Section B

ZEOLITE-Y ENCAPSULATED RUTHENIUM COMPLEX OF DIMETHYL GLYOXIME

Chapter IV

Section- A

ZEOLITE -Y ENCAPSULATED RUTHENIUM COMPLEXES OF ANTHRANILIC ACID AND 4-AMINOBENZOIC ACID

4A.1. INTRODUCTION

Encapsulated metal complexes using the amino acids anthranilic acid (AA) and 4-aminobenzoic acid (ABA) as ligands are found to have an immense variety of applications, as they possess great catalytic and bio-mimetic properties. The encapsulated complexes of the two isomeric amino-benzoic acids have not yet been reported. Hence it was considered worthwhile to encapsulate these simple compounds inside the zeolite cages and to study whether any structural changes occur due to this confinement and to determine the influence of the encapsulation upon their characteristic properties.

There are many ways in which the amino group in an aromatic ring differs from their aliphatic analogues. The amino benzoic acids are rigid preferentially allowing a planar arrangement, and the delocalisation of the electron pair on the nitrogen atom towards the aromatic ring decreases their basic nature. All the unique properties of the above ligands allow them to act as good catalysts in many important reactions. The structure of ligands anthranilic acid and 4-aminobenzoic acid are given in figures 4A.1. and 4A.2. respectively.

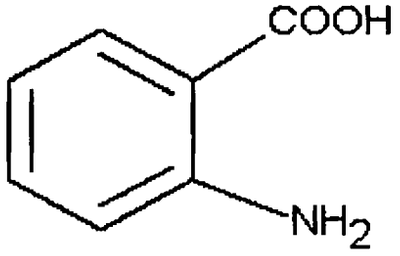

Figure 4A.1. Structure of anthranilic acid (AA)

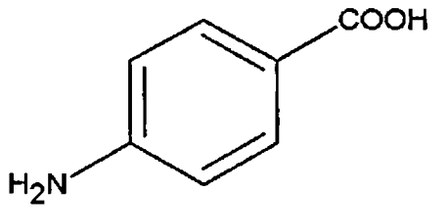

Figure 4A.2. Structure of 4-aminobenzoic acid (ABA)

4A.2. EXPERIMENTAL

The details concerned with the purification of the two ligands used for the formation of the zeolite encapsulated complexes are presented in chapter II. The metal exchanged zeolite was also prepared according to the procedure already described.

4A.2.1. Synthesis of zeolite encapsulated ruthenium complexes of anthranilic acid (AA) and 4-aminobenzoic acid (ABA)

The flexible ligand method[1] was employed for the preparation of zeolite-encapsulated complexes of AA and ABA of ruthenium. This method of synthesis involves the reaction of the ligand under study with the metal already introduced within the supercages of the zeolite.

The ligand anthranilic acid was mixed with the metal exchanged zeolite RuY such that the ligand to metal ratio is approximately 2. This ratio is maintained keeping in view the percentage of metal present in the modified zeolite-Y form. The above mixture was taken in a glass ampule, sealed and heated at a constant temperature of about 120°C for about 6 hours to ensure complete complexation. The evidence for the formation of the complexes is indicated by the slight colour changes occurring during encapsulation. A similar procedure is adopted for preparing RuYABA where the temperature is maintained at 140°C. The complexes thus synthesized were filtered and then soxhlet extracted with methanol and acetone until the extracting solvent became colourless. The process of soxhlet extraction was employed to remove any species adsorbed on the surface of the zeolite. The filtered complexes were back exchanged by stirring with 0.01 M NaCl solution for 24 hours to replace the uncomplexed metal ions with sodium ions. The zeolite containing the metal complexes was then made chloride

free by washing with distilled water and drying in an air oven at 100°C for 2 hours. The complexes thus obtained were stored in vacuum over anhydrous calcium chloride.

4. A.3. ANALYTICAL METHODS

Various characterization methods were employed to study the different properties of the synthesized metal complexes and the details of these techniques are already presented in chapter II.

4. A.4. RESULTS AND DISCUSSION

The ability of the encapsulated complexes of aminobenzoic acids to act as heterogeneous catalysts depends on various factors like the nature of the exchanged cation, the degree of ion exchange, coordination, distribution of the cations through the lattice[2] and electronic structure of the transition metal centers.

4. A.4.1. Chemical analysis

Chemical analysis was done to obtain an idea about the composition of the sample and the degree of ion exchange. The analytical data of the zeolite complexes RuYAA and RuYABA are given in table 4A.1. The Si/Al ratio is retained as 2.6 even after complex formation indicating the absence of any dealumination.

Table 4 A.1. Analytical data of the encapsulated complexes

Sample	% Si	% Al	% Na	% Ru	% C	% H	% N
RuYAA	20.49	8.02	6.28	1.2	0.83	1.80	0.15
RuYABA	20.61	7.98	6.98	1.3	0.90	1.76	0.45

The metal percentage and CHN analysis confirm the formation of the metal complexes in the zeolite cavities. These values suggest the formation of 1: 2 complexes inside the cages. There is the possibility for the presence of traces of metal ions occluded even after the final sodium exchange. The encapsulation of complexes involves the

breaking of metal-oxygen bonds in the zeolite structure and the formation of new bonds with the atoms present in ligands[3].

4.A.4.2. Surface area and pore volume analysis

The data obtained by the BET method in an atmosphere of nitrogen is given in table 4A.2.

Table 4.A.2. Surface area and pore volume data

Sample	Surface area (m^2/g)	% Loss	Pore volume (cc/g)	% Loss
RuY	682		0.35	
RuYAA	532	22	0.28	18.28
RuYABA	548	19.65	0.27	20.56

The significant reduction in surface area and pore volume as a result of the encapsulation of complexes within the zeolite pores is due to the blocking of the pores by the formation of the metal complexes[4]. The decrease in surface area values suggests the formation of metal complexes inside the zeolite cages.

4A.4.3. X-ray diffraction studies

The X-ray diffraction patterns of RuYAA and RuYABA appear similar to the parent zeolite-Y and ruthenium exchanged zeolite. This shows that the zeolite framework has retained its crystallinity on encapsulation. The XRD patterns of the above mentioned complexes are depicted in figure 4A.3. The analysis of the XRD pattern reveals the presence of large transition metal complexes either within the zeolite structure or on the external surface of the zeolite[5, 6].

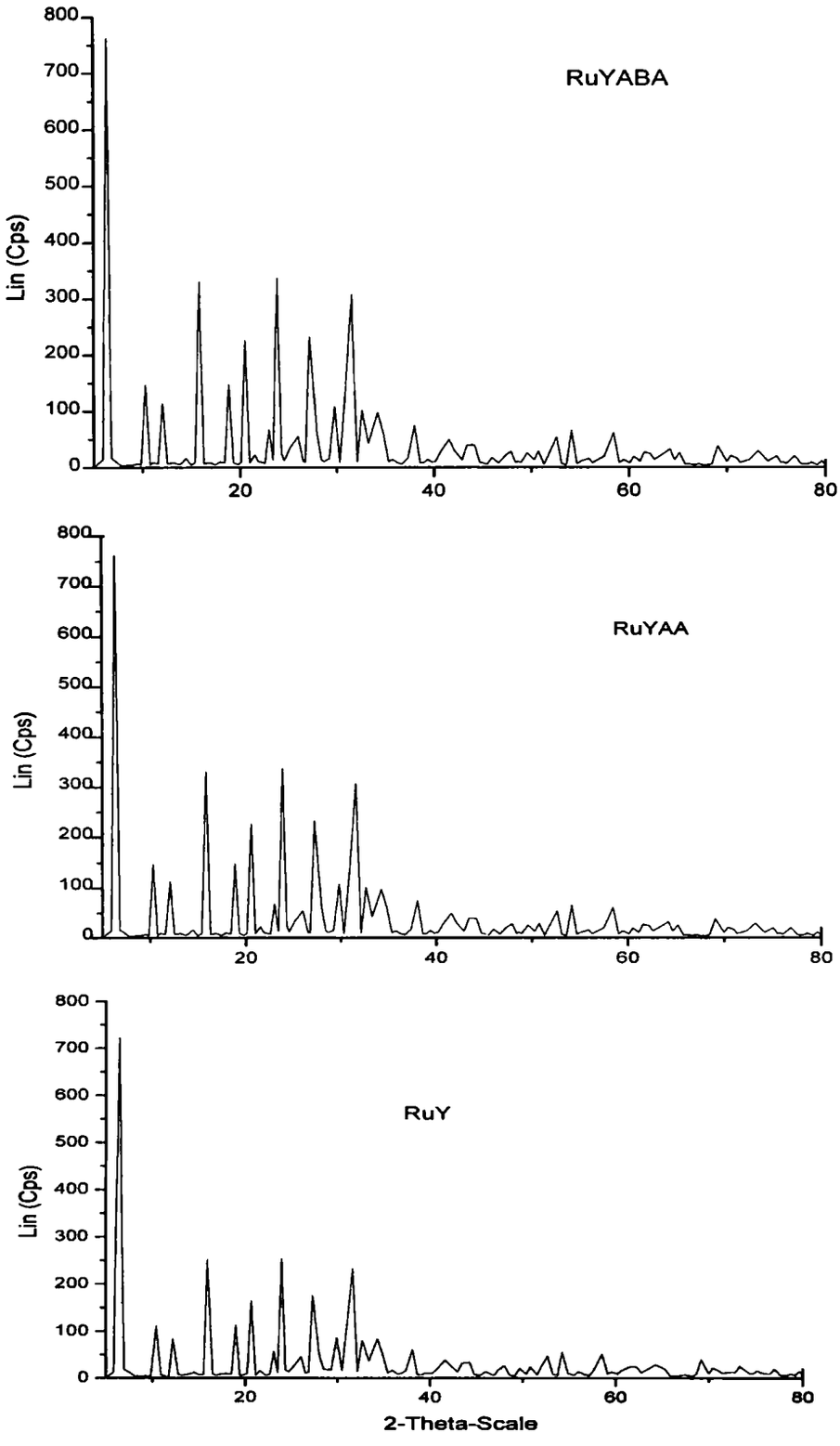

Figure 4A.3. XRD spectra of (i) RuY (ii) RuYAA (iii) RuYABA

4A.4.4. SEM analysis

This is an effective technique to determine the effectiveness of the process of purification by which extraneous materials on the surface of the zeolite are removed. The SEM of RuYAA and RuYABA before and after soxhlet extraction shows the removal of various species adsorbed on the surface of the zeolite. The corresponding scanning electron micrographs are given in figures 4A.4 and 4A.5. The complexes formed inside the zeolite cages remain trapped and are not able to come out. Thus the method of soxhlet extraction can be used for the complete removal of the surface complexes.

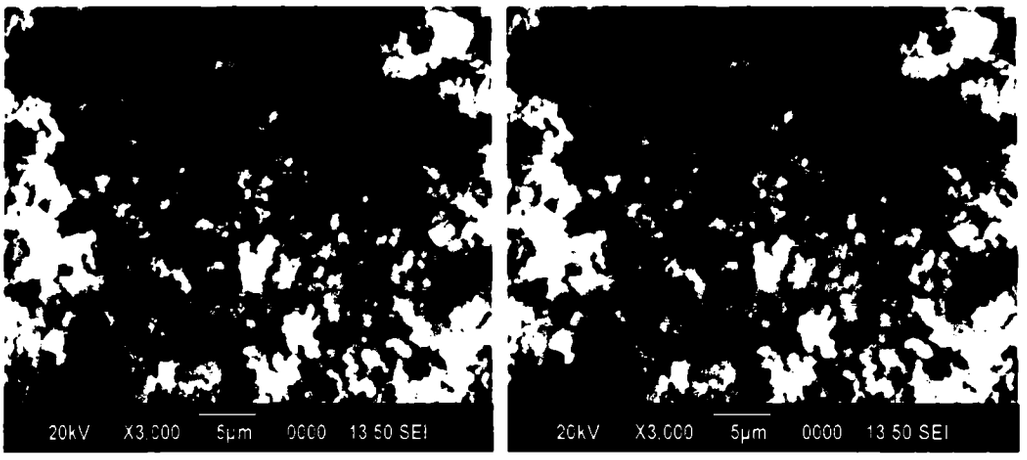

(i) (ii)

Figure 4A.4. Scanning electron micrographs of RuYAA (i) before and (ii) after soxhlet extraction

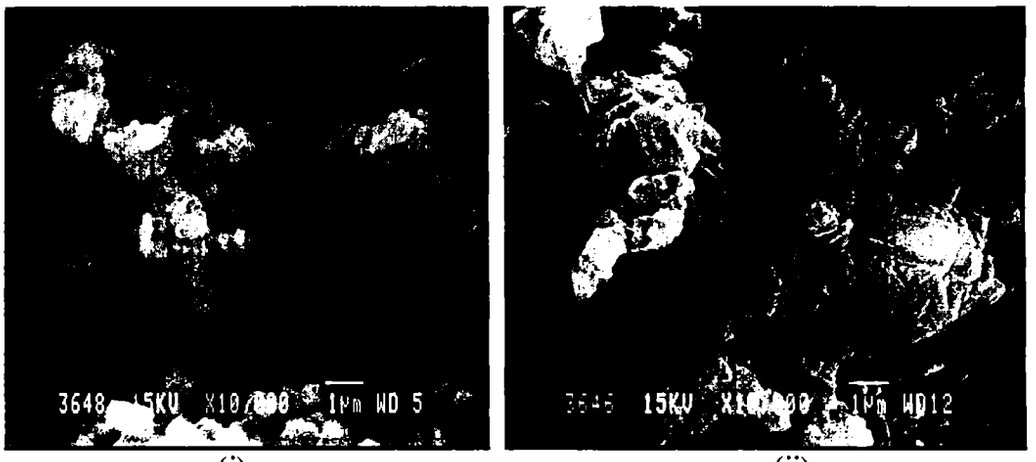

(i) (ii)

Figure 4A.5. Scanning electron micrographs of RuYABA (i) before and (ii) after soxhlet extraction

4.A.4.5. TG analysis

The TG/DTG curves of RuYAA and RuYABA were recorded from room temperature to 1000°C at a heating rate of 10°C per minute in an atmosphere of nitrogen. The figures 4A.6 and 4A.7 depict the TG/DTG and TG/DSC curves of the prepared samples. The thermo analytical data of these complexes are represented in the table 4A.3.

Table 4A.3. Thermogravimetric data of the encapsulated ruthenium complexes

Complex	Temp. range of decomposition (°C)	% weight loss	Nature of DSC Curve
RuYAA	25-100	19.42	Endothermic
	100-300	13.0	Endothermic
	300-500	2.65	Endothermic
	500-800	3.82	Endothermic
	800-900	1.47	Exothermic
RuYABA	30-100	16.45	Endothermic
	100-300	11.51	Endothermic
	300-500	2.3	Endothermic
	500-600	0.66	Exothermic

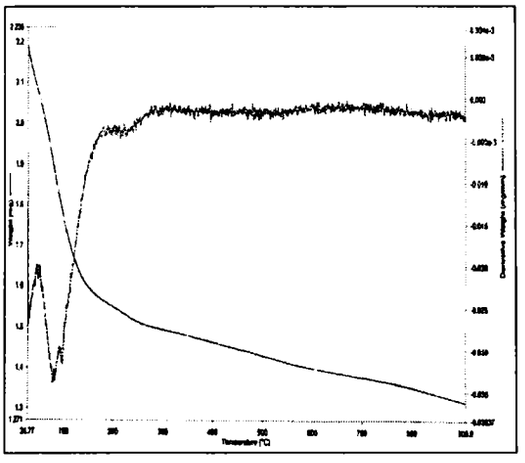

Figure 4A.6(a) TG/DTG curve of RuYAA

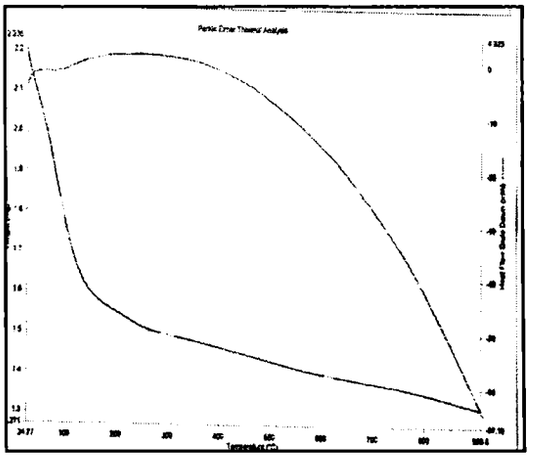

Figure 4A.6(b) TG/DSC curve of RuYAA

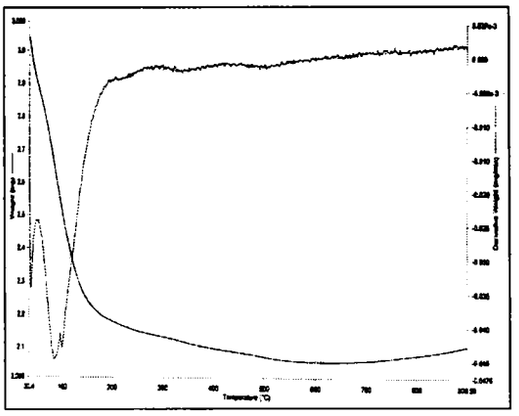

Figure 4A.7(a) TG/DTG curve of RuYABA

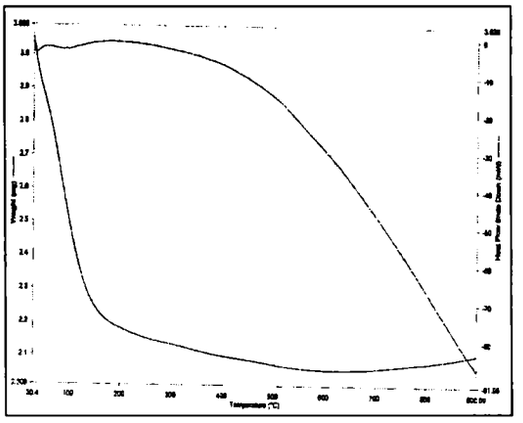

Figure 4A.7(b) TG/DSC curve of RuYABA

TG analysis provides an approximate idea about the decomposition temperature of the supported complexes. The loss of water molecules in the zeolite cages is shown in the range 25-300°C. The decomposition of the complex and partial decomposition of the zeolite cage also occurs in this range. The small mass loss in different stages of decomposition is an indication of the low percentage of metal complexes in zeolite cages. For RuYABA, two main stages of decomposition were observed. As there is only a low concentration of metal complexes within the zeolite cage, a vague idea about the decomposition of the complex was obtained. The first stage of mass loss up to 180°C is due to the loss of water molecules present in the zeolite cavities. The second stage begins at 180°C, which may be due to the decomposition of the ligand. The total mass loss for RuYABA is 31.84%. This indicates the high thermal stability of the zeolite complex and low loading of the metal complex in the cavities.

4.A.4.6. FTIR spectra

The figures 4A.8 and 4A.9 shows the IR spectra of the ligands AA, ABA and their encapsulated complexes. The spectral data of the ligands and the complexes RuYAA and RuYABA are presented in the table 4A.4. The ligand bands in the prepared complexes that are not masked by the prominent zeolite bands can be easily identified from the table. The encapsulation inside the zeolite cages is evident from the IR spectral studies on such type of complexes[7].

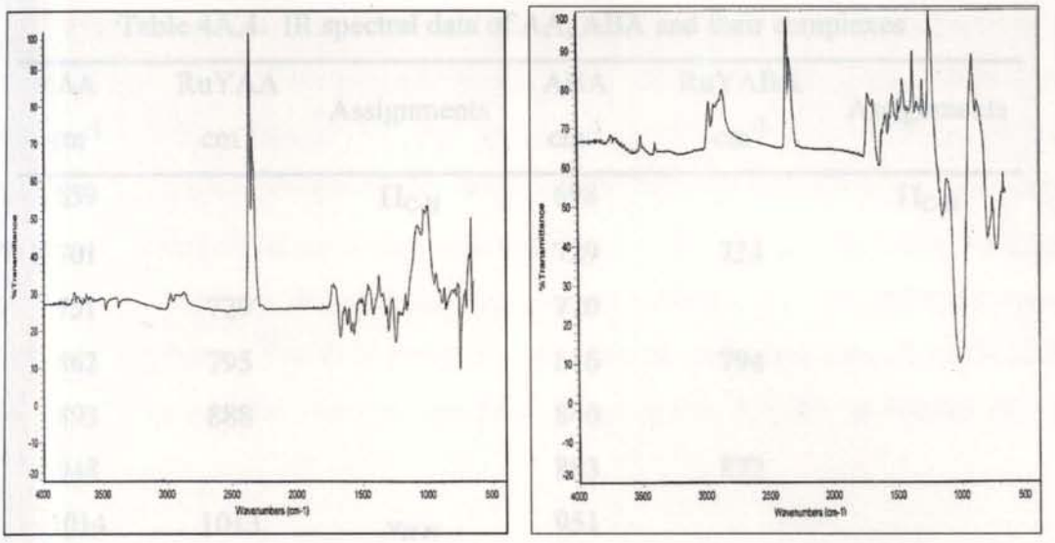

Figure 4A.8. IR spectra of AA and RuYAA

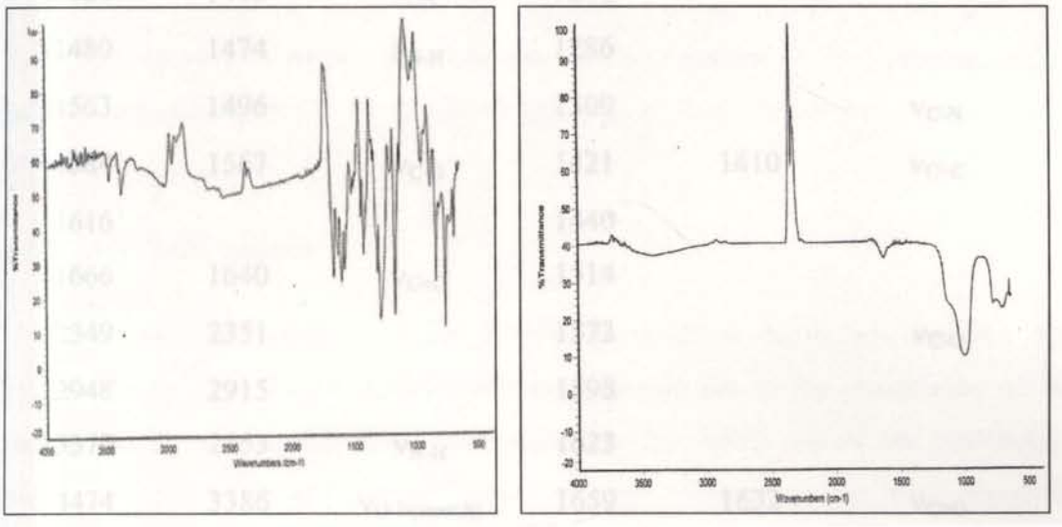

Figure 4.A.9. IR spectra of ABA and RuYABA

Table 4A.4. IR spectral data of AA, ABA and their complexes

AA cm^{-1}	RuYAA cm^{-1}	Assignments	ABA cm^{-1}	RuYABA cm^{-1}	Assignments
659		Π_{C-H}	698		Π_{C-H}
701			729	724	
751	729		770		
862	795		816	794	
893	888		840		
948			883	872	
1014	1013	ν_{N-N}	951		
1047			1021	1005	ν_{N-N}
1244			1128	1125	ν_{symC-C}
1300	1271	ν_{C-N}	1172		
1420	1408	$\nu_{C=C}$	1208		
1480	1474	δ_{N-H}	1286		
1563	1496		1309		ν_{C-N}
1584	1567	ν_{C-O}	1421	1410	$\nu_{C=C}$
1616			1440		
1666	1640	$\nu_{C=O}$	1514		
2349	2351		1573		ν_{C-O}
2948	2915		1598		
3370	2953	ν_{N-H}	1623		
3474	3386	$\nu_{O-H(stretch)}$	1659	1632	$\nu_{C=O}$
	3465		2284		
			2538	2349	
			2915		
			2950		
			3222		
			3361		ν_{N-H}
			3458		$\nu_{O-H(stretch)}$

The band at 1300 cm^{-1} in the spectrum of the recrystallized anthranilic acid may be attributed to the C-N stretching vibration of the primary amino group. This band shifts to a lower frequency of 1271 cm^{-1} in the encapsulated complex, which can be due to the coordination of nitrogen of anthranilic acid to ruthenium metal on complexation. The $\nu_{C=O}$ stretching vibration occurring at around 1666 cm^{-1} in the pure ligand is shifted to 1640 cm^{-1}. This indicates coordination of the carboxyl group to the ruthenium metal ion in the complexes. The O-H stretching vibration of water seen around 3300- 3500 cm^{-1} in the encapsulated complex indicates the presence of water molecules of the zeolite.

The vibration at 1309 cm^{-1} present in RuYABA is assigned to C-N stretching vibration. This band might have shifted to a lower region in the complex. But this is not clearly visible since it gets merged with other peaks. The band corresponding to carbonyl stretching vibration occurring around 1659 cm^{-1} in the pure ABA has shifted to a lower frequency of 1632 cm^{-1} which provides a clear evidence for the complexation of the C=O group in RuYABA. Many bands clearly observed in the spectrum of the ligand are not visible in the encapsulated complex as they are masked by the zeolite bands.

4A.4.7. Electronic spectra

The electronic spectra of the zeolite encapsulated complexes RuYAA and RuYABA were taken in the diffuse reflectance mode due to the insolubility of the complexes[8]. Data regarding the d-d transitions in the visible region and the charge-transfer transition in the UV region[9-11] were obtained. We get an indication about the structure of the complexes from the spectral bands in the electronic spectra. These facts combined with other useful analytical techniques like EPR and FTIR confirm the structure of the complexes. The electronic spectrum of the complex RuYAA is given in figure 4A.10 and the tentative assignments of the absorption peaks obtained are given in table 4A.5.

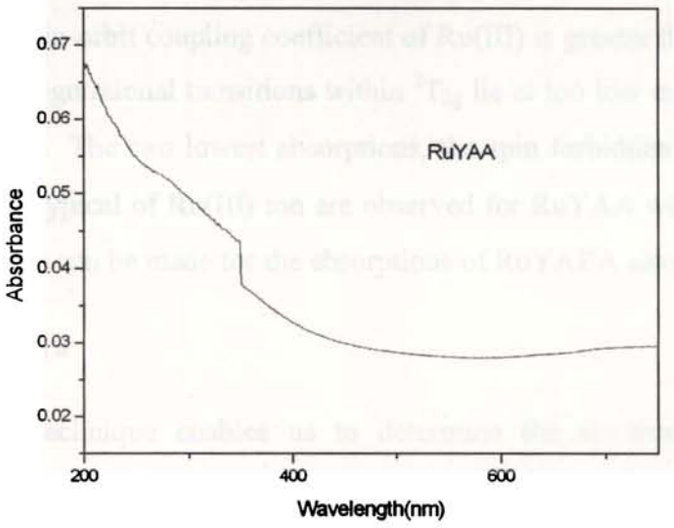

Figure 4A.10. Electronic spectrum of RuYAA

Table 4A.5. Electronic spectral data

Sample	Absorbance Max.		Tentative Assignments
	nm	cm^{-1}	
RuYAA	260	38460	Charge transfer
	320(sh)	31250	$A_{2g}, {}^2T_{1g} \leftarrow {}^2T_{2g}$
	575	17390	${}^4T_{1g} \leftarrow {}^2T_{2g}$
	881(sh)	11350	${}^4T_{2g} \leftarrow {}^2T_{2g}$
	950	10530	${}^4T_{1g} \leftarrow {}^2T_{2g}$
RuYABA	256	39060	Charge transfer
	325(sh)	30770	$A_{2g}, {}^2T_{1g} \leftarrow {}^2T_{2g}$
	574	17420	${}^4T_{1g} \leftarrow {}^2T_{2g}$
	875(sh)	11430	${}^4T_{2g} \leftarrow {}^2T_{2g}$
	952	10500	${}^4T_{1g} \leftarrow {}^2T_{2g}$

RuYAA show absorptions at 38460, 31250, 17390, 11350 and 10530 cm^{-1} that indicate an octahedral geometry. The ground state of Ru(III) is ${}^5T_{2g}$ owing to the t_{2g}^5 configuration of the Ru(III) ion in an octahedral environment[12]. The excited states corresponding to this configuration are ${}^2A_{2g}$, ${}^2T_{1g}$ and ${}^2E_g$. The charge transfer absorption bands of six coordinate Ru(III) complexes occur at relatively low energies.

Many of the d-d bands are frequently obscured due to very large crystal field parameters. The spin-orbit coupling coefficient of Ru(III) is greater than that of Fe(III). Therefore intraconfigurational transitions within $^2T_{2g}$ lie at too low energies and cannot be well understood. The two lowest absorptions, the spin forbidden $^4T_{1g} \leftarrow {}^2T_{2g}$, $^4T_{2g} \leftarrow {}^2T_{2g}$, which are typical of Ru(III) ion are observed for RuYAA with low intensities. Similar assignments can be made for the absorptions of RuYABA also.

4A.4.8. EPR Spectra

The EPR technique enables us to determine the electronic state and the symmetry of the ligand field that provides several pieces of information on the immediate environment. Hence the technique renders to localize the cations in the different sites existing in the zeolite framework. The parameters of the electron paramagnetic spectra enable us to calculate the delocalization of the unpaired electron.

The EPR parameters of the ruthenium-exchanged zeolite undergo slight changes on complexation, which is further proof for the formation of encapsulated complexes. The EPR spectra of the various samples recorded at LNT are presented in the figures 4A.11 and 4A.12 and the data are represented in the table 4A.6.

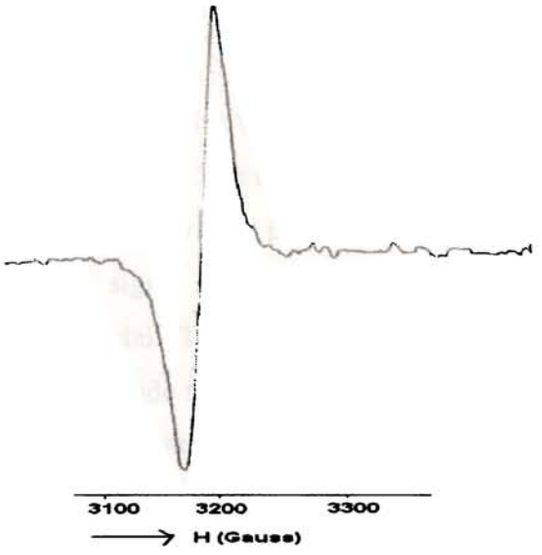

Figure 4A.11. EPR spectrum of RuYAA

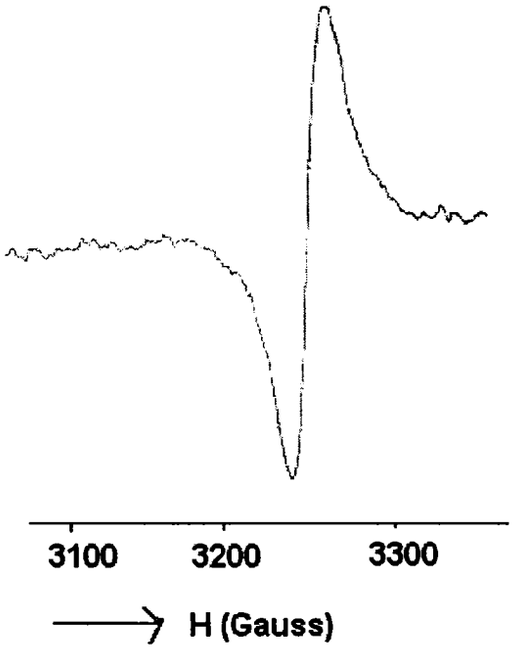

Figure 4A.12. EPR spectrum of RuYABA

Table 4A.6. EPR spectral parameters

Complex	EPR parameters
RuYAA	$g_{\parallel} = 1.99$; $g_{\perp} = 2.03$
RuYABA	$g_{\parallel} = 2.01$; $g_{\perp} = 2.1$

RuYAA is found to be EPR active which points out the possibility for ruthenium to exist as Ru(III) ion in this complex. The anisotropic nature of RuYAA and RuYABA is indicated by the presence of two g values presenting an axial symmetry[13]. The small hyperfine splitting of the EPR signal is indicative of the involvement of the nitrogen atom in coordination with the metal. The complex is assigned a six coordinate structure on the basis of the observations made from EPR spectra[14, 15]. The axial symmetry of the encapsulated complexes is consistent with the presence of a paramagnetically active Ru(III) ion.

Section- B

ZEOLITE-Y ENCAPSULATED RUTHENIUM COMPLEX OF DIMETHYLGLYOXIME

4B.1. INTRODUCTION

Studies about the transition metal complexes of dimethylglyoxime have gained great popularity since the last few decades[16]. The metal complexes of dimethylglyoxime act as good reagents in synthetic organic chemistry[17-20]. Notable among them is cobaloxime(II) which is actually bis(dimethylglyoximato)cobalt(II) described by Tschugaev in 1905[21]. The catalytic activity of cobaloxime in hydrogenation and oxidation reactions has made it necessary to study the structure and bonding in such type of complexes. Metal containing oxime complexes are used in medicine. Technetium(V) and copper(II) complexes with vicinal dioximes are used as cerebral and myocardial perfusion imaging agents[22]. The substitution of two hydrogen bridges with metal complexes yields polynuclear compounds with which magnetic interactions can be studied[23].

The coordination chemistry of chelating dioxime ligands with first row transition metals[24-27] have been the subject of study for a long period of time in view of their role as biological model compounds[28-30], dioxygen carriers[31, 32] and catalysts in chemical processes[33-35]. The dioxime ligands are capable of coordinating metal ions as neutral dioximes and as monoanionic dioximates through the dissociation of one oxime proton[36]. Though the oxime complexes of 3d metal ions[37, 38] have been widely studied, more importance is given to symmetrically disubstituted glyoximes[39, 40]. The chemistry of monosubstituted glyoximes were also investigated[41, 42]. Studies are also conducted on macromolecules attached to dioximes[43].

The spectroscopic and redox properties of Co(II), Ni(II) and Cu(II) complexes with ligands such as N-(1-(2-aminoethyl)piperazine)-phenylglyoxime, N-(1-(2-aminoethyl)piperazine)-glyoxime and N,N'-bis(1-(2-aminoethyl)piperazine)-glyoxime

are reported[44]. Ruthenium complexes with benzaldoxime have been synthesized and their catalytic activities for oxygenation, carbonylation and hydroformylation have been studied[45]. Studies were conducted on complexes of $RuCl_2(PPh_3)_3$ (where PPh_3 = triphenyl phosphine) with dioximes such as DMG, 1,2-cyclohexanedione dioxime and diphenyl glyoxime[46]. Encapsulated cobalt dimethylglyoxime complex, $Co(dmg)_2$-X acts as catalyst for the selective oxidation of propene to formaldehyde and acetone as reported by Diegruber *et al.*[47]

All these fascinating properties of dimethylglyoxime complexes have prompted us to synthesize and characterize zeolite encapsulated Ru(III) complex of DMG. The behaviour of encapsulated dimethylglyoxime complex is expected to be quite different from that of simple dimethylglyoxime complex due to their interaction with the zeolite framework. The complex RuYDMG is thus an attractive system for catalytic studies. In this chapter, details regarding the synthesis and characterization of Y-zeolite encapsulated complex of Ru(III) with dimethyl glyoxime are presented. The structure of dimethylglyoxime is given below in figure 4B.1.

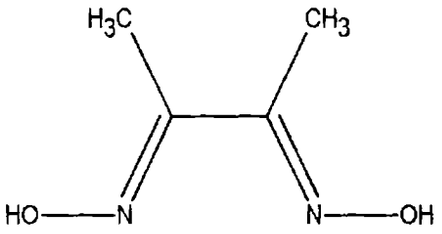

Figure 4B.1. Structure of dimethylglyoxime (DMG)

4B.2. EXPERIMENTAL

4B.2.1. Materials

The details concerned with the purification of dimethylglyoxime (DMG) obtained from Merck are given in chapter II. The ruthenium-exchanged zeolite used in the synthesis of encapsulated DMG complex was prepared according to the procedure described in chapter II.

4B.2.2. Synthesis of zeolite encapsulated ruthenium complex of dimethylglyoxime

Ruthenium exchanged zeolite was thoroughly mixed with dimethylglyoxime such that the ligand to metal ratio is slightly greater than 2. The metal content present in ion exchanged zeolite play a decisive role in determining the amount of ligand to be used in synthesis. The mixture was taken in a sealed glass ampule and heated at 150°C for about 6 hours to ensure maximum complexation. The resulting encapsulated complex RuYDMG was soxhlet extracted with methanol for about 24 hours to remove the surface species present, which may include the uncomplexed ligands also. The uncomplexed metal ions and the protons released from the ligand to zeolite during the process of complex formation were removed by ion exchange with sodium chloride solution (0.01 M, 250 ml, 24 hrs). The encapsulated complex thus obtained was filtered, washed to remove chloride ions, finally dried at about 110°C for two hours and stored in vacuum over anhydrous calcium chloride.

The equations representing the exchange of ruthenium ions with sodium-exchanged zeolite to form the corresponding ruthenium exchanged zeolite and the back exchange of uncomplexed metal ions after complexation can be represented as follows.

$$Ru^{3+}_{(aq)} + Na_3Y_{(s)} \rightarrow 3\ Na^{+}_{(aq)} + RuY_{(S)}$$

$$RuY_{(S)} + DMG_{(s)} \rightarrow \text{Ru-Y-DMG}$$

$$3\ Na^{+}_{(aq)} + Ru^{3+}Y\ \text{Ru-DMG} \rightarrow Ru^{3+}_{(aq)} + Na_3^{+}Y\ \text{Ru-DMG}_{(s)}$$

4B.3. ANALYTICAL METHODS

The characterization techniques include chemical analysis, surface area and pore volume analysis, X-ray diffraction patterns, SEM analysis, FTIR spectra, diffuse reflectance spectra, TG analysis, EPR studies etc. All these methods are described in detail in chapter II.

4B.4. RESULTS AND DISCUSSION

4B.4.1. Chemical analysis

The results of the chemical analysis of the complex RuYDMG is given in the table 4B.1. From the analytical data, it is clear that the Si/Al ratio of 2.6 is retained here

as in the case of ruthenium exchanged zeolite. There is well-documented evidence of the retention of the zeolite framework on encapsulation of metal complexes through flexible ligand method[48, 49]. The ruthenium content in the complex is found to be very low as only a portion of the metal present in RuY has undergone complexation with DMG within the voids of zeolite cages. The rest of the metal ions were removed by ion exchange with NaCl solution. The low content of metal ion might be one of the reasons for the enhanced catalytic activity of the encapsulated complexes. Similar to simple DMG complexes, we expect a ligand to metal ratio of 2. But it was found to be slightly less than the expected value of 2 as traces of free metal ions remain in the zeolite lattice evenafter back exchange with Na^+ ions. However metal ions present in trace quantities do not have any profound effect on the spectral and magnetic properties of the encapsulated complexes as reported earlier[50].

Table 4B.1. Analytical Data of the Encapsulated Complexes

Sample	% Si	% Al	% Na	% Ru	% C	% H	% N
RuY	20.49	8.02	6.28	1.98			
RuYDMG	20.11	8.35	6.72	0.90	0.36	2.87	0.21

4B.4.2. Surface area and pore volume

The loss in surface area and pore volume of the encapsulated DMG complex of ruthenium in comparison with RuY is given in table 4B.2. The surface area decreases by 22.43% and pore volume decreases by 15.3%. The pronounced lowering of these values is a strong proof for the encapsulation of metal complexes inside the zeolite cavities[51].

Table 4B.2. Surface area and pore volume data

Sample	Surface area (m^2/g)	% Loss	Pore volume (cc/g)	% Loss
RuY	682		0.35	
RuYDMG	529	22.43	0.30	15.30

4B.4.3. X-ray diffraction patterns

The XRD pattern of RuYDMG is found to be very much similar to that of RuY and it is presented in the figure 4B.2. The similarity in the patterns indicate that the zeolite framework remain uncollapsed during the synthesis of the complex. The XRD patterns are a good indicator of the crystallinity of the complex.

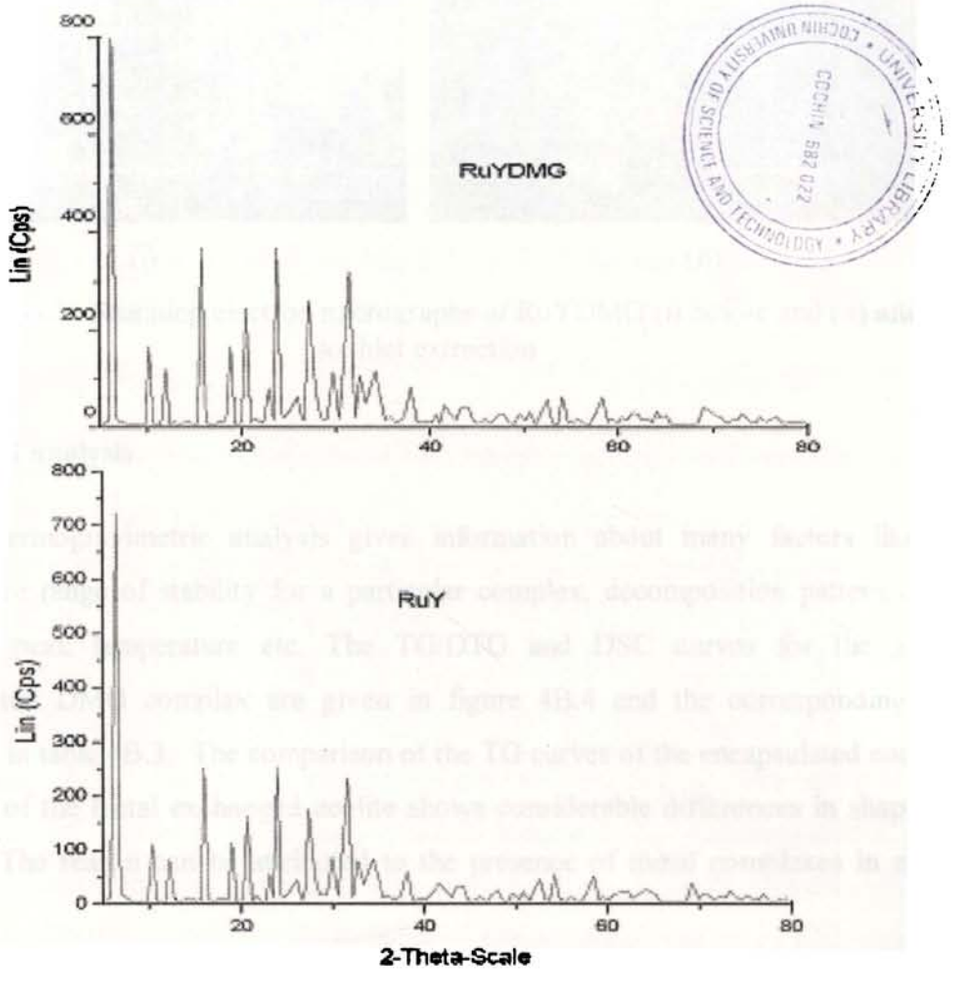

Figure 4B.2. XRD patterns of RuY and RuYDMG

4B.4.4. SEM analysis

The scanning electron micrographs of the complex taken before and after soxhlet extraction with methanol are given in the figure 4B.3. The clear zeolite surfaces of the encapsulated complex after soxhlet extraction indicate that the surface species present can be removed[52, 53].

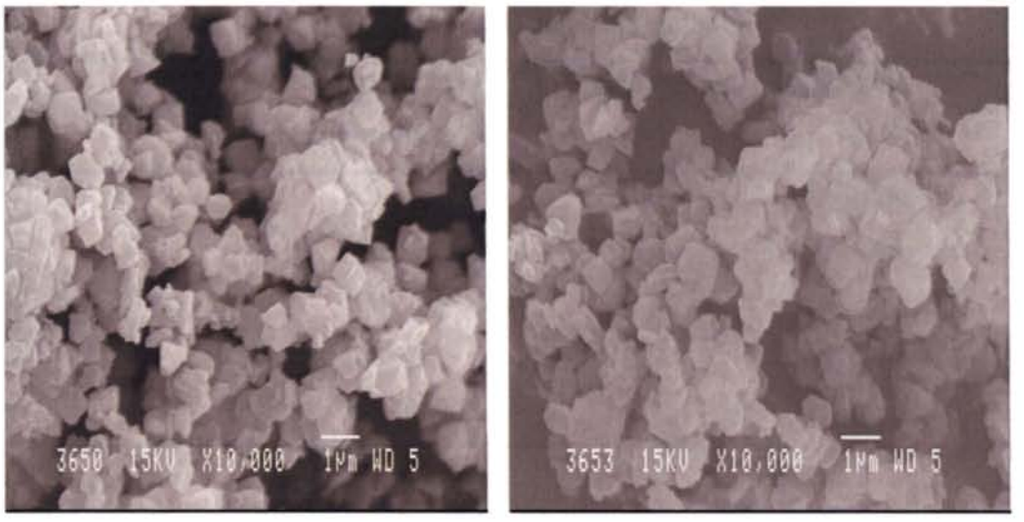

(i) (ii)

Figure 4B.3. Scanning electron micrographs of RuYDMG (i) before and (ii) after soxhlet extraction

4B.4.5. TG analysis

Thermogravimetric analysis gives information about many factors like the temperature range of stability for a particular complex, decomposition pattern of the complex, peak temperature etc. The TG/DTG and DSC curves for the zeolite encapsulated DMG complex are given in figure 4B.4 and the corresponding data presented in table 4B.3. The comparison of the TG curves of the encapsulated complex with that of the metal exchanged zeolite shows considerable differences in shape and pattern. The reason can be attributed to the presence of metal complexes in zeolite cavities.

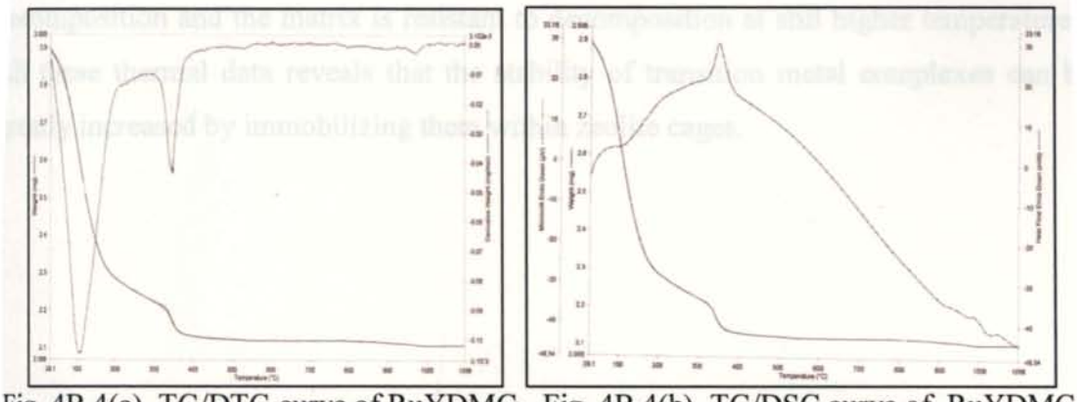

Fig. 4B.4(a) TG/DTG curve of RuYDMG Fig. 4B.4(b) TG/DSC curve of RuYDMG

Table 4B.3. TG/DSC data of RuYDMG

Complex	Temp. range of decomposition (°C)	Weight loss (%)	Nature of DSC curve
RuYDMG	35-100	16.9	Endothermic
	100-300	17.8	Endothermic
	300-500	2.8	Endothermic
	500-800	2.9	Endothermic
	800-1000	2.1	Exothermic

There are many factors influencing the nature of decomposition of the complex. These factors include the nature of the atmosphere employed for analysis, the nature and size of the sample under study, the physical state of the sample, the heating rate etc.

The compound is stable at room temperature. The decomposition starts at 35°C and the major decomposition is observed between 35°C and 300°C. The mass loss in the temperature range 35 – 300°C is due to the removal of intrazeolite and coordinated water molecules. The DTG peak temperature for this stage is observed at 106°C. The subsequent weight loss may be due to the decomposition of encapsulated complex with the peak temperature at 344°C. The total mass loss for this complex is found to be approximately 42%. The decomposition consists of four stages. The initial stage is characterized by the removal of water, which is followed by the decomposition of the complex present in the zeolite cavities. The decomposition is almost complete when the temperature reaches 600°C. Beyond this temperature, there is no noticeable decomposition and the matrix is resistant to decomposition at still higher temperatures. All these thermal data reveals that the stability of transition metal complexes can be greatly increased by immobilizing them within zeolite cages.

4B.4.6. FTIR spectra

The IR spectra of DMG and encapsulated DMG complex are shown in figure 4B.5 and IR spectral bands of DMG and RuYDMG are presented in table 4B.4. In the case of free DMG ligand, two absorptions each have been reported for C=N and N-O vibrations. These two bands can be due to unequal C=N and N-O linkages. The D_{2h} symmetry of dimethyl glyoxime gives two types of infrared active vibrations which might be responsible for this particular behavior of the ligand.

The bands due to N-O stretching frequency occur at 980 cm^{-1} and 1143 cm^{-1} for free DMG. The bands observed at 1439 cm^{-1} and 1521 cm^{-1} can be assigned to C=N stretching vibration. In the formation of the corresponding encapsulated complex, the bands due to C=N stretching frequencies have been found to shift towards lower frequencies that suggest coordination through nitrogen atom of the ligand DMG to the metal. The band at 1439 cm^{-1} is shifted to 1411 cm^{-1} and that at 1521 cm^{-1} is shifted to 1482 cm^{-1}. The peak expected due to N-O stretching vibration is not observed in the spectrum of the complex since the broad band of the zeolite masks it.

A band around 3600 cm^{-1} in DMG is attributed to the -OH stretching frequency. In the spectra of the complex, this region does not show any significant change, as it is difficult to distinguish them from the overlap with γ_{O-H} of water molecules present in the zeolite lattice. Moreover bands at 1500-1600 cm^{-1} due to the stretching vibrations of benzene rings are seen in the spectrum of the zeolite complex. This is a clear indication of the formation of complex within the supercages of the zeolite as there are no prominent zeolite bands at this position.

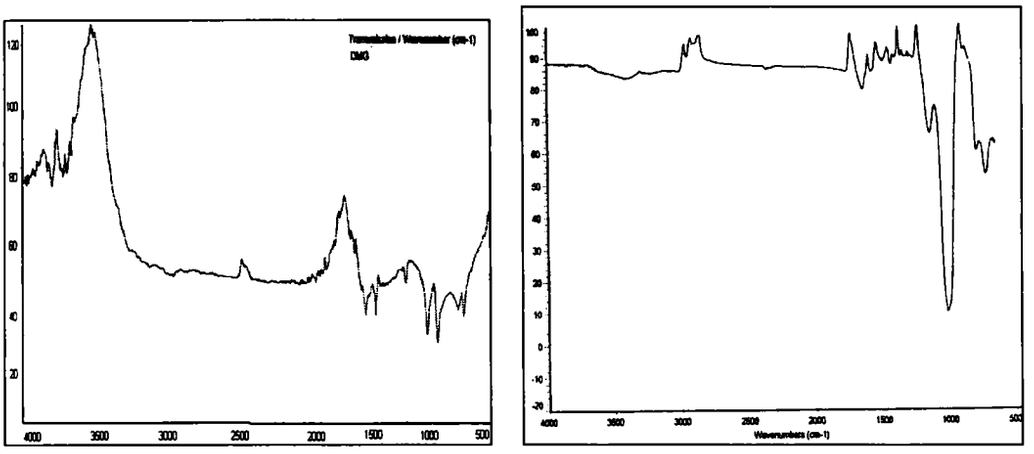

Figure 4B.5. Infrared spectra of DMG and RuYDMG

Table 4B.4. IR spectral data of DMG and RuYDMG

DMG (cm^{-1})	RuYDMG (cm^{-1})	Assignments
625	595	$\nu_{zeolite}$
708	662	
751	800	
904	1018	
980		$\nu_{N-O\ (stretch)}$
1143	1150	$\nu_{N-O\ (stretch)}$
1368		δ_{N-H}
1439	1411	$\nu_{C=N}$
1521	1482	$\nu_{C=N}$
1634	1534	$\nu_{C-O\ (H-bonded)}$
1668	1662	$\nu_{C-O\ (free)}$
1731	1726	
1759	1760	
1810		
2395	2392	
2874		
3629	3578	$\nu_{free\ O-H}$
3696	3642	
3778	3666	
3913	3790	

4B.4.7. Electronic spectra

The optical reflectance data were analysed by means of Kubelka-Munk method and they were recorded as a plot of percentage reflectance against wavelength. The electronic transitions in the DMG complex and their tentative assignments are given in the table 4B.5. Absorption bands in the spectra of all zeolite samples are of low intensity due to the low concentration of metal ions in the zeolite. Certain bands characteristic of the zeolite lattice appear in the spectra of all samples which can be due to the different overtones and various combinations of the stretching and bending vibrations of water molecules[54]. All these bands and charge transfer transitions make it rather difficult to interpret the electronic spectra.

The higher oxidising power of Ru(III) permit the intense charge transfer transitions to appear in the visible region[55] thus masking the characteristic d-d bands of very low intensity. The bands at 11350 cm^{-1} and 17390 cm^{-1} in the spectrum of RuYDMG are due to spin-forbidden d-d transitions. All these findings suggest an octahedral geometry. The oxygen atoms in the zeolite matrix may participate in the octahedral coordination[56] which can be proved from the EPR spectral data. There is no clear proof for the participation of water molecules in the coordination sphere of RuYDMG.

Table 4B.5. Electronic spectral data

Sample	Absorbance Max.		Tentative Assignments
	nm	cm^{-1}	
RuYDMG	260	38460	Charge transfer
	320	31250	$A_{2g}, {}^2T_{1g} \leftarrow {}^2T_{2g}$
	575	17390	${}^4T_{1g} \leftarrow {}^2T_{2g}$
	950	11350	${}^4T_{2g} \leftarrow {}^2T_{2g}$
	881	10530	${}^4T_{1g} \leftarrow {}^2T_{2g}$

4B.4.8. EPR spectra

The EPR spectrum of RuYDMG was recorded at liquid nitrogen temperature and it is given in the figure 4B.6.

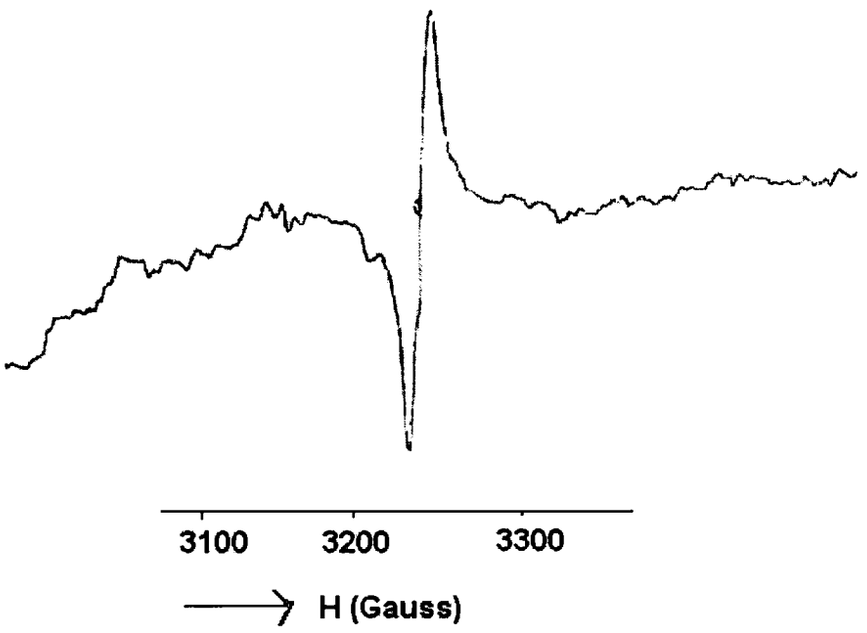

Figure 4B.6. EPR spectrum of RuYDMG

The nature of the spectrum suggests an octahedral environment for the complex. A slight anisotropy of the octahedral geometry is indicated by the $g_{\parallel}$ value of 2.14 and the $g_{\perp}$ value of 2.03.

References

1. Herron, N. Inorg.Chem. **1986**, 25, 4714.
2. Rabo, J.A.; Poutsma, M. Second. Intern. Conf. on Molecular Sieve Zeolites, Worcester **1970**, p.210.
3. Lunsford, J.H.; Vansant, E.F. J. Chem.Soc. Faraday Trans II, **1973**, 19, 1028.
4. Balkus, K.J.Jr.; Gabrielov, A.G. J. Inclusion Phenom. Mol. Recogn. Chem. 1995, 21,159.
5. Quayle, W.H.; Lunsford, J.H. Inorg. Chem. **1982**, 21, 97.
6. Quayle, W.H.; Peeters, G.; De Roy, G.L.; Vansant, E.F.; Lunsford, J.H. Inorg. Chem. **1982**, 21, 2226.
7. Edgardo, P.M.; Nyole, G.; Fabio, L.; Acosta, D.D.; Pasquale, P.; Aldo, L.G.; Patricio, R.; Bernard, D. J. Phys. Chem. **1933**, 97, 12819.
8. Delabie, A.; Pierloot, K.; Groothaert, M.H.; Weckhuysen, B.M.; Schoonheydt, R.A. Microporous and Mesoporous Materials, **2000**, 37, 209.
8. Kortum, G. Reflectance Spectroscopy: Principles, Methods and Applications, Springer - Verlag, Berlin, **1969**.
10. Kellerman, R.; Diffuse Reflectance and Photoacoustic Spectroscopies, Delgan, W.N.; Haller, G.L.; Kellerman, R.; Lunsford, J.H. (Eds.) Spectroscopy in Heterogeneous Catalysis , Academic Press, New York, **1979**, 86.
11. Schoonhydt, R.A. Diffuse reflectance Spectroscopy, Delanny, F.(Ed.); Characterization of Catalysis, Marcel Dekker, New York, **1984**, P-220.
12. Lever, A.B.P. "Inorganic Electronic Spectroscopy", Elsevier, Amsterdam, **1984.**
13. Chinnusamy, V.; Muthusamy, G.; Natarajan, K. Synth.React.Inorg.Met.-Org.Chem. **1994**, 24, 4, 561-564.
14. Viswanathamurthi, P.; Natarajan, K. Synth. React. Inorg. Met.-Org. Chem. **1998**, 28,437-447.
15. Ramesh, R.; Suganthy, P.K.; Natararajan, K. Synth. React. Inorg. Met.-Org. Chem. **1996**, 26 (1) 47-60.

16. Schrauzer, G.N. Acc. Chem. Res. **1968**, 97 I.

17. Nemeth, S.; Szeverenvi, Z.; Simandi, L.I. Inorg. Chim. Acta. **1980**, 44 L, 107.

18. Nemeth, S.; Simandi, L.I. J. Mol. Catal. **1982**, 14, 87.

19. Diegruber, H.; Plath, P.J.; Schulz- Ekloff, G. J. Mol. Catal ; **1984**, 24, 115.

20. Tollman, C.; Herron, H. Symposium on Hyrocarbon Oxidation, 194th National Meeting of the American Chemical Society, New Orleans, LA, **1987**, Aug 30-Sept 4.

21. Tschugaev, Z. Anorg. Chem. **1905**, 46, 144.

22. Prushan, M.J.; Addison, A.W.; Butcher, R.J. Inorg. Chim. Acta, **2000**, 300, 992.

23. Luneau, D.; Oshio, H.; Okawa, H.; Kidas, S. J. Chem. Soc. Dalton Trans, **1990**, 2283.

24. Lance, K.A.; Goldsky, K.A.; Busch, D.H. Inorg. Chem. **1990**, 29, 2428.

25. Muller, J.G.; Grzybowski, J.J.; Takeuchi, K.J. Inorg. Chem. **1986**, 25, 2665.

26. Pomposo, F.; Stynes.D.V. Inorg. Chem. **1983**, 22, 569.

27. Bakac, A.; Brynildson, M.E.; Espenson, J.H. Inorg. Chem. **1986**, 25, 4108.

28. Chakravorty, A. Coord. Chem. Rev, **1974**, 13, 1.

29. Schrauzer, G.N.; Sibert, J.W. J. Am. Chem. Soc. **1970**, 92, 7078.

30. Toscano, P.J.; Seligson, A.L.; Curran, M.T.; Skrobutt, A.T.; Sonenberger, D.C. Inorg. Chem. **1989**, 28, 166.

31. Schrauzer, G.N.; Sibert, J.W. J. Am. Chem. Soc. **1970**, 92, 1551.

32. Tovrog, B.S.; Kitko, D.J.; Drago, R.S. J. Am. Chem. Soc. **1976**, 98, 5144.

33. Rochinbauer, A.; Eyor, M.; Kwiecinsky, M.; Tyrlik, S. Inorg. Chim. Acta, **1982**, 58, 237.

34. Okamoto, T.; Oka, S. Tetrahedron Lett., **1981**, 22, 2191.

35. Nemeth, S.; Simandi, L. J. Mol. Catal., **1982**, 14, 87.

36. Ovcharenko, V.I.; Fokin, S.V.; Reznikov, V.A.; Ikorskii, V.V.; Romanenko, G.V.; Sagdeev, R.Z. Inorg. Chem.**1998**, 37, 2104.

37. Xu, D.; Gu, J.; Xu, L.; Liang, K.; Xu, Y. Polyhedron, **1998**, 17, 231.

38. Birkelbach, F.; Weyhermuller, T.; Lengen, M.; Gerdan, M.; Trautwein, A.X.; Weighdart, K.; Chaudhuri, P. J. Chem. Soc. Dalton Trans, **1997**, 4529.

39. Gul, A.; Bekaroglu, O. J. Chem. Soc. Dalton Trans., **1983**, 2537.

40. Ahsen, V.; Gokceli, F.; Bekaroglu, O. J. Chem. Soc. Dalton Trans., **1987**, 1827.

41. Ozean, E.; Mirzaoglu, R. Synth. React. Inorg. Met.- Org.Chem., **1988**, 18, 559.

42. Tas, E.; Ulusoy, M.; Guler, M. Synth. React. Inorg. Met.- Org. Chem., **2004**, 37 (7) 1221.

43. Vural, U.S.; Sevindir, H.C. Macromol. Rep. **1994**, A31(Suppl.5), 673.

44. Kilic, A.; Tas, E.; Gumgum, B.; Yilmaz, I. Journal of Coordination Chem, **2007**, 60, 11, 1233-1246.

45. Khan, M.M.T.; Kureshy, R.I.; Khan, N.H. J.Coord.Chem..**1993**, 28, 67-72.

46. Fukuchi, T.; Miki, E.; Mizumachi, K.; Isimov, K. Chem. Lett., **1987**, 1133.

47. Diegruber, H.; Plath, P.J.; Schulz-Ekloff, G. J. Mol. Catal. **1984**, 24, 115.

48. Strutz, J.; Diegruber, H.; Jaeger, N.I.; Moseler, R. Zeolites, 3, **1983**, 102.

49. Mizun, K.; Lunsford, J.H. Inorg. Chem. **1983**, 22, 3483.

50. Enrist, S.; Traa, Y.; Deeg, O. Stud. Surf. Sci and Catal. **1994**, 84B, 925.

51. Mukherjee, A.K.; Ray, P. J. Ind. Chem .Soc. **1955**, 32 , 581.

52. Thomas, J.M.; Catlow, C.R.A. Progr. Inorg. Chem. **1988**, 35, I.

53. Raja, R.; Ratnasamy, P. J. Catal. **1997**, 170, 244.

54. Klier, K.; Kellerman, R.; Hutta, P.J. J. Chem. Phys. **1974**, 61, 4224.

55. Greenwood, N.N.; Earnshaw, A. 'Chemistry of the Elements', Pergamon Press, **1984**.

56. Diegruber, H.; Plath, P.J. Stud. Surf. Sci. and Catal. **1982**, 12 , 23.

Chapter V

ZEOLITE-Y ENCAPSULATED RUTHENIUM COMPLEXES OF THE SCHIFF BASES DERIVED FROM PYRIDINE CARBOXALDEHYDES

Chapter V

ZEOLITE-Y ENCAPSULATED RUTHENIUM COMPLEXES OF THE SCHIFF BASES DERIVED FROM PYRIDINE CARBOXALDEHYDES

5.1. INTRODUCTION

The ligands of the type C_5H_4N-2-CH=N-C_6H_4-p-X where X= H, Me, OMe, Cl, NO_2, COOH prepared by the condensation of pyridine-2-carboxaldehyde with different aromatic amines act as a series of N, N'- donor Schiff base ligands and form half sandwich pentamethylcyclopentadienyl ruthenium(II) phosphine complexes[1]. The spectral studies on complexes with the ligand N-2-pyridylmethylidine-2-hydroxy-phenylamine obtained by the reaction of pyridine-2-carboxaldehyde with 2-aminophenol revealed a distorted octahedral geometry[2]. Mixed chelate ruthenium(III) complexes were synthesized using tridentate Schiff base ligands derived by condensation of pyridine-2-carboxaldehyde with 2-aminobenzoic acid and their catalytic efficiency examined in oxidation reactions for cyclohexene, cyclohexane, cyclohexanol, toluene and benzyl alcohol.

In view of the interesting properties of Schiff base complexes, zeolite encapsulated ruthenium complexes of the Schiff bases N,N'-bis(3-pyridylidene)-1,2-phenylenediamine (PCO); N,N'-bis(3-pyridylidene)-1,4-phenylenediamine (PCP) ; N,N'-bis(2-pyridylidene)-1,2-phenylenediamine (CPO) and N,N'-bis(2-pyridylidene)-1,4-phenylenediamine (CPP) derived from the reactions of pyridine carboxaldehydes with ortho and para-phenylenediamines have been synthesized. The present chapter gives a detailed picture of the synthesis and characteristic properties of ruthenium complexes with the Schiff bases PCO, PCP, CPO and CPP.

EXPERIMENTAL

The method of preparation of the ligands PCO, PCP, CPO and CPP are ented in chapter II. The structures of the ligands are given in figures 5.1- 5.4. The enium exchanged zeolite for the synthesis of encapsulated complexes was prepared ɪrding to the ion exchange method.

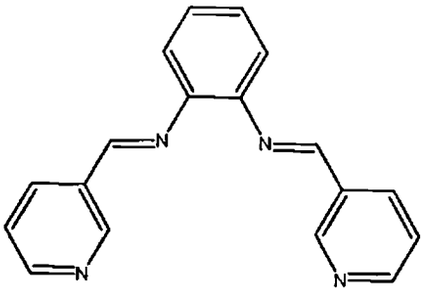

Figure 5.1. Structure of N,N'-bis(3-pyridylidene)-1,2-phenylenediamine (PCO)

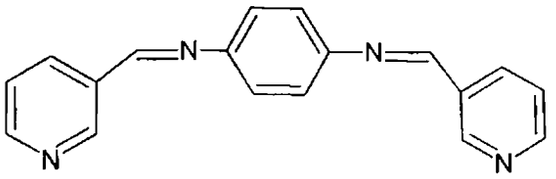

Figure 5.2. Structure of N,N'-bis(3-pyridylidene)-1,4-phenylenediamine (PCP)

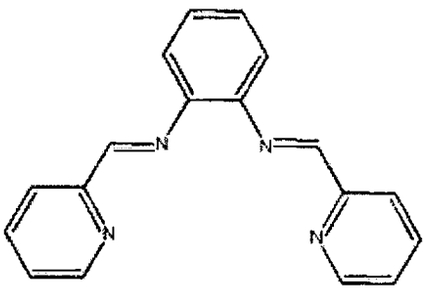

Figure 5.3. Structure of N,N'-bis (2-pyridylidene)-1,2-phenylenediamine (CPO)

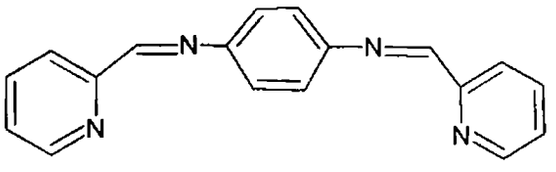

Figure 5.4. Structure of N,N'-bis (2-pyridylidene)-1,4-phenylenediamine (CPP)

5.2.1. Synthesis of zeolite encapsulated ruthenium complexes of N,N'-bis (3-pyridylidene)-1,2-phenylenediamine(PCO); N,N'-bis(3-pyridylidene)-1,4-phenylenediamine (PCP); N,N'-bis (2-pyridylidene) -1,2-phenylenediamine (CPO); N,N'-bis (2-pyridylidene)-1,4-phenylenediamine (CPP)

The zeolite encapsulated metal complexes of PCO, PCP, CPO and CPP were prepared by adopting the flexible ligand method[3]. The ligand was dissolved in ethanol and the metal exchanged zeolite was added to it corresponding to a ligand to metal ratio of approximately 2:1. The mixture was refluxed on a water bath for about 6 hours. The ligands form complexes inside the zeolite cages by breaking the metal- lattice oxygen bonds[4]. The complexes obtained were filtered and then soxhlet extracted with methanol until the extracting solvent became colourless to remove the free ligand and the complexes formed on the surface of the zeolite. The purified complexes were then stirred with 0.1 M NaCl for 24 hours to re-exchange the uncomplexed metal ion. The complexes were finally dried at 100°C and kept over anhydrous calcium chloride in a desiccator.

5.3. ANALYTICAL METHODS

The details of the various analytical methods employed to characterize the synthesized metal complexes are given in chapter II.

5.4. RESULTS AND DISCUSSION

5.4.1. Chemical analysis

The analytical data of the different Schiff base complexes are given in table 5.1. The percentages of carbon, hydrogen and nitrogen in the encapsulated complexes suggest the formation of metal complexes inside the zeolite cages. The information about the CHN values indicate the complexes as placed inside the supercages of the zeolite framework. The silica- alumina ratio of the zeolite complexes is 2.6, which is in the range typical of zeolite Y. This rules out the possibility of loss in crystalline nature of the zeolite framework on encapsulation as reported in earlier studies[5, 6]. The metal percentages were determined by ICP-AES method but the exact percentage of metal in the complexes cannot be found out accurately as there are remote chances for some

of complexes within the zeolite pores. The lowering of surface area is usually interpreted as due to the blocking of zeolite pores[9-11] as revealed by studies conducted by Balkus and Gabrielov. Thus zeolites in addition to the expected benefits of conventional hybrid catalysts can play a major catalytic role by imposing high diffusional selectivity, altered stereochemistry and stabilization of encapsulated structures[12]. The drastic decrease of surface area values is a clear evidence for the formation of encapsulated complexes[13]. The surface area and pore volume data are represented in table 5.2.

Table 5.2. Surface area and pore volume data

Sample	Surface area (m^2/g)	% Loss	Pore volume (cc/g)	% Loss
RuY	682		0.35	
RuYPCO	306	55.13	0.18	47.92
RuYPCP	296	56.60	0.17	49.36
RuYCPO	386	43.40	0.22	36.80
RuYCPP	361	47.07	0.20	43.32

5.4.3. X-ray diffraction patterns

X ray powder diffraction method can be effectively used to identify the zeolite structure[14] and its crystalline nature, estimation of the purity of individual zeolites and determination of the unit cell parameters[15]. The XRD patterns of the encapsulated Ru(III) complexes are given in figure 5.5. The comparison of these patterns with the parent zeoliteY and the metal exchanged zeolite indicates that the crystalline structure of the parent zeolite is well maintained even after the process of encapsulation. Similar observations have been made earlier in the case of zeolite encapsulated complexes[16-18]. But there are chances for the collapse[19] of zeolite framework if the pH of the medium is less than four.

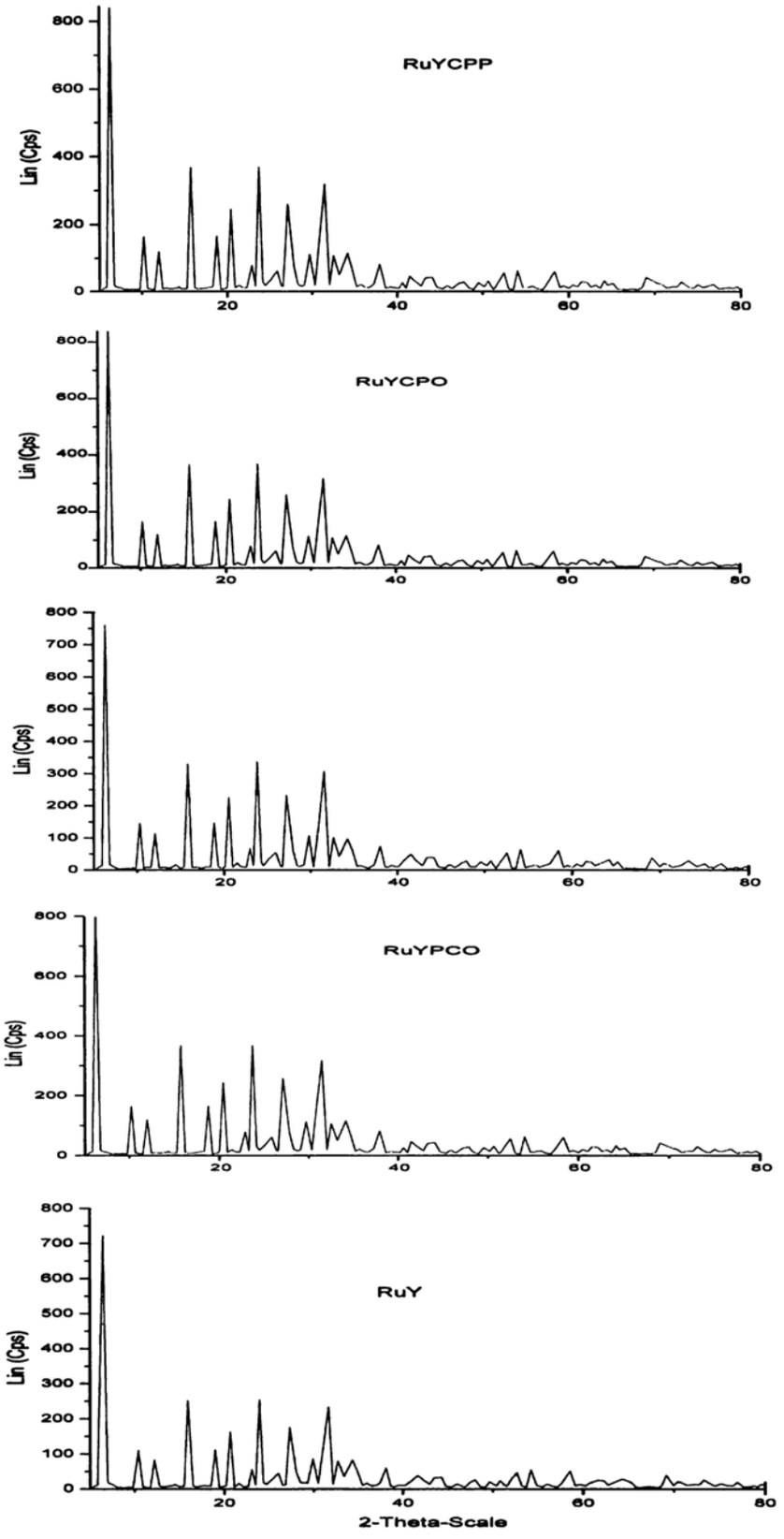

Figure 5.5. XRD patterns of (i) RuY (ii)RuYPCO (iii) RuYPCP(iv) RuYCPO (v) RuYCPP

5.4.4.SEM analysis

The scanning electron micrographs of the encapsulated complexes taken before and after soxhlet extraction are represented in figures 5.6 and 5.7. They indicate the absence of complexes on the external surface. SEM of the supported complexes is a clear evidence of the formation of well-defined complex structures free of metal ions or complexes on the external surface after soxhlet extraction. The extraneous species adsorbed on the surface of the zeolite can be successfully removed by soxhlet extraction with the correct solvent. The major advantage of this method of purification is that only the surface adsorbed species are removed by this method. This is due to the trapping of complexes inside the supercages of the zeolite, which hinders their ability to come out.

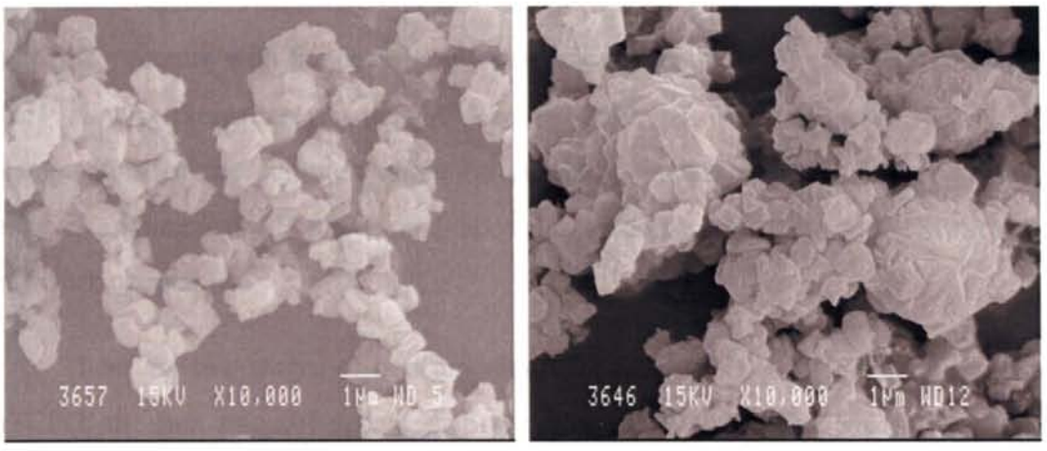

(i) (ii)

Figure 5.6. Scanning electron micrographs of RuYPCO (i) before and (ii) after soxhlet Extraction

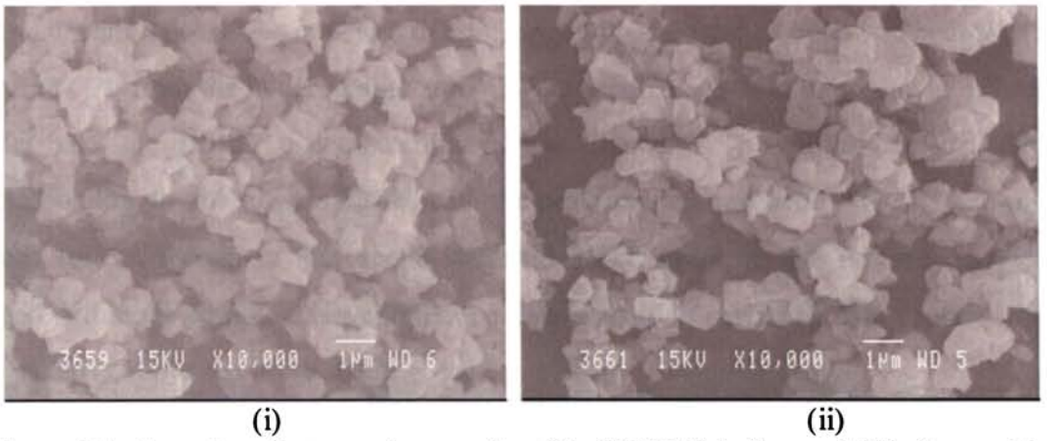

(i) (ii)

Figure 5.7. Scanning electron micrographs of RuYCPP (i) before and (ii) after soxhlet extraction

5.4.5. TG analysis

TGA and DSC were used to characterize metal complexes encapsulated in zeolite. The TG/DTG and DSC curves obtained for the encapsulated PCO, PCP, CPO and CPP complexes in an atmosphere of nitrogen at a heating rate of 10°C per minute are represented in figures 5.8-5.11 and the data are tabulated in table 5.3. Two stages of decomposition are observed for RuYPCO. The first stage in the temperature range of 40-180°C corresponds to the loss of coordinated water along with the physisorbed water. The percentage mass loss of 2.4 in the temperature range 180-600°C is consistent with the decomposition of the synthesized complex. For RuYPCP, during the initial stage of decomposition starting from 40°C and continuing till 200°C, a weight loss of 22.9% has occurred. This stage indicates the removal of water entrapped in the cages of the zeolite structure with the peak temperature occurring at 105°C. The decomposition occurs slowly thereafter. A weight loss of 2.6% is observed upto 400°C. The decomposition of the complex might be occurring in this region. Then a constant weight is maintained till 850°C and above this temperature the destruction of the framework occurs.

There are two stages of decomposition for both CPO and CPP complexes. In RuYCPO, the first stage of decomposition occurs till 200°C. The weight loss during this initial stage of 40-200°C is 23.7% and the peak temperature is 100°C. The above weight loss can be due to the removal of occluded water present in the sample. The second broad peak in the range of 200-350°C representing the steady loss of about 2.9% is an indication of the decomposition of the organic part of the complex. The mass loss for RuYCPP from the initial temperature till 200°C corresponds to the removal of lattice water and the partial decomposition of the ligand. The difference in weight corresponding to this stage is 22.8% with the peak temperature being 111°C. The small steady loss of weight in the second stage till 300°C confirms the destruction of the ligand within the complex. Beyond that no decomposition occurs till 900°C after which the collapse of the zeolite structure occurs.

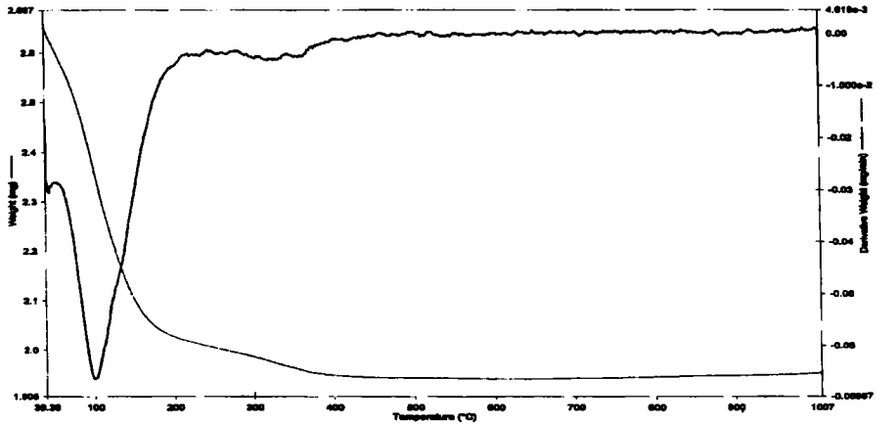

Figure 5.8.(a) TG/DTG of RuYPCO

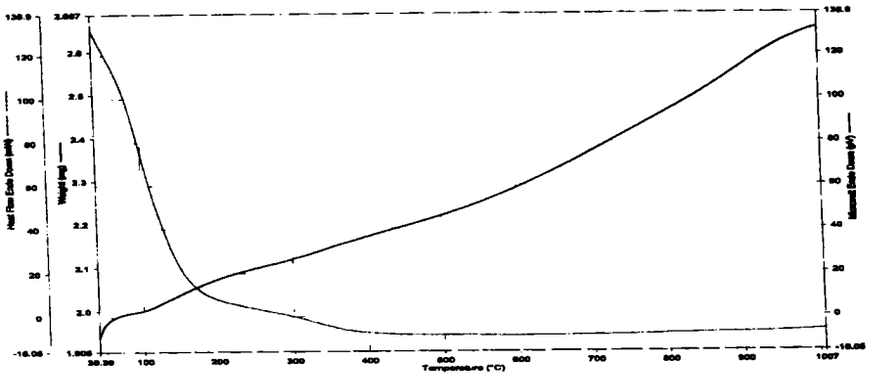

Figure 5.8.(b) TG/DSC of RuYPCO

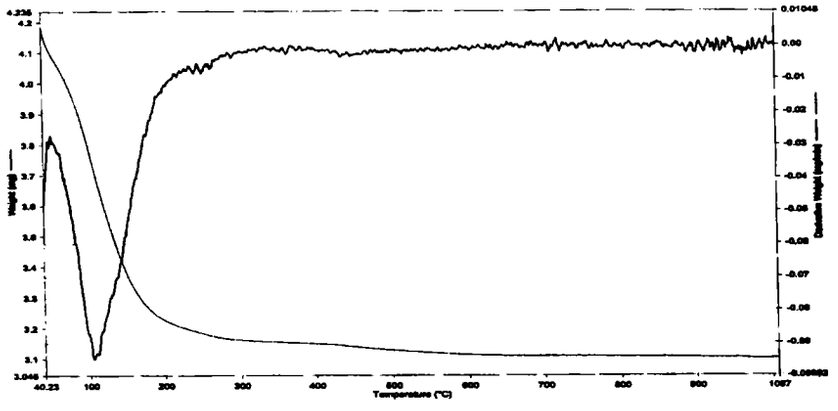

Figure 5.9.(a) TG/DTG of RuYPCP

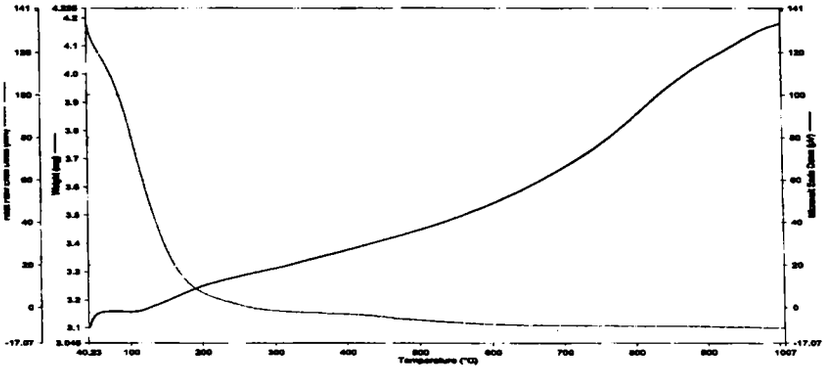

Figure 5.9.(b) TG/DSC of RuYPCP

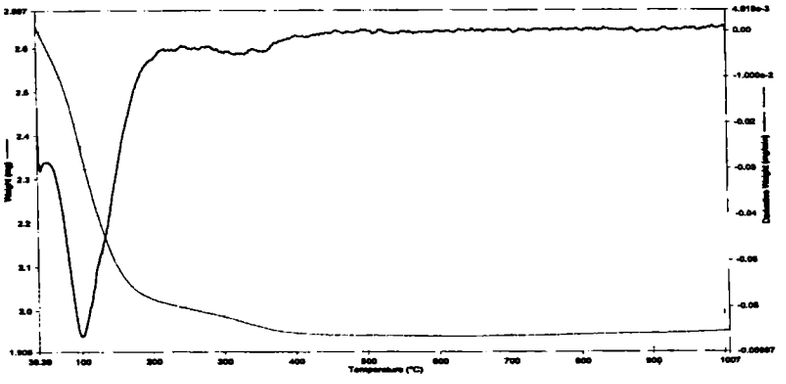

Figure 5.10.(a) TG/DTG of RuYCPO

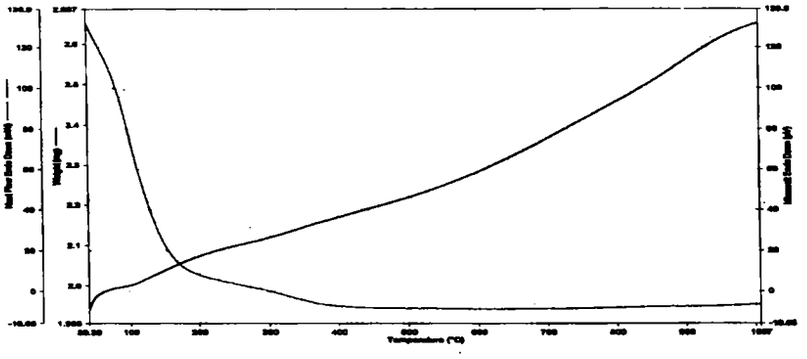

Figure 5.10.(b) TG/DSC of RuYCPO

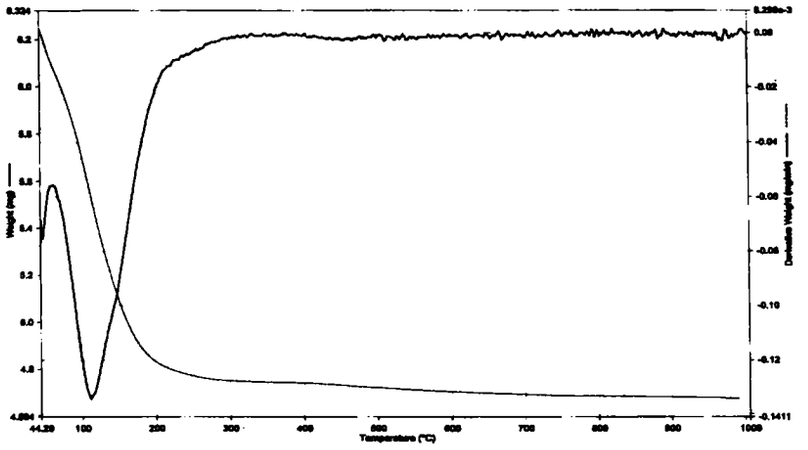

Figure 5.11.(a) TG/DTG of RuYCPP

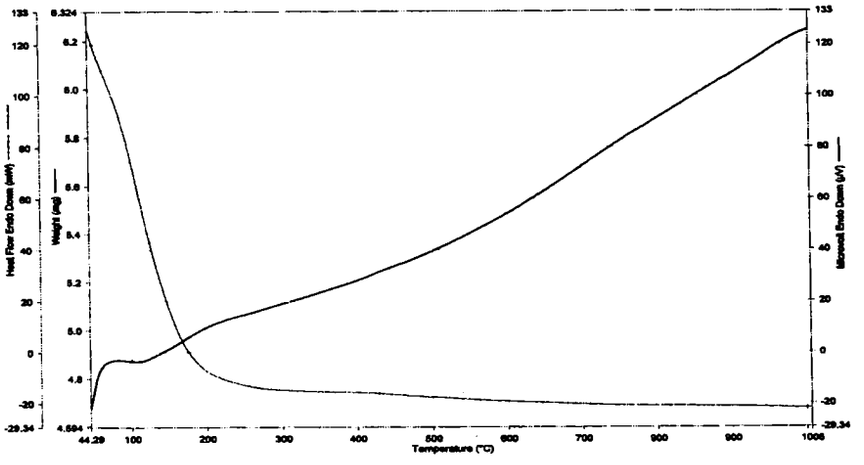

Figure 5.11.(b) TG/DSC of RuYCPP

Table 5.3. TG/ DTA data of encapsulated complexes

Compound	Temperature range (°C)	Weight loss (%)	Nature of DSC curve
RuYPCO	40-180	21.8	Endothermic
	180-600	2.4	Exothermic
RuYPCP	40-200	22.9	Endothermic
	200-600	2.6	Exothermic
RuYCPO	40-200	23.7	Endothermic
	200-700	2.9	Exothermic
RuYCPP	44-200	22.8	Endothermic
	200-650	2.0	Exothermic

5.4.6. FTIR spectra

The IR spectra of the ligands and their corresponding encapsulated complexes are given in figures 5.12- 5.15. The spectral data are presented in the table 5.4 and 5.5.

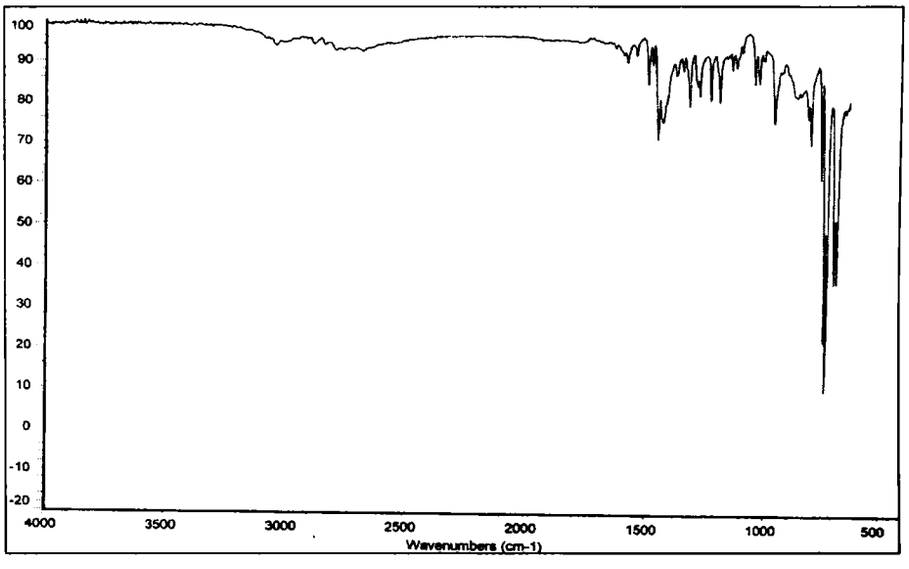

Figure 5.12. IR spectrum of PCO

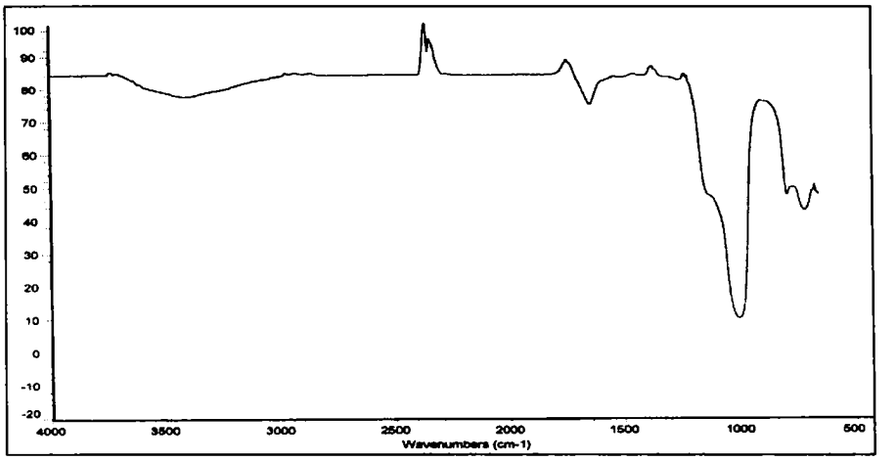

Figure 5.12. IR spectrum of RuYPCO

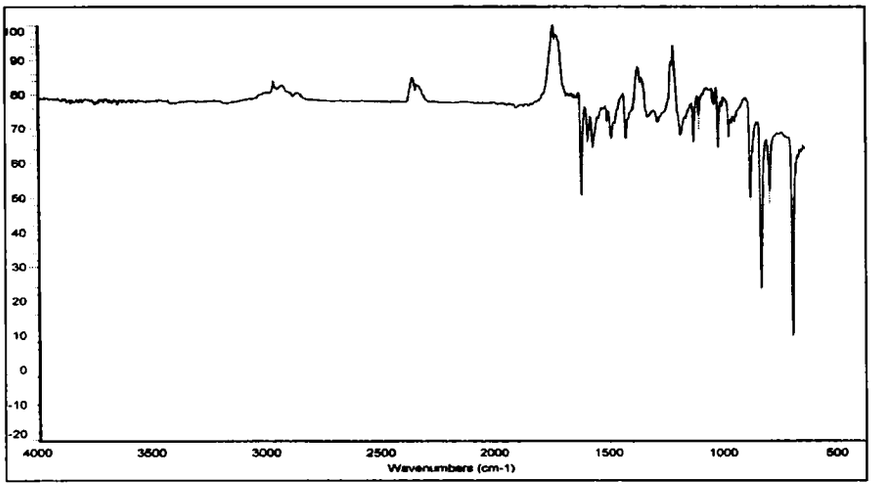

PCP

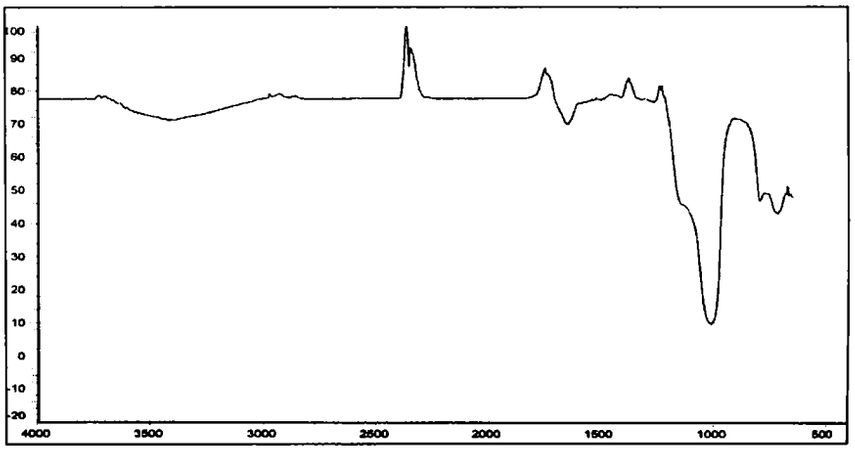

Figure 5.13. IR spectra of PCP and RuYPCP

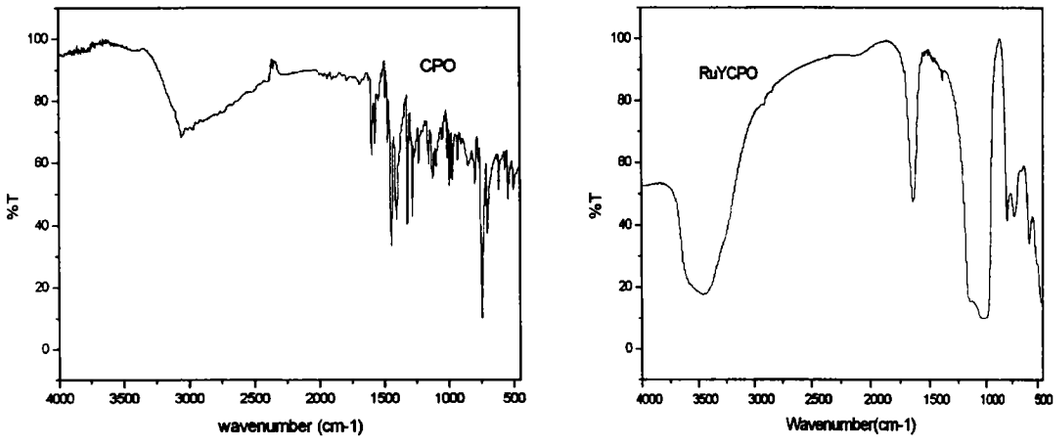

Figure 5.14. IR spectra of CPO and RuYCPO

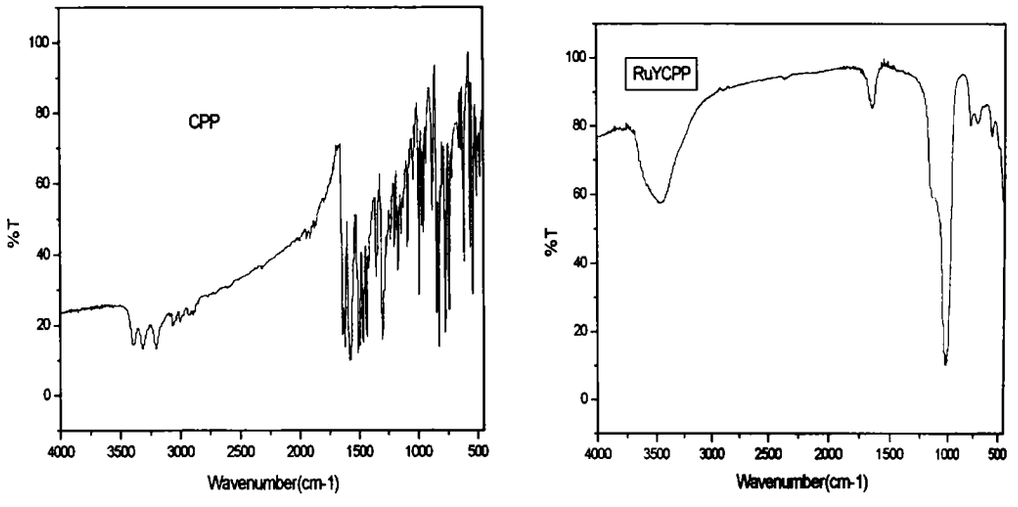

Figure 5.15. IR spectra of CPP and RuYCPP

Table 5.4. IR spectral data of PCO, RuYPCO, PCP and RuYPCP.

PCO (cm^{-1})	RuYPCO (cm^{-1})	Assignments	PCP (cm^{-1})	RuYPCP (cm^{-1})	Assignments
712	714		701	714	
754			799	789	
769	789		837		
812			882		
961			976		
	1001	$\nu_{zeolite}$		1005	$\nu_{zeolite}$
1025		ν_{O-H}	1023		ν_{O-H}
1043		ν_{C-N}	1106		
1190			1130		
1228			1187		
1273			1286		
1316			1424		
1427			1489		δ_{NH}
1448			1569		
1489			1590	1570	$\nu_{C=N}$
1540		δ_{NH}	1619	1638	$\nu_{O-H(stretch)}$
1578	1556	$\nu_{C=N}$		2345	
	1639	$\nu_{O-H(stretch)}$			
	2345				

The stretching vibration due to the presence of azomethine nitrogen seen at 1578 cm^{-1} in the spectrum of the pure ligand PCO is shifted to the lower energy region of about 1556 cm^{-1} in the spectrum of the corresponding encapsulated complex indicating the involvement of azomethine nitrogen in coordination. The peak at 1043 cm^{-1} can be attributed to ν_{C-N} of the ligand. However this band is not visible in the encapsulated complex and could be due to the fact that they are obscured by the broad zeolite bands found around 1000 cm^{-1}. There are some bands seen around 700 cm^{-1} that can be due to the rocking and wagging modes of water. The bands at 1639 cm^{-1} and around 3000 cm^{-1} in the spectrum of RuYPCO is due to the OH stretching and bending vibrations of water. Many peaks of the ligand can be seen in the zeolite-encapsulated complexes in the region where the zeolite peaks are not present. This is a clear indication of trapping of metal complexes within the supercages of the zeolite framework.

The band at 1590 cm^{-1} in the spectrum of PCP is due to $\nu_{C=N}$ vibration. The encapsulated complex RuYPCP shows a red shift of about 20 cm^{-1} in the band due to azomethine group, which suggests that the ligand is coordinated to the metal atom through this nitrogen. Corresponding to the OH bending vibration of water, bands are observed around 1638 cm^{-1}. Most bands characteristic of the ligands are masked by the broad asymmetric stretching mode of the internal tetrahedra in the zeolite framework. As in the case of PCO complex, the band at 1005 cm^{-1} masks the peak due to ν_{C-N}.

There is a peak at 1592 cm^{-1} in the spectrum of the ligand, CPO which is attributed to the azomethine nitrogen of the ligand. On complexation, this band is found to be shifted to lower frequencies of about 1576 cm^{-1}, which confirms that the azomethine nitrogen is coordinated to the metal. The peak at 1045 cm^{-1} is due to ν_{C-N} of the ligand. It is not seen in the zeolite-encapsulated complex, RuYCPO as the broad zeolite band around 1024 cm^{-1} obscures them. The zeolite peaks are more intense than those of the ligands in the encapsulated complexes. The asymmetric stretching vibrations of $(Si/Al)O_4$ units of the zeolite structure contributes the band seen at 1024 cm^{-1}. Similar bands are observed at 1638 and 3463 cm^{-1} for the zeolite structure. The stretching due to the OH groups of the zeolite is shown by the broad band around 3000cm^{-1}.

Table 5.5. IR spectral data of CPO, RuYCPO, CPP and RuYCPP

CPO (cm^{-1})	RuYCPO (cm^{-1})	Assignments	CPP (cm^{-1})	RuYCPP (cm^{-1})	Assignments
401			407		
430	458		478	462	
499			507		
540			540		
566	577		614	577	
614			717		
701	723		738	715	
743			776		
796	791		829	818	ν_{coord} H_2O
828	820	ν_{coord} H_2O	882	790	
928			992		
971				1022	$\nu_{zeolite}$
			1039		ν_{C-N}
994			1087		
	1024	$\nu_{zeolite}$	1120	1114	ν_{symC-C}
1045		ν_{C-N}			
1121			1167		
1151	1135	ν_{symC-C}	1229		
1227			1295		
1260			1352	1355	δ_{NH}
1279			1434		$\nu_{C=C}$
1315	1324	δ_{NH}	1458		
1401	1384		1512		
1441		$\nu_{C=C}$	1581	1541	$\nu_{C=N}$
1467			1622		
1488			1638	1640	
1568			1911		
1592	1576	$\nu_{C=N}$	1945		
	1638	$\nu_{zeolite}$			
1685			3065		
3056			3205		
	3463	$\nu_{zeolite}$			
			3315		
			3391	3454	$\nu_{zeolite}$

The IR spectra of all encapsulated complexes are characterized by bands in the region 1500-1600 cm^{-1} due to stretching vibrations of benzene rings. No zeolite bands are present at this region, so these bands confirm the formation of encapsulated complexes. The peak at 1581 cm^{-1} due to the presence of azomethine nitrogen in CPP shows blue shift to a lower frequency of 1541 cm^{-1} in the spectrum of the complex RuYCPP indicating the involvement of that nitrogen in the encapsulation of the complex. The bands due to NH can be assigned in the region around 3300-3400 cm^{-1}, which undergo slight change of frequency in the encapsulated complexes due to changes in environment brought about by the coordination of ligand with the metal.

5.4.7. Electronic spectra

The ground state of d^5 Ru(III) ion with t^5_{2g} electronic configuration is $^2T_{2g}$. The first excited doublet levels in the order of increasing energy are $^2A_{2g}$ and $^2T_{1g}$ due to $t^4_{2g}e^1_g$ configuration[20]. The electronic spectra of the complexes show some characteristic bands in the 230-300 nm region which can be assigned as charge transfer bands. The prominent charge transfer bands of the type $L_{\pi y} \rightarrow t_{2g}$ lying in the low energy region obscure the weaker d-d transitions. The other bands occurring at 550-400nm have been assigned to $^2T_{2g} \rightarrow {}^2A_{2g}$ transitions. These transitions are in confirmity with assignments made for similar octahedral Ru(III) complexes[21, 22]. The nature of the electronic spectra and the assignment of the bands point towards an octahedral geometry around the ruthenium ion in the complexes[23]. The data obtained from the electronic spectra and the corresponding assignments are represented in the table 5.6.

Table 5.6. Electronic Spectral Data

Sample	Absorbance Max.		Tentative Assignments
	nm	cm^{-1}	
RuYPCO	238	42020	Charge transfer
	310(sh)	32260	$^2A_{2g}, {}^2T_{1g} \leftarrow {}^2T_{2g}$
	430	23260	$^2E_g \leftarrow {}^2T_{2g}$
	605(sh)	16530	$^4T_{1g} \leftarrow {}^2T_{2g}$
	880(sh)	11360	$^4T_{2g} \leftarrow {}^2T_{2g}$
	944	10590	$^4T_{1g} \leftarrow {}^2T_{2g}$
RuYPCP	240	41670	Charge transfer
	308(sh)	32470	$^2A_{2g}, {}^2T_{1g} \leftarrow {}^2T_{2g}$
	436	22940	$^2E_g \leftarrow {}^2T_{2g}$
	610(sh)	16390	$^4T_{1g} \leftarrow {}^2T_{2g}$
	878(sh)	11390	$^4T_{2g} \leftarrow {}^2T_{2g}$
	945	10580	$^4T_{1g} \leftarrow {}^2T_{2g}$
RuYCPO	244	40980	Charge transfer
	309(sh)	32360	$^2A_{2g}, {}^2T_{1g} \leftarrow {}^2T_{2g}$
	449	22270	$^2E_g \leftarrow {}^2T_{2g}$
	600(sh)	16670	$^4T_{1g} \leftarrow {}^2T_{2g}$
	892(sh)	11210	$^4T_{2g} \leftarrow {}^2T_{2g}$
	955	10470	$^4T_{1g} \leftarrow {}^2T_{2g}$
RuYCPP	240	41670	Charge transfer
	305(sh)	32790	$^2A_{2g}, {}^2T_{1g} \leftarrow {}^2T_{2g}$
	447	22370	$^2E_g \leftarrow {}^2T_{2g}$
	612(sh)	16340	$^4T_{1g} \leftarrow {}^2T_{2g}$
	880(sh)	11360	$^4T_{2g} \leftarrow {}^2T_{2g}$
	950	10530	$^4T_{1g} \leftarrow {}^2T_{2g}$

5.4.8. EPR spectra

The Ru(III) system with d^5 configuration is a good probe of the geometry and the nature of coordination in encapsulated complexes as the g values obtained from the EPR spectra are found to be really sensitive to very small changes occurring during the linkage of the metal to the ligand[24]. The solid state EPR spectra of the ruthenium complexes were recorded at room temperature. The EPR absorption in the ground state of the molecules corresponds to transitions between the lowest Kramer's doublet levels. Each of the complexes exhibits two g values (table 5.7.) indicating anisotropic nature of the encapsulated complexes. The EPR spectra are represented in figures 5.16- 5.19.

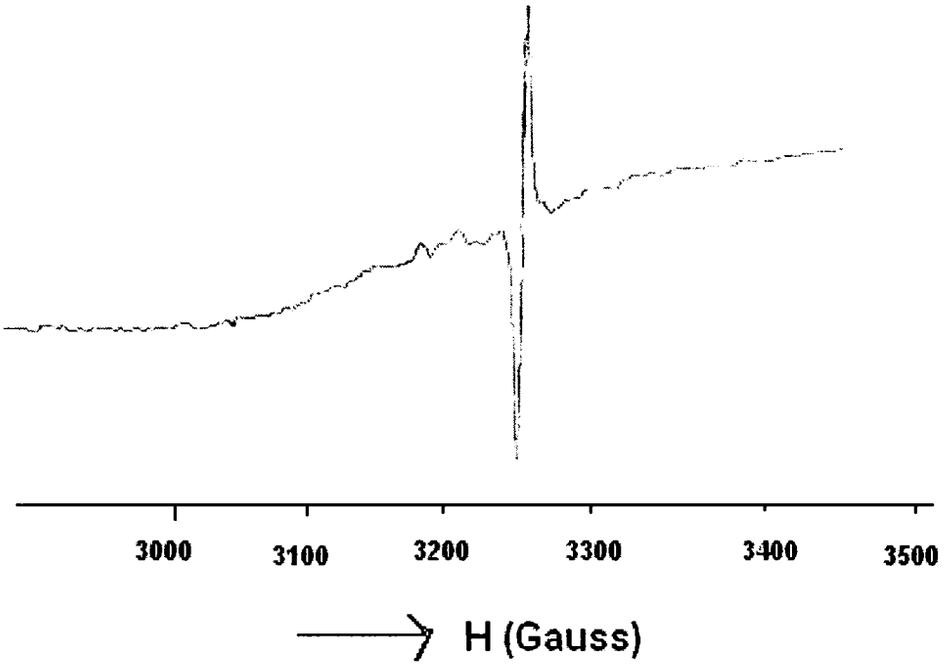

Figure 5.16. EPR spectrum of RuYPCO

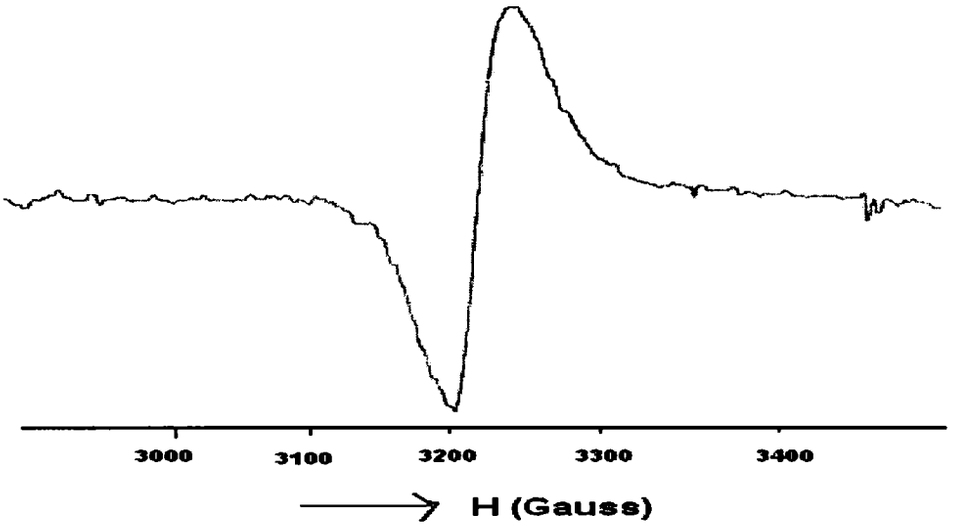

Figure 5.17. EPR spectrum of RuYPCP

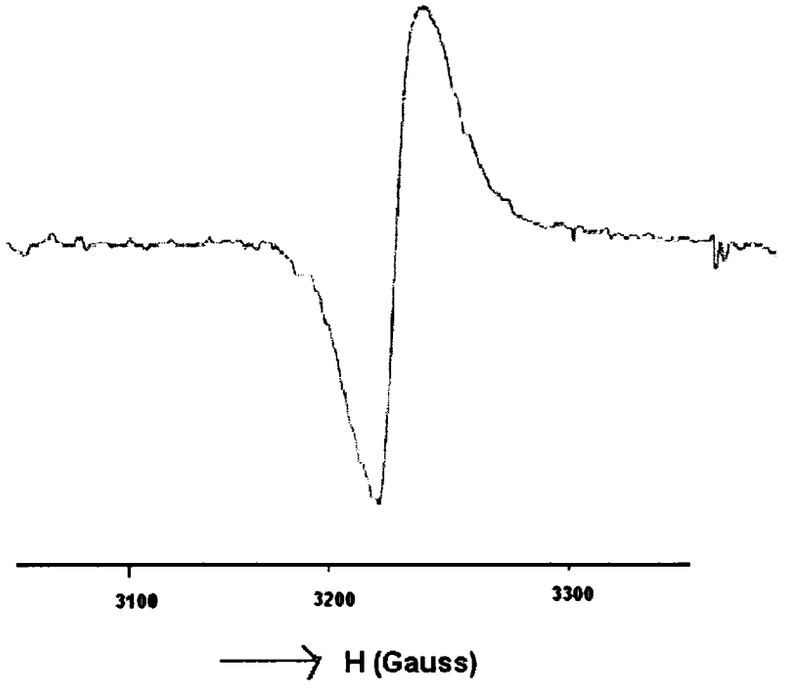

Figure 5.18. EPR spectrum of RuYCPO

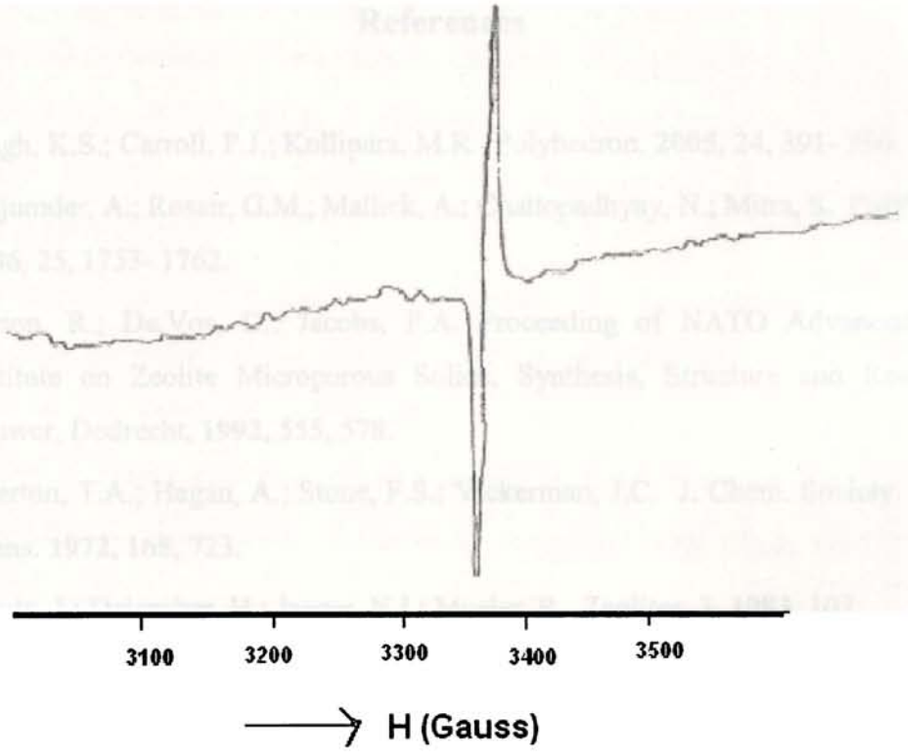

Figure 5.19. EPR spectrum of RuYCPP

Table 5.7. EPR spectral parameters

Complex	EPR parameters
RuYPCO	$g_{\parallel} = 2.03$; $g_{\perp} = 2.14$
RuYPCP	$g_{\parallel} = 2.05$; $g_{\perp} = 2.18$
RuYCPO	$g_{\parallel} = 2.13$; $g_{\perp} = 2.05$
RuYCPP	$g_{\parallel} = 2.11$; $g_{\perp} = 2.14$

The EPR spectral data suggest the possibility of an octahedral geometry for ruthenium complexes[25] and the existence of ruthenium in +3 state.

References

1. Singh, K.S.; Carroll, P.J.; Kollipara, M.R. Polyhedron. **2005**, 24, 391- 396.
2. Majumder, A.; Rosair, G.M.; Mallick, A.; Chattopadhyay, N.; Mitra, S. Polyhedron. **2006**, 25, 1753- 1762.
3. Parton, R.; De.Vos, D.; Jacobs, P.A. Proceeding of NATO Advanced study institute on Zeolite Microporous Solids, Synthesis, Structure and Reactivity, Kluwer, Dodrecht, **1992**, 555, 578.
4. Egerton, T.A.; Hagan, A.; Stone, F.S.; Vickerman, J.C. J. Chem. Society. Farady Trans. **1972**, 168, 723.
5. Strutz, J.; Deigruber, H.; Jaeger, N.I.; Mosler, R. Zeolites, 3, **1983**, 102.
6. Mizuno, K.; Lunsford, J.H. Inorg. Chem. **1983**, 22, 3483.
7. Kumar, M.; Asian J. Chem.6, **1994**, 3, 576.
8. Kumar, M.; Arabinda Kumar, S. Asian. J. Chem. 6, **1994**, 4, 782.
9. Balkus, Jr. K.J.; Gabrielov, A.G. J. Inclusion Phenom. Mol. Recogn. Chem. **1995**, 21, 159.
10. Varkey, S.P.; Jacob, C.K. Ind. J. Chem. **1998**, 37A, 407.
11. Paez-Mozo, E.; Gabiunas, N.; Luccaccioni, F.; Acosta, D.D.; Patrono, P.; Ginestra, A.L.; Ruiz, P.; Delmon, B. J. Phys. Chem. **1993**, 97, 12819.
12. Bein,T.; Jacobs, P.A. J. Chem. Soc. Faraday Trans. **1983**, 79, 1819; **1984**, 80, 1391.
13. Paez-Mozo, E.; Gabriunas, N.; Lucaccioni, F.; Acosta, D.D.; Patrono, P.; Ginestra, A.L.; Ruz, P.; Delmon, B. J. Phys. Chem. **1993**, 97, 12819.
14. Ballmoos, R.V. Collection of simulated XRD powder patterns for zeolites, b Butterworths, London , **1984**.
15. Szostak, R. Molecular Seives: Principles of Synthesis and Identification , Van Nostrand Reinhold, New York, **1989**, 83.

16. Xavier, K.O.; Chacko, J.; Yusuff, K.K.M. J. Mol. Catal. A: Chemical, **2002**, 178, 275.

17. Meyer, G.; Wohrle, D.; Mohl.; Schulz- Ekloff.G. Zeolites, **1984**, 4, 30.

18. Phani, K.L.N.; Pitchumani, S.; Ravichandran, S. Langmuir, **1993**, 9, 2455.

19. Menon, P.G. Lectures on Catalysis, 41st Ann. Meeting, Ind. Acad. Science, Ed:S. Ramasheshan, **1971**.

20. Jayabalakrishnan, C.; Karvembu, R.; Natarajan, K. Synthesis and Reactivity in Inorganic and Metal-organic chemistry, **2002**, 32, 6, 1099-1113.

21. Boucher, L.J. Inorg. Nucl. Chem. **1974**, 36, 531.

22. Ramesh, R. Inorg. Chem. Communication. **2004**, 7, 274-276.

23. Dharmaraj, N.; Natarajan,K. Synth. React. Inorg. Met - Org. Chem. **1997**, 27, 601-618.

24. Mehdi, O.K.; Agarwala, U. Inorg. Chem. **1980**, 19,5.

25. Khan, M.M.T.; Srinivas,D.; Kureshy,R.I.; Khan.,N.H. Inorg. chem. **1990**, 29, 2320-2326.

Chapter VI

CATALYTIC ACTIVITY OF ZEOLITE ENCAPSULATED COMPLEXES IN THE DECOMPOSITION OF HYDROGEN PEROXIDE

Chapter VI

CATALYTIC ACTIVITY OF ZEOLITE ENCAPSULATED COMPLEXES IN THE DECOMPOSITION OF HYDROGEN PEROXIDE

6.1. INTRODUCTION

Hydrogen peroxide is industrially and chemically important since it participates in a variety of reactions. It is used as an oxidant for the synthesis of fine chemicals, drugs and pharmaceuticals.[1-3] and serves as the source of oxygen in many oxidation and epoxidation reactions. Controlled partial oxidation is found to be more effective with sacrificial oxidants[4] such as hydrogen peroxide or alkylhydroperoxides than with molecular oxygen or air[5-9]. These sacrificial oxidants have been used in catalytic systems involving tailored transition-metal complexes or metal substituted polyoxometalates either in a homogeneous state encapsulated in molecular sieves or anchored to the inner surfaces of mesoporous silica[10-14].

The decomposition of hydrogen peroxide is represented by the standard reaction,

$$2\,H_2O_2 \rightarrow 2\,H_2O + O_2$$

Many transition metal complexes are known to catalyze the above reaction and the rate of catalysis is greatly affected by the nature and structure of the heterogeneous complexes. The decomposition of hydrogen peroxide is considered as a standard reaction to test the catalytic activity of metal complexes and the activity of metal complexes in this particular reaction can be compared to the action of enzymes like catalase and peroxidase[15].

6.2. EXPERIMENTAL

6.2.1. Materials used

Zeolite encapsulated ruthenium complexes of anthranilic acid, 4-aminobenzoic acid, dimethylglyoxime, SSC, SOD, SPD, PCO, PCP, CPO and CPP are used for catalytic studies. The details regarding the synthesis of pure complexes, metal exchanged zeolites and zeolite-encapsulated metal complexes have been described earlier. Hydrogen peroxide solution (30%, Merck) was used without further purification.

6.2.2. Procedure for the decomposition of hydrogen peroxide

Hydrogen peroxide was taken in a reaction vessel of 50 ml capacity placed on a magnetic stirrer. All the encapsulated complexes selected for catalytic study were activated by heating to about 120°C for two hours. The required amount of catalyst was placed over the H_2O_2 in a plastic float. The catalytic activity was studied by noting the oxygen evolved and a gas burette was used for collecting the evolved oxygen. The gas burette was filled with 20% sodium chloride solution acidified with dilute hydrochloric acid and coloured using methyl red. The levels of solution in both arms of the burette were equalized at zero and the reaction flask was sealed. The reaction was initiated by switching on the magnetic stirrer. Then the catalyst got dispersed in H_2O_2 solution and the reaction progresses. The decomposition of hydrogen peroxide liberates oxygen and the evolved oxygen gets collected in the right arm of the gas burette. The volume of oxygen collected was noted at intervals of 5 minutes and the experiment was continued for 60 minutes. The reaction was then followed under different conditions by varying different parameters like the amount of catalyst, volume of hydrogen peroxide, the polarity of the solvent and addition of certain solvents. The used catalysts were recovered, washed with acetone and heated at 120°C for 2 hours and reused. The experimental set up used is given in figure 6.1.

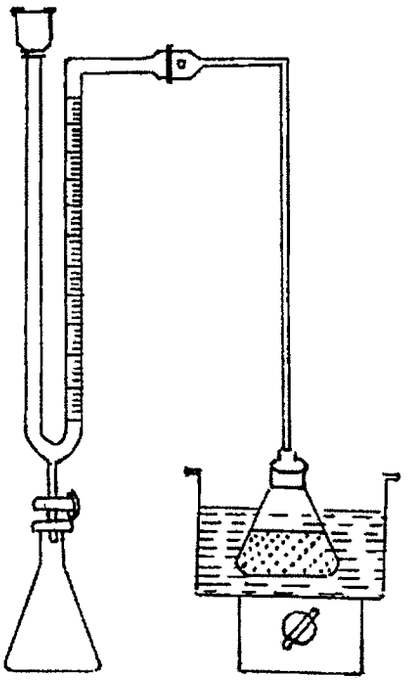

Fig.6.1. Experimental set up for the study of hydrogen peroxide decomposition

6.3. RECYCLING STUDIES

The used catalysts were separated from the reaction mixture, washed with acetone several times and dried at 120°C for two hours in an oven. The decomposition reaction was then carried out in the presence of recycled catalysts in order to check the leaching of metal ions. Characterization of the recycled catalysts was done using XRD, IR and electronic spectroscopy. The similarity of the XRD patterns of the fresh catalysts with that of the recycled catalysts indicated the retention of their crystalline nature even after the reaction. The IR and electronic spectra of the recycled catalysts were similar to those of fresh sample, which suggests that the zeolite-encapsulated complexes undergo no change in their structure even after the regeneration process.

RESULTS

4.1. Screening studies

Zeolite encapsulated ruthenium complexes of anthranilic acid (AA), 4-aminobenzoic acid (ABA), dimethylglyoxime (DMG) and the Schiff bases SSC, SOD, SPD, PCO, PCP, CPO and CPP were evaluated for their activity in the decomposition of 30% H_2O_2 at room temperature. The results of the screening studies are given in table 6.1. Further the percentage conversions are represented graphically in figure 6.1. The catalytic activity exhibited by the complexes employed for the reaction study has been explained in terms of the redox potential of the metal ion and geometry of the complexes[16, 17]. The activity exhibited by the synthesized Ru(III) complexes might be probably due to favourable redox potentials.

Table 6.1
Activity of various zeolite encapsulated complexes in the decomposition of 30% H_2O_2 at room temperature

Serial no:	Catalyst used	Activity of the catalyst (ml min^{-1} $mmol^{-1}$)
	RuY	41.82
1	RuYSSC	348.6
2	RuYSOD	185.9
3	RuYSPD	173.3
4	RuYAA	101.8
5	RuYABA	100.6
6	RuYDMG	116.2
7	RuYPCO	123.6
8	RuYPCP	88.2
9	RuYCPO	179.9
10	RuYCPP	179.3

Reaction conditions:

Amount of catalyst	10 mg
Volume of H_2O	10 ml
Volume of 30% H_2O_2	10 ml
Temperature	30°C
Time	60 minutes

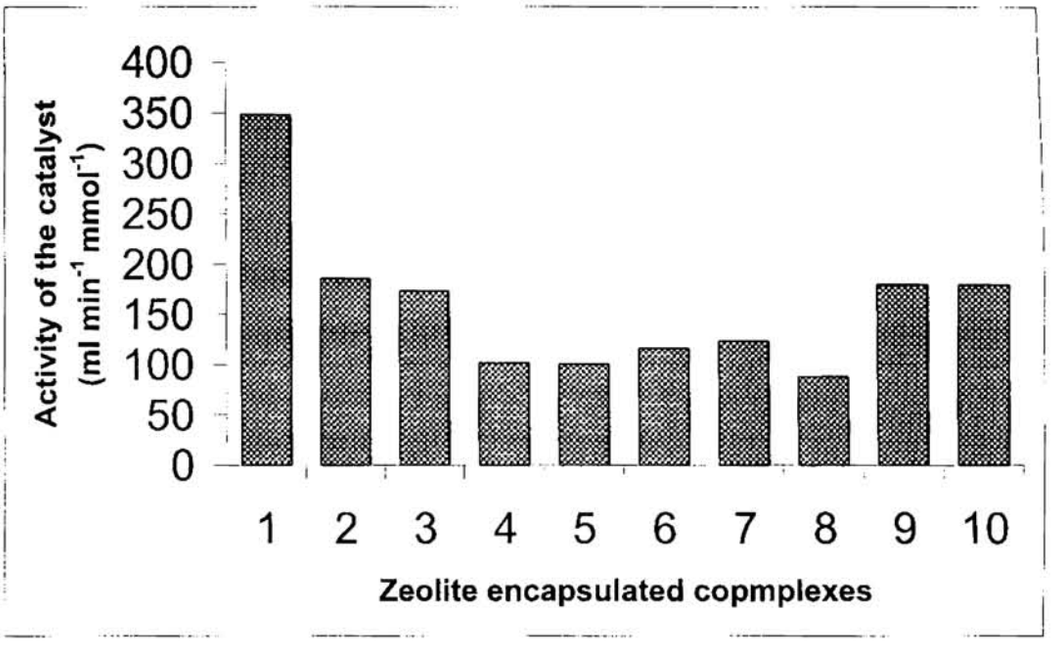

Figure 6.1. Screening study using all the zeolite encapsulated complexes in the decomposition of hydrogen peroxide.

From the data it can be seen that RuYSSC is the most active catalyst and RuYPCP is the least active. The comparison of the catalytic activities of RuYAA and RuYABA shows there is only a slight difference in their activities. The catalytic effect largely depends on the type of ligand used.

6.4.2. Blank run

The blank test for the decomposition reaction was conducted under the conditions same as that of screening studies. But no catalyst was added for the reaction. No measurable volume of oxygen was collected even after 60 minutes. Ruthenium exchanged zeolite was then used to study the decomposition reaction under identical conditions.

6.4.3. Effect of various parameters on the decomposition of H_2O_2

The different factors influencing the decomposition reaction were studied in order to have a clear picture of the nature of the various catalysts used. The influence of the following parameters on the decomposition reaction was studied.

1. Amount of catalyst
2. Volume of H_2O_2 used
3. Solvent polarity of the reaction mixture
4. Addition of pyridine
5. Using recycled catalyst

6.4.3.1. Effect of the amount of catalyst

The influence of the amount of catalyst on the reaction was studied. For this purpose, the amount of catalyst was increased from 10 mg to 30 mg keeping all other factors the same. The decomposition reaction was conducted for all the complexes under the same conditions. It can be observed that when the amount of catalyst was increased, there was an increase in activity. The results obtained are shown in table 6.2 and represented graphically in figure 6.2.

Table 6.2

Effect of the amount of catalyst on the decomposition of H_2O_2

Serial. No:	Zeolite encapsulated complex	Activity of the catalyst (ml min^{-1} $mmol^{-1}$)		
		Amount of catalyst (mg)		
		10	20	30
1	RuYSSC	348.6	450.3	711.8
2	RuYSOD	185.9	276.4	340.1
3	RuYSPD	173.3	262.6	340.8
4	RuYAA	101.8	130.7	188.8
5	RuYABA	100.6	137.4	194.4
6	RuYDMG	116.2	154.9	232.4
7	RuYPCO	123.6	167.1	199.8
8	RuYPCP	88.2	115.8	146.1
9	RuYCPO	179.9	236.8	274.7
10	RuYCPP	179.3	240.9	292.2

Reaction conditions:

Volume of H_2O	10 ml
Volume of 30% H_2O_2	10 ml
Temperature	30°C
Time	60 minutes

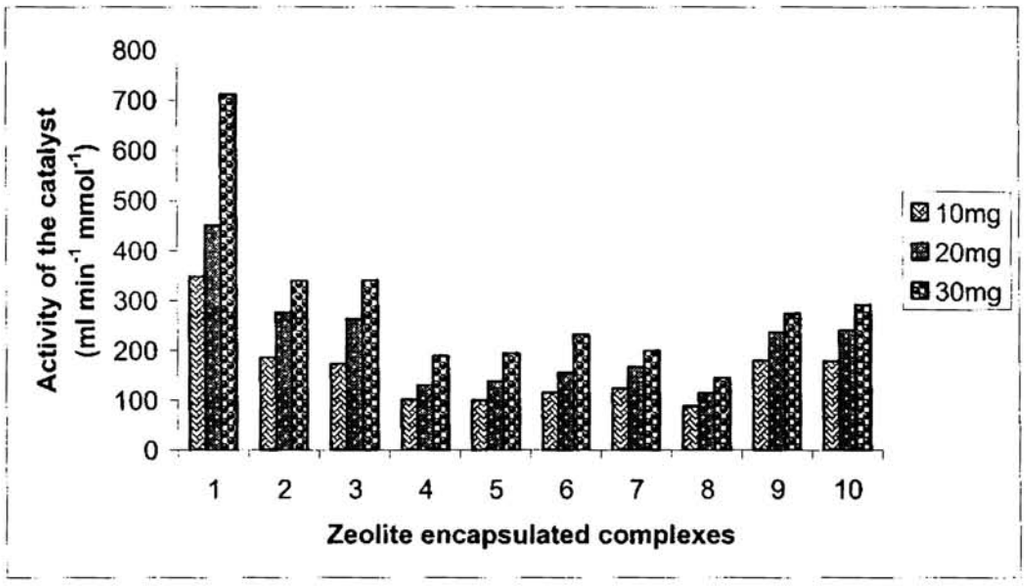

Figure 6.2. Effect of the amount of catalyst in the decomposition of hydrogen peroxide.

6.4.3.2. Effect of the volume of H_2O_2

The influence of the amount of hydrogen peroxide on the decomposition reaction was studied by varying the amount of H_2O_2 keeping the total volume of hydrogen peroxide and water mixture constant. All the other reaction conditions were kept the same. The results of these reactions with different complexes are given in table 6.3 and the graphical representation in figure 6.3. From the data obtained, it was observed that when the volume of H_2O_2 increases, the activity also increases for all complexes.

Table 6.3

Effect of H_2O_2: H_2O volume ratios on the decomposition of hydrogen peroxide

Serial. no:	Zeolite encapsulated complex	Activity of the catalyst (ml min^{-1} $mmol^{-1}$)			
		H_2O_2: H_2O ratio (ml)			
		5:15	10:10	15:5	20:0
1	RuYSSC	290.5	348.6	450.3	660.9
2	RuYSOD	154.1	185.9	244.5	308.3
3	RuYSPD	128.5	173.3	217.9	273.8
4	RuYAA	72.6	101.8	152.5	188.8
5	RuYABA	80.5	100.6	154.2	181.0
6	RuYDMG	92.0	116.2	154.9	232.4
7	RuYPCO	105.3	123.6	188.9	247.0
8	RuYPCP	60.7	88.2	118.6	159.9
9	RuYCPO	132.6	179.9	265.3	312.6
10	RuYCPP	128.2	179.3	276.9	317.9

Reaction conditions:

Amount of catalyst	10 mg
Temperature	30°C
Time	60 minutes

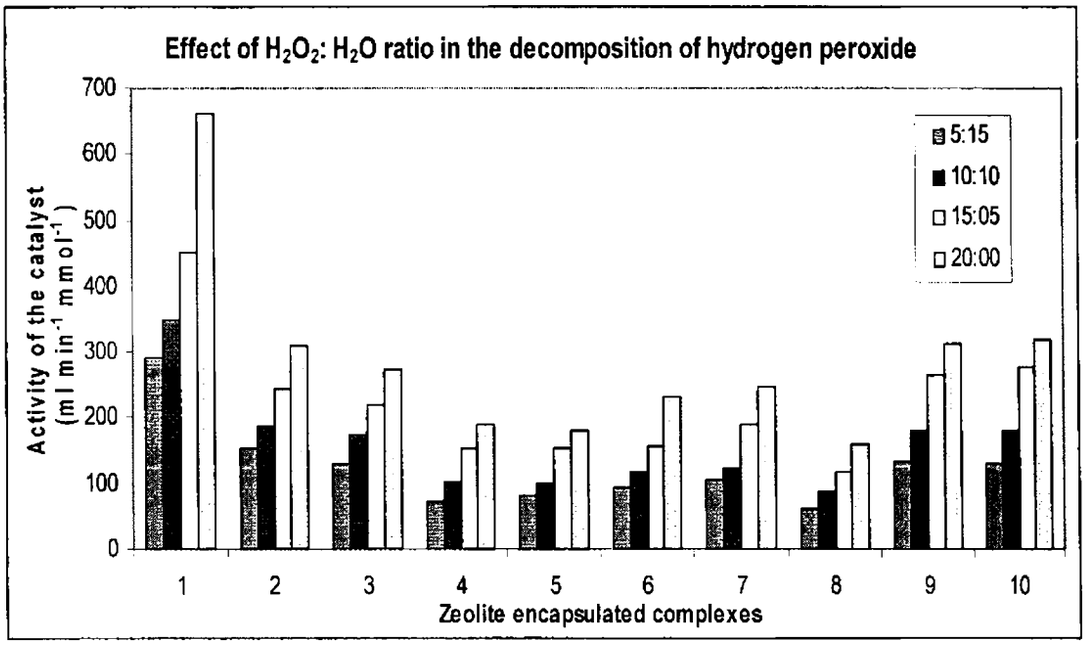

Figure 6.3. Effect of H_2O_2: H_2O ratio in the decomposition of hydrogen peroxide.

6.4.3.3. Effect of the variation of solvent polarity of the reaction mixture

The decomposition reaction was conducted by adding methanol to the reaction mixture keeping the total volume of water and methanol constant in order to study the influence of solvent polarity on the reaction rate. Table 6.4 shows the results obtained for all the complexes encapsulated inside the zeolite cages. The data is represented graphically in figure 6.4. The addition of methanol slows down the decomposition of hydrogen peroxide in all the cases.

Table 6.4

Effect of solvent polarity of the reaction mixture on the decomposition reaction

Serial. No:	Zeolite encapsulated complex	Activity of the catalyst (ml min^{-1} $mmol^{-1}$)		
		H_2O: CH_3OH ratio (ml)		
		10:0	9:1	8:2
1	RuYSSC	348.6	283.3	232.4
2	RuYSOD	185.9	116.9	79.7
3	RuYSPD	173.3	106.2	61.5
4	RuYAA	101.8	69.0	54.5
5	RuYABA	100.6	73.8	53.6
6	RuYDMG	116.2	63.0	43.6
7	RuYPCO	123.6	101.7	65.4
8	RuYPCP	88.2	60.7	41.4
9	RuYCPO	179.9	132.6	99.5
10	RuYCPP	179.3	138.4	82.0

Reaction conditions:

Amount of catalyst	10 mg
Volume of H_2O_2	10 ml
Temperature	30°C
Time	60 minutes

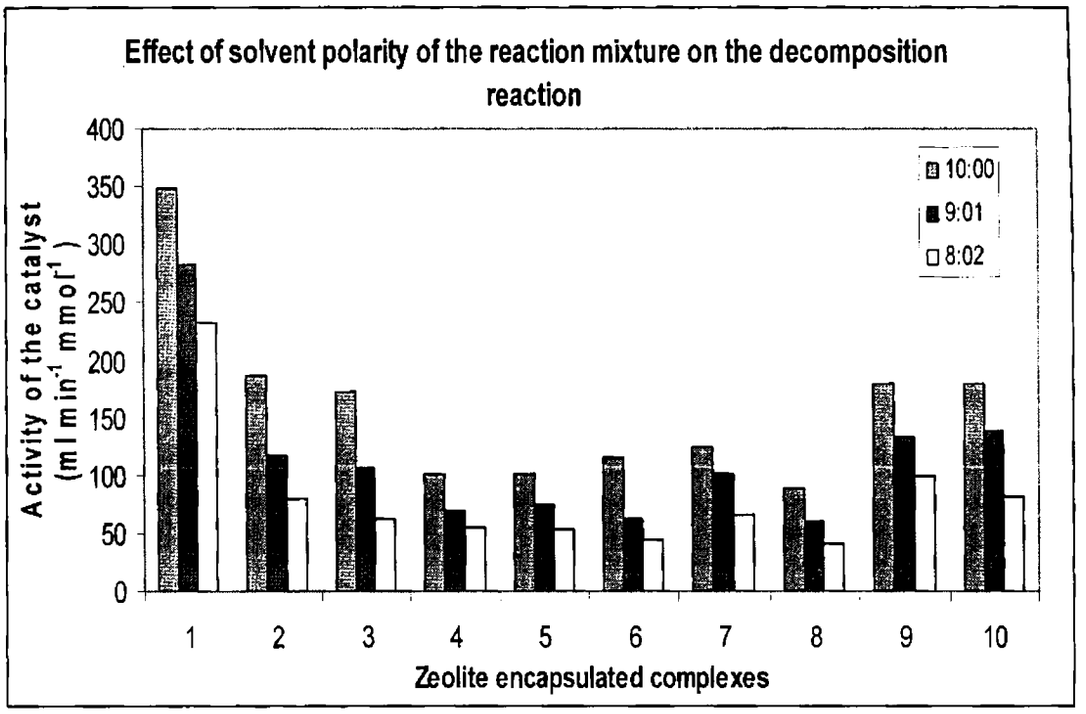

Figure 6.4. Influence of solvent polarity in the decomposition of hydrogen peroxide.

6.4.3.4. Effect of pyridine on the reaction

The influence of pyridine on the decomposition reaction was studied by adding traces of pyridine to the reaction mixture. Two-three drops of pyridine were added to the reaction mixture keeping other conditions intact. The addition of pyridine results in an increase in oxygen evolution, which is suggestive of an increase in the rate of decomposition of H_2O_2. The various experiments conducted with the encapsulated complexes indicate that the activity shows a substantial increase. The experimental results are given in table 6.5 and figure 6.5.

Table 6.5

Effect of the addition of pyridine on the decomposition reaction

Serial no:	Catalyst Used	Activity of the catalyst (ml min^{-1} $mmol^{-1}$)
1	RuYSSC	704.5
2	RuYSOD	403.9
3	RuYSPD	407.9
4	RuYAA	214.3
5	RuYABA	207.8
6	RuYDMG	227.6
7	RuYPCO	283.3
8	RuYPCP	206.9
9	RuYCPO	407.4
10	RuYCPP	420.4

Reaction conditions:

Amount of catalyst	10 mg
Volume of H_2O	10 ml
Volume of H_2O_2	10 ml
Temperature	30°C
Time	30 minutes

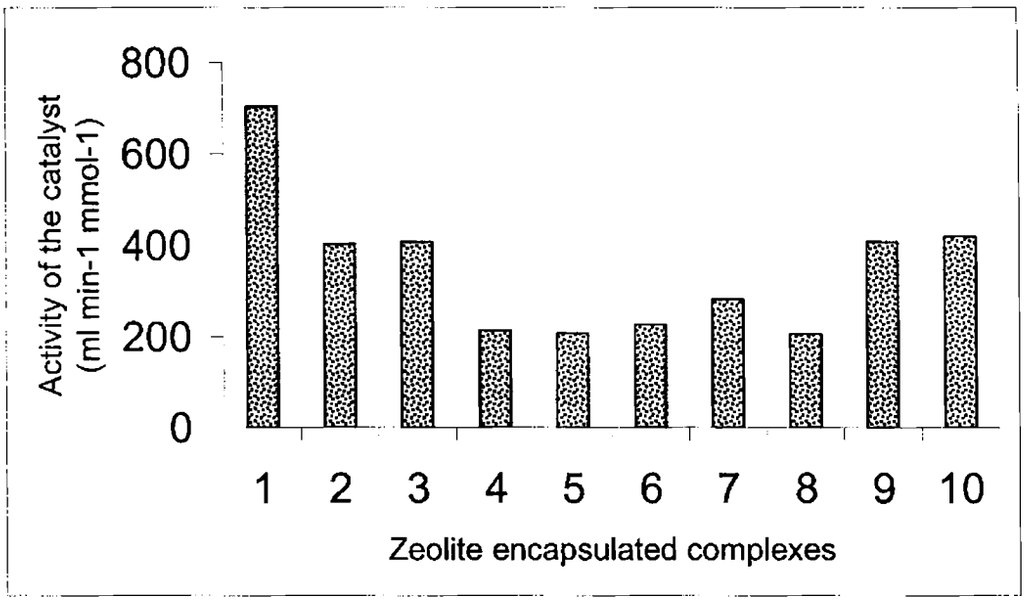

Figure 6.5. Effect of the addition of pyridine in the decomposition of hydrogen peroxide

6.4.3.5. Recycling studies

All the catalysts used were removed from the reaction mixture by filtration. The recovered catalysts were used again for decomposition studies after washing them with acetone and drying at 110°C for two hours. Recycling studies were conducted using the complexes RuYSSC, RuYSOD, RuYSPD, RuYAA, RuYABA, RuYDMG, RuYPCO, RuYPCP, RuYCPO and RuYCPP under identical conditions and the details of the recycling studies are given in table 6.6. The comparison of the activities of the fresh and the recycled samples are represented by the graph in figure 6.6.

The complexes RuYSSC, RuYSOD, RuYSPD, RuYAA, RuYABA and the different complexes synthesized from pyridine carboxaldehyde were able to retain their activity that indicates the stability of the zeolite-encapsulated complexes. The complex RuYDMG was found to loose some of its activity.

Table 6.6. Results of recycling studies

Serial no:	Catalyst Used	Activity of the catalyst (ml $min^{-1}mmol^{-1}$)	
		Fresh sample	Recycled sample
1	RuYSSC	348.6	334.1
2	RuYSOD	185.9	170.1
3	RuYSPD	173.3	162.0
4	RuYAA	101.8	94.4
5	RuYABA	100.6	97.2
6	RuYDMG	116.2	87.2
7	RuYPCO	123.6	112.6
8	RuYPCP	88.2	82.7
9	RuYCPO	179.9	165.8
10	RuYCPP	179.3	174.3

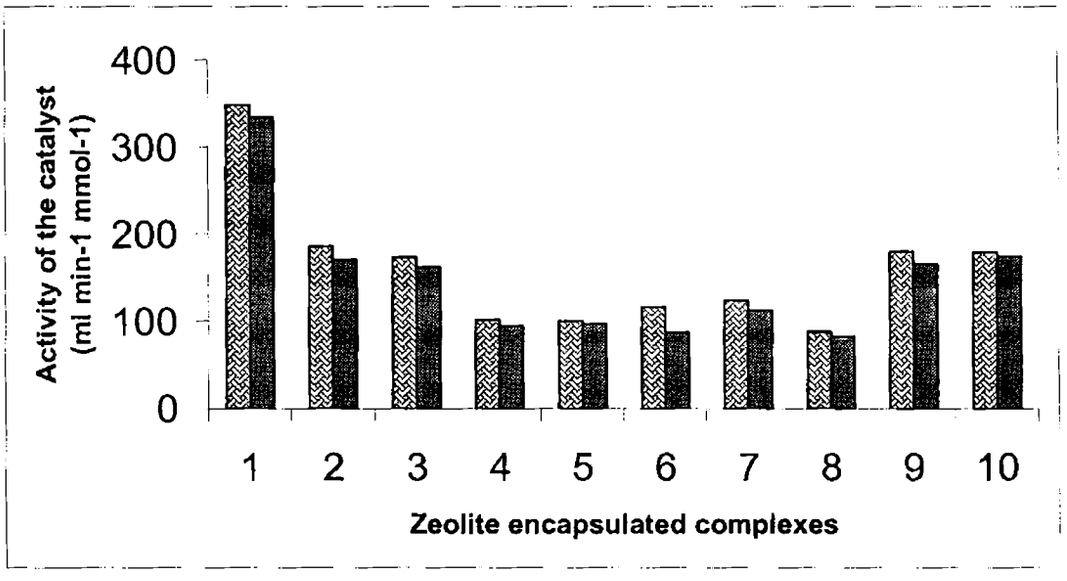

Figure 6.6. Comparative studies of the activity of fresh and recycled samples in the decomposition of hydrogen peroxide.

6.4.4. Activity of neat complexes of ruthenium in the decomposition of H_2O_2.

The neat complexes of ruthenium with the various ligands like SSC, SOD, SPD, AA, ABA, DMG, PCO, PCP, CPO and CPP were tested for their activity in the decomposition of hydrogen peroxide. The results of the screening experiments are presented in the table 6.7 gives an idea about the increase in activity upon encapsulation. It can be concluded from the experimental data that the encapsulated complexes are relatively more active than the neat ones. The heterogenization of the homogeneous metal complexes isolates the metal complexes so as to prevent their dimerization, increase their ruggedness and separability and result in beneficial interaction between the complexes and the support[18-20].

Table 6.7. Screening studies using neat complexes of ruthenium

Serial no:	Catalyst Used	Activity of the catalyst (ml $min^{-1}mmol^{-1}$)
1	RuSSC	1.42
2	RuSOD	1.58
3	RuSPD	1.24
4	RuAA	0.48
5	RuABA	0.67
6	RuDMG	0.27
7	RuPCO	1.16
8	RuPCP	1.02
9	RuCPO	1.60
10	RuCPP	1.31

6.5. DISCUSSION

Ruthenium exchanged zeolite and zeolite- encapsulated complexes were used as catalysts in the decomposition reaction. On comparing their activities, it can be seen that zeolite encapsulated ruthenium complexes exhibit higher activity than the metal exchanged zeolites and simple complexes. RuYSSC was found to be the most active catalyst. There are reports about the enhanced activity of supported catalysts which maybe due to the greater stability of encapsulated complexes when compared to simple

complexes. Another possibility is the formation of a modified catalyst precursor that is involved in the rate-determining step of the reaction. It has been reported that metal complexes accelerate the decomposition of hydrogen peroxide if they are coordinately unsaturated or if they have coordinated water molecules at one or more sites readily available for substitution by HOO^- or H_2O_2.

Many mechanisms have been proposed for the decomposition of hydrogen peroxide. The reaction proceeds by the oxidation or reduction of the substrate. A plausible mechanism involving a change in the oxidation states of the metal, which can be applied for zeolite-encapsulated complexes, is as follows.

$$2H_2O_2 \rightarrow 2HOO^- + 2H^+$$

$$2\,(LM)^{n+} + 2HOO^- \rightarrow 2\,(LM)^{(n-1)+} + 2HOO^{\cdot}$$

$$2HOO^{\cdot} \rightarrow O_2 + H_2O_2$$

$$2\,(LM)^{(n-1)+} + H_2O_2 \rightarrow 2\,(LM)^{n+} + 2OH^-$$

The overall reaction can be represented by the equation

$$2H_2O_2 \rightarrow O_2 + 2H_2O$$

The catalytic activity of the complex depends on the redox potential of the metal ion, which plays a major role in the decomposition reaction.

Yet another mechanism involves the formation of an intermediate peroxo species. Free H_2O_2 molecules yield HOO^- that generates the peroxo intermediate by their action on the complex.

$$H_2O_2 \rightarrow H^+ + HOO^-$$

$$(LM)^{n+} + HOO^- \rightarrow LM(HOO)^{(n-1)+}$$

The peroxide entity in the transition state can be highly reactive as suggested by Sharma and Schubert[21]. There should be at least two free vacant coordination sites at the metal ion for this mechanism to occur. The complexes with less than two free sites on the metal ion are found to be inactive. The presence of vacant coordination sites

obtained by the loss of labile water molecules might facilitate the formation of peroxo intermediates due to the bidentate nature of peroxide ion. The peroxo intermediates are found to be highly reactive species which lead to an increase in the rate of decomposition of H_2O_2. A change in the colour of the complexes during the reactions is suggestive of the decomposition reaction proceeding through the formation of peroxo intermediate species or might be due to a change in the oxidation state of the complex.

Earlier studies by Sharma and Schubert suggest that the catalytic activities of the complexes are largely influenced by the nature of the ligands. The ligands attached to the metal ion exert a strain around them that leads to an increase in their catalysis[22]. The chelate ring size also plays a major role in determining catalytic activity and 6-membered chelate rings are found to exhibit greater activity. The kinetics of reactions remains the same for supported and non-supported catalysts. The advantage lies in the significant increase in the rate of the reaction. Experimental studies haves proved the enhanced activity with supported catalysts.

Attempts were made to study the decomposition of hydrogen peroxide using different optimum reaction conditions. The various experiments conducted showed that the catalytic activity of the encapsulated complexes selected for study follows the order of RuYSSC > RuYSOD >RuYCPO > RuYCPP> RuYSPD> RuYPCO >RuYDMG RuYAA > RuYABA >RuYPCP. The geometry and structural properties of the complexes explain the variation in their activity.

The rate of the reaction is greatly influenced by the amount of catalyst added. When more amount of catalyst was used, there was a subsequent reaction enhancement. The increase in reaction rate was found to be greater for RuYSSC, the most active catalyst. There was a considerable change in the rate of the reaction on increasing the volume of hydrogen peroxide. The addition of methanol shows a different trend. The polarity of methanol is lower than that of water and when methanol is added to the reaction medium, the decomposition reaction slows down due to the decrease in polarity.

Catalytic studies were conducted with the addition of pyridine and it was found to enhance the reaction to a greater extent. Pyridine acts as a base in this reaction and

the basicity exerts a strong influence on the activity of the encapsulated complexes in different catalytic reactions. It aids the decomposition of H_2O_2 to the reactive HOO^- species and results in the acceleration of the decomposition reaction. Mechanism I was more favored in these cases, as there was no decrease in activity observed by addition of pyridine. If the reaction follows mechanism II, there might be chances for pyridine to coordinate to the metal thereby lowering the vacant coordination sites for interaction with HOO^-. Moreover the ligands tune the metal and vary the redox potential of metal ion, which in turn decide the catalytic activity of the complex.

The reaction was then carried out using recycled catalysts. All the complexes could retain their activity, which is an indicative of the stability of the zeolite-encapsulated complexes.

References

1. Sheldon, R.A.; Van Santen, R.A. (Eds.). Catalytic Oxidation Principles and Applications, World Scientific Pulishing, Singapore, **1995.**
2. Cota, H.M.; Katan, T.; Chin, M.; Schoenweis, F.J. Nature, **1964**, 203, 1281.
3. Tamagaki, S.; Sasaki, M.; Tagaki, W. Bull. Chem. Soc. Jpn. 1989, 62, 153.
4. Buxendak, J.H. Adv. Catal. **1952**, 4, 39.
5. Thomas, J.M.; Raja, R.; Sankar, G.; Bell, R.G. Acc. Chem. Res., **2001**,34, 191-200.
6. Tatsumi, T.; Yanagisawa, K.; Asano, K.; Nakamura, M.; Tominaga, H. Zeolites Microporous Crystals, **1994**, 83, 417.
7. Okuhara, T.; Mizuno, N. Adv. Catal. **1996**, 41, 113.
8. Thomas, J.M. New microcrystalline catalysts. Philos. Trans. R. Soc. **1990**, 333, 173.
9. TMaschmeyer, T.; Thomas, J.M.; Sankar, G.; Olyroyd, R.D.; Shannon, I.J.; Kleptko, J.A.;.Masters, A.F.; Beattle, J.K.; Catlow, C.R.A. Angew. Chem. Int. Ed. Engl. **1997**, 36, 1639.
10. Hayashi, T.; Kishida, A.; Mizuno, N. Chem. Commun. **2000**, 381.
11. Herron, N.; Tolman, C.A. J. Am. Chem. Soc. **1987**, 109, 2837.
12. Ratnasamy, C.; Murugkar, A.; Padhye, S. Ind. J. Chem. **1996**, 35A, 1-3.
13. Raja, R.; Ratnasamy, P. Stud. Surf. Sci. Catal. **1996**, 101, 181.
14. Raja, R.; Ratnasamy, P. U.S.Patent. 5, **1998**, 767, 320.
15. Sigel, H. Angew.Chem. Int. Ed. **1969**, 8, 3, 167.
16. Joshi, R.; Limiye, S.N. Oxidn. Commun. **1998**, 21, 3, 337.
17. Mochida, I.; Takeshita, K. J. Phys. Chem. **1974**, 78, 16, 1653.
18. Moreau, J.J.E.; Man, M.W.C. Coord. Chem. Rev, **1998**, 178-180, 1073.
19. Choplin, A.; Quignard, F. Coord. Chem. Rev, **1998**, 178-180, 1679.
20. De Vos, D.E.; Dams, M.; Sels, B.F.; Jacobs, P.A. Chem. Rev, **2002**, 102, 3615.
21. Sharma, V.S.; Schubert, J. Inorg. Chem. 10, **1971**, 2, 251.
22. Wang, J.H. Account Chem. Res. **1970**, 3, 90.

Chapter VII

OXIDATION OF CYCLOHEXANOL USING ZEOLITE ENCAPSULATED METAL COMPLEXES AS CATALYSTS

Chapter VII

OXIDATION OF CYCLOHEXANOL USING ZEOLITE ENCAPSULATED RUTHENIUM COMPLEXES AS CATALYSTS

7.1. INTRODUCTION

Many fundamental reactions in organic synthesis involve oxidation of organic compounds. The oxidation of alcohols to aldehydes and ketones is an important reaction in the viewpoint of large-scale industrial production. Oxidation with molecular oxygen usually requires very high temperature and pressure and is less preferred. Moreover, oxidation by certain reagents release substances toxic to the environment. Hence taking into consideration environmental protection and economic concerns, new oxidants are developed for effective oxidation reactions. Studies involving the use of ruthenium complexes to catalyze oxidation of alcohols by oxygen atom donors are reported[1, 2]. Well-documented literature is available on the use of primary oxidants like iodobenzene[3], alkylhydroperoxides[4], p-cyano-N,N-dimethylaniline-N-oxide[5] and molecular oxygen[6]. The results obtained from these studies have made it clear that high valent metal-oxo species is responsible for the oxidation reactions. The oxidation of some important alcohols catalyzed by ruthenium complexes was carried out by Sharpless *et al*[7].

The oxidation of cyclohexanol is an industrially important reaction. The major product formed during this oxidation reaction is cyclohexanone which is used for the production of adipic acid[8] and caprolactum[9]. Eventhough a mixture of cyclohexanone and cyclohexanol is acceptable for nylon production; cyclohexanone is desirable as the sole oxidation product in a variety of chemical syntheses[10, 11]. Numerous experiments have been conducted to develop new catalysts so as to aid the oxidation of cyclohexanol under mild conditions with high selectivity for a particular end product by using different oxidising agents[12, 13]. In order to avoid the difficulty of separating the catalyst from the products during homogeneous catalysis, efforts have been extended to develop

some heterogeneous catalysts for these reactions. A major milestone in this context is the incorporation of metal complexes inside zeolite cavities[14]. The activity of this heterogeneous system mainly depends on the correct choice of solvent, which determines the polarity of the medium, and also on the size of the substrate that is to be adsorbed at the catalytic surface[15]. The presence of promoters or co - reactants plays a major role in the reduction of induction period and in the increase in the amount of cyclohexanol conversion with high selectivity for the desired product. The heteronuclear caboxylato clusters of cobalt and manganese encapsulated in zeolite cages showed remarkable activity in the oxidation of cyclohexane, cyclohexanol and cyclohexanone to adipic acid[16].

Oxidation of cyclohexanol with tert-butyl hydroperoxide using Cu(Salen)Y as catalyst is found to be very effective with a conversion of 50% having 90% selectivity[17]. Tert-butyl hydroperoxide (TBHP) is an environment friendly and cheap oxidant[18]. It also acts as an important source of oxygen for oxidation[19] and hence widely used as oxidant for the liquid phase oxidation reaction of ethyl benzene[20]. There are reports of effective use of peroxides for alcohol oxidation and epoxidation of olefins using copper supported catalysts[21] at room temperature. Jacobs *et al.* prepared a composite catalyst system by incorporating phthalocyanine complex of iron in zeolite-Y embedded in a polydimethylsiloxane membrane mimicking cytochrome P-450 which oxidized cyclohexane at room temperature at rates similar to those of the enzymes[22]. The oxidation of cyclohexane, cyclohexene and benzyl alcohol using TBHP as the oxidant was achieved by copper amino acid complexes encapsulated in zeolite-Y[23].

Highly efficient catalytic oxidation of cyclohexane over copper doped titania structure are studied in detail[24]. Iron, aluminium and mixed Fe-Al pillared clays were tested for catalytic activity in the oxidation of cyclohexanol with hydrogen peroxide[25]. The oxidation of cyclohexane to cyclohexanol, cyclohexanone and adipic acid has been investigated with phthalocyanines and substituted phthalocyanines of copper, cobalt and iron encapsulated in zeolite X andY using molecular oxygen and alkyl (tertiary butyl, cyclohexyl and cumyl) hydroperoxides as the oxidants[26]. The catalytic efficiency of encapsulated complexes are much higher than the neat complexes and the rate of oxidation with copper substituted phthalocyanine embedded within the zeolite matrix

with TBHP can reach up to 90%. The isolated metal complex is the active site. The variation of solvents exerts a major influence on product distribution. The rates of oxidation with alkyl hydroperoxides decrease with increase in their molecular cross section, which suggests that the active site is located inside zeolite cavities and not on the external surface.

Ruthenium complexes with a variety of ligands including polypyridyl, Schiff base, macrocyclic and polyaminopolycarboxylate donors are known to activate H_2O_2 in oxidation reactions[27-31]. The reaction of $[RuHCl(CO)(PPh_3)_2(Z)]$ where Z = PPh_3, pyridine or piperidine with tridentate Schiff bases derived by condensing anthranilic acid with acetyl acetone, salicylaldehyde, o-vanillin and o-hydroxy acetophenone give a variety of hexa-coordinated ruthenium(II) complexes which behave as efficient catalysts for oxidising primary alcohols to aldehydes[32]. There are also reports on the dehydrogenation of cyclohexanol to cyclohexanone in the presence of Y_2O_3/ ZrO_2 as catalysts[33]. Oxidation of cyclohexane to cyclohexanol and cyclohexanone were investigated using supported gold catalysts under mild conditions of temperature and pressure[34] and they exhibit same activity as that of supported Pt and Pd catalysts. The selectivity is solely a function of conversion, which is a function of reaction time. But this catalytic process is not highly beneficial, as high selectivity under mild conditions cannot be maintained at higher concentrations.

In the present study, cyclohexanol oxidation using TBHP in the presence of zeolite encapsulated complexes of SSC, SOD, SPD, AA, ABA, DMG, PCO, PCP, CPO and CPP were investigated and the results of these studies are presented in this chapter.

7.2. EXPERIMENTAL

7.2.1. Materials used

Zeolite encapsulated ruthenium complexes of anthranilic acid, 4-aminobenzoic acid, dimethylglyoxime, SSC, SOD, SPD, PCO, PCP, CPO and CPP were used as catalysts for the study of oxidation reaction and the details of their synthesis have been described earlier. The catalytic activities of zeolite Y, metal exchanged zeolite and pure metal complexes were also investigated.

7.2.2. Experimental set up

The reaction was carried out in a round-bottom flask fitted with a reflux condenser. The required amount of substrate was taken in a suitable solvent. The specified amount of catalyst was added and the oxidation initiated by the addition of the oxidant. The whole set up was taken in an oil bath and stirred magnetically using a stirrer for the required time at a particular temperature. The flask was cooled after the experiment and the catalyst removed by filtration. The product and the unreacted substrate were analyzed using a gas chromatograph to estimate the conversion. The amount of various components in the mixture was determined from the peaks that appeared on the recorder. The GC parameters were quantified by the authentic product samples prior to the analysis.

7.2.3. Procedure for cyclohexanol oxidation

The oxidation of cyclohexanol with 70% TBHP as the oxidant and chlorobenzene as solvent at 90^0C was carried out in the presence of zeolite encapsulated complexes. The product, cyclohexanone was analyzed by GC using a carbowax column. The reaction was carried out under different conditions to study the influence of different factors like reaction time, amount of catalyst, temperature, oxidant to substrate ratio etc. All the GC results obtained are reproducible within ±0.3%. The appropriate choice of the amount of catalyst and the reaction conditions are crucial for catalytic effect. The catalysts were recycled and used to study the oxidation reactions. Characterization of the catalyst at the end of the oxidation reaction revealed that no leaching of metal occurred during the reaction. This suggests that the metal complexes selected for study are intact inside the zeolite cages.

7.3. RESULTS

7.3.1. Screening studies

The zeolite encapsulated ruthenium complexes of the ligands AA, ABA, DMG and the Schiff bases SSC, SOD SPD, PCO, PCP, CPO and CPP in the liquid phase were evaluated for their activity for the partial oxidation of cyclohexanol to cyclohexanone using t-butyl hydroperoxide in chlorobenzene solvent at 90°C keeping the oxidant to

substrate ratio as 2. The percentage conversion of cyclohexanol was noted after 4 hours and the activities corresponding to different complexes are presented in table 7.1 and the results are represented graphically in figure 7.1. From the extensive activity studies, it can be pointed out that among all the complexes RuYSSC and RuYSOD are more active whereas RuYDMG is the least active showing only 39% conversion. The complexes obtained by the condensation of pyridine carboxaldehydes with the two isomers of phenylenediamines show almost identical percentage conversion.

Table 7.1

Results of screening studies using zeolite encapsulated complexes for cyclohexanol oxidation using TBHP

Serial no:	Catalyst Used	% Conversion
1	RuYSSC	78.4
2	RuYSOD	63.5
3	RuYSPD	58.3
4	RuYAA	46.9
5	RuYABA	50.8
6	RuYDMG	39.0
7	RuYPCO	59.2
8	RuYPCP	55.4
9	RuYCPO	56.5
10	RuYCPP	52.7

Reaction conditions:

Amount of catalyst	20 mg
Oxidant to substrate mole ratio	2
Solvent used	Chlorobenzene
Temperature	90°C
Time	4 hours

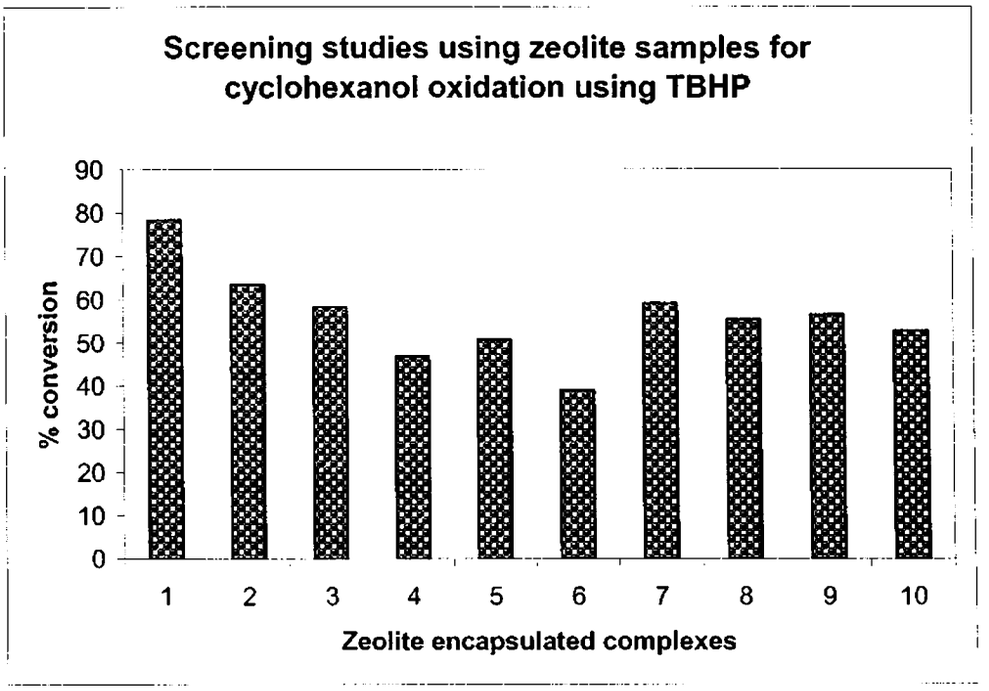

Figure 7.1. Screening studies using all the synthesized zeolite complexes for cyclohexanol oxidation using TBHP.

7.3.2. Blank run

The blank run was conducted at 90°C keeping the conditions same as that of screening experiments but without any catalyst. No conversion occurred even after four hours duration, which indicates that TBHP by itself will not aid the oxidation of cyclohexanol in the absence of catalyst.

7.3.3. Factors influencing the oxidation of cyclohexanol

The effects of various parameters on catalysis were studied by varying the following factors.

1. Amount of catalyst
2. Reaction time
3. Oxidant to Substrate ratio
4. Temperature
5. Solvent

7.3.3.1. Influence of the amount of catalyst

The extent to which oxidation proceed depends on the amount of catalyst present in the reaction mixture. Therefore the influence of catalyst was studied by varying the amount of catalyst from 20 mg to 60 mg. The percentage conversion of cyclohexanol showed no substantial increase with increase in the amount of catalyst; hence 20 mg of catalyst was used for detailed studies. The data showing the conversion of cyclohexanol on varying the amount of catalyst are presented in table 7.2. Further the percentage conversions are represented graphically in figure 7.2.

Table 7.2. Effect of the amount of catalyst on the oxidation of cyclohexanol

Serial No:	Zeolite encapsulated complex	% Conversion of Cyclohexanol		
		Amount of catalyst (mg)		
		20	40	60
1	RuYSSC	78.4	80.3	86.5
2	RuYSOD	63.5	64.5	69.3
3	RuYSPD	58.3	60.2	63.4
4	RuYAA	46.9	48.6	52.6
5	RuYABA	50.8	54.5	56.2
6	RuYDMG	39.0	40.4	45.5
7	RuYPCO	59.2	62.3	68.3
8	RuYPCP	55.4	59.7	63.6
9	RuYCPO	56.5	62.3	65.0
10	RuYCPP	52.7	56.9	60.2

Reaction conditions:

Oxidant to Substrate ratio	2
Solvent Used	Chlorobenzene
Temperature	90°C
Time	4 hours

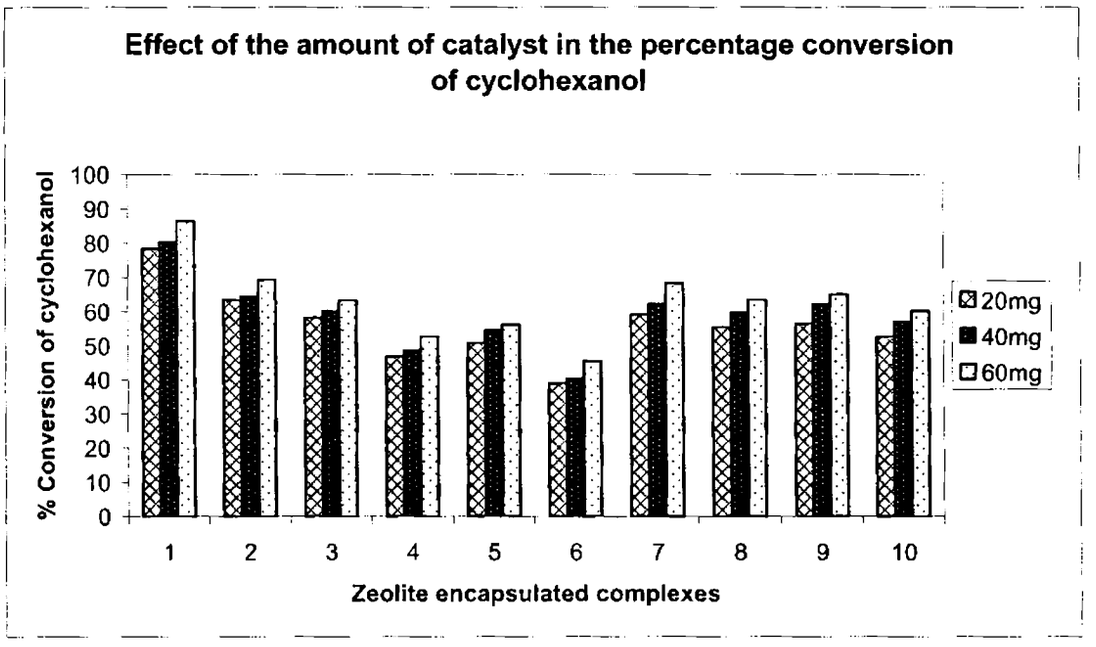

Figure 7.2. Influence of the amount of catalyst for cyclohexanol oxidation using TBHP

7.3.3.2. Influence of reaction time

In order to find out the influence of time on the percentage conversion of cyclohexanol, the oxidation reaction was conducted for different durations varying from one hour to four hours. Aliquots of the reaction mixture was withdrawn and subjected to gas chromatographic analysis for products and the results of the above studies are presented in table 7.3. Figure 7.3 is the corresponding graphical representation. The conversion was found to increase considerably with time for all the complexes studied. For two hours very little conversion was found to occur for all complexes and for RuYSOD and RuYSPD almost no product formed during two hours, which can be considered as the induction period. But when the reaction was allowed to proceed after four hours, darkening of the solution was observed indicating tar formation or tarry products. So the optimum time for the reaction was set as four hours.

Table 7.3. Effect of reaction time on the oxidation of cyclohexanol

Serial no:	Zeolite encapsulated complex	% Conversion of Cyclohexanol			
		Reaction time (h)			
		1	2	3	4
1	RuYSSC	10.0	26.1	48.2	78.4
2	RuYSOD	0.5	8.2	36.4	63.5
3	RuYSPD	0.3	7.6	30.9	58.3
4	RuYAA	2.8	14.5	31.2	46.9
5	RuYABA	3.4	15.0	33.5	50.8
6	RuYDMG	0.5	2.9	29.5	39.0
7	RuYPCO	4.3	21.6	36.4	59.2
8	RuYPCP	4.0	18.6	33.5	55.4
9	RuYCPO	4.1	19.6	35.1	56.5
10	RuYCPP	3.1	15.2	29.5	52.7

Reaction conditions:

Amount of catalyst	20 mg
Oxidant to substrate ratio	2
Solvent used	Chlorobenzene
Temperature	90°C

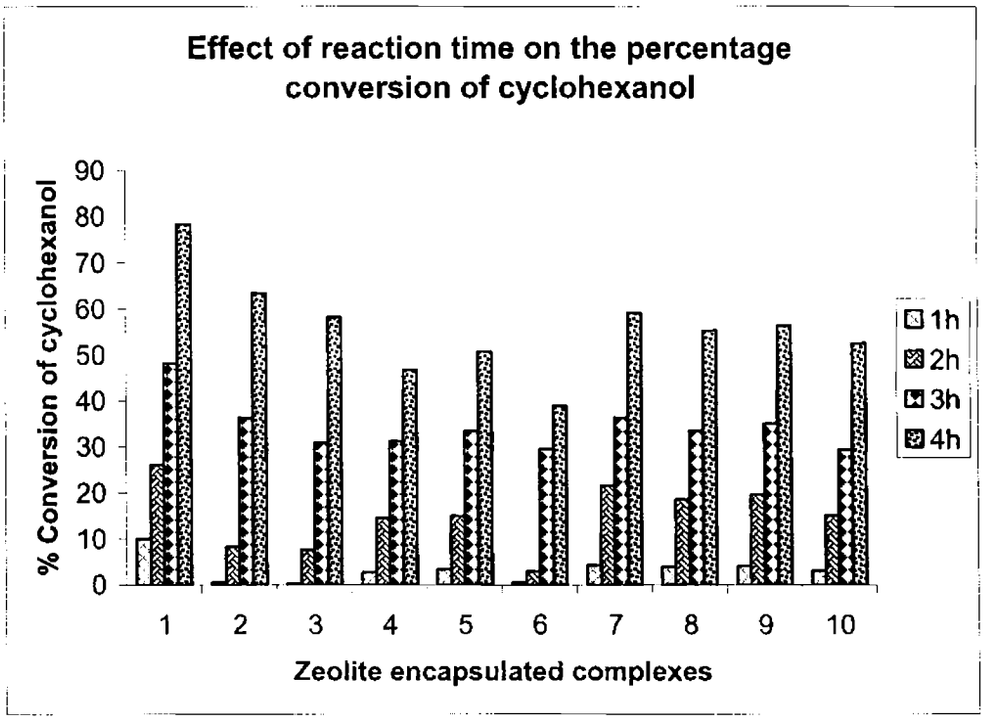

Figure 7.3. Influence of reaction time in cyclohexanol oxidation using TBHP

7.3.3.3. Influence of oxidant to substrate ratio

The oxidation reactions were conducted under identical conditions by varying the oxidant to substrate ratio. The results involving the variation of the ratio for the synthesized complexes RuYSSC, RuYSOD, RuYSPD, RuYAA, RuYABA, RuYDMG, RuYPCO, RuYPCP, RuYCPO and RuYCPP are given in table 7.4 and figure 7.4. A substantial increase in percentage conversion was noted as the oxidant to substrate ratio increased. Higher percentage conversion occurred at the ratio of 2 and further increase of the oxidant to substrate ratio produced no significant increase in the conversion of cyclohexanol. Hence the mole ratio 2 was taken as the optimum for further studies.

Table 7.4. Effect of oxidant to substrate ratio on the oxidation of cyclohexanol

Serial no:	Zeolite encapsulated complex	% Conversion of Cyclohexanol			
		Oxidant to substrate mole ratio			
		0.5	1	2	3
1	RuYSSC	38.2	56.8	78.4	81.4
2	RuYSOD	26.7	48.4	63.5	64.2
3	RuYSPD	19.3	37.6	58.3	59.
4	RuYAA	15.5	23.2	46.9	47.8
5	RuYABA	16.7	24.5	50.8	52.3
6	RuYDMG	7.9	16.5	39.0	42.5
7	RuYPCO	18.3	26.4	59.2	61.5
8	RuYPCP	15.5	22.7	55.4	60.9
9	RuYCPO	17.0	25.5	56.5	61.0
10	RuYCPP	12.4	19.0	52.7	58.9

Reaction conditions:

Amount of catalyst	20 mg
Solvent used	Chlorobenzene
Temperature	90°C
Time	4 hours

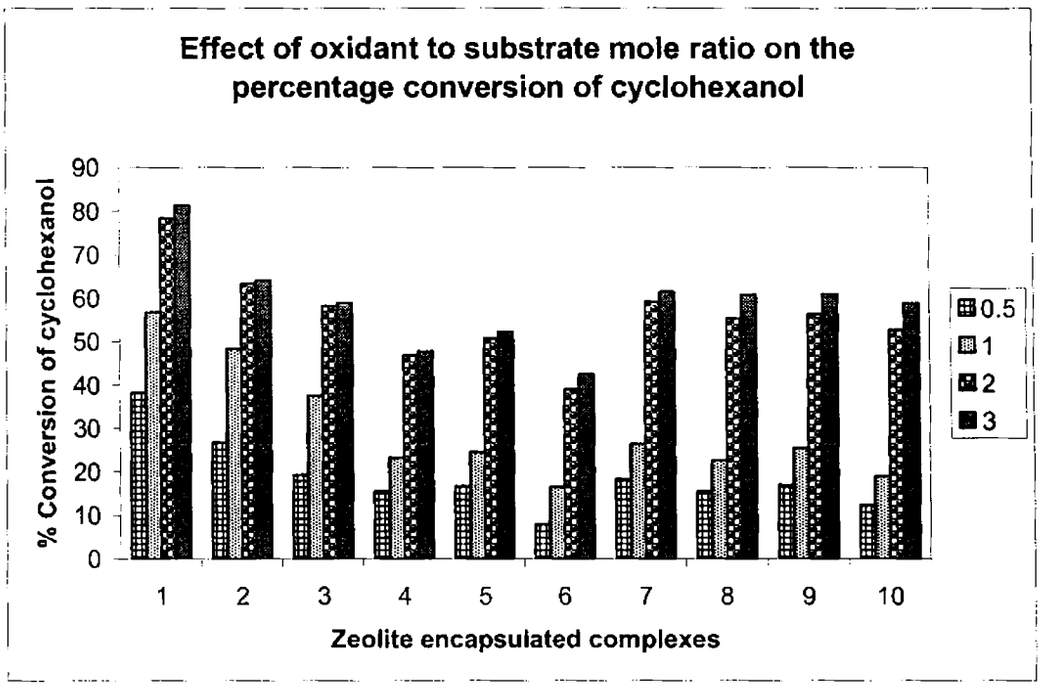

Figure 7.4. Influence of oxidant to substrate ratio in cyclohexanol oxidation using TBHP

7.3.3.4. Influence of temperature

The oxidation reaction for the complexes under study RuYSSC, RuYSOD, RuYSPD, RuYAA, RuYABA, RuYDMG, RuYPCO, RuYPCP, RuYCPO and RuYCPP were conducted under identical conditions at three different temperatures 50°C, 70°C and 90°C to find out the optimum temperature for the reaction. The results obtained for the various encapsulated complexes are presented in table 7.5. The percentage conversion increases with increase of temperature in the case of all the above-mentioned catalysts as evident from the graph 7.5. The maximum conversion occurred at 90°C and it was selected as the optimum temperature for detailed studies.

Table 7.5. Effect of temperature on the oxidation of cyclohexanol

Serial no:	Zeolite encapsulated complex	% Conversion of Cyclohexanol		
		Temperature (°C)		
		50	70	90
1	RuYSSC	33.3	55.2	78.4
2	RuYSOD	25.5	33.2	63.3
3	RuYSPD	19.8	25.4	58.3
4	RuYAA	10.2	22.7	46.9
5	RuYABA	13.3	24.5	50.8
6	RuYDMG	8.2	16.3	39.0
7	RuYPCO	20.3	42.6	59.2
8	RuYPCP	19.6	41.0	55.4
9	RuYCPO	20.2	41.9	56.5
10	RuYCPP	18.6	36.6	52.7

Reaction conditions:

Amount of catalyst		20 mg
Oxidant to substrate ratio		2
Solvent used		Chlorobenzene
Time	:	4 hours

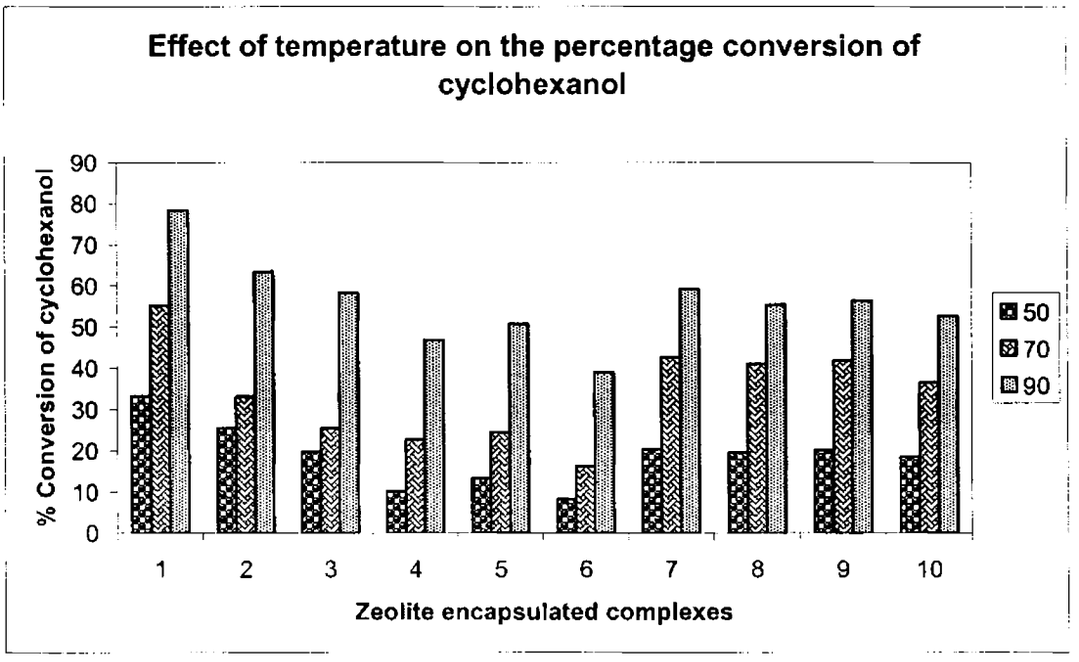

Figure 7.5. Influence of temperature in cyclohexanol oxidation using TBHP

7.3.3.5. Influence of solvents

The catalytic activity was carried out in different solvents like toluene, water, methanol and chlorobenzene with a view to find out the most suitable solvent. The results presented in table 7.6 and figure 7.6 show that chlorobenzene give a higher percentage conversion when compared to other solvents. Hence further catalytic studies were conducted using chlorobenzene as the solvent. Methanol gave the least conversion.

Table 7.6. Catalytic activity of the complexes in different solvents

Serial no:	Zeolite encapsulated complex	% Conversion of Cyclohexanol			
		Solvents Used			
		Toluene	Water	Methanol	Chlorobenzene
1	RuYSSC	42.6	27.6	12.9	78.4
2	RuYSOD	29.6	18.4	10.7	63.5
3	RuYSPD	24.6	17.2	9.3	58.3
4	RuYAA	20.3	12.2	7.4	46.9
5	RuYABA	27.6	14.5	9.8	50.8
6	RuYDMG	16.4	9.2	2.9	39.0
7	RuYPCO	34.5	28.9	10.3	59.2
8	RuYPCP	32.6	20.9	8.6	55.4
9	RuYCPO	34.1	24.8	9.1	56.5
10	RuYCPP	26.8	20.7	8.5	52.7

Reaction conditions:

Amount of catalyst		20 mg
Oxidant to substrate ratio		2
Temperature		90°C
Time	:	4 hours

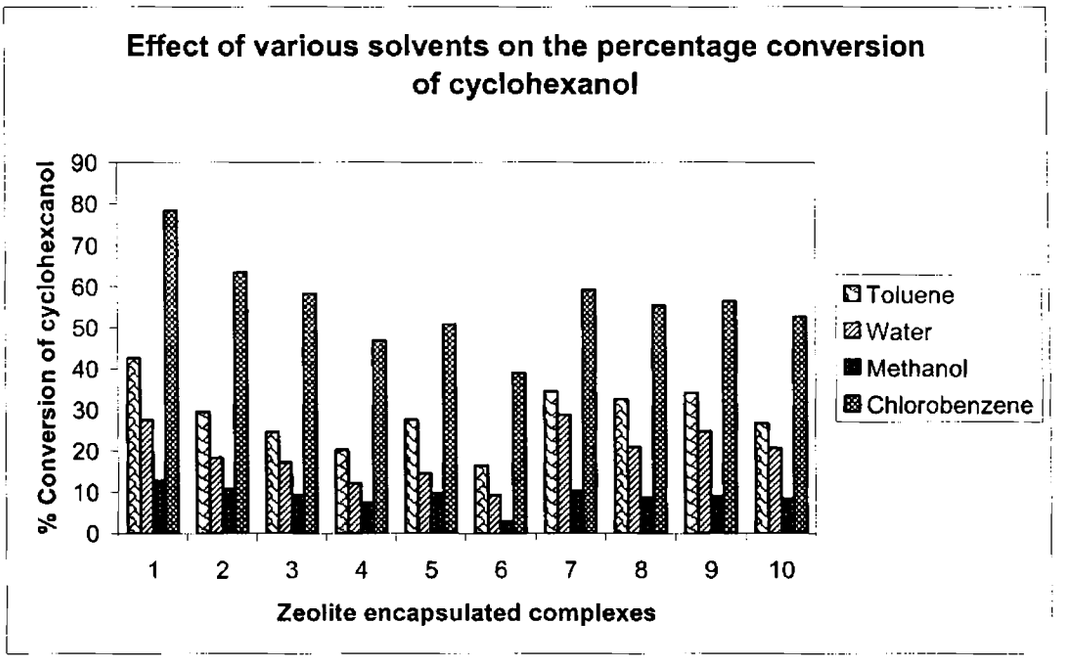

Figure 7.6. Influence of solvents in cyclohexanol oxidation using TBHP

7.3.4. Recycling studies

The encapsulated complexes RuYAA, RuYABA, RuYDMG, RuYSSC, RuYSOD, RuYSPD, RuYPCO, RuYPCP, RuYCPO and RuYCPP employed for oxidation studies were separated from the reaction mixture, washed with acetone several times and dried in oven to remove the impurities attached to the catalyst. The retention of the zeolite structure can be proved from the similar XRD patterns. Then reactions were carried out using recycled catalyst under the same conditions. The percentage conversions of the recycled catalysts are given in table 7.7. A graphical comparison of the activities of the fresh and recycled samples is presented in figure 7.7. The similar activity and spectroscopic properties of the recycled catalyst indicated the preservation of the structural integrity of the synthesized complexes.

Table 7.7. Results of recycling studies

Serial no:	Sample used	Fresh sample	Recycled sample	Third Run
1	RuYSSC	78.4	72.5	70.6
2	RuYSOD	63.5	52.4	51.8
3	RuYSPD	58.3	48.6	45.4
4	RuYAA	46.9	42.1	41.9
5	RuYABA	50.8	48.4	46.6
6	RuYDMG	39.0	26.2	25.7
7	RuYPCO	59.2	55.5	52.8
8	RuYPCP	55.4	52.5	50.1
9	RuYCPO	56.5	50.6	50.2
10	RuYCPP	52.7	48.3	46.4

Reaction conditions:

Amount of catalyst		20 mg
Oxidant to substrate mole ratio		2
Solvent used	:	Chlorobenzene
Temperature		90°C
Time		4 hours

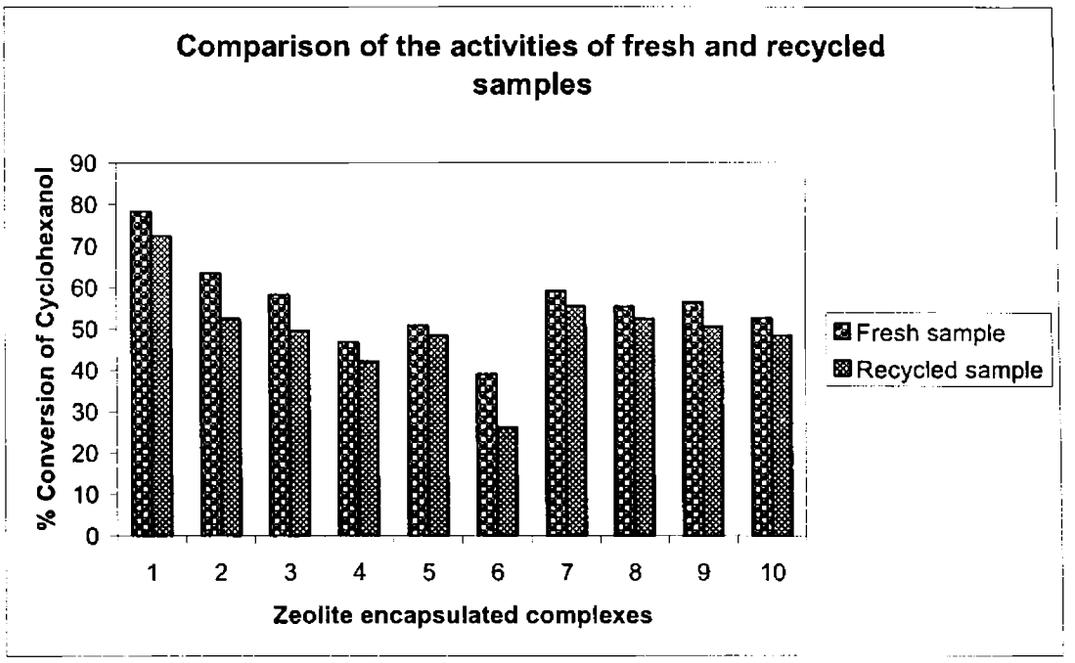

Figure 7.7. Comparative studies of the activity of fresh and recycled samples in the oxidation of cyclohexanol using TBHP

7.3.5. Oxidation of cyclohexanol using neat ruthenium complexes

The percentage conversion of cyclohexanol was studied by adding neat ruthenium complexes of anthranilic acid, 4-aminobenzoic acid, dimethylglyoxime and the Schiff bases prepared from salicylaldehyde and pyridine carboxaldehydes. The comparison of the activities of the pure complexes with that of their corresponding encapsulated complexes indicated that there is a considerable increase in the catalytic activity on encapsulation. This significant increase may be due to the change in the geometry of the complex during encapsulation. The absence of catalytic activity for pure zeolite proves beyond doubt that the metal ions trapped inside the zeolite pores largely contributes to the catalytic properties. The results are presented in table 7.8. The figure 7.8 gives a comparative picture of the catalytic activities of the neat and encapsulated complexes.

Table 7.8

Results of screening studies with the simple ruthenium complexes for the oxidation of cyclohexanol using TBHP as the oxidant

Serial no:	Catalyst used	% Conversion
1	RuSSC	40.6
2	RuSOD	25.5
3	RuSPD	20.9
4	RuAA	20.4
5	RuABA	22.5
6	RuDMG	14.2
7	RuPCO	21.6
8	RuPCP	19.4
9	RuCPO	20.8
10	RuCPP	18.6

Reaction conditions:

Amount of catalyst	20 mg
Oxidant to substrate ratio	2
Solvent used	Chlorobenzene
Temperature	90°C
Time	4 hours.

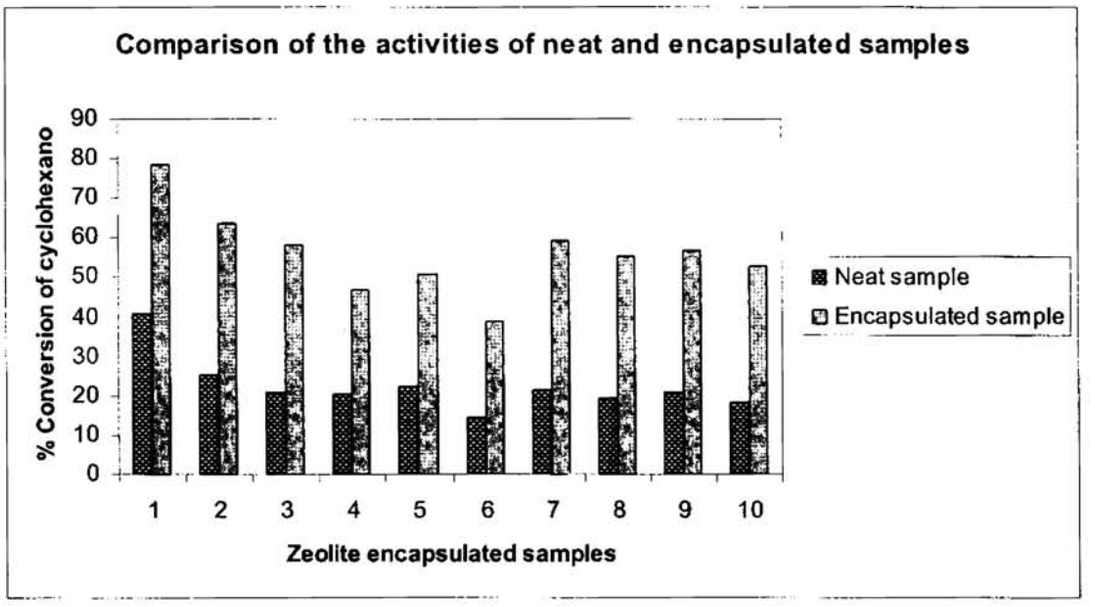

Figure 7.8. Comparative studies of the activity of neat and encapsulated samples in the oxidation of cyclohexanol using TBHP

7.4. DISCUSSION

The zeolite encapsulated complexes of anthranilic acid, 4-aminobenzoic acid, dimethylglyoxime, the Schiff bases SSC, SOD, PCO, PCP, CPO and CPP were used to catalyse the oxidation of cyclohexanol. The catalysts used for this oxidation reaction are activated by combining them it with a porous support like zeolite[35, 36]. The comparisons of their catalytic activities indicate that RuYSSC acts as the most effective catalyst in this oxidation reaction followed by RuYSOD. RuYAA and RuYABA exhibit almost the same activity whereas RuYDMG is found to be the least active.

The enhanced activity exhibited by encapsulated complexes can be attributed to several factors. The distortion of the molecular geometry from planarity to a puckered structure, greater depletion of electron density at the site of metal ion facilitating nucleophilic attack by anionic reagents are identified as the reasons for the increased catalytic activity[37].

The oxidation reaction did not take place in the absence of catalyst. Hence investigations were conducted on the availability of oxygen for oxidation. The source

of oxygen required for the conversion of primary alcohols to aldehydes may be through the formation of an intermediate Ru(V)-oxo complex[38, 39]. Experimental studies have pointed out that catalysis using ruthenium complexes occur through higher oxidation states of ruthenium, which can be readily achieved through oxidation with common co-oxidants[40].

The study of the effect of different parameters on the reaction reveals that there is an induction period during the course of the reaction. The percentage conversion of cyclohexanol is found to increase with time, which suggests that the oxidation proceeds, by a free radical mechanism. But when the reaction was allowed to proceed after an optimum time, darkening of the reaction mixture occurs.

Zeolite encapsulated complexes act as heterogeneous catalysts and offer several advantages when compared to homogeneous catalysts. They can be separated from the reaction mixture by simple methods like filtration. Another advantage lies in the fact that they can be recycled which enables continuous processing. Also it reduces the problem of environmental pollution by different chemical reagents. The use of encapsulated complexes as catalysts allows the cyclohexanol oxidation process to follow a heterogeneous- homogeneous reaction mechanism.

The oxidation reactions were also conducted with NaY, RuY and simple ruthenium complexes. No significant conversion occurs with NaY supporting the fact that zeolite support by itself doesnot ensure oxidation. The yield with RuY and neat complexes is found to be very low when compared with supported catalysts. The encapsulated ruthenium complexes are held firmly inside the zeolite pores by electrostatic forces of attraction, which enhances their catalytic activity.

Oxidation of cyclohexanol with TBHP is accompanied by the parallel decomposition of the oxidant. This accounts for the excess amount of oxidant when compared with the substrate required for the reaction. The oxygen gas evolved during the parallel reaction aids the process of oxidation. Cyclohexanol oxidation that is of first order is not greatly affected by the change in concentration of the peroxide. However the decomposition reaction follows second order, which makes it largely dependent on the concentration of peroxide.

The reaction was conducted with varying amounts of catalyst to study the influence of the amount of catalyst. The percentage conversion of cyclohexanol increases only by a small extent with increase in the amount of catalyst. The excess amount of catalyst increases the number of active sites thereby enhancing the reaction. Experimental results have showed that cyclohexanol oxidation is a slow process. It takes about four hours for the reaction to be complete and running the reaction for a period more than the optimum time results in the formation of undesired products. All the encapsulated complexes showed very little conversion for about two hours after which the percentage conversion shows a considerable increase. The product formed with RuYSOD is negligible during the initial phase. The requirement of a longer reaction time of about four hours for the conversion is probably due to diffusion limitations for zeolite catalysts.

The oxidant to substrate ratio too plays an important role in the reaction. The optimum oxidant to substrate ratio was found to be 2. Further increase in the amount of oxidant poses the risk of a parallel decomposition reaction that may deactivate the catalysts. In order to study the effect of temperature, the reaction was conducted at three different temperatures 50°C, 70°C and 90°C. The percentage conversion increased on raising the temperature and maximum yield was obtained at 90°C. So 90°C was selected as the optimum temperature for further studies. The effect of different solvents on the reaction was studied and these studies reveal that chlorobenzene is the best solvent for cyclohexanol oxidation. The percentage conversion was found to be minimum with methanol. Therefore all further studies were conducted using chlorobenzene as the solvent.

An important advantage of zeolite-encapsulated complexes is their ability to be recycled. The recycling studies were done after washing the used samples several times with acetone and heating them in an oven. They were able to retain their activity that can be taken as a solid evidence for the stability of the complexes inside the zeolite pores. RuYSOD and RuYDMG loose some of their activity when compared to the fresh sample. The retention of catalytic activity by recycled samples is a proof of their ability to withstand the regeneration process.

References

1. Thronback, J.R.; Wilkinson, G. J. Chem. Soc. Dalton Trans, **1978**, 110.
2. Hendawy, A.M.EL.; Alkubaisi, A.H. Polyhedron, **1993**, 12, 2343.
3. Ziegler, D.M. Ann. Rev, Biochem. **1984**, 54.
4. Lappins, A.G.; McAuley, A. J. Chem. Soc. A, **1975**, 1560.
5. Gilbert, J.A.; Eggleston, D.S.; Murphy, W.R.; Gerstem, S.W.; Hodgson, D.J.; Meyar, T.J. J. Am. Chem. Soc. **1985**, 107, 3855.
6. Ayoka, G.A.; Olatunji, M.A. Polyhedron, **1983**, 2, 577.
7. Sharpless, K.B.; Akashi, K.; Oshima, K. Tetrahedron. Lett. **1976**, 2, 2503.
8. Ulrich, H.; Raw Materials for Industrial Polymers, Hanser Publishers, Munich, Oxford Univ. Press, Oxford, **1988**, 142.
9. Weissermel, K.; Horpe, H.J.; Industrial Organic Chemistry, 2nd edit. VCH press, Weinheim, **1993**.
10. Sheldon, R.A.; Van Santen, R.A.; Catalytic oxidation Applications World Scientific Publishing, Singapore, **1995**.
11. Szment, H.H. Organic Building blocks of the Chemical Industry, Wiley, NewYork, 1989; Iwamoto, M.; Kusano, H.; Kagawa, S. Inorg. Chem., **1983**, 22, 3366.
12. Moody, C.J.; O'Connell, J. Chem. Commun. **2000**, 1311.
13. Almquist, C.B.; Biswas, P. Appl. Catal. A : Gen, **2001**, 214, 259.
14. Carvalho, W.A.; Varaldo, P.B.; Wallau, M.; Schuchardt, U. Zeolites, **1997**, 18, 408.
15. Lin, S.S.; Weng, H.S. Appl. Catal. A: Gen, **1994**, 118, 21.
16. Chavan, S.A.; Srinivas, D.; Ratnasamy, P.J. Catal. **2002**, 212, 39.
17. Sharpless, K.B.; Verhoeven, T.R. Aldirichimica Acta. **1979**, 12, 63.
18. Scheldon, R.A. Stud. Surf. Sci. Catal. **1990**, 55, 1.
19. Sakhtivel, A.; Dapurkar, E.S.; Selvam, P. Catalysis Letters, **2001**, 77.

20. Wekhuysen, B.M.; Verberchmoes, A.A.; Vannijvel, I.P.; Pelgrims, J.A.; Buskens, P.L.; Jacobs, P.A.; Schoonheydt, R.A. Angew. Chem. Int. Ed. Engl. **1995**, 34, 23-24.

21. Vangham D.E.W. Catal. Today. **1988**, 2, 187.

22. Parton, R.F.; Vankelecom, I.; Benzoukhanova, C.P.; Casselman, M.; Uytterhoeven, J.; Jacobs, P.A. Nature, **1994**, 370, 541.

23. Murphy, B.P. Coord. Chem. Rev, **1993**, 124, 3.

24. Yao, W.; Fang, H.; Ou, E.; Wang, J.; Yan, Z. Catalysis Communication, **2008**, V.7, 387-390.

25. Kurian, M.; Sugunan, S. Reaction Kinetics and Catalysis Letters, **2005**, 85, 1, 37-44.

26. Raja, R.; Ratnasamy, P. Catalysis Letters, **2007**, V.48, 1-10.

27. Gallagher, L.A.; Meyer, T.J. J. Am. Chem. Soc. **2001**, 123, 5308.

28. Nakata, N.; Takeda, T.; Mihara, J.; Hamada, T.; Trie, R.; Katsuki, T. Chem. Eur. J. **2001**, 7, 3776.

29. Miyata, A.; Muakami, M.; Trie, R.; Katsuki, T. Tetrahedron Lett. **2001**, 42, 7067.

30. Takeda, T.; Trie, R.; Katsuki, T. Synlett. 1999, 7, 1166.

31. Takeda, T.; Trie, R.; Katsuki, T.; Shinoda, Y. Synlett. **1999**, 7, 1157.

32. Jayabalakrishnan, C.; Karvembu, R.; Natarajan, K. Transition Metal Chemistry, **2002**, 27: 790-794.

33. Ilyas, M.; Ikramullah, Catalysis Communications, **2004**, 5, 1, 1-4.

34. Yi-Jun, X.; Philip, L.; Dan, E.; Albert, C.; Roberts,M.; Graham, H. Catalysis Letters, **2005**, Vol.101, 175-179.

35. Figueras,F. Catal. Rev, Sci. Eng. **1988**, 30, 457.

36. Khan, M.M.T.; Sreelatha, C.;.Mirza, S.A.; Ramachandriah, G.; Abdi, S.H.R. Inorg. Chem. Acta. **1988**, 154, 102.

37. Srinivas, D.; Sivasanker, S. Catalysis Surveys from Asia, **2003**, 7, 2-3.

38. Goldstein, A.S.; Drago, R.S. J. Chem. Soc. Chem. Commun. **1991**.

39. Leung, W.H. Inorg. Chem. **1989**, 28, 4619.

40. Zsigmond, A.; Notheisz, F.; Frater, Z.; Backvall, J.E. in Heterogeneous Catalysis and Fine Chemicals IV, Blaser, H.U.; Baiker, A.; Prins.R.(Eds.); Elsevier Science B.V 453, 197.

Chapter VIII

ZEOLITE ENCAPSULATED RUTHENIUM COMLEXES: CATALYSTS FOR HYDROXYLATION OF PHENOL

Chapter VIII

ZEOLITE ENCAPSULATED RUTHENIUM COMPLEXES: CATALYSTS FOR HYDROXYLATION OF PHENOL

8.1. INTRODUCTION

The application of transition metal complexes of Schiff bases as catalysts have gained considerable importance in the past few decades. Many characteristic properties of Schiff bases like induction of substrate chirality, tuning of metal centered electronic factor, enhancement of stability of heterogeneous complexes etc. contribute to this growing interest in the catalytic study of such complexes[1-9]. The study of ruthenium complexes to catalyse the oxidation of alcohols by oxygen atom donors has been reported[10, 11]. Also studies on oxidation using hydroperoxide in the presence of different metals are conducted[12].

The fundamental reaction in the synthesis of many industrially important organic compounds involves the oxidation of alcohols to aldehydes and ketones and these oxidation reactions are realized in practice by various oxidising agents[13]. A major drawback regarding the widely used oxidants is their toxicity to the environment. So it has become increasingly important to develop new catalysts for various oxidative purposes that pose minimum threat to the environment.

The major challenge in the present field of organic synthesis is product selectivity. Experiments on shape catalytic studies have led to major advancements in organic synthesis. Reports on product selectivity and shape selectivity were first put forward by Weisz and coworkers[14, 15]. Weisz has suggested that the actual need of a catalyst in a particular reaction is to provide selectivity to direct chemical transformation along a specific desired path.

Eventhough homogeneous metal complexes act as effective catalysts for oxidation reactions; they cannot be easily recovered from the reaction mixture. The separation of these catalysts often requires tedious procedures, which causes a substantial increase in the production cost during large-scale industrial applications. All these drawbacks of homogeneous catalysts can be overcome by the use of heterogeneous catalysts. Zeolite encapsulated metal complexes or 'zeoenzymes' are widely used heterogeneous catalysts and they are prepared by trapping metal complexes inside the zeolite pores[16]. The advantage of these catalysts lies in the fact that they can be easily removed by filtration which results in considerable reduction in cost.

The hydroxylation of phenol with hydrogen peroxide is an environment-friendly catalytic process and it yields dihydroxybenzenes such as hydroquinone and catechol. Both of them find various applications as antioxidants, photography chemicals and polymerization inhibitors and they are also used in pesticides, flavouring agents and medicines. Catechol can be used as an organic sensitizer in a photoelectrochemical cell[17].

There are reports of simple metal oxides and supported oxides such as Fe_2O_3, Co_3O_4, CuO/SiO_2, Fe_2O_3/Al_2O_3, MoO_3, V_2O_5 and TiO_2 colloidal particles used in the catalysis of phenol hydroxylation[18-23]. Complex oxides with transition metals like $La_{1.9}Sr_{0.1}CuO_4$ V-Zr-O were also employed for similar reactions[24, 25]. But the conversion of phenol by such catalysts is not high enough to be used for industrial purposes. Though the hydroxylation of phenol can also be brought by iron oxide nanoparticles trapped within macroporous resins[26], the decomposition of such catalysts hinder their catalytic activity. Iron based complex oxides Fe-Si-O, Fe-Mg-O and Fe-Mg-Si-O synthesized by coprecipitation method[27] exhibit a speedy reaction rate in the hydroxylation reaction. A heterogeneous-homogeneous free radical reaction mechanism might be the reason for the increased reaction rate.

The first commercial application of the metallosilicate TS-1 in the hydroxylation of phenol was done by Enichem in 1986[28-30]. Active research conducted on the catalytic importance of various metallosilicates has been reported[31-33]. The low reaction rate, complicated methods of synthesis and high expenses associated with such catalysts

posed a major limitation to their commercial application. Some new types of catalysts such as copper hydroxyl phosphate[34] and heteropoly compounds of copper[35] have also been investigated to study the reaction rate of phenol hydroxylation.

The catalysts widely used for phenol hydroxylation in the liquid phase with hydrogen peroxide are mainly transition metal containing zeolites such as TS-1, TS-2, Ti-MCM-41, V-ZSM-11 and Cu-ZSM-5[36-42]. All these molecular sieves possess attractive catalytic properties even though their slow reaction rates restrict their wide application in industrial synthesis. Extensive research has been done on the use of transition metal framework- substituted zeolites[43-49] in similar reactions. These studies have pointed out that simple transition metal ion exchanged zeolites can act as effective oxidants for phenol hydroxylation if the size of the zeolite pores is large enough to allow the reaction to occur. It has been recently reported that $Fe^{2+}$and Co^{2+} ion-exchanged Naβ zeolite is very active in phenol hydroxylation in aqueous medium even at room temperature[50]. The Cu^{2+} exchanged NaY, HY, Hβ and HZSM-5 zeolites were used for hydroxylation studies with hydrogen peroxide[51]. The effect of various parameters like reaction time, temperature and the molar ratio of phenol to H_2O_2 on the rate of reaction were studied. It has been observed that the type of zeolite and the amount of metal exchanged into the zeolite play a decisive role in the determination of catalytic activity.

The iron incorporated mesoporous silica material Fe-HMS possesses high catalytic activity and very high selectivity to dihydroxybenzene for the hydroxylation of phenol. But the product distribution was found to be different from that over the microporous TS-1 zeolite[52]. The zeolite-Y encapsulated complexes of copper, cobalt and vanadium phthalocyanines prepared by the ligand synthesis method were tested as catalysts for phenol hydroxylation[53]. The difference in activity can be explained on the basis of the differences in the location and accessibility of the different complexes, differences in the interaction with the zeolite framework etc. The performances of the encapsulated complexes are also influenced by the presence of uncomplexed metal ions. The method of synthesis of the zeolite complexes has a marked effect on the ratio of products formed. It has been observed that complexes prepared by 'zeolite synthesis

method' yielded more hydroquinone than catechol whereas catalysts synthesized by the 'in situ ligand synthesis method' yielded more amount of catechol[54].

The encapsulation of metal complexes inside the zeolite ring bring about several modifications in their properties like surface area, pore volume, potential gradient etc. These desirable changes in properties of the zeolite structure enable them to act as efficient catalysts for oxidation reactions in the presence of hydrogen peroxide, which also includes phenol hydroxylation. The use of zeolite complexes to catalyse these types of oxidative reactions in the presence of hydrogen peroxide has been well documented[55]. There are many vacant coordination sites available for the metal ions entrapped within the supercages of the zeolite which might be one of the reasons for their catalytic activity.

The zeolite encapsulated ruthenium complexes of SSC, SOD, SPD, AA, ABA, DMG, PCO, PCP, CPO and CPP were used as catalysts to study the oxidation of phenol using hydrogen peroxide, the major product being the p-isomer, hydroquinone. The importance of the reaction selected for study lies in the products formed from the substrate. The two major products obtained during the hydroxylation of phenol, hydroquinone and catechol act as useful intermediates in the large scale production of many industrially important reagents[56, 57]. The details of the experiment and the results are presented in this chapter.

8.2. EXPERIMENTAL

8.2.1. Materials

The syntheses of the simple and encapsulated metal complexes for catalytic studies are described earlier.

8.2.2. Reaction procedure

The required amount of phenol, water, oxidant and the specific catalyst was taken in a round-bottom flask fitted with a reflux condenser and a temperature controllable oil bath. The mixture was stirred for a definite period of time using a magnetic stirrer. The catalytic reaction was repeated using different reaction conditions

which are specified for each experimental setup. After the reaction, the catalyst was separated by filtration and the products were analyzed with a GC to determine the percentage conversion. The chromatograms indicate the presence of different products, which were ascertained by injection of standards as well as by standard calibration mixture (prepared from individual compounds). The products were confirmed by GC-MS analysis. An SE-3 column was used for the analysis and the parameter selected for quantification of a particular component is the peak area. The reaction was carried out by varying the factors like temperature, reaction time, amount of catalyst, solvent used and oxidant to substrate ratio. The reactions were also carried out using the recycled catalyst. All the GC results are reproducible within ±0.3%.

8.3. RESULTS

8.3.1. Screening studies

The catalytic activity of ruthenium exchanged zeolite and the zeolite encapsulated ruthenium complexes of SSC, SOD, SPD, AA, ABA, DMG, PCO, PCP, CPO and CPP in the hydroxylation of phenol using hydrogen peroxide at room temperature are presented in table 8.1 and the reaction conditions employed are also given below the table. RuYSSC was found to be the most effective catalyst for phenol hydroxylation with 94.4% conversion and 76% hydroquinone selectivity. Among all the catalysts studied, RuYDMG was the least effective in terms of percentage conversion. The reaction rate is found to be negligible in the absence of catalysts. It was observed from experiments that parent zeolite NaY by itself, before the incorporation of transition metal ions into its lattice structure is not active for the catalytic reaction. The activities of the encapsulated complexes synthesized from pyridine 3-carboxaldehyde are more or less the same as that obtained from pyridine-2-carboxaldehyde.

Table 8.1. Activity of ruthenium encapsulated zeolite and various zeolite encapsulated metal complexes on percentage conversion of phenol

Catalyst Used	% Conversion	% Hydroquinone	% Catechol	% Benzoquinone	% others	HQ/ CAT
RuY	18.6	9.4	6.8	1.83	0.57	1.38
RuYSSC	94.4	76.0	16.2	0.60	0.55	4.69
RuYSOD	83.7	48.9	33.4	0.55	0.92	1.46
RuYSPD	81.7	46.9	32.6	0.68	1.42	1.44
RuYAA	87.6	45.8	39.5	1.10	1.22	1.16
RuYABA	87.2	46.0	40.4	0.29	0.58	1.14
RuYDMG	79.9	42.7	35.3	1.25	0.76	1.21
RuYPCO	87.3	56.8	28.2	1.50	0.80	2.01
RuYPCP	85.4	52.8	27.4	4.23	0.92	1.93
RuYCPO	90.8	63.7	24.5	1.95	0.68	2.6
RuYCPP	90.2	63.1	26.1	0.02	1.02	2.42

Reaction conditions

Volume of phenol		1 ml
Volume of H_2O_2		5 ml
Volume of solvent (water)		5 ml
Duration	:	4 h
Temperature		70°C
Weight of catalyst		50 mg

8.3.2. Blank run

The reaction was repeated using the same conditions as that of screening studies but without adding any catalyst. No hydroquinone was obtained even after four hours of reaction. Only some dark tarry products were formed which could not be clearly identified.

8.3.3. Effect of various factors on phenol hydroxylation

The catalytic activity was investigated using various reaction conditions of temperature, amount of catalyst, time, oxidant to substrate ratio etc. in order to find out the optimum conditions for the hydroxylation reaction. The different factors selected for study are

1. Reaction time
2. Temperature
3. Amount of catalyst
4. Solvent used
5. Oxidant to substrate ratio (H_2O_2: Phenol ratio)

8.3.3.1. Influence of reaction time

The influence of time on the percentage conversion of phenol was studied by conducting the reactions for different durations varying from one hour to four hours. The reactions were carried out in the presence of complexes RuYSSC, RuYSOD, RuYAA, RuYABA, RuYCPO and RuYCPP. The dependence of the catalytic activity on the reaction time is displayed in table 8.2. It can be clearly pointed out that the effective conversion of phenol and the percentage of hydroquinone formed increases with the increase of the contact time.

Table 8.2 Influence of reaction time on percentage conversion of phenol

Catalyst Used	Reaction time (h)	% Conversion	% Hydroquinone	% Catechol	% Benzoquinone	% others
RuYSSC	1	10.5	6.1	2.1	2.32	
	2	67.4	54.4	10.4	2.39	0.20
	3	85.6	72.3	11.6	1.45	0.22
	4	94.4	76.0	16.2	0.60	0.55
RuYSOD	1	6.4	4.2	0.9	1.22	0.10
	2	45.1	26.4	16.6	1.34	0.75
	3	78.2	45.4	31.3	0.65	0.85
	4	83.8	48.9	33.4	0.55	0.92
RuYAA	1	10.0	6.6	3.0	0.40	
	2	48.3	25.6	19.3	2.50	0.85
	3	68.4	40.2	25.6	1.60	1.02
	4	87.6	45.8	39.5	1.10	1.22
RuYABA	1	10.3	5.4	3.9	0.96	
	2	46.3	24.8	20.7	0.52	0.26
	3	67.5	42.1	24.6	0.35	0.44
	4	87.3	46.0	40.4	0.29	0.58
RuYCPO	1	18.0	12.3	5.5		0.24
	2	54.2	37.5	13.6	2.76	0.38
	3	81.3	60.6	17.8	2.4	0.52
	4	90.8	63.7	24.5	1.95	0.68
RuYCPP	1	15.0	10.4	3.3	1.22	0.09
	2	49.0	32.4	15.1	0.82	0.65
	3	76.4	56.8	18.1	0.56	0.92
	4	90.2	63.1	26.1	0.02	1.02

Reaction conditions:

Volume of phenol		1 ml
Volume of H_2O_2	:	5 ml
Volume of solvent (water)	:	5 ml
Temperature		30°C
Weight of catalyst		50 mg

No significant change occurred during the initial phase of the reaction but there was a considerable increase in the rate of the reaction after the induction period. The length of the induction period depends on the nature of the active components and their crystallite size. RuYSSC was found to be the most effective. A higher percentage conversion of about 94.4% was obtained with 76% selectivity for hydroquinone after 4 hours. But when the reaction was allowed to proceed after that period, some darkening of the reaction mixture occurs. This indicates that undesirable products are formed after the fixed time. Hence the optimum time was fixed as 4 hours. The other Schiff base encapsulated ruthenium complexes showed similar reactions. But the percentage conversion was found to be less when compared with RuYSSC. The catalytic activities with RuYAA and RuYABA were found to be almost equal. The Schiff base complexes, RuYCPO and RuYCPP give more or less the same amount of conversion after the specific time. Though the conversion of phenol and selectivity for hydroquinone increases with time, the amount of benzoquinone formed decreases with time. This is in good agreement with previous results with TS-1 catalysts[58, 59]. The formation of comparatively higher amounts of benzoquinone during the initial stages of the reaction is due to the fast over-oxidation of hydroquinone by the large concentration of H_2O_2. But as time progresses, the benzoquinone formed probably gets converted into other products like benzophenones. There are also chances for the oxidation of H_2O_2 by benzoquinone resulting in the formation of hydroquinone and oxygen[60].

8.3.3.2. Influence of reaction temperature

The phenol hydroxylation reaction was carried out initially at room temperature. The dependence of percentage conversion on temperature was studied by carrying out the reaction at three different temperatures, 30°C, 50°C and 70°C. The results of these reactions are presented in table 8.3.

Table 8.3 Influence of reaction temperature on percentage conversion of phenol

Catalyst Used	Temperature (°C)	% Conversion	% Hydroquinone	% Catechol	% Benzoquinone	% others
	30	86.8	70.4	14.9	0.92	0.58
RuYSSC	50	88.6	74.8	12.1	1.25	0.46
	70	94.4	76.0	16.2	1.60	0.55
	30	76.9	42.5	33.3	0.44	0.62
RuYSOD	50	82.7	45.4	36.2	0.66	0.48
	70	83.7	48.9	33.4	0.55	0.92
	30	66.2	38.2	23.4	2.75	1.82
RuYAA	50	76.1	40.4	28.7	5.56	1.38
	70	87.6	45.8	39.5	1.10	1.33
	30	62.4	37.6	23.1	0.96	0.78
RuYABA	50	80.6	44.5	34.2	1.02	0.84
	70	87.2	46.0	40.4	0.29	0.58
	30	81.8	54.4	26.2	1.06	0.09
RuYCPO	50	85.1	61.8	21.5	1.22	0.57
	70	90.8	63.7	24.5	1.95	0.68
	30	84.9	59.8	23.0	1.12	0.82
RuYCPP	50	86.5	60.6	23.6	1.45	0.86
	70	90.2	62.1	25.1	2.02	1.02

Reaction conditions:

Volume of phenol		1 ml
Volume of H_2O_2		5 ml
Volume of solvent (water)	:	5 ml
Weight of catalyst		50 mg
Duration		4h

The influence of temperature is found to be similar for all the complexes under study. The catalysts employed are found to be active even at room temperature. But the reaction rate can be further enhanced by raising the temperature from 30°C to 50°C and then to 70°C. Reactions carried at temperatures higher than 70°C results either in the decomposition of the products or in the formation of tarry products. The formation of a significant amount of tar products and the rapid decomposition of H_2O_2 in a non-productive manner at temperatures greater than 70°C makes it the optimum temperature for maximum conversion. This is found contrary to the properties exhibited by titanosilicate catalysts, which show high catalytic activity at higher temperatures even after 6 hours.

8.3.3.3. Influence of the amount of catalyst

The reaction was carried out using varying amounts of metal encapsulated complexes with a view to determine the influence of the amount of catalyst. The percentage conversion values obtained with these studies are given in table 8.4.

Table 8.4. Influence of the amount of catalyst on the hydroxylation reaction

Catalyst Used	Weight of catalyst (mg)	% Conversion	% Hydroquinone	% Catechol	% Benzoquinone	% others
	20	66.2	56.1	9.8	0.25	0.09
RuYSSC	40	91.6	73.8	16.5	0.88	0.46
	50	94.4	76.0	16.2	1.6	0.55
	20	55.2	35.7	19.1	0.26	0.11
RuYSOD	40	80.4	46.4	32.6	0.58	0.86
	50	83.7	48.9	33.4	0.55	0.92
	20	46.4	28.7	15.3	2.28	0.09
RuYAA	40	79.2	42.9	29.8	5.46	1.05
	50	87.6	45.8	39.5	1.10	1.33
	20	49.9	31.1	18.3	0.35	0.15
RuYABA	40	81.5	44.4	36.5	0.38	0.19
	50	87.2	46.0	40.4	0.29	0.58
	20	68.8	50.5	16.8	0.98	0.56
RuYCPO	40	89.3	60.2	26.9	1.50	0.75
	50	90.8	63.7	24.5	1.95	0.68
	20	65.6	48.5	15.4	1.05	0.65
RuYCPP	40	88.8	56.6	29.6	1.88	0.76
	50	90.2	62.1	25.1	2.02	1.02

Reaction conditions:

Volume of phenol	1 ml
Volume of H_2O_2	5 ml
Volume of solvent (water)	5 ml
Temperature	70°C
Duration	4h

On increasing the catalyst amount, the degree of conversion increased for all complexes as expected. When the catalyst amount was increased from 20 mg to 40 mg, there is a tremendous increase in the amount of product formed. However further increase in the weight of the catalyst did not have any noticeable effect on the percentage conversion.

8.3.3.4. Influence of oxidant to substrate ratio

The oxidant used in this particular reaction is hydrogen peroxide. Phenol hydroxylation using different ruthenium encapsulated complexes was carried out under the same reaction conditions by varying the volume of hydrogen peroxide and keeping the volume of phenol constant. The results obtained are summarized in table 8.5.

Table 8.5. Influence of H_2O_2 to phenol ratio on percentage conversion of phenol

Catalyst Used	Volume of H_2O_2 (ml)	% Conversion	% Hydroquinone	% Catechol	% Benzoquinone	% others
RuYSSC	4	76.9	58.2	15.4	2.40	0.88
	5	94.4	76.0	16.2	1.60	0.55
	6	97.6	78.2	17.6	0.95	0.87
RuYSOD	4	59.9	35.5	22.6	0.96	0.85
	5	83.7	48.9	33.4	0.55	0.92
	6	86.9	49.8	35.6	0.46	1.04
RuYAA	4	72.7	38.2	31.3	1.88	1.34
	5	87.6	45.8	39.5	1.10	1.33
	6	91.7	49.2	40.7	0.94	0.89
RuYABA	4	77.1	39.3	35.7	1.24	0.86
	5	87.2	46.0	40.4	0.29	0.58
	6	90.2	47.7	41.6	0.25	0.62
RuYCPO	4	81.7	57.4	21.6	1.98	0.76
	5	90.8	63.7	24.5	1.95	0.68
	6	91.5	64.6	25.2	0.58	1.09
RuYCPP	4	82.1	57.2	21.6	2.36	0.97
	5	90.2	62.1	25.1	2.02	1.02
	6	91.1	63.4	26.6	0.64	0.45

Reaction conditions:

Volume of phenol	:	1 ml
Volume of solvent (water)		5 ml
Temperature		30°C
Weight of catalyst		50 mg
Duration		4h

These studies indicate that the oxidation reaction increases with increase in the volume of hydrogen peroxide till a certain volume. But further increase in the volume of H_2O_2 is detrimental as some dark mass is obtained after four hours of reaction. The increase in the amount of phenol converted with increase in the oxidant to substrate mole ratio agrees well with other previously obtained results. The hydroquinone to catechol ratio remains almost unchanged, which indicates their insensitivity to the change of molar ratio of H_2O_2 to phenol.

8.3.3.5. Influence of solvents

The activity studies of the encapsulated complexes were carried under similar conditions in different solvents like water, methanol, acetone and chlorobenzene. The data obtained with these studies are tabulated in table 8.6.

Table 8.6. Influence of various solvents on percentage conversion of phenol

Catalyst Used	Solvent Used	% Conversion	% Hydroquinone	% Catechol	% Benzoquinone	% others
RuYSSC	Water	94.4	76.0	16.2	1.60	0.55
	Acetone	88.6	66.1	18.8	2.47	1.20
	Methanol	75.6				
	Chlorobenzene	68.7				
RuYSOD	Water	83.7	48.9	33.4	0.55	0.92
	Acetone	79.3	45.6	31.7	0.76	1.22
	Methanol	68.5				
	Chlorobenzene	66.9				
RuYAA	Water	87.6	45.8	39.5	1.10	1.33
	Acetone	73.4	40.7	28.6	2.35	1.78
	Methanol	68.9				
	Chlorobenzene	62.2				
RuYABA	Water	87.2	46.0	40.4	0.29	0.58
	Acetone	80.7	40.8	36.2	1.88	1.78
	Methanol	70.4				
	Chlorobenzene	65.6				
RuYCPO	Water	90.8	63.7	24.5	1.95	0.68
	Acetone	82.9	60.8	19.8	1.56	0.73
	Methanol	68.8				
	Chlorobenzene	70.5				
RuYCPP	Water	90.2	63.1	26.1	0.02	1.02
	Acetone	81.5	59.2	20.5	0.84	0.95
	Methanol	70.4				
	Chlorobenzene	64.2				

Reaction conditions:

Volume of phenol	1 ml
Volume of H_2O_2	5 ml
Volume of solvent	5 ml
Temperature	30^0C
Weight of catalyst	50 mg
Duration	4h

Among all the solvents studied, water was found to be the best solvent with a higher rate of conversion. When acetone, methanol and chlorobenzene are used as solvents for the reaction, the catalytic activity reduces to a great extent, which may be due to the adsorption of the solvents on the active species of the catalysts. Acetone showed less percentage conversion and lower selectivity towards hydroquinone. The formation of tarry products with methanol and chlorobenzene suggested that they could not be used as solvents for this particular oxidation reaction. The arrangement of bulky solvent molecules induces a kinetic barrier for the approach of the substrate molecules towards the active sites of the catalyst. This will favour the oxidation of the solvent and lower the product yield.

8.3.4. Recycled catalyst

The oxidation reactions were carried out using recycled catalyst under identical conditions. Once the oxidation reaction is over, the catalyst was separated by filtration from the reaction mixture, washed with acetone several times. Then it was dried at 80°C in an oven to remove any impurities present. There was no change in its crystal structure as indicated by the X- ray diffraction pattern of the used catalyst. The FTIR spectra of the recycled catalysts were also found to be similar to that of the fresh catalyst. All the encapsulated complexes could retain their catalytic activity, which indicates their stable nature. The percentage conversion of the recycled catalysts is given in table 8.7. The comparison of the activities of the fresh and used samples showed that there is some loss of activity for recycled catalysts. These results are also presented in the table.

Table 8.7. Catalytic activity of recycled catalysts

Catalyst Used	% Conversion	% HQ	% Catechol	% Benzoquinone	% others	% loss of activity
RuY	16.1	8.2	5.8	1.24	0.87	13.44
RuYSSC	91.7	74.6	15.8	0.46	0.88	2.86
RuYSOD	79.7	46.4	31.8	0.42	1.12	4.78
RuYSPD	77.5	45.5	30.6	0.63	0.78	5.14
RuYAA	82.7	43.4	37.5	1.09	0.74	5.59
RuYABA	83.4	44.9	37.4	0.57	0.48	4.36
RuYDMG	74.7	40.7	32.3	0.75	0.96	6.51
RuYPCO	82.5	54.8	26.1	0.85	0.74	5.49
RuYPCP	80.4	52.8	25.9	1.23	0.48	5.85
RuYCPO	87.3	61.6	23.7	1.32	0.65	3.85
RuYCPP	86.4	60.2	24.5	0.96	0.72	4.21

Reaction conditions:

Volume of phenol	1 ml
Volume of H_2O_2	5 ml
Volume of solvent	5 ml
Temperature	30°C
Weight of catalyst	50 mg
Duration	4h

The recycling studies have shown that RuYSSC showed almost the same percentage conversion after recycling. This means that the encapsulated complex has not undergone any significant changes during the reaction. Recycled RuYPCO, RuYPCP, RuYCPO and RuYCPP exhibit similar activity to that of the fresh sample with small decrease in percentage conversion and hydroquinone selectivity. Among all the complexes studied, the least active RuYDMG was the most deactivated.

8.3.5. Activity of neat complexes of ruthenium in phenol hydroxylation

The neat complexes of ruthenium with the various ligands like AA, ABA, DMG, SSC, SOD, SPD, PCO, PCP, CPO and CPP were tested for the percentage conversion of phenol in the presence of hydrogen peroxide. The results of the screening experiments are presented in table 8.8. From the experimental data it is clear that the encapsulated complexes are relatively more active than the neat ones. The heterogenization of the homogeneous metal complexes stabilizes them and enhances their catalytic properties. However the ratio of hydroquinone to catechol remained almost the same as in the case of encapsulated complexes.

Table 8.1. Activity of neat complexes of ruthenium on percentage conversion of phenol

Catalyst Used	% Conversion	% Hydroquinone	% Catechol	% Benzoquinone	% others	HQ/ CAT
RuSSC	75.2	58.6	14.2	0.86	1.55	4.13
RuSOD	65.7	36.8	27.2	0.78	0.89	1.35
RuSPD	68.4	39.1	27.5	1.02	0.76	1.42
RuAA	80.0	42.4	35.6	0.87	1.16	1.19
RuABA	84.9	43.8	39.7	0.45	0.92	1.10
RuDMG	61.1	32.8	26.9	0.65	1.08	1.24
RuPCO	72.3	48.4	22.6	0.55	0.78	2.14
RuPCP	66.4	41.6	21.9	1.69	1.18	1.89
RuCPO	90.8	58.6	19.8	1.95	0.68	2.95
RuCPP	90.2	53.2	20.6	0.02	1.02	2.58

Reaction conditions:

Volume of phenol	1 ml
Volume of H_2O_2	5 ml
Volume of solvent (water)	5 ml
Duration	4 h
Temperature	70°C
Weight of catalyst	50 mg

8.4. DISCUSSION

The zeolite encapsulated ruthenium complexes of SSC, SOD, DMG, ABA, AA, PCO, PCP, CPO and CPP have been employed to study the hydroxylation of phenol. The reactions were conducted in the presence as well as in the absence of catalysts. A comparison of the catalytic reactions indicates that encapsulated complexes show much higher activity in comparison with neat complexes and ion exchanged zeolites. Among all the encapsulated complexes selected for study, RuYSSC is found to be the one yielding highest amount of the desired product, hydroquinone. The effectiveness of the RuYSSC complex is supported by its higher conversion values. It showed 94.4% conversion and 76% selectivity for hydroquinone. The Schiff base encapsulated complexes RuYSOD, RuYSPD, RuYPCO, RuYPCP, RuYCPO and RYCPP are also active with small differences in the amount of hydroquinone formed.

The hydroxylation of phenol can give a variety of products. On GC analysis of the reaction mixture after completion of the reaction it is clear that there is a distribution of products that include hydroquinone, catechol, benzoquinone, benzophenones etc. Hydroquinone and catechol are the major products formed during the course of the reaction.

There are chances for the oxidation reaction to occur at the external surface as well as inside the pores of the zeolite. Hydroquinone is formed due to catalytic reactions taking place inside the zeolite pores whereas reactions occurring on the external surface of the zeolite result in the formation of the other product, catechol[61]. Some dark coloured tarry substances whose identification is difficult are also obtained when the reaction proceeded after an optimum period. In all these cases of catalysis, the formation of hydroquinone as the major product is indicative of the hydroxylation reactions occurring inside the zeolite cages. The catalytic activity of the metal ion is greatly influenced by its environment and the coordination of the ligands during the formation of complexes also plays a major role in enhancing the catalytic properties[62].

On completion of the reaction, the aqueous phase was separated from the organic phase and tested for the presence of ruthenium ion. No leaching of complexes

has occurred. The complexes undergo no change, as they remain intact inside the zeolite cages.

No appreciable amount of hydroquinone was formed on carrying out the reaction with ruthenium-exchanged zeolite. Thus the presence of zeolite alone does not ensure hydroxylation reaction. Also the metal ions by themselves will not act as good catalysts in this reaction. Zeolite encapsulated complexes show higher activity compared to the corresponding simple complexes. The site isolation theory clearly explains these disparities. There are very strong electrostatic forces of attraction existing between the zeolite and the complex that prevent their escape from the zeolite cages. The deactivation by multimolecular association is thus ruled out completely. The free movement of complexes within the zeolite framework aids in their catalytic activity.

The influence of different factors on the oxidation reaction was studied by employing different reaction conditions of time, temperature, amount of catalyst, various solvents, oxidant to substrate ratio etc. The reaction was conducted for different durations varying from one hour to four hours. During the initial phase, only a small amount of hydroquinone was formed. It was considered as the induction period and after that period, the percentage conversion is found to increase rapidly with time. The optimum time required for the conversion to be complete was four hours. The continuation of the reaction beyond the stipulated time yields unwanted products. These observations point to the possibility of a free radical mechanism.

Variations in the amount of catalyst used for study showed that increase in the amount of catalyst results in an increase in the rate of conversion. This may be due to the increase in the number of active sites. The increase in the weight of catalyst from 20 mg to 40 mg made a significant increase in the formation of the product hydroquinone but further increase of amount from 40 mg to 50 mg shows only a little increase. This shows that maximum product formation occurred with a certain amount of catalyst. The increase in the addition of catalyst above a certain optimum limit has no significant effect on the conversion.

The optimum temperature for the reaction was found to be 70° since maximum yield was obtained at that temperature. The reactions were carried out similarly at two more temperatures, 30°C and 50°C. Generally most reactions are expected to increase with temperature and similar effect is observed in this particular reaction. The increase in hydroquinone percentage with increase in temperature can be attributed to several reasons. The decomposition of hydrogen peroxide at higher temperatures to produce radicals that accelerate the rate of oxidation could be one reason. Moreover, at increased temperatures there are chances of side reactions resulting in the formation of other products along with the major product.

The study of the effect of oxidant to substrate ratio showed that the amount of the oxidant plays a decisive role in deciding the catalytic activity of these encapsulated complexes. A large increase in the volume of H_2O_2 has a negative impact on the reaction since very high concentration of the oxidant results in the rapid oxidation of phenol giving unwanted products.

It has been already reported that solvents have a distinct influence on phenol hydroxylation over microporous titanosilicate zeolites[63]. Experimental studies have proved that the catalytic activity is maximum when the solvent used is water. The use of methanol and chlorobenzene as solvents give dihydroxy benzenes in small amounts that can be due to the low solubility of hydrogen peroxide in these solvents. The reactive phenol radicals maybe removed by these solvents resulting in lowering of activities. Moreover the activity coefficient of phenol in water is much higher than in any other solvents and this might be the reason for the enhanced catalytic activity in water medium[64].

The study of recycled catalysts is significant on account of economical considerations. The separation of the encapsulated complexes from the reaction medium can be done by simple procedures like filtration. The activities shown by the recycled catalysts are much higher compared to the free complexes. The intactness of the complexes within the zeolite cages enhances their possibility of recycling. All the complexes under study were recycled and used for catalytic studies. The percentage conversion data proves beyond doubt that they can be recycled and further used.

Many factors contribute to the high efficiency of zeolite complexes in this catalytic reaction. The coordination sites occupied by the labile water molecules are readily available for the reactants to interact with the metal ions entrapped within the supercages of the zeolite, which might be one of the reasons for their high catalytic activity. Furthermore, other parameters like shape selectivity, electric field gradient inside the zeolite pores, surface area and pore volume play a decisive role in deciding the redox properties of the encapsulated transition metal complexes. The low concentration of metal in the encapsulated complexes enhances their catalytic activity.

Though there are many possible mechanisms for the hydroxylation of phenol, the experimental studies conducted above indicate a free-radical mechanism[65]. The abstraction of a hydrogen atom from phenol results in the formation of the more reactive phenoxy radical. The phenoxy radical makes the aromatic ring more susceptible towards oxidaion reactions. Mayer *et al.* have reported a heterogeneous- homogeneous free radical mechanism for these types of reactions in liquid phase[66]. According to the scheme presented by Meyer, the free radicals are formed on the catalyst surface and the radicals undergo propagation and termination in solution. There are two ways of generating free radicals. The catalytic surface may trigger the decomposition of hydrogen peroxide into radicals. The acidic sites of zeolite accelerate the formation of highly reactive $H_3O_2^+$ species, which attack the benzene ring leading to the formation of hydroquinone and catechol. There are also chances for the activation of phenol molecules facilitating the formation of phenoxy radicals.

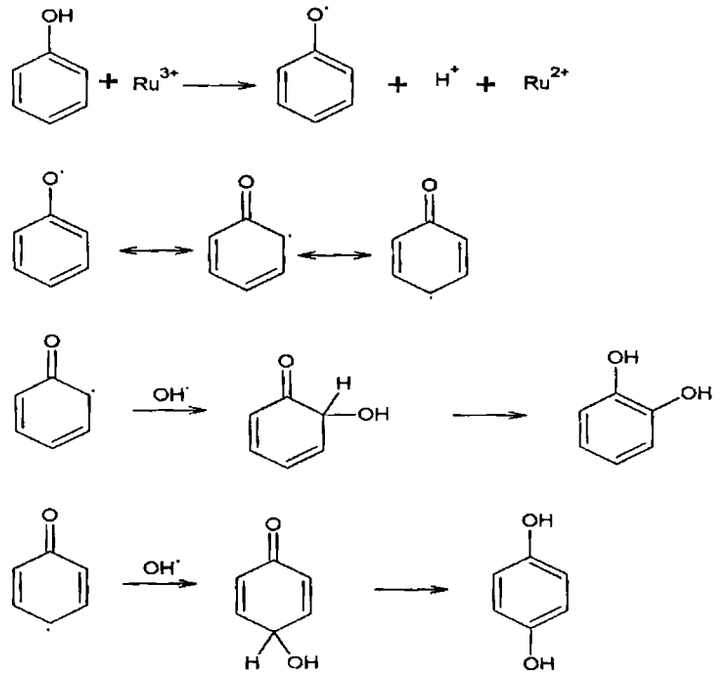

Scheme I Mechanism of phenol hydroxylation

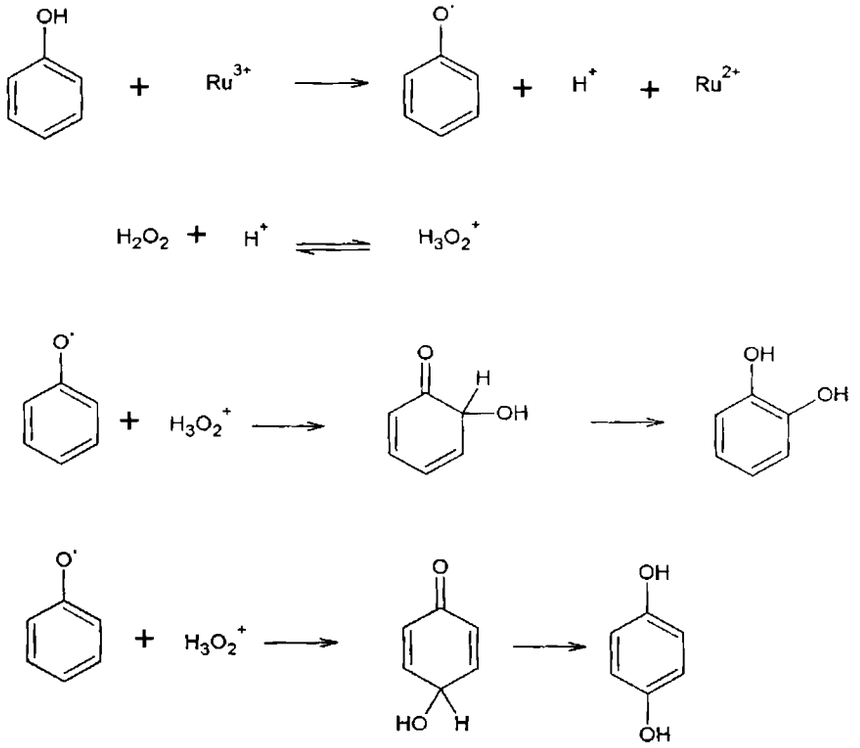

Scheme II Mechanism of phenol hydroxylation

In both schemes the first step is the reaction between the zeolite complex and phenol resulting in the production of phenoxy radicals by abstraction of hydrogen which is the initiation step. The phenoxy radical undergoes reaction in two ways. The radical undergoes rearrangement and the attack of $OH^{\cdot}$ radicals constitute the propagation step in solution. The formation of hydroquinone and catechol in varying amounts can be explained by the different sites of attack by the $OH^{\cdot}$ radical. The scheme 2 involves the utilization of $H_3O_2^+$ radicals in the propagation of the reaction chain. The presence of zeolite supported complexes accelerates the formation of $H_3O_2^+$ by the presence of acidic sites of zeolites. Hence we can propose that the hydroxylation proceeds through the mechanism as in scheme 2. Another factor supporting this mechanism is the increase in reactivity with increase in the concentration of hydrogen peroxide.

References

1. Murray, K.S.; Aust. J. Chem. **1978**, 31, 203.
2. Nakajima, K.; Ando, Y.; Mano, H.; Kojima, M. Inorg. Chim. Acta, **1998**, 274, 184.
3. Doine, H. Bull. Chem. Soc. Japan, **1995**, 58, 1327.
4. Pal, S.N.; Pal, S. Inorg. Chem. **2001**, 40, 4807.
5. De Clereq, B.; Verpoort, F. Macromolecules, **2002**, 35, 8943.
6. De Clereq, B.; Verpoort, F. Adv. Synth. Catal. **2002**, 34, 639.
7. De Clereq, B.; Lefebvre, F.; Verpoort, F. Appl. Catal. A, **2003**, 247, 345.
8. Opstal, T.; Verpoort, F. Synlett. **2002**, 6, 935.
9. Opstal, T.; Verpoort, F. Angew. Chem. Int. Edit. **2003**, 42, 2876.
10. Thronback, J.R.; Wilkinson, G. I.Chem. Soc. Dalton Trans, **1978**, 110.
11. Hendawy, A.M..EL.; Alkubaisi, A.H. Polyhedron, **1993**, 12, 2343.
12. Iyun, J.F.; Ayoko, G.A.; Lawal, H.M. Trans. Met. Chem. **1992**, 17, 16.
13. Weisz, P.B.; Frilette, V.J. J. Phy. Chem. **1960**, 64, 382.
14. Weisz, P.B.; Frilette, V.J.; Maatman, R.W.; Mower, E.B. J. Catal. I, **1962**, 307.
15. Jacob, C.R.; Varkey, S.P.; Ratnasamy, P. Appl. Catal. A. **1998**, 168, 353.
16. Parton, R.F.; De Vos, D.E.; Jacobs, P.A. in Proceedings of the NATO Advanced Study Institute on Zeolite Microporous Solids : Synthesis, Structure and Reactivity, Derouane, E.G.; Lemos, F.; Naccache, C.; Ribeiro, F.R. (Eds.); Kluwer, Dodrecht, **1992**, 555, 578.
17. Tennakone, K.; Kumara, G.R.; Kumarasinghe, A.R.; Sirimanne, P.M.; Wijayantha, K.G.U. Photochem. Photobiol. A: Chem. **1996**, 94 (2-3), 217- 220.
18. Imamura, S.M.; Gjjutsu, **1981**, 22, 201.
19. Ai, M. J.Catal. **1978**, 54, 223.
20. Njnibeako, A. Prepr. Canad. Symp. Catal. **1977**, 5, 170.
21. Al-Hayck, N. Water Res. **1985**, 19, 657.
22. Tatarinova, T.A. Kinet. Katal. **1985**, 23, 54.
23. Goldstein, S.; Czapski, G.; Robani, J. J. Phys. Chem. **1994**, 98, 6586.
24. Yang, R.B.; Xiao, F.S.; Wu, D.; Lui, Y.; Qiu, S.I.; Xu, R.R. Catal. Lett. **1997**, 49, 49.

25. Yang, R.B.; Xiao, F.S.; Wu, D.; Lui, Y.; Qiu, S.I.; Xu, R.R. Catal. Today **1997**, 51, 39.
26. Wang, D.Y.; Liu, Z.Q.; Liu, F.Q. Appl. Catal. A. **1998**, 174, 25.
27. Xiong, C.; Chen, Q.; Lu, W.; Gao, H.; Lu, W.; Gao, Z. Catalysis Letters **2000**, 69, 231-236.
28. Esposito, A.; Taramasso, M.; Neri, C. U.S. Patent 4, **1983**, 396, 783.
29. Thangaraj, A.; Kumar, R.; Ratnasamy, P. J. Catal. **1991**, 131 (1) 294-297.
30. Martens, J.A.; Buskens, P.; Jacobs, P.A. Appl. Catal. A: Gen. **1983**, 99 (1), 71-84.
31. Arends, I.W.C.E.; Sheldon, R.A.; Wallau, M.; Schuchardt, U. Angew. Chem. Int. Ed. Engl. **1997**, 36 (11),1144-1163.
32. Ulagappan, N.; Krishnasamy,V. J. Chem. Soc. Commun. **1995**, 373-374.
33. Chou, B.; Tsai, J.L.; Cheng, S. Microporous Mesoporous Mater. **2001**, 48 (1-3), 309- 317.
34. Xiao, F.S.; Sun,J.; Meng, X.; Yu, R.; Yuan, H.; Jiang, D.; Qiu, S.; Xu, R. Appl. Catal. A: Gen. **2001**, 207 (1-2), 267-271.
35. Zhang, H.; Zhang, X.; Ding, Y.; Yan, L.; Ren, T.; Suo, J. New J. Chem, **2002**, 26, 376-377.
36. Taramasso, M.; Pergeo, G.; Notari, B. US Patent **1983**, 44105019.
37. Thangaraj, A.; Kumar, R.; Ratnasamy, P. Appl. Catal. **1990**, 57, L1.
38. Reddy, J.S.; Kumar, R.; Ratnasamy, P. Appl. Catal. **1990**, 58, L1.
39. Reddy, J.S.; Sivasanker, S. Catal. Lett. **1994**, 11, 241.
40. Jiri, K.R.; Amost, Z.; Jiri, H. Collect Czech. J. Chem. Soc. Chem. Commun. **1995**, 60, 451.
41. Hari, P.R.; Ramaswamy, A.V. Appl. Catal. A, **1993**, 93, 123.
42. Yu, J.F.; Zhang, C.L.; Yang, Y.; Wu, T.H. Chin. J. Catal. **1997**, 18, 230.
43. Thangaraj, A.; Kumar, R.; Ratnasamy, P. J. Catal. **1991**, 131, 294.
44. Reddy, J.S.; Sivasanker, S.; Ratnasamy, P. J. Mol. Catal. **1992**, 71, 373.
45. Tuel, A.; Ben Taarit, Y. Appl. Catal A: General ,**1993**, 102, 69.
46. Allian, M.; Germain, A.; Cseri, T.; Figueras, F. Stud. Surf. Sci. Catal, **1993**, 78, 455.
47. Martens, J.A.; Buskens, P.; Jacobs, P.A. Appl. Catal. A : General, **1993**, 99, 71.

48. Vlagappan, N.; Rishasang, V. J. Chem. Soc. Chem. Commun. **1995**, 374.
49. Serrano, D.P.; Li, X.; Davis, M.E. J. Chem. Soc. Chem.Commun. **1992**, 745.
50. Wang, J.; Park, J.N.; Wei, X.Y.; Lee, C.W. Chem. Commun. **2003** , 5, 628- 629.
51. Wang, J.; Park, J.N.; Jeong, H.C.; Choi, K.S.; Wei, X.Y.; Hong, S.I.; Lee, C.W. Energy and Fuels, **2004**, 18, 470-476.
52. Liu, H.; Lu, G.; Guo, Y.; Guo, Y.; Wang, J. Nanotechnology, **2006**, 17, 997-1003.
53. Seelan, S.; Sinha, A.K.; Srinivas, D.; Sivasanker, S. Bull. Catal. Soc. India I, **2002**, 29.
54. Raja, R.; Ratnasamy, P. Stud. Surf. Sci. Catal. **1996**, 101, 181.
55. Iyun, J.F.; Ayoko, G.A.; Lawal, H.M. Trans. Met. Chem. **1992**,17, 16.
56. Draths, K.M.; Frost, J.W. J. Am. Chem. Soc. **1991**, 113, 9361.
57. Draths, K.M.; Frost,J.W. J. Am. Chem. Soc. 1995, 117, 2395.
58. Thangaraj, A.; Kumar, R.; Ratnasamy, P. J. Catal. **1991**, 131, 294.
59. Reddy, J.S.; Sivasanker, S.; Ratnasamy, P. J. Mol. Catal. **1992**, 71, 373.
60. Allian, M.; Germain, A.; Figueras, F. Catal. Lett. **1994**, 28, 409.
61. Martens, J.A.; Buskens, P.; Jacobs, P.A. Appl. Catal. A : Gen. **1993**, 99 (1) 71-84.
62. Sharma, V.S.; Schubert, J. Inorg. Chem. **1971**, 10, 251.
63. Tuel, A.; Moussa-Khouzarni, S.; Tarrit, Y.B.; Naccache, C. J.Mol. Catal. **1991**, 6845.
64. Subramanyan, Louis, B.; Viswanathan, B.; Renken, A.; Varadarajan, T.K. Eurasian Chem. Tech. J. **2001**, 3.5963.
65. Bellussi, G.; Perego, C. Handbook of Heterogeneous Catalysis, 5 ; Ertl, G.; Knozinger, H.; Weitkamp, J. Wiley- VCH, New York, 2329, 1997.
66. Meyer, C.; Clement, G.; Balaceanu, J.C. in.Proc.3rd Int.Congr. on Catalysis, **1965**, 1, 184.

SUMMARY AND CONCLUSION

Catalysis is an area of research, which plays a key role in modern chemical technology. Infact, catalysis form the backbone of chemical industry as the application of catalytic science and engineering in the industries provide us with various materials like fertilizers, fuels, medicines, food additives, organic reagents etc. The kinetic phenomena of catalysis are broadly classified into three- homogeneous, heterogeneous and biological (enzymatic) catalysis. Transition metal complexes constitute a major class of homogeneous catalysts and their performance can be enhanced by varying the coordination environment around the metal atom or by altering the ligands attached to them. But the increasing need for the development of environment friendly products and processes have put many restrictions on the use of homogeneous catalysts. The disadvantages associated with them have prompted chemists to design more efficient catalysts that combine the advantages of both homogeneous and heterogeneous systems.

Heterogenization involves the immobilization of homogeneous transition metal complexes on various organic and inorganic supports. The most commonly used supports are zeolites, alumina, silica and organic polymers. In accordance with this aim, transition metal complexes of ruthenium were encapsulated within the supercages of zeolite Y. The rigid inorganic zeolite matrices with cavities and channels of molecular dimensions of different sizes and shapes form an interesting class of supports as they provide the shape selectivity for certain reactions. The properties of zeolites like high thermal stability, well defined and large internal surface area and the ability to impose size and shape selectivity on the product distribution make them attractive solid supports for complexes. The work presented in this thesis is mainly centered on the synthesis and characterization of some encapsulated transition metal complexes and the catalytic activity of the synthesized complexes in certain organic reactions. The thesis is divided into eight chapters.

Chapter 1 presents a general introduction of zeolite-encapsulated complexes and their utility as catalysts in different reactions. The role of zeolites as active supports

for many organic syntheses and as enzyme mimics is also presented in detail. The reports throwing light on the reason behind the tremendous interest in the research of the chemistry and bonding of various transition metals especially ruthenium are collected and presented. The scope of the present study is also included in this chapter.

Chapter 2 contains details regarding the materials used, methods employed for the preparation of ligands, metal exchanged zeolite and the characterization techniques used to study the nature and geometry of the synthesized complexes. The methods used to characterize the complexes are chemical analysis, CHN analysis, XRD studies, scanning electron micrographs, thermogravimetric studies, surface area and pore volume analysis, diffuse reflectance spectra, FTIR, EPR studies etc. The hydroxylation of phenol and oxidation of cyclohexanol was monitored with the help of gas chromatograph.

The synthesis and characterization of zeolite encapsulated Ru(III) complexes of the Schiff bases salicylaldehyde semicarbazone (SSC), N,N'-bis(salicylaldimine)-*o*-phenylenediamine (SOD) and N,N'-bis(salicylaldimine)-*p*-phenylenediamine (SPD) are described in **chapter 3**. The ion exchanged zeolite, RuY was prepared from the sodium exchanged form by the method of ion exchange. The zeolite encapsulated ruthenium complex of the Schiff base SSC was prepared from the ruthenium-exchanged zeolite using the intrazeolite synthesis by complexation method. The complexes of SOD and SPD were obtained by flexible ligand method. All the complexes were purified by the method of soxhlet extraction. The Si to Al ratio of the encapsulated forms is found to be approximately same as that of the ion exchanged zeolite, which indicates the retention of the zeolite structure even after encapsulation. The comparison of the XRD patterns of the complexes with the metal exchanged form proves that there is no collapse of zeolite framework. The lowering of surface area and pore volume values is an indication of the formation of metal complexes inside the zeolite pores. The absence of surface adsorbed species is obtained from the SEM pictures taken before and after soxhlet extraction.

The IR spectra give an idea about the site of coordination of ligands to the metal. Though strong zeolite peaks mask some bands of the complex, the shifts in the position of bands indicate the point of attachment. The band occurring at 1485cm^{-1} in the pure

SSC ligand due to C=N stretching vibration of the azomethine group gets shifted to a lower frequency of 1427 cm^{-1} in the zeolite encapsulated semicarbazone indicating the involvement of azomethine nitrogen in coordination. The shift of the band assigned to carbonyl vibration is indicative of the complexation involving the participation of the carbonyl group. Similarly the IR bands observed in SOD and SPD due to azomethine nitrogen show shift to a lower energy region proving the coordination of ligand to metal using that nitrogen. On the basis of electronic spectral data and EPR studies, an octahedral geometry was tentatively assigned for the zeolite encapsulated ruthenium complexes, RuYSSC, RuYSOD and RuYSPD. The thermal stability of the complexes is obtained from the TG/DTG data. The stages of decomposition and the percentage loss in weight give a rough idea of the amount of intrazeolite metal complex formed.

Chapter 4 is divided into two sections- Section A and Section B. The section A describes the preparation and characterization of zeolite-Y complexes of anthranilic acid (AA) and 4-aminobenzoic acid (ABA) whereas the second section deals with the dimethylglyoxime (DMG) complex. The Si/ Al ratio of 2.6 and the XRD patterns of the encapsulated complexes indicate that the zeolite framework has retained its crystallinity even on encapsulation. The decrease in surface area and pore volume values is a direct proof of the formation of metal complexes. The presence of well-defined samples of encapsulated metal complexes with clear boundaries in SEM taken after soxhlet extraction shows the removal of surface species. The band corresponding to $\nu_{C=O}$ stretching vibration occurring at 1666 cm^{-1} and 1659 cm^{-1} in the spectrum of AA and ABA shift to a lower frequency of 1640 cm^{-1} and 1632 cm^{-1} respectively indicating the participation of carbonyl group in complex formation. The bands due to C=N stretching frequencies have been found to shift towards lower frequencies in RuYDMG, which suggests coordination through nitrogen atom of the ligand to the metal. TG curves give an idea about the different stages of decomposition. The decomposition of the aminobenzoic acids occurs in two stages- first stage corresponds to the loss of water molecules present in the zeolite cavities and the second stage corresponds to the decomposition of the ligand. The electronic spectra of the complexes show that ruthenium complexes possess octahedral geometry. The spin forbidden $^4T_{1g} \leftarrow {}^2T_{2g}$, $^4T_{2g} \leftarrow {}^2T_{2g}$ transitions which are typical of Ru(III) ion are observed for RuYAA and

RuYABA with low intensities. The EPR spectra is indicative of the presence of a paramagnetically active Ru(III) in all the complexes and the small hyperfine splitting of the EPR signal points out the involvement of the nitrogen atom in coordination with the metal.

Chapter 5 describes the synthesis and characterization of zeolite Y encapsulated Ru(III) complexes of the Schiff bases N,N'-bis (3-pyridylidene)-1,2-phenylenediamine (PCO); N,N'-bis(3-pyridylidene)-1,4-phenylenediamine (PCP); N,N'-bis(2-pyridylidene)-1,2-phenylenediamine (CPO) and N,N'-bis(2-pyridylidene)-1,4-phenylenediamine (CPP) derived from the reactions of pyridine carboxaldehydes with ortho and para-phenylenediamines. The complexes synthesized by flexible ligand method were purified by soxhlet extraction. The retention of the Si/Al ratio of zeolite-Y indicate that there is no loss in crystallinity of the zeolite structure by encapsulation. This is further confirmed by the similar XRD patterns. Reduction in surface area and pore volume value of the complexes compared to ruthenium-exchanged zeolite suggests encapsulation within the supercages of the zeolite. The IR spetral data indicate the coordination sites of the ligands to the metal. The stretching vibration due to azomethine nitrogen seen at 1578 cm^{-1} in the spectrum of the pure ligand PCO, is shifted to the lower energy region of about 1556 cm^{-1} in the spectrum of the corresponding encapsulated complex indicating the involvement of azomethine nitrogen in coordination. The band at 1590 cm^{-1}in the spectrum of PCP is due to $\nu_{C=N}$ vibration. The encapsulated complex RuYPCP shows a red shift of about 20 cm^{-1} in the band due to azomethine group, which suggests that the ligand is coordinated to the metal atom through this nitrogen. The peaks due to the presence of azomethine nitrogen in CPO and CPP show blue shift to lower frequency in the zeolite samples indicating the involvement of that nitrogen in the formation of the complex. The electronic spectra of the complexes show some characteristic bands in the 230-300 region which can be assigned as charge transfer bands. The bands around 627-620 nm and 406-362 nm were assigned to d-d transitions. These transitions are in conformity with assignments made for similar octahedral Ru(III) complexes. The solid state EPR spectra of the ruthenium complexes were recorded at room temperature. The presence of two g values for the encapsulated complexes refers to the anisotropic nature and presents an axial symmetry. The EPR spectra is consistent with the presence of a paramagnetically active Ru(III)

ion. Two stages of decomposition are observed for all the complexes derived from pyridine carboxaldehyde. The first stage of decomposition till 200°C corresponds to the loss of coordinated water along with the physisorbed water. The mass loss in the second stage is consistent with the decomposition of the synthesized complex. Then a constant weight is maintained till 850°C and above this temperature, the destruction of the framework occurs.

Chapter 6 contains a detailed study of the decomposition of hydrogen peroxide in the presence of encapsulated complexes of SSC, SOD, SPD, AA, ABA, DMG, PCO, PCP, CPO and CPP. Among all the complexes synthesized, RuYSSC was found to be the most active catalyst. A comparative study of the activities of the simple complexes and the zeolite samples revealed that encapsulated forms act as more effective catalysts in the decomposition reaction. This might be due to the shape selectivity of the zeolite pore and the presence of vacant coordination sites or active sites in the complex. The effects of various parameters like amount of catalyst, volume of hydrogen peroxide, solvent polarity of the reaction mixture and action of pyridine on the decomposition of H_2O_2 were studied. The activity increase with increase in the weight of the catalyst used and the addition of methanol slowed down the decomposition reaction, which indicate the involvement of HOO^- species in the catalytic reaction. The addition of pyridine to the reaction mixture results in an increase in the reaction rate which confirms HOO^- as the active species in the decomposition. The activities of the recycled catalysts were studied and the small decrease in activity is due to the increased stability of the encapsulated complexes when compared to their neat analogues.

Chapter 7 of the thesis presents the results obtained by our studies on cyclohexanol oxidation using 70% THBP in the presence of zeolite encapsulated complexes of SSC, SOD, SPD, AA, ABA, PCO, PCP, CPO and CPP. The product formed cyclohexanone and the unreacted substrate were analyzed using a gas chromatograph to estimate the percentage conversion. The reaction was carried out under different conditions to study the influence of different factors like reaction time, amount of catalyst, temperature, oxidant to substrate ratio etc. An estimation of the catalyst at the end of the oxidation reaction revealed that no leaching of metal occurred during the reaction, which suggests that the zeolite samples selected for study are intact.

The comparison of their catalytic activities indicates that RuYSSC acts as the most effective catalyst in this oxidation reaction followed by RuYSOD. RuYAA and RuYABA exhibit almost the same activity whereas RuYDMG is found to be the least active. The percentage conversion with RuY and neat complexes is found to be very low in comparison with supported catalysts. The encapsulated ruthenium complexes are held firmly inside the zeolite pores by electrostatic forces of attraction that enhances their catalytic activity. The percentage conversion of cyclohexanol showed no substantial increase with increase in the amount of catalyst; hence 20 mg of catalyst was used for detailed studies. Experimental results have showed that there is an optimum time for the completion of the reaction and when the reaction was allowed to proceed after the stipulated time, unwanted products are formed. All the encapsulated complexes showed very little conversion for about two hours after which the percentage conversion shows a considerable increase. The requirement of a longer reaction time of about four hours for the conversion is probably due to diffusional limitations for zeolite catalysts. The catalytic activity showed a strong dependence on the oxidant to substrate ratio and the optimum oxidant to substrate ratio was found to be 2. Further increase in the amount of oxidant poses the risk of a parallel decomposition reaction that may deactivate the catalysts. The reaction was studied at three different temperatures 50°C, 70°C and 90°C in order to determine the influence of temperature on the oxidation. The percentage conversion increased on raising the temperature. The maximum conversion was observed at 90°C and so it was selected as the optimum temperature for further studies. Chlorobenzene appears to be the best solvent for cyclohexanol oxidation when compared to other solvents like toluene, water and methanol. The recycling studies were done after washing the used samples several times with acetone and heating them in an oven. They were able to retain their activity, which can be taken as a solid evidence for the stability of the complexes inside the zeolite pores and their ability to withstand the regeneration process.

Chapter 8 of the thesis deals with the catalytic activity of ruthenium-exchanged zeolite and the zeolite encapsulated complexes of SSC, SOD, SPD, AA, ABA, DMG, PCO, PCP, CPO and CPP in the hydroxylation of phenol using hydrogen peroxide. The products were analyzed with a GC to determine the percentage conversion and the chromatograms indicate the presence of different products like hydroquinone, catechol,

benzoquinone, benzophenone etc. The major product formed is hydroquinone. From the screening studies, RuYSSC was found to be the most effective catalyst for phenol hydroxylation with 94.4% conversion and 76% hydroquinone selectivity. The influence of different factors like reaction time, temperature, amount of catalyst, effect of various solvents and oxidant to substrate ratio in the catalytic activity were studied in order to find out the optimum conditions for the hydroxylation reaction. The influence of time on the percentage conversion of phenol was studied by conducting the reactions for different durations varying from one hour to four hours. There is an induction period for all the complexes and the length of the induction period depends on the nature of the active components. Though the conversion of phenol and selectivity for hydroquinone increases with time, the amount of benzoquinone formed decreases with time. This is probably due to the decomposition of benzoquinone formed during the initial stages of the reaction into other degradation products like benzophenones. The effect of temperature was studied by carrying out the reaction at three different temperatures, 30°C, 50°C and 70°C. Reactions carried at temperatures higher than 70°C result either in the decomposition of the products or in the formation of tarry products. Activity increased with increase in the amount of the catalyst up to a certain level. However further increase in the weight of the catalyst did not have any noticeable effect on the percentage conversion. The catalytic studies indicate that the oxidation reaction increases with increase in the volume of hydrogen peroxide till a certain volume. But further increase in the volume of H_2O_2 is detrimental as some dark mass is obtained after four hours of reaction. The catalytic activity is largely dependent on the nature of the solvent and maximum percentage conversion occurred when the solvent used is water. The intactness of the complexes within the zeolite cages enhances their possibility of recycling and the activities of the recycled catalysts show only a slight decrease when compared to the fresh samples.